



**Teck Coal Environmental Office**  
Bag Service 2000, 421 Pine Avenue  
Sparwood, B.C. Canada V0B 2G0

+1 250 425 3331 Tel  
[www.teck.com](http://www.teck.com)

## **Technical Report Overview**

**Report:** Calcite Effects to Fish Incubation Conditions 2016

**Overview:** This report provides the results from a 2016 investigation into the relationship between calcite and the incubation conditions for Westslope Cutthroat Trout eggs in the Upper Fording River.

This report was prepared for Teck by Ecofish Research Ltd.

### **For More Information**

If you have questions regarding this report, please:

- Phone toll-free to 1.855.806.6854
- Email [feedbackteckcoal@teck.com](mailto:feedbackteckcoal@teck.com)

Future studies will be made available at [teck.com/elkvalley](http://teck.com/elkvalley)

# Teck Coal Ltd

## Calcite Effects to Fish Incubation Conditions



Prepared for:

**Teck Coal Limited**  
Suite 1000 – 205 9th Street  
Calgary, AB, T2G 0R3

May 17, 2017

Prepared by:

**Ecofish Research Ltd.**

and

**Westslope Fisheries Ltd.**



Photographs and illustrations copyright © 2017

Published by Ecofish Research Ltd., Suite F, 450 8<sup>th</sup> St., Courtenay, B.C., V9N 1N5

For inquiries contact: Technical Lead [documentcontrol@ecofishresearch.com](mailto:documentcontrol@ecofishresearch.com) 250-334-3042

**Citation:**

Wright, N., D. West, T. Jensma, S. Cope, M. Hocking, and T. Hatfield. 2017. Calcite Effects to Fish Incubation Conditions. Consultant's report prepared for Teck Coal by Ecofish Research Ltd, and Westslope Fisheries Ltd. May 17, 2017.

**Certification:** *Certified. Stamped version on file*

**Senior Reviewer:**

Todd Hatfield, Ph.D., R.P.Bio. No. 927  
Senior Environmental Scientist/Project Manager

**Technical Leads:**

Morgan Hocking, Ph.D., R.P. Bio. No. 2752  
Fisheries Biologist

David West, M.Sc., P.Eng. No. 186132  
Water Resources Engineer

Nicole Wright, Ph.D., AScT. No. 30520  
Senior Hydrologist

**Disclaimer:**

This report was prepared by Ecofish Research Ltd. for the account of Teck Coal Ltd. The material in it reflects the best judgement of Ecofish Research Ltd. in light of the information available to it at the time of preparation. Any use which a third party makes of this report, or any reliance on or decisions to be made based on it, is the responsibility of such third parties. Ecofish Research Ltd. accepts no responsibility for damages, if any, suffered by any third party as a result of decisions made or actions, based on this report. This numbered report is a controlled document. Any reproductions of this report are uncontrolled and may not be the most recent revision.

## EXECUTIVE SUMMARY

Calcite formation has been observed in the tributaries downstream of Teck mining activities, at some locations in the Fording River and, to a lesser extent, in the Elk River and in reference streams unaffected by mining. Conditions of high calcite presence in tributaries are hypothesized to affect spawning success through several mechanisms including access to useable spawning gravels, incubation conditions, rearing conditions for juveniles, and food (e.g., production of invertebrate prey). This report provides results from investigations into the linkage between calcite and incubation conditions. Calcite accumulations are hypothesized to reduce flow and dissolved oxygen in the interstitial spaces of spawning gravel by interfering with exchange of surface water and hyporheic water. Teck Coal Limited (Teck) commissioned a phased study approach to assess incubation conditions (as represented by dissolved oxygen and flow) in relation to calcite levels. The study assessed the following general impact hypothesis:

H1: Observed calcite conditions on stream substrates have no effect on hyporheic flow and DO.

Study sites were selected within the upper Fording River watershed to represent both mainstem and tributary spawning habitat used by Westslope Cutthroat Trout (*Oncorhynchus clarkii lewisi*) in the upper Fording River and to represent the full range of calcite conditions based on previous calcite monitoring. Spawning was visually confirmed (i.e., redds, spawning fish) at the sites selected in the upper Fording River, Clode Creek Settling Pond System, and lower Greenhills Creek.

A field study was conducted during the Westslope Cutthroat Trout spawning season in late June and again during the summer growing period in late August and early September 2016, to measure calcite index (CI), hyporheic conditions (i.e., DO concentration at depth and hyporheic flow), as well as other naturally varying potential covariates (i.e., key fish habitat variables, hyporheic water quality, substrate composition, and surface hydrology). Flow and DO were measured with a piezometer standpipe in the Fording River (low calcite presence), Clode Creek Settling Pond System (low to moderate calcite presence), and Greenhills Creek (low to high calcite presence).

Two methods were employed to measure hyporheic flow: a hydraulic head method and a temperature method. Results were used to model relationships between hyporheic conditions and the CI taking into consideration site characteristics and covariates (e.g., % fines).

### *Antecedent Streamflow and Precipitation*

Flow data collected at the mouth of the Fording River (Water Survey of Canada Station, WSC, 08NK018) and precipitation data collected at Environment Canada's (EC) Sparwood climate station (1152899) provide a continuous data record with which to characterize streamflow and precipitation prior to the study periods. Discharge measurements were collected during each sampling period at each target stream to determine the flow on the day at which hyporheic conditions were measured.

*FHAP and Fish Observations*

Modified fish habitat surveys (FHAP) were completed in the habitat unit upstream, downstream and within each calcite study site. The surveys were completed during the first field visit (June 18 to June 23, 2016). During field work Westslope Cutthroat Trout or redds were observed in each of the three study streams, but not in all of the study reaches.

*Calcite Index Measures*

Surface calcite levels were measured using the calcite index. CI varied spatially throughout the study area, as expected from previous studies. The lowest CI was measured in the Fording River (all sites <0.50). The CI at the Clode Creek Settling Pond System sites ranged from 1.00 to 1.22, and CI at the Greenhills Creek sites ranged from 0.50 to 2.64; generally increasing with distance upstream in the tributary. Calcite occurrence was also assessed in relation to depth, but was not measured with the same method as surface calcite measurements. Calcite occurred only at the surface in the Fording River, whereas calcite occurred to greater depths at the Clode Creek Settling Pond System and Greenhills Creek sites.

CI was measured at two scales: a mesohabitat scale typical of the standard CI measurements in the broader calcite monitoring program, and a smaller area near each piezometer site intended to represent the spatial scale of a redd. There was generally minimal difference in CI between the two spatial scales, suggesting little variation of CI within the mesohabitat. The exception was in Greenhills Creek, where GH\_GH1 and GRE-CA05 exhibited greater differences in CI between the two measurement scales.

*Hyporheic Dissolved Oxygen Concentration*

Dissolved oxygen (DO) and general water quality parameters were measured in the hyporheic zone (the saturated interstitial area beneath and alongside a streambed, where there is a mixing of shallow groundwater and surface water) at several depths in June 2016 (surface, 10 cm and 30 cm depth) and again in August/September 2016 (surface, 10 cm, 30 cm and approx. 50 cm) at all the study sites.

At the Fording River sites, with low CI, DO exhibited a well-saturated condition ranging from 76.4 % to 90.7 % saturation and 9.00 mg/L to 10.86 mg/L concentration at all sites over both sampling periods. Water temperature ranged from 6.4 °C to 9.7 °C. In general, the lowest DO values were recorded at depth; little variation in water temperature at depth was observed.

At the Clode Creek Settling Pond System sites, with low to moderate calcite index scores, DO generally exhibited a well-saturated condition ranging from 75.5% to 93.4% saturation and a concentration of 8.45 mg/L to 9.84 mg/L over both sampling periods. Water temperature ranged from 10.9 °C to 12.5 °C. In general, the lowest DO values were recorded at depth; little variation in water temperature at depth was observed.

In Greenhills Creek, where CI score ranged from low to high, DO exhibited a well-saturated condition at all depths in two of the seven sites: GRE-CA03 and GH\_GH1. DO at these sites

ranged from 81.0% to 87.2% saturation and 8.35 mg/L to 9.70 mg/L concentration. Water temperature at these sites changed minimally with depth and ranged from 10.2 °C to 14.6 °C, over the study periods. The remaining sites exhibited variable DO concentration between sites and at depth ranging from 0.99 mg/L to 10.58 mg/L. Average DO at three of the sites was below the minimum instantaneous (6 mg/L) BC water quality guidelines at depths between ~ 19 cm and 50 cm (GRE-CA01, GRE-CA02, GH-CTF). These results suggest exchange with surface water may be limited at these depths and conditions for incubation may be compromised. At GRE-CA01 and GRE-CA02, poor surface water exchange may be due, in part, to high % fines at depth. It should be noted that DO was above the guidelines at 10 cm depth in all cases. The less stringent 30-day guideline of 8 mg/L was not met at GRE-CA01, GRE-CA02, GRE-CA05, GRE-CA06 and GH\_CTF at depths below ~ 10 cm.

The lowest DO levels were recorded at GRE-CA02; the dominant substrate at GRE-CA02 is sand and fines, therefore interstitial spaces at depth and the exchange of gases with the surface water are both likely to be limited. Temperature decreased with depth at this site by approximately 1 °C. DO saturation typically increases with decreased temperature; however, this was not observed suggesting that mixing with surface flow was not occurring at this depth/site. CI at this site ranged from 0.50 to 0.69.

Variability in the data between the three piezometer sites was most pronounced (>18% RSE to maximum of 70% RSE) for DO in Greenhills Creek suggesting heterogeneity between the piezometer sites.

#### *Hyporheic Flow*

Groundwater exchange rate was modelled using two different methods. Exchange rates were modelled with (1) Darcy's equation using measured hydraulic head and hydraulic conductivity estimates based on grain size distribution relations, and (2) using substrate thermal gradient time series along with the one-dimensional flow and heat-transport equations using 1DTempPro.

Hydraulic head was measured during the first study period (June 2016) at two different depths within the streambed, approximately 10 cm and 30 cm, as these depths bracket the likely redd depths for Westslope Cutthroat Trout in the Upper Fording River. An additional hydraulic head measurement was made at ~50 cm depth (where possible) in August/September. The average hydraulic head generally increased (became more positive) with depth at all sites, indicating downwelling; although, the magnitude of the hydraulic gradient with depth varied by site.

Groundwater exchange rates estimated with Darcy's equation were found to have unrealistically high downwelling values at some sites. The variance and magnitude of these results are greater than those found in other studies. Hydraulic head measurements varied more than expected within the same transect and at different depths, providing evidence of high microhabitat-scale heterogeneity, as well as potential issues with the measurement technique caused by sometimes large (up to 6 cm) fluctuations in water level inside and outside the piezometer. Hydraulic conductivity estimates

derived from grain size distribution relations also had a high level of uncertainty. The hyporheic flow estimates derived from the hydraulic head method are therefore considered to be unreliable; though the positive relationship between hydraulic head and depth at all sites, indicating downwelling flow, is valid.

Groundwater exchange rate was also modelled at seven sites distributed between Fording River (FRD-CA01), Clode Creek Settling Pond System (CLO-CA01), and Greenhills Creek (GRE-CA01, GRE-CA03, GRE-CA05, GRE-CA06, and GH-CTF) using the temperature method. Thermistors were installed at three depths (0, 10 and 40 cm) for a minimum of five days during each of the June 2016 and August/September 2016 study periods.

The temperature method using the hydraulic conductivity optimization module in 1DTempPro produced more realistic and reliable results than the hydraulic head method. During June, downwelling ranged from 3.5 m/d at GH-CTF to 25.6 m/d at GRE-CA06, with an average of 13.6 m/d. During August/September, downwelling ranged from 6 m/d at CLO-CA01 to 34.4 m/d at GRE-CA03, with an average of 19.4 m/d. The rate of downwelling in August/September varied from 38% to 494% of the June rate, with an average increase of 235%. The RMS error of the 1DTempPro model runs ranged from 0.015°C to 0.167°C with an average of 0.083°C, which is lower than the thermistor accuracy of 0.2°C. The greatest sources of uncertainty in the temperature-based hyporheic exchange estimates were associated with piezometer measurement uncertainty, site-scale heterogeneity, and the potential of increased rates caused by bed disturbance during equipment installation. The variability in hyporheic exchange rates between sites was expected to be largely due to difference in geomorphic conditions (i.e., natural differences in slope, substrate, and channel planform between the streams), and location of equipment installation relative to riffles. The low number of sites (n=7) and lack of replication made it difficult to detect an effect from calcite.

#### *Modelling of Calcite versus Physical Parameters*

The relationship between calcite index and hyporheic dissolved oxygen and flow was modeled using a model selection procedure and fitting a series of linear mixed-effects models using the “lme4” and “MuMIn” packages for R statistical software (Bates *et al.* 2015). Three separate models were fit for each key response variable: dissolved oxygen concentration, hyporheic flow from the hydraulic head method, hyporheic flow from the temperature method. The predictor variables included in each model were calcite index score and habitat and sampling variables hypothesized to affect hyporheic conditions (depth in substrate, water temperature, water quality, water depth, flow, substrate composition, season, site). Predictor variables include fixed effects (variables that we are interested in and test directly) and random effects (variables that we are less interested in but need to account for in the analysis).

For dissolved oxygen, the top model included CI score, depth in substrate, the CI score\*depth in substrate interaction, and percent fines as predictors. At shallow depths in the substrate, CI score did not have a strong effect on dissolved oxygen conditions. In contrast, at deeper depths in the substrate increasing CI Score led to decreasing dissolved oxygen in the substrate.

Hyporheic flow calculated via the hydraulic head method increased with increasing depth, but was not affected by CI score. The top model included only depth in the substrate as a predictor, while the averaged model included percent fines.

Hyporheic flow calculated via the temperature method was not predicted strongly by CI score or any of the habitat variables. The intercept-only model was the top model.

### *Conclusions*

The CI measured at the mesohabitat scale shows good agreement with CI measured within the mesohabitat near each piezometer site, suggesting that the CI score at the mesohabitat scale is representative of calcite presence and concretion at the piezometer sites intended to represent the scale of a Westslope Cutthroat Trout redd. There was little variation in CI score by season (June vs. August/September). Although there was consistency in calcite cover within each mesohabitat across sites and seasons, there was high spatial and temporal variance in other variables (response and predictor variables) within the sites.

CI score was an important predictor of DO in the substrate, but not of hyporheic flow as measured with the hydraulic head or temperature methods. Hyporheic flow estimates from the hydraulic head method were considered mostly unreliable in predicting absolute magnitude of flow, but are considered valid to indicate direction of flow and relative magnitude. Hyporheic flow estimates from the temperature method were restricted by the low number of sites ( $n=7$ ), lack of replication within mesohabitats, and high variation between sites; this made it difficult to assess the effect of calcite. The model for dissolved oxygen predicts that average instantaneous DO would decrease to below 8 mg/L at a depth of 30 cm and a CI score of  $\sim 2.3$ . At a depth of 50 cm, average instantaneous DO is predicted to decrease to below 6 mg/L at a CI score of near 3.

The average redd depth for Westslope Cutthroat Trout is between 10 and 30 cm. Our model thus predicts that average DO concentrations during incubation will be above the instantaneous minimum threshold for buried embryos/alevins of 6 mg/L from the BC Guidelines for Protection of Aquatic Life at all levels of calcite in the stream.

However, the model predictions of DO represent *mean* conditions, and exceedances of the BC Guidelines are expected at sites with high CI and high % fines. We conclude that sites with high levels of calcite are likely to experience some reduction in incubation conditions for Westslope Cutthroat Trout, and thus we reject the impact hypothesis  $H_1$ . We caution that this is a small dataset and the effect of calcite on DO is most apparent at depths that are deeper than typical redd depths of Westslope Cutthroat Trout. These results should be considered by Teck and the Environmental Monitoring Committee in relation to future work on calcite and potential effects to Westslope Cutthroat Trout in the Elk Valley watershed.

TABLE OF CONTENTS

**EXECUTIVE SUMMARY ..... II**

**LIST OF FIGURES ..... IX**

**LIST OF TABLES ..... XI**

**LIST OF MAPS..... XII**

**LIST OF APPENDICES ..... XII**

**1. INTRODUCTION ..... 1**

    1.1. IMPACT HYPOTHESIS ..... 2

**2. STUDY SITES ..... 3**

    2.1. STUDY AREA ..... 3

    2.2. SITE SELECTION..... 3

    2.3. DESCRIPTION OF SELECTED SITES ..... 4

        2.3.1. *Mainstem Upper Forging River*..... 4

        2.3.2. *Clode Creek Settling Pond System*..... 4

        2.3.3. *Greenhills Creek*..... 4

    2.4. ANTECEDENT STREAMFLOW AND PRECIPITATION ..... 8

**3. METHODS..... 9**

    3.1. FISH HABITAT, CALCITE, AND HYPORHEIC CONDITIONS ..... 9

        3.1.1. *Fish Habitat Assessment and Fish Observations*..... 9

        3.1.2. *Calcite Index Measures and Substrate Composition*..... 11

        3.1.3. *Hyporheic Dissolved Oxygen Concentration*..... 14

        3.1.4. *Surface Hydrology* ..... 16

        3.1.5. *Hyporheic Flow* ..... 17

    3.2. TESTING THE IMPACT HYPOTHESIS..... 20

        3.2.1. *Modelling of Hyporheic Conditions vs Calcite Index*..... 20

**4. RESULTS..... 21**

    4.1. FISH HABITAT, CALCITE INDEX, AND HYPORHEIC CONDITIONS ..... 21

        4.1.1. *Fish Habitat Assessment and Fish Observations*..... 21

        4.1.2. *Calcite Measures and Substrate Composition*..... 24

        4.1.3. *Surface Hydrology* ..... 31

        4.1.4. *Hyporheic Dissolved Oxygen Concentration*..... 31

        4.1.5. *Hyporheic Flow* ..... 37

    4.2. TESTING THE IMPACT HYPOTHESIS..... 49

        4.2.1. *Statistical Modelling of Hyporheic Conditions vs. Calcite*..... 49

---

**5. DISCUSSION AND CONSIDERATIONS..... 53**

5.1. FISH HABITAT, CALCITE INDEX, AND HYPORHEIC CONDITIONS ..... 53

5.2. TESTING THE IMPACT HYPOTHESIS ..... 55

**REFERENCES..... 57**

**PROJECT MAPS..... 62**

**APPENDICES ..... 67**

**LIST OF FIGURES**

Figure 1. Effect pathway diagram linking calcite on the streambed to fish production. ....2

Figure 2. Daily average flow data collected at the WSC 08NK018 hydrometric station and precipitation at EC’s Sparwood climate station prior to and during the June 17-26 and August 29-September 6, 2016 measurement periods. ....8

Figure 3. A CI piezometer site consisted of three piezometer sites located in a transect within a mesohabitat (e.g., run or riffle). ....12

Figure 4. Summary of CI at Fording River sites, 2016.....27

Figure 5. Summary of CI at Clode Creek Settling Pond System sites, 2016.....27

Figure 6. Summary of CI at Greenhills Creek sites, 2016. ....28

Figure 7. Dissolved oxygen in relation to depth measured at the Fording River and Clode Creek Settling Pond System sites in a) June and b) August/September 2016. Water quality guidelines (WQG) include long-term average minimum DO of 8 mg/L and instantaneous DO minimum guideline 6 mg/L (MOE 2016). ....33

Figure 8. Dissolved oxygen in relation to depth measured at the Greenhills Creek sites in a) June and b) August/September 2016. Water quality guidelines (WQG) include long-term average minimum DO of 8 mg/L and instantaneous DO minimum guideline 6 mg/L (MOE 2016).....34

Figure 9. Water temperature in relation to depth measured at the Fording River and Clode Creek Settling Pond System sites in a) June and b) August/September 2016. Water quality guidelines (WQG) include optimum water temperature range for the incubation of Cutthroat Trout (Oliver and Fiddler 2001).....35

Figure 10. Water temperature in relation to depth measured at the Greenhills Creek sites in a) June and b) August/September 2016. Water quality guidelines (WQG) include the optimum water temperature range for incubation of Cutthroat Trout (Oliver and Fiddler 2001)....36

Figure 11. Hydraulic head measured at depth in Fording River and Clode Creek Settling Pond System in a) June and b) August/September 2016.....39

Figure 12. Hydraulic head measured at depth in Greenhills Creek in a) June and b) August/September 2016.....40

Figure 13. Modelled K values using the K optimizer module in 1DTempPro.....44

Figure 14. Modelled groundwater exchange rates using the K optimizer module in 1DTempPro. ....46

Figure 15. Scatterplot of DO in the substrate versus CI score. Lines indicate the predicted relationships between DO and CI at different depths in the substrate based on the model that best predicts DO.....50

Figure 16. Model averaged coefficients (with 95% confidence intervals) indicating the most important variables predicting hyporheic dissolved oxygen. RVI = Relative Variable Importance scores, where a score of 1 indicates that a predictor variable occurs in all top models with  $\Delta AICc < 4$ . p-values represent probability that the coefficient is equal to 0. 51

Figure 17. Model averaged coefficients (with 95% confidence intervals) indicating the most important variables predicting hyporheic flow using the hydraulic head method. RVI = Relative Variable Importance scores, where a score of 1 indicates that a predictor variable occurs in all top models with  $\Delta AICc < 4$ . p-values represent probability that the coefficient is equal to 0. ....52

Figure 18. Model averaged coefficients (with 95% confidence intervals) indicating the most important variables predicting hyporheic flow using the temperature method. RVI = Relative Variable Importance scores, where a score of 1 indicates that a predictor variable occurs in all top models with  $\Delta AICc < 4$ . p-values represent probability that the coefficient is equal to 0. ....53

**LIST OF TABLES**

Table 1. Calcite study sites including watercourse, calcite character, and nomenclature used to reference sites within the report. ....6

Table 2. Physical parameters, units of measure and equipment used during FHAP. ....10

Table 3. Minimum size criteria for tertiary habitat unit types.....11

Table 4. Substrate classification scheme. ....13

Table 5. Study site locations and water quality sampling dates. ....14

Table 6. Water quality sampling parameters and meters. ....14

Table 7. Typical range of specific conductivity, pH and dissolved oxygen in BC watercourses.....16

Table 8. BC MOE Guidelines for the Protection of Aquatic Life for dissolved oxygen (mg/L)....16

Table 9. Summary of FHAP results at each calcite study site, June 18 to June 23, 2016. ....23

Table 10. Westslope Cutthroat Trout observations recorded during field trips for Calcite Study, 2016.....24

Table 11. Summary of CI and calcite depth at piezometer and mesohabitat sites, 2016. ....26

Table 12. Substrate size (mm) composition in the Fording River measured in the mesohabitat (meso) and piezometer (piez) sites in June and August/September 2016. ....29

Table 13. Substrate size (mm) composition in Clode Creek Settling Pond System measured at the mesohabitat (meso) and piezometer (piez) sites in June and August/September 2016. ....29

Table 14. Substrate size (mm) composition in Greenhills Creek (GRE-CA01, GRE-CA02 and GRE-CA03) measured at the mesohabitat (meso) and piezometer (piez) sites in June and August/September 2016.....30

Table 15. Groundwater exchange rate calculated with Darcy’s equation using GSD based K estimates.....42

Table 16. Modelled groundwater exchange rates using the K optimizer module in 1DTempPro. ....45

Table 17. Theoretical wetted length based on downwelling rates modelled with 1DTempPro, assuming all downwelling flows are lost.....47

Table 18. Summary of top models for each of three response variables representing hyporheic conditions.....50

**LIST OF MAPS**

Map 1. Calcite study sites and overview map.....7

Map 2. Clode Creek and Fording River Calcite Monitoring Sites, FHAP Type and Discharge Locations.....63

Map 3. Greenhills Creek Calcite Monitoring Sites, FHAP Type and Discharge Locations .....64

Map 4. Greenhills Creek, GH-CTF Calcite Monitoring Site and FHAP Type.....65

Map 5. Greenhills Creek GRE-CA06 Calcite Monitoring Site. FHAP Type and Discharge Location .....66

**LIST OF APPENDICES**

- Appendix A. Calcite Study Site Photographs.**
- Appendix B. Fish Habitat Assessment Procedure (FHAP) data and photographs.**
- Appendix C. Substrate grain distribution plots.**
- Appendix D. Summary of surface hydrology results.**
- Appendix E. Water quality and hydraulic head data tables and QA/QC.**
- Appendix F. Figures from fixed hydraulic conductivity 1DTempPro runs 2016.**
- Appendix G. Figures from optimized hydraulic conductivity 1DTempPro runs 2016.**

## 1. INTRODUCTION

Teck Coal Limited (Teck) currently operates steelmaking coal mines within the Elk River watershed in Southwestern British Columbia. Calcite formation has been observed in the tributaries downstream of Teck mining activities, at some locations in the Fording River and, to a lesser extent, in the Elk River and in reference streams unaffected by mining. Calcite is created by the reaction between dissolved calcium ( $\text{Ca}^{2+}$ ) and carbonate ( $\text{CO}_3^{2-}$ ) ions under conditions that can occur naturally, but can be enhanced when water passes through waste rock from mining. A number of seasonal factors can contribute to the precipitation or dissolution of calcite, including physical forces (e.g., scouring of the substrate during high flow turbid periods), water flow and water chemistry (water temperature, pH, composition of dissolved ions and minerals); therefore, timing and location of calcite formation can be challenging to predict (Minnow Environmental 2016).

In the Elk River watershed, there are wide ranges in the spatial extent of calcite cover, as well as seasonal fluctuations in calcite cover. For example, there are areas with minimal calcite formation and areas where calcite can completely cover portions of the stream bed, making the gravels largely immovable. There are concerns that high levels of calcite may have an effect on fish in the region. The upper Fording River and tributaries were the focus of this initial study for calcite effects because habitat use by fish is well known in this part of the watershed and fish values are high (Cope *et al.* 2016).

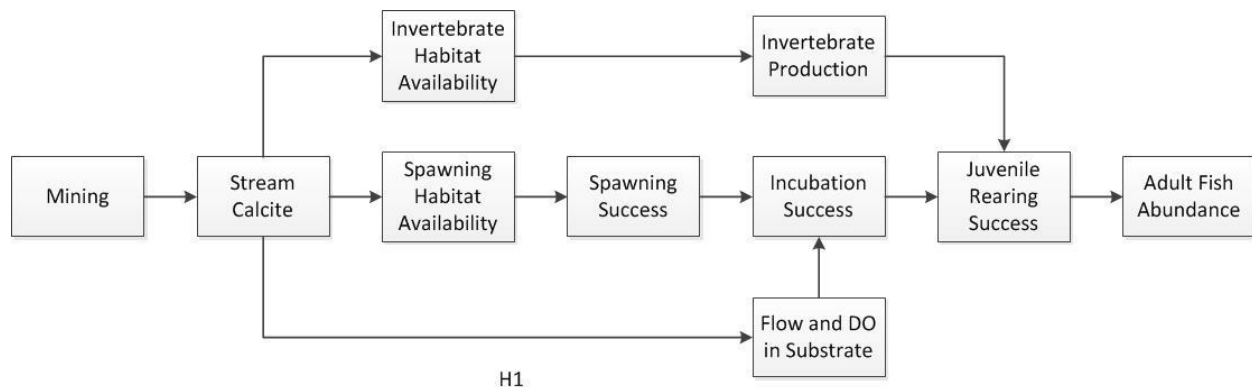
In the Elk Valley Water Quality Plan, Teck committed to continuing a program of monitoring and management for calcite with the objective of understanding and managing mine-related calcite formation such that streambed substrates in the Elk and Fording rivers and their tributaries can support abundant and diverse communities of aquatic plants, benthic invertebrates, and fish comparable to those in reference areas (Teck 2014). Instream calcite levels are measured using a calcite index (CI) that combines extent of calcite presence and level of concretion or immovability of the substrate. Teck's requirements for monitoring biological effects as part of its Regional Aquatic Effects Monitoring Program (RAEMP) include:

“Teck shall complete the assessment to determine the potential relationships between calcite and benthic invertebrate community structure, periphyton productivity and fish spawning and incubation success. Teck shall work in collaboration with the Ministry and Ktunaxa Nation representatives ideally in a monitoring committee forum to prepare study designs for work proposed in 2015 and 2016.”

High calcite levels are hypothesized to affect Westslope Cutthroat Trout (*Oncorhynchus clarkii lewisi*) and other fish species through several mechanisms including usability of spawning gravels, incubation conditions, rearing conditions for juveniles, and food (stream periphyton and invertebrate production; Figure 1). Other factors unrelated to calcite also influence spawning and incubation success, which complicates assessing effects of calcite on biological resources of interest. For example, water temperature is an important parameter for success of incubation and rearing, but is not expected to be affected by calcite.

The objective of this study is to investigate one mechanism in the effect pathway described in Figure 1, specifically the hypothesis that calcite accumulation on and within a streambed reduces hyporheic flow and dissolved oxygen (DO) concentrations at depth, thus affecting fish survival during incubation. In essence, the research question is, assuming fish spawn at a site, what effect does calcite have on incubation conditions? The question was addressed by examining physical conditions within the hyporheic zone in relation to calcite; the hyporheic zone is the saturated interstitial region beneath and alongside a streambed, where there is mixing of shallow groundwater and surface water. Water flowing in the stream channel flows into the subsurface materials of the streambed and then returns to the stream. Calcite accumulations are hypothesized to reduce flow at depth in the interstitial spaces between spawning gravel by interfering with exchange of water between the surface water and hyporheic water, resulting in poor gas/nutrient levels and diminished DO concentrations. The average redd depth for Westslope Cutthroat Trout is between 10 and 30 cm (DeVries 1997, Weaver and Fraley 1993).

**Figure 1. Effect pathway diagram linking calcite on the streambed to fish production.**



### 1.1. Impact Hypothesis

The link between calcite and hyporheic conditions was assessed by testing the following impact hypothesis (Figure 1), which is posed as a null hypothesis.

H1: Observed calcite conditions on stream substrates have no effect on hyporheic flow and DO.

To address this hypothesis, flow and oxygen levels were measured using a piezometer in the hyporheic zone of the upper Fording River and tributaries in late June and again in late August and early September 2016. Hyporheic flow was also estimated using thermistors buried in the streambed.

The impact hypothesis was tested by modelling hyporheic conditions (i.e., DO concentration at depth and hyporheic flow) as a function of CI and habitat characteristics of the study sites. Measured hyporheic DO concentrations were also compared to the BC guidelines for the protection of buried salmonid life stages for Westslope Cutthroat Trout.

This pilot study was designed to test the feasibility and effectiveness of field methods and to build upon existing studies characterizing the extent of calcite presence and formation in the Project area (Minnow Environmental 2014, Robinson *et al.* 2016, Minnow Environmental 2016).

## 2. STUDY SITES

### 2.1. Study Area

The study was conducted in the upper Fording River watershed above Josephine Falls (Map 1). The Fording River is a tributary to the Elk River and is located within the Regional District of East Kootenay, in south-eastern British Columbia (BC). The Fording River drainage basin is located on the western slope of the Rocky Mountains and encompasses an area of approximately 621 km<sup>2</sup> with a mean annual discharge at the mouth of 7.93 m<sup>3</sup>/s (Water Survey Canada Station 08NK018). The river flows 78 km in a southerly direction from its headwaters immediately west of the British Columbia – Alberta boundary and the continental divide to its confluence with the Elk River near Elkford, BC.

Josephine Falls is a natural barrier to fish migration and Westslope Cutthroat Trout is the only fish species occurring upstream of the falls. The Westslope Cutthroat Trout population above Josephine Falls is considered a fluvial headwater population restricted to the approximately 57.5 km portion of the upper Fording River (plus tributaries) between Josephine Falls at 20.5 river kilometre (rkm) and the upstream limit of fish distribution in the headwaters between 73.0 and 78.0 rkm.

### 2.2. Site Selection

Study sites were selected within the upper Fording River to represent both mainstem and tributary spawning habitat used by Westslope Cutthroat Trout in the upper Fording River (Cope *et al.* 2016, Minnow Environmental 2016, Beswick 2007) and to represent the full range of calcite conditions based on previous calcite monitoring (Minnow Environmental 2016, Robinson *et al.* 2016) (Map 1, Table 1). Spawning was visually confirmed (i.e., redds, spawning fish) at the sites selected in the upper Fording River, Clode Creek Settling Pond System, and lower Greenhills Creek (i.e., lowermost 400 m below the hanging culvert barrier at the Fording highway crossing (Cope *et al.* 2016).

Sites within upper Greenhills Creek (i.e., 5.8 km of stream channel above the Fording River highway crossing) were added to represent high calcite conditions (i.e., CI greater than 2.0, Robinson *et al.* 2016). This was done to ensure hyporheic investigations encompassed the widest range of site conditions possible. The calcite index can range between 0.00 and 3.00 and calcite conditions previously reported for the selected sites (or adjacent areas) ranged from 0.00 to 2.90 (Minnow Environmental 2016, Robinson *et al.* 2016). Beswick (2007) identified fish presence within the upper reaches of Greenhills Creek; however, spawning has not been confirmed nor was it expected at these high calcite locations. Minnow Environmental (2016) reported calcite indices were less than 1.00 at all but one redd location in the spring (i.e., conditions during redd site selection by Westslope Cutthroat Trout). This observation is consistent with preference for areas with relatively low calcite

conditions. It was hypothesized that this was a result of spawning trout preferentially selecting areas with moveable gravels, and thus avoiding areas where calcite concretion makes substrates immovable (Minnow Environmental 2016).

### 2.3. Description of Selected Sites

#### 2.3.1. Mainstem Upper Fording River

The selected mainstem sites are located within Fording River Operations and have relatively high densities of spawning, juvenile rearing and adult rearing Westslope Cutthroat Trout (Cope *et al.* 2016, Lister and Kerr Wood Leidal 1980). The three selected sites represent documented mainstem spawning habitat (Cope *et al.* 2016, Lister and Kerr Wood Leidal 1980) with low CI (< 1.00, Minnow Environmental 2016).

Conditions within and nearby the mainstem upper Fording River sites have been described as ranging from 9.9 m to 25.0 m wetted width, <1% stream gradient, gravel-cobble dominant-subdominant bed material, and mean water depths of ~ 50 cm. Actively spawning Westslope Cutthroat Trout and redds have been documented in the immediate area (Cope *et al.* 2016).

#### 2.3.2. Clode Creek Settling Pond System

The selected Clode Creek Settling Pond System study sites are located within Fording River Operations and represent documented tributary spawning habitat adjacent to the mainstem upper Fording River sites (Cope *et al.* 2016, Oliver 1999, Wright *et al.* 2001). The lower reach of Clode Creek Settling Pond System was diverted into a constructed settling pond and outflow channel. A constructed fish passage barrier at the outlet of the settling pond restricts Westslope Cutthroat Trout access to all but the lowermost 0.2 km of the Clode Creek Settling Pond System constructed works. The habitat below the culvert barrier is fed primarily by settling pond outflows (Windward *et al.* 2014). Two study sites were selected within this lowermost 0.2 km reach, where low to moderate CI values have been observed (0.76 – 1.33; Minnow Environmental 2016) and relatively high densities of spawning fish have been documented (Cope *et al.* 2016, Oliver 1999).

Conditions within the lowermost 0.2 km reach of the Clode Creek Settling Pond System have been described as a constructed channel with approximately 3.0 m wetted width, <1% stream gradient, gravel-cobble dominant-subdominant bed material with instream vegetation, and mean water depths of ~15 cm (Cope *et al.* 2016). The lower site in the present study is a small side-channel within the active (i.e., bankfull) channel of the upper Fording River and has a 3.0 m mean wetted width, low gradient (< 0.5%), gravel-fines dominant-subdominant bed material, and mean water depths of ~15 cm. Actively spawning Westslope Cutthroat Trout and redds have been documented at both sites and fine particulates have been identified as a concern for incubation success and fry rearing within the substrate interstitial environment (Cope *et al.* 2016).

#### 2.3.3. Greenhills Creek

Greenhills Creek is located entirely within Greenhills Operations (GHO) mine property. Greenhills Creek can be divided into three stream segments with two Westslope Cutthroat Trout components;

1) the lowermost reach with fish connectivity to the mainstem upper Fording River, 2) Greenhills settling pond which is isolated from the Fording River by a fish barrier, and 3) the upper reaches connected to the settling pond. Five study sites were selected in the reach below the settling pond and two sites were selected above the settling pond. The uppermost reach of the headwaters has been covered by waste rock from East Spoil (Beswick 2007). The calcite indices generally increase from low to high as one moves up Greenhills Creek to the headwaters (Minnow Environmental 2016, Robinson *et al.* 2016).

#### 2.3.3.1. Lower Section Greenhills Creek

The lower section (below the Fording Road highway) is restricted to the lowermost 0.5 km downstream of a hanging culvert on the Ministry of Highways Fording Road. This culvert, a second hanging culvert immediately upstream, and the dam spillway on the GHO settling pond are complete barriers to upstream movements by upper Fording River Westslope Cutthroat Trout (Cope *et al.* 2016, Beswick 2007). Similar to Clode Creek Settling Pond System, lower Greenhills Creek spawning habitat receives settling pond outflows with water quality concerns related to elevated concentrations of mine related constituents (Windward *et al.* 2014). Lower Greenhills Creek has low to moderate CI sites (0.10 to 1.60) and generally increases with distance upstream (Minnow Environmental 2016). The lower section is used by Westslope Cutthroat Trout for spawning and, to a lesser extent, fry and juvenile rearing (Cope *et al.* 2016, Beswick 2007). Documentation of spawning and rearing use dates back to 1979 before development of GHO (BC Research 1981).

Conditions at study sites within the lower Greenhills Creek section have been generally described as 2.2 m wetted width, <1% stream gradient, gravel-fines dominant-subdominant bed material and mean water depths of ~15 cm. Fine particulates were identified as a concern for incubation success and fry rearing within the substrate interstitial environment (Cope *et al.* 2016). Actively spawning Westslope Cutthroat Trout and redds have been documented in the immediate area (Cope *et al.* 2016).

#### 2.3.3.2. Upper Section Greenhills Creek

The upper section of Greenhills Creek extends upstream approximately 100 m from the hanging culvert on Fording Road to a second hanging culvert, then 50 m further upstream to the dam spillway of the GHO settling pond. Site GH-GH1 represents this isolated section of stream channel. From its confluence with the settling pond, Greenhills Creek continues upstream for 5.8 km, with an additional 3.0 km of its headwaters covered by waste rock from East Spoil (Beswick 2007). Above the settling pond, Beswick (2007) identified three reaches. Reaches 1 and 2 represent 4.9 km of fish-bearing stream channel. Reach 3 represents the uppermost 0.9 km and was classified as non-fish bearing (Beswick 2007). Although spawning habitat has not been specifically identified, adult, juvenile and fry have been captured throughout these reaches (Beswick 2007). Upper Greenhills Creek represents sites with high CI (2.5 – 2.9, Robinson *et al.* 2016), but has no actively used spawning habitat (Minnow Environmental 2016, Cope *et al.* 2016).

Conditions at study sites within the upper Greenhills Creek sections have been described as ranging from 1.4 m to 3.0 m wetted width, 4% stream gradient, cobble-boulder dominant-subdominant bed material, and mean water depths in the 18 to 23 cm range (Beswick 2007). Adult, juveniles and fry have been captured throughout reaches 1 and 2, but specific spawning locations have not been confirmed (Beswick 2007).

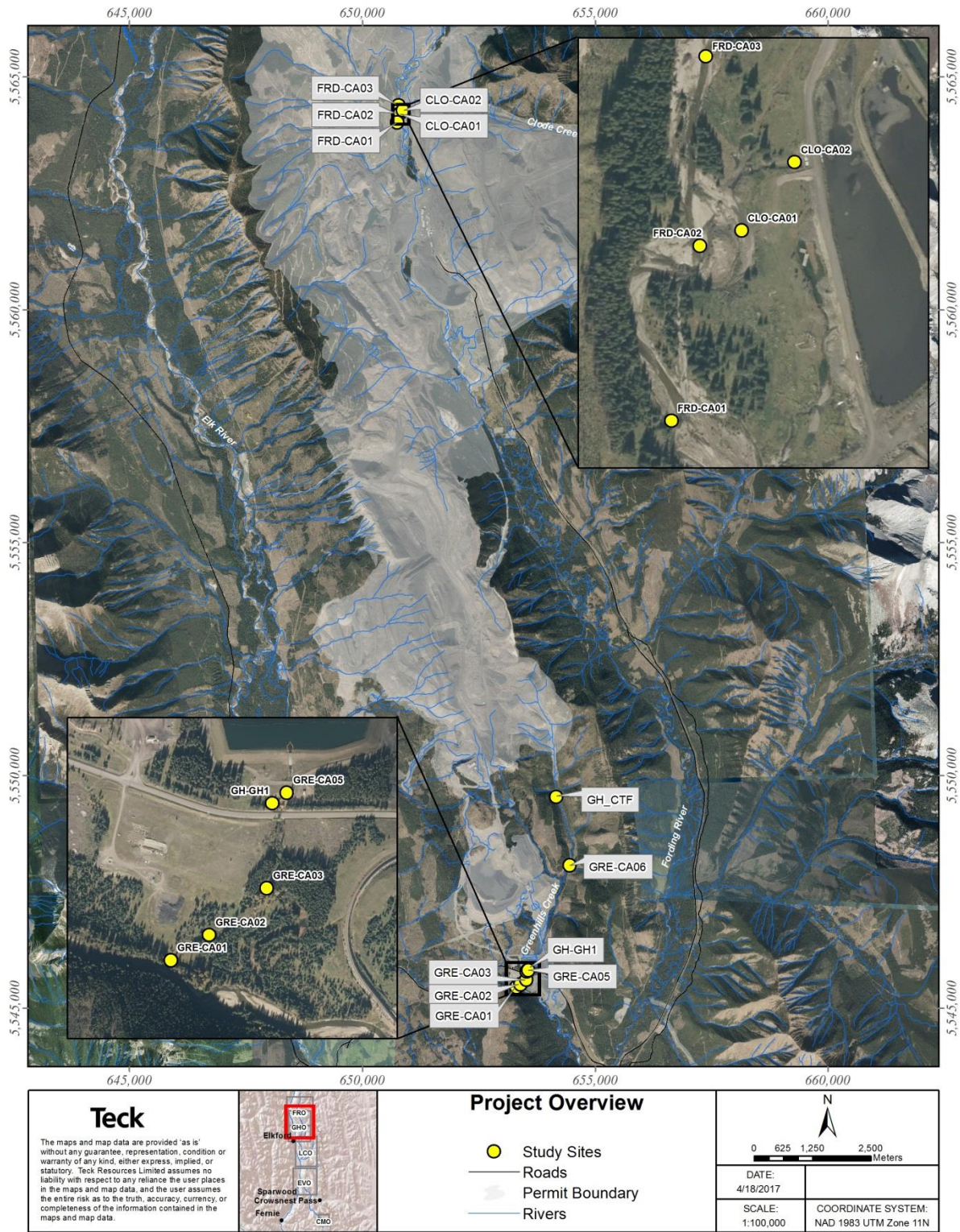
**Table 1. Calcite study sites including watercourse, calcite character, and nomenclature used to reference sites within the report.**

Watercourse	Character	C.I. Range <sup>1</sup>	Site	UTM Coordinates (Zone 11U)		Elevation (masl) <sup>2</sup>
				Easting	Northing	
Fording River	low level of calcite presence	0.29	FRD-CA01	650747	5564030	1674
			FRD-CA02	650775	5564202	1674
			FRD-CA03	650781	5564388	1674
Clode Creek Settling Pond System	low to moderate level of calcite	0.76 - 1.33	CLO-CA01	650816	5564217	1675
			CLO-CA02	650868	5564284	1675
Greenhills Creek (lower)	low to moderate level of calcite presence	0.1 - 1.60	GRE-CA01	653314	5545461	1491
			GRE-CA02	653396	5545515	1492
			GRE-CA03	653520	5545616	1495
Greenhills Creek (upper)	high level of calcite presence	2.5 - 2.9	GH_GH1	653537	5545800	1503
			GRE-CA05	653563	5545821	1502
			GRE-CA06	654451	5548079	1651
			GH_CTF	654165	5549540	1742

<sup>1</sup> Previously reported in Minnow Environmental (2016) and Robinson *et al.* (2016).

<sup>2</sup> Elevation was determined from Google Earth.

Map 1. Calcite study sites and overview map.



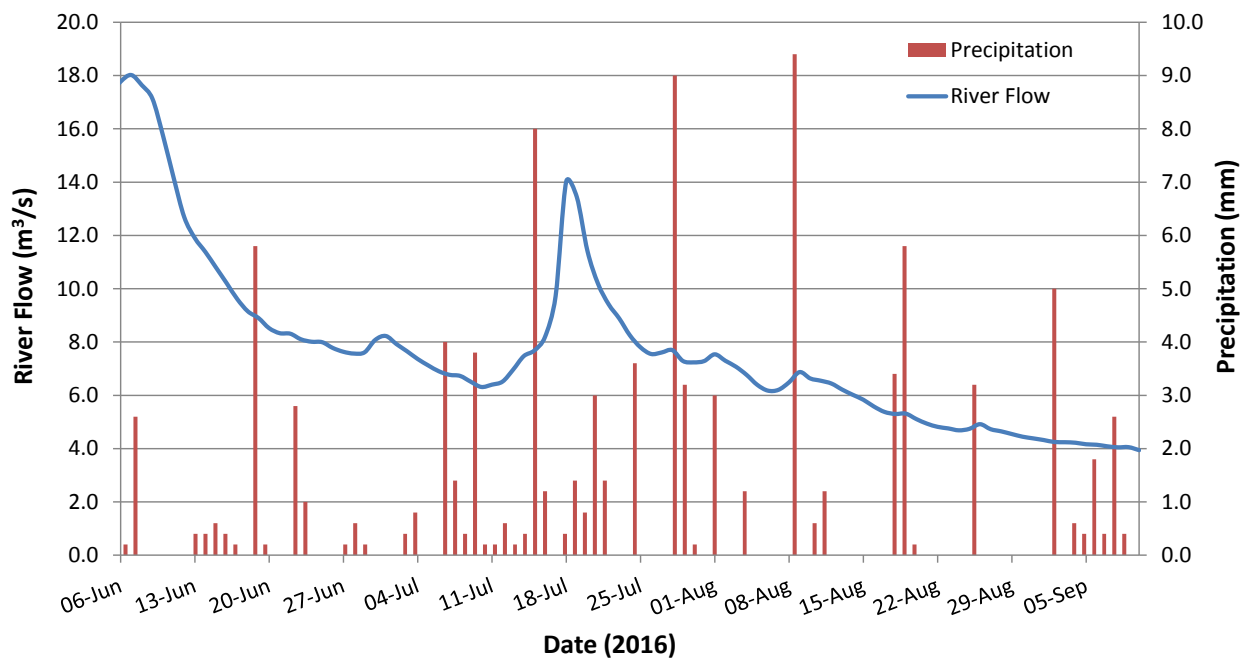
2.4. Antecedent Streamflow and Precipitation

Hyporheic conditions are likely to be influenced by precipitation and streamflow prior to and during periods of observation. Flow data collected at the mouth of the Fording River (Water Survey of Canada Station, WSC, 08NK018) and precipitation data collected at Environment Canada’s (EC) Sparwood climate station (1152899) provide a continuous data record with which to characterize conditions prior to the study periods. Discharge measurements were collected at each target stream to determine the flow on the day at which hyporheic conditions were measured (see Section 3.1.4 and 4.1.3).

The Fording River data show a decline in flows from a peak of 18.28 m<sup>3</sup>/s on June 7 to approximately half that value at the start of the June study period (June 17-26); flows continued to decline throughout the study period (Figure 2); an average 0.027 m<sup>3</sup>/s decline in flow was observed for all streams during the June field study. Precipitation prior to and during the June study period was low; only 8 mm of rain fell in the two weeks prior to the study and 4.8 mm during the study.

Flows at the mouth of the Fording River also showed a steady decline during the August 29 to September 6 study period (Figure 2); an average 0.013 m<sup>3</sup>/s decline in flow was observed for all streams. Prior to the study, flows had been declining since a 14.57 m<sup>3</sup>/s peak flow event on July 18, with modest responses to precipitation inputs (Figure 2). Antecedent precipitation prior to the August/September study period was low; 12.6 mm of rain fell in the week prior to the study and 7.8 mm during the study.

**Figure 2. Daily average flow data collected at the WSC 08NK018 hydrometric station and precipitation at EC’s Sparwood climate station prior to and during the June 17-26 and August 29-September 6, 2016 measurement periods.**



### 3. METHODS

#### 3.1. Fish Habitat, Calcite, and Hyporheic Conditions

This section describes the methods used to measure the stream habitat variables at each site, including calcite cover, substrate composition and hyporheic conditions (DO and flow) hypothesized to influence salmonid incubation success. The selected study sites occur across a gradient of pre-existing calcite levels and other naturally varying potential covariates such as substrate size and channel morphology (Table 1, Table 2). Measurements were taken in areas representative of spawning habitat during the spawning season in late June and again during the late summer growing period in late August and early September 2016. Exact study dates were June 17-26 and August 29-September 6, 2016. The same field crew was used throughout to ensure consistency in field techniques and methods. All sites and measurements were photo documented; a sample of these photos is presented in Appendix A.

Hyporheic conditions were measured at each of the sampling sites: DO (see Section 3.1.3); hyporheic flow measured using hydraulic head (see Section 3.1.5.1) and hyporheic flow measured using temperature (see Section 3.1.5.2). Hyporheic DO and hydraulic head were measured with piezometers.

Within each mesohabitat, piezometers were installed at three sites that span the cross section of the river (e.g., river right, mid-channel, and river left). The piezometers were spaced across the stream at approximately  $\frac{1}{4}$ ,  $\frac{1}{2}$ , and  $\frac{3}{4}$  of the wetted width. Piezometers were custom made to be robust, reusable, and ensure tight contact between the bed material and the piezometer. The body of the piezometer was made of 1" S40 stainless steel with an inner diameter of 26 mm. A stainless steel drive point tip was welded to the bottom of the body and a manual slide hammer was permanently attached to aid installation. The piezometer screen was comprised of 10  $\sim$ 7 mm diameter perforations drilled into the lower 0.14 m of the body. A wood dowel was inserted into the piezometer during installation to prevent suspended sediment and small substrate from entering the screen.

The piezometers were driven vertically into the streambed substrate to the desired depth and left to equilibrate to ensure that water level had stabilized (see Section 3.1.5.1 for further details on equilibrium times). The water quality probes and water level tape were lowered into the standpipe piezometer to take measurements. Once the measurements were recorded, the probes/tape were removed and the piezometer was driven deeper or moved to another location and allowed to equilibrate prior to completing another set of measurements.

##### 3.1.1. Fish Habitat Assessment and Fish Observations

A modified Level 1 Fish Habitat Assessment Procedure (FHAP), as described by Johnston and Slaney (1996), was used to quantify fish habitat at a mesohabitat scale at each study site. The habitat unit immediately upstream, immediately downstream, and the study unit itself were assessed using the modified FHAP; exceptions occurred where upstream or downstream units did not occur due to

proximity of the study unit to a barrier (e.g., culvert) or the Fording mainstem. Habitat unit types were classified according to definitions in Johnston and Slaney (1996). Table 2 lists the physical parameters surveyed along with the units of measurement and the equipment used. Parameters were measured rather than estimated wherever possible. Estimates were made for pool depths greater than 1.5 m, dominant and subdominant bed materials, and percent cover.

Habitat units were classified as pools, glides, runs, riffles and cascades. Johnston and Slaney (1996) recommend using only pools, glide, riffle, cascade and “other”; however, we added “run” to better define the habitat units. Units were additionally classified by location within the stream as primary, secondary, and tertiary. Primary habitat units occupy more than 50% of the wetted width of the main channel. Secondary units occupy secondary channels, and tertiary units are embedded within primary units but meet the minimum size criteria (Table 3).

Total wetted areas and bankfull areas were determined by summing the wetted areas and bankfull areas of individual habitat units within a given reach. For each habitat unit type, the average wetted and bankfull areas, widths, depths, and gradients were determined by averaging data from individual units within a given reach. Photographs of each habitat unit were taken.

Substrate was classified according to a modified Wentworth scale into the following categories: fines (<2 mm), gravel (2 to 64 mm), cobble (64 to 256 mm), boulder (256 to 4,000 mm) and bedrock (>4,000 mm) (Lewis *et al.* 2004). The dominant and subdominant substrate type within each habitat unit was estimated based on coverage area. Dominant and subdominant substrate types within a reach were then determined from the percentage of habitat units in which a particular substrate type was either dominant or subdominant (further described in Section 3.1.2).

Observations of fish, redds, and egg presence were recorded during field work, and estimated fish length in mm was documented.

**Table 2. Physical parameters, units of measure and equipment used during FHAP.**

Parameter	Unit	Measured or Estimated	Equipment Used
Bankfull Width	m	Measured	Rangefinder
Bed Material Type	n/a	Visual Estimate	Visual
Cover Proportions	n/a	Visual Estimate	Visual
Cover Types	n/a	Visual Estimate	Visual
Gradient	%	Measured	Clinometer
Habitat Unit Length	m	Measured	Rangefinder
Maximum Pool Depth	m	Measured	Meter Stick
Wetted Depth	m	Measured	Meter Stick
Wetted Width	m	Measured	Rangefinder

**Table 3. Minimum size criteria for tertiary habitat unit types.**

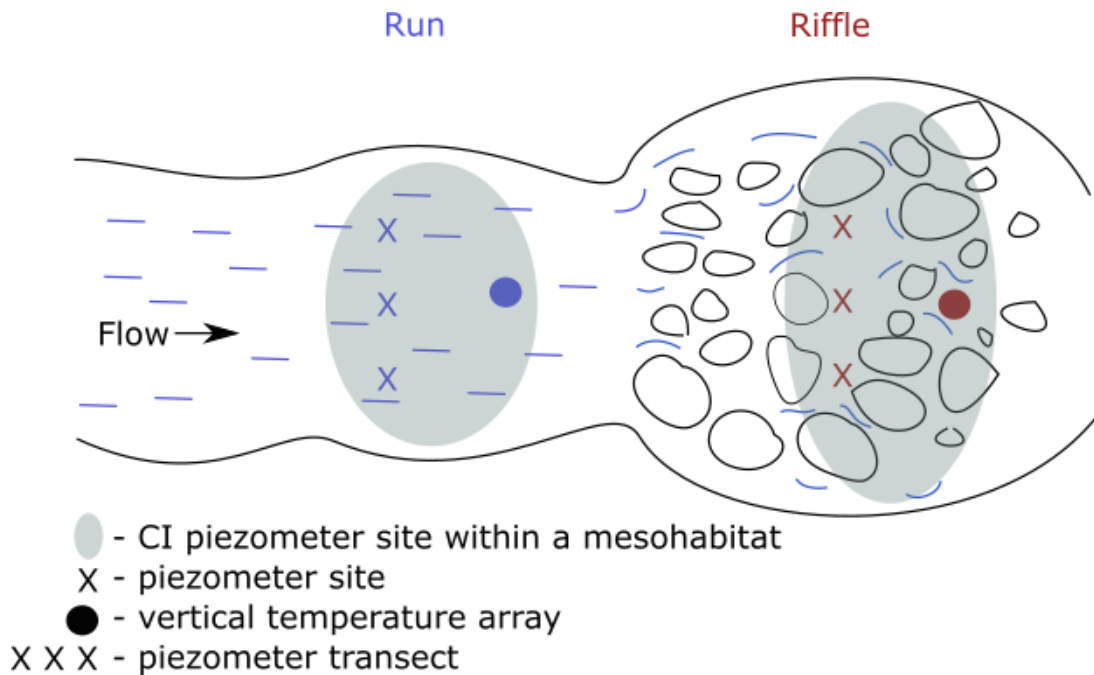
Bankfull Channel Width (m)	Minimum Area (m <sup>2</sup> )	Minimum Residual Depth (m)
0 - 2.5	1.0	0.20
2.5 - 5	2.0	0.40
5 - 10	4.0	0.50
10 - 15	6.0	0.60
15 - 20	8.0	0.70
> 20	10.0	0.80

### 3.1.2. Calcite Index Measures and Substrate Composition

CI was measured at the mesohabitat unit scale and again at a smaller spatial scale within the mesohabitat corresponding to the primary location of hyporheic conditions data collected for this study. CI was measured based on the practices and procedures used by Teck in their Calcite Monitoring Program (Robinson and MacDonald 2014, Minnow Environmental 2016, Robinson *et al.* 2016). Prior to field work, the crew received training in determining calcite presence/absence and CI procedures from Kevin Atherton, Teck's Superintendent of Calcite Management. The procedures employed in this study are described below.

To maintain consistency with the Teck Calcite Monitoring program, calcite data were collected at a mesohabitat scale. At each mesohabitat site, the observer systematically moved over the site, stopping every one, two or three steps to randomly select a pebble  $\geq 2$  mm in diameter (i.e., gravel or larger) along a stream section of variable length (20 to 100 m). If the substrate selected was  $< 2$  mm in diameter, this was noted and another pebble was chosen to ensure a total count of 100 pebbles. Within each mesohabitat unit, three piezometers were installed along a transect to collect hyporheic water quality data (dissolved oxygen, water temperature, pH and specific conductivity) and flow data (Figure 3; see Section 3.1.3 and 3.1.4). The area immediately surrounding the piezometers, referred to hereafter as the CI piezometer site, was sampled for calcite to obtain information at a spatial scale reflecting individual piezometer sites and a scale more representative of individual Westslope Cutthroat Trout redds than the entire mesohabitat unit. This information was also used to describe within-mesohabitat variability in calcite and substrate conditions. The area of a CI piezometer site varied depending on site conditions, but was on average  $\sim 8.5$  m<sup>2</sup> at Greenhills Creek, 13.5 m<sup>2</sup> at Clode Creek Settling Pond System, and 25.5 m<sup>2</sup> at Fording River sites. The average area is based on the channel width measured at the piezometer transects and the  $\sim 3$  m length of the river that was sampled for CI.

**Figure 3.** A CI piezometer site consisted of three piezometer sites located in a transect within a mesohabitat (e.g., run or riffle).



A total of 100 pebbles were sampled for each CI measurement and the following information was recorded for each pebble:

- The concretion score: if the pebble was removed with negligible resistance (not concreted, score = 0), notable resistance but removable (partially concreted, score = 1), or immovable (fully concreted, score = 2);
- Absence or presence of calcite (score = 0 or 1 respectively); and
- The b-axis length of the pebble, to the nearest mm. Pebbles less than 5 mm (b-axis) were recorded as fines for the purpose of CI calculations.

Additional substrate classification was recorded for fines and sand (<2 mm) (Table 4) and the FHAP unit type (R = riffle, C = cascade, P = pool, G = glide) was also recorded and mapped.

To sample the CI piezometer sites, an additional 100 pebbles were evaluated. This approach was designed to be consistent with the approach used in Minnow (2016). The data recorded from pebbles that were located in both the mesohabitat and the piezometer site were used for both CI calculations. For example, if 40 pebbles overlapped the two sites an additional 60 pebbles were evaluated in the piezometer site and an additional 60 in the mesohabitat. In most cases both the piezometer and the larger mesohabitat were sampled at each site; however, in a few cases the mesohabitat site was not large enough (CLO-CA02, GRE-CA05) and/or the substrate was too fine (GRE-CA02), or largely composed of bedrock and mostly concreted (GRE-CA06 and GH\_CTF),

to warrant including an additional 100 pebbles at the piezometer site. In these cases, a “combined” mesohabitat/piezometer site was surveyed with a minimum of 50 pebbles (or larger substrate) sampled at the piezometer site. This overlap occurred at sites where the stream substrate was relatively homogenous.

The results for each area were then expressed as a CI score using the following equation:

$$CI = CP + CC$$

where,

*CI = Calcite Index*

$$CP = \text{Calcite Presence Score} = \frac{\text{Number of pebbles with calcite}}{\text{Number of pebbles counted}}$$

$$CC = \text{Calcite Concretion Score} = \frac{\text{Sum of pebble concretion scores}}{\text{Number of pebbles counted}}$$

**Table 4. Substrate classification scheme.**

Substrate Type	Substrate Category	Size Range (mm)
Fines and Sand	Clay	<0.0039
	Silt	0.0039-0.0625
	Sand	0.0625-2
Gravel	Small Gravels	2-16
	Large Gravels	16-64
Cobble	Small Cobble	64-128
	Large Cobble	128-256
Boulders	-	256-4000
Bedrock	-	>4000

Calcite presence at depth and vertical substrate characteristics were measured at each site to a depth of approximately 35 cm during the June 17 to 26, 2016 sampling period and to a depth of approximately 50 cm during the August 30 to September 2, 2016 period. Sediment samples were taken at four depth intervals (approximately 0-7 cm, 10-15 cm, 30-35 cm and 38-50 cm). For each depth interval, the percent composition of different substrate class sizes and the vertical extent (depth) of calcite presence was recorded. In some cases the sampling depth that could be achieved was limited due to the presence of bedrock.

Substrate measurements were grouped according to the Wentworth Scale (Table 4). The distribution of substrate size or grain size distribution (GSD) was reported as: (a) a cumulative percentage of grain size (mm) and (b) the number of grains in increasing size categories (mm). Particles <2 mm were assigned a value of 1 mm for the sake of plotting and representative grain size calculation.

### 3.1.3. Hyporheic Dissolved Oxygen Concentration

DO and water temperature were measured during the first study period (June 2016) at approximately 0, 10 cm and 30 cm depths at each piezometer site. In the late summer sampling period, DO, water temperature, pH and conductivity were measured at approximately 0, 10 cm, 30 cm and 50 cm depths (Table 5, Table 6).

The actual depth recorded in the field varied slightly from those listed above due to sediment infiltration within the piezometer or inability to install the piezometer deeper due to bedrock and/or high calcite concretion.

**Table 5. Study site locations and water quality sampling dates.**

Watercourse	Site	Sampling Dates
Fording River	FRD-CA01	25-Jun-2016, 5-Sep-2016
	FRD-CA02	25-Jun-2016, 5-Sep-2016
	FRD-CA03	22-Jun-2016, 6-Sep-2016
Clode Creek Settling Pond System	CLO-CA01	25-Jun-2016, 4-Sep-2016
	CLO-CA02	23-Jun-2016, 4-Sep-2016
Greenhills Creek	GRE-CA01	19-Jun-2016, 30-Aug-2016
	GRE-CA02	19-Jun-2016, 3-Sep-2016
	GRE-CA03	21-Jun-2016, 3-Sep-2016
	GH_GH1	20-Jun-2016, 2-Sep-2016
	GRE-CA05	20-Jun-2016, 2-Sep-2016
	GRE-CA06	26-Jun-2016, 1-Sep-2016
	GH_CTF	26-Jun-2016, 1-Sep-2016

**Table 6. Water quality sampling parameters and meters.**

Parameter	Units	Meter
pH	pH units	YSI Pro Plus
Specific Conductivity	µS/cm	YSI Pro Plus
Water Temperature	°C	YSI ProODO (Optical Dissolved Oxygen), YSI Pro Plus
Air Temperature	°C	Alcohol thermometer
Dissolved Oxygen	mg/L	YSI ProODO (Optical Dissolved Oxygen)
Dissolved Oxygen	% saturation	YSI ProODO (Optical Dissolved Oxygen)

### 3.1.3.1. QA/QC and Data Analysis

*In-situ* meters were maintained and calibrated and water quality sampling procedures followed the guidelines of the British Columbia Field Sampling Manual (Clark 2003) and the Ambient Fresh Water and Effluent Sampling Manual (RISC 2003).

All field data were entered into Ecofish's proprietary data management platform, EcoDAT. This data management platform has built-in rigorous QA/QC protocols. Hardcopy data from field forms were transcribed into EcoDAT and entries were visually compared by a second person to check for data entry errors.

The data were screened to remove suspect data by first evaluating the hydraulic head data to ensure that the piezometer was equilibrated with the hyporheic flow. Suspect data corresponding to field constraints including excessive infiltration of fines in the piezometer were also removed. High variability (low precision) between piezometer data within the site was evaluated based on the RISC guidelines for relative standard error (RSE) (RISC 1998); specifically, data should be viewed with caution if the RSE for triplicates is >18%.

Water quality summary statistics (average, minimum, maximum and standard deviation) were calculated for each sampling site and each sampling depth based on the results recorded at the three piezometer sites (n=3). Actual depths were noted for those cases where the measurement depth varied within the three sites.

Summary statistics for dissolved oxygen (% saturation and mg/L), water temperature (°C), pH and specific conductivity (µS/cm) were generated for each site at each measured depth. In most cases, the average was calculated from three single measurements (n=3) taken at piezometer sites within a mesohabitat unit (i.e., at river right, mid-channel and at river left).

DO may decrease with depth assuming reduced gas exchange with the surface water or infiltration of groundwater, which is typically lower in DO in comparison to surface water (MOE 1997b). Where an unusual trend was observed or if the trends between sites were markedly different, the data were depicted graphically to facilitate interpretation.

Data were compared to typical ranges in BC watercourses (Table 7) and the applicable BC MOE water quality guidelines for DO (Table 8). The minimum acceptable water quality guidelines instantaneous concentration of DO (mg/L) for the protection of buried life stages is 6 mg/L. Water temperature data were also compared to the provincial optimum water temperature ranges for Cutthroat Trout incubation (9.9-12.0 °C; Oliver and Fidler 2001).

**Table 7. Typical range of specific conductivity, pH and dissolved oxygen in BC watercourses.**

Parameter	Unit	Typical Range in BC	Reference
Specific Conductivity	µS/cm	The typical value in coastal British Columbia streams is 100 µS/cm, while interior streams range up to 500	RISC (1998)
pH	pH units	Natural fresh waters have a pH range from 4 to 10, and lakes tend to have a pH ≥ 7.0.	RISC (1998)
Dissolved Oxygen	mg/L	In BC surface waters are generally well aerated and have DO concentrations greater than 10 mg/L	MOE (1997a)
Dissolved Oxygen	% saturation	In BC surface waters are generally well aerated and have DO concentrations close to equilibrium with the atmosphere (i.e., close to 100% saturation)	MOE (1997a)

**Table 8. BC MOE Guidelines for the Protection of Aquatic Life for dissolved oxygen (mg/L).**

BC Guidelines for the Protection of Aquatic Life <sup>1</sup>			
	Life Stages Other Than Buried Embryo/Alevin	Buried Embryo/Alevin <sup>2</sup>	Buried Embryo/Alevin <sup>2</sup>
Dissolved Oxygen Concentration	Water column mg/L O <sub>2</sub>	Water column mg/L O <sub>2</sub>	Interstitial Water mg/L O <sub>2</sub>
Instantaneous minimum <sup>3</sup>	5	9	6
30-day mean <sup>4</sup>	8	11	8

<sup>1</sup> MOE (1997a) and MOE (1997b)

<sup>2</sup> For the buried embryo / alevin life stages these are in-stream concentrations from spawning to the point of yolk sac absorption or 30 days post-hatch for fish; the water column concentrations recommended to achieve interstitial dissolved oxygen values when the latter are unavailable. Interstitial oxygen measurements would supersede water column measurements in comparing to criteria.

<sup>3</sup> The instantaneous minimum level is to be maintained at all times.

<sup>4</sup> The mean is based on at least five approximately evenly spaced samples. If a diurnal cycle exists in the water body, measurements should be taken when oxygen levels are lowest (usually early morning).

### 3.1.4. Surface Hydrology

A number of physical factors in addition to calcite are likely to influence hyporheic conditions, and measurements were taken to allow assessment of these as covariates during analysis. Water depth and water velocity were measured at each piezometer site on the day at which hyporheic conditions were measured. Water depth was measured as surface level to streambed using a meter stick. Water

velocity was measured at the piezometer as the average water column velocity using a Swoffer meter, following RISC (2009) standards.

Discharge measurements were collected to determine the flow on the day at which hyporheic conditions were measured. Due to the large distance between some of the Greenhills study sites, Greenhills Creek was divided into upper and lower reaches, and separate flow measurements were collected at each. The flow at each transect was assumed to be representative of all sites within each target stream or reach.

Discharge measurements were collected twice in June and twice in August/September (once at the start of the study and again at the end) at Fording River, Clode Creek Settling Pond System, and upper and lower Greenhills Creek. For the majority of flow measurements, velocities at a transect were measured with a standard USGS magnetic head current meter (Price AA or Pygmy) and water depths were taken with a 1.4 m top-set wading rod. The midsection method (a velocity-area method; RISC 2009, Rantz *et al.* 1982) was used to estimate discharge at each transect. The transect locations were recorded so that flow measurements were taken at the same sites in June and in August/September.

### 3.1.5. Hyporheic Flow

#### 3.1.5.1. Hydraulic Head Method

Hyporheic flow was measured using the hydraulic head method at each piezometer site. The vertical head gradient (VHG) was calculated as the water level inside the piezometer minus water level outside the piezometer (recorded in m below the top of the piezometer), divided by the distance between the streambed and the midpoint of the piezometer perforations or screen. The VHG was used to estimate the extent of upwelling from or downwelling to the streambed at a site. Positive vertical hydraulic head indicates downwelling flow, whereas negative vertical hydraulic head indicates upwelling flow. Flow direction was defined in this way to be consistent with the USGS software (1DTempPro) used for the temperature modelling.

Hydraulic head was measured during the first study period (June 2016) at two different depths within the streambed, approximately 10 cm and 30 cm, as these depths bracket the likely redd depths for Westslope Cutthroat Trout. An additional hydraulic head measurement was made at ~50 cm depth (where possible) in August/September to confirm groundwater flow direction observed at the 10 and 30 cm depths. To measure hydraulic head, a piezometer was driven vertically into the streambed substrate to a depth of 10 cm and left to equilibrate for a minimum of 20 minutes. The equilibration time was determined by undertaking measurements every 5 minutes for 60 minutes (more time was not required) at three sites, taking care to test equilibrium times at sites with different substrate conditions. Trends in water level, DO, and temperature were assessed over this duration and were used to ensure that sufficient equilibration time was allowed before each measurement during the study. Water surface elevations were measured from the top of the piezometer using an electronic interface measuring tape (Solinst; 1 mm accuracy). Water level measurements were repeated a minimum of three times at each piezometer depth and each

piezometer site (e.g., river right, mid-channel and river left) to ensure sufficient equilibrium time (i.e., water levels inside and outside of the piezometers remained consistent and stable for a minimum of 20 minutes) and to account for water fluctuations due to turbulence in the stream (up to 6 cm), and/or human error in reading the measuring tape. The standpipe piezometer was then driven further into the streambed substrate to a depth of 30 cm and hydraulic head measurements were repeated. An additional hydraulic head measurement was made at ~50 cm depth (where possible) in August/September. This procedure was repeated at subsequent sites (e.g., river right, mid-channel and river left), spaced evenly across the stream.

The downwelling or upwelling rate from each site and date was calculated using VHG and Darcy's equation (Kalbus *et al.* 2006). Hydraulic conductivity (K) of each site was estimated based on grain size distributions and modelled using 1DTempPro (Koch *et al.* 2015). Hydraulic conductivity represents the ease with which a fluid can move through substrate, and is highly correlated to porosity. The modelled K values were also applied to each VHG measurement to assess the variation of groundwater exchange at different depths, and laterally across each transect.

#### 3.1.5.2. Temperature Method

Hyporheic flow was also estimated at seven study sites using the temperature method. The propagation of diurnal heat fluxes from a streambed into a stream can be used to estimate groundwater recharge and discharge from the stream to the streambed. Groundwater exchange rates were modelled using stream temperature profiles and one-dimensional flow and heat-transport equations using 1DTempPro (Koch *et al.* 2015). Using a known VHG, 1DTempPro can be used to numerically solve for an optimal K value that results in a similar modelled thermal gradient time series to that observed in the field. Alternatively, an estimated K and measured VHG can be used to model groundwater exchange, with the accuracy of the estimate assessed by comparing the RMS of the resulting modelled thermal gradient time series to that observed in the field.

To obtain continuous measurements of stream bed temperature, two Onset Tidbit V2 temperature data loggers were installed in a vertical array at approximate depths of 10 cm and 40 cm within the sediment. A third temperature data logger was installed at the water column-substrate interface, fitted with a radiation shield with holes drilled through to allow water through flow. Temperature was continuously recorded at 2-min intervals. Temperature arrays were installed at well-mixed locations bracketing features that have the potential to provide good spawning habitat, where strong hyporheic exchange would be expected, and in close proximity to the piezometer sites (<6 m). The thermistor arrays were installed at seven of the study sites: one on the Fording River (FRD-CA01) and Clode Creek Settling Pond System (CLO-CA01), and five on Greenhills Creek (GRE-CA01, GRE-CA03, GRE-CA05, GRE-CA06, and GH-CTF).

Installation of the temperature data loggers consisted of digging a 40-cm deep hole within the streambed, installing a logger at this depth, backfilling the hole to a 10-cm depth to install the second logger, and then backfilling the hole so that the bed surface was approximately even with the surrounding surface. Substrate was set aside in an attempt to backfill the hole with the same

substrate as that removed. Implications of this method on the flow exchange results are discussed in section 4.1.5.3.

Thermistor arrays were installed concurrent with VHG measurements described in section 3.1.5.1. Interstitial water temperature was recorded for a minimum of 5 days. The arrays were removed at the end of the study in June and reinstalled in August in similar locations.

Running 1DTempPro requires a VHG value at the same depth as the deepest thermistor. To determine the VHG at this depth, the measured VHG values at each site were linearly extrapolated from the ~30 cm depth during June, and linearly interpolated between the ~30 cm and 50 cm depth for August/September.

To determine if modelled downwelling rates were realistic and to distinguish between hyporheic and groundwater exchange, the theoretical wetted channel length was calculated assuming downwelling flows were lost from the channel and no inflows. This channel length was calculated by dividing discharge measured at some point during the thermistor installation period by downwelling rate and average channel width. A long theoretical wetted channel length suggests the channel could be losing flow that is replenished by inflows, whereas a short theoretical channel length suggests that downwelling was more likely hyporheic and returned to the channel.

#### 3.1.5.3. Initial hydraulic conductivity and porosity estimation

Initial K estimates were obtained using empirical curves and equations relating K to GSD detailed below. The estimates were then refined using the numerical optimization approach in 1DTempPro described in Section 3.1.5.2. Initial K estimates were taken as the average of values obtained using the recommended method of Salarashayeri and Siosemarde (2012) and the curves prepared by She *et al.* (2006). The estimates based on Salarashayeri and Siosemarde (2012) used a relationship dependent on GSD D10, D50, and D60 (i.e., the value of the grain diameter at 10%, 50%, and 60% in the cumulative GSD), and the estimates based on She *et al.* (2006) relied on visual estimation of fines content and fines composition. Due to the lack of fines characterization at GH-CTF, the table presented in Domenico and Schwartz (1990) was used assuming the material resembled fine sand or medium silt. Porosity was also estimated based on grain size distribution for each site using the curves prepared by She *et al.* (2006), which provided estimates based on sand content and fines composition.

The K of the streambed was modelled as a uniform layer to allow application of the K optimization module using 1DTempPro. Optimizing the K of multiple layers is not possible in the current version of 1DTempPro (Koch *et al.* 2015). Each of the substrate columns assessed was relatively uniform except for GRE-CA01 and CLO-CA01, which had a surface layer of coarser material. The benefits of assuming uniform streambed stratigraphy and using the 1DTempPro optimizer tool are believed to outweigh the uncertainty introduced by this assumption.

#### 3.1.5.4. Heat transport properties parameterization

A sensitivity analysis was completed using the GRE-CA01 June study data to test the sensitivity of modelled groundwater exchange rates to physical substrate properties and to parameterize constants. The parameters required for 1DTempPro that were assessed included K (m/s), porosity (-), thermal conductivity (W/m°C), sediment heat capacity (J/m<sup>3</sup>C), dispersivity (m), and vertical head gradient (m). The variance of groundwater exchange rate estimates was analyzed using the upper, lower, and average estimates of each of these parameters found in the literature. The parameter estimate that produced the lowest RMSE of modelled thermal gradient was used for the rest of the modelling. It was assumed that each site would have a similar thermal conductivity, sediment heat capacity, and dispersivity due to the similarities in local geology.

### 3.2. Testing the Impact Hypothesis

#### 3.2.1. Modelling of Hyporheic Conditions vs Calcite Index

Relationships between CI and hyporheic DO and flow were investigated using a model selection procedure and fitting a series of linear mixed-effects models using the “lme4” and “MuMIn” packages for R statistical software (Bates *et al.* 2015). Three separate models were fit, one for each key response variable: 1) dissolved oxygen concentration; 2) hyporheic flow from the hydraulic head method; and 3) hyporheic flow from the temperature method. The predictor variables included in each model were habitat and sampling variables hypothesized to affect hyporheic conditions (CI, depth in substrate, water temperature, water quality, water depth, water velocity, substrate composition, season, and site). Predictor variables include fixed effects (variables that we are interested in and test directly [CI, depth in substrate, water temperature, water quality, water depth, water velocity, substrate composition, season]) and random effects (variables that we are less interested in but need to account for in the analysis [site]). Model selection techniques were used to assess the relative importance of each predictor variable, including CI, in explaining hyporheic conditions (e.g., Zuur *et al.* 2009, Grueber *et al.* 2011).

In the first step of the model selection procedure, data were explored to screen the variables to include in each model. Predictor variables that were highly correlated with one another were excluded due to multicollinearity. In addition, variables with a low number of observations (e.g., specific conductivity and pH) were also excluded. The following predictor variables were used in the analysis: site, season, CI score, depth in substrate, average substrate size, percent fines, flow, water temperature, water depth, and a CI score\*depth in substrate interaction term. The CI score\*depth interaction term was included as a predictor because it was hypothesized that the relationship between surface CI and hyporheic conditions would vary by depth of measurement in the substrate. All of the predictor variables were modelled as fixed effects, with the exception of site, which was modelled as a random effect. The predictor variables were all scaled by subtracting their respective means, and dividing by twice their respective standard deviations, to allow for direct comparisons of predictor effects at the same scale (see Grueber *et al.* 2011). When hyporheic flow was analyzed as the response variable, it was also scaled because the data included extremely low values and large

outliers. For the model with hyporheic flow from the temperature method as a predictor, neither depth in substrate nor the CI score\*depth interaction were included in the model because this method was not applied in the field at different depths in the substrate.

Once the initial ‘global model’ was determined, the second step of the model selection procedure involved an all-model-combinations model selection approach where candidate models containing all possible combinations of each predictor variable were competed against one another to find the model that best predicted hyporheic conditions. To prevent overfitting, the candidate models were limited to a maximum of four predictors. For each candidate model, the goodness of fit was quantified using Akaike Information Criterion, corrected for small sample sizes (AICc), which balances model simplicity with variance explained. A subset of the candidate models was then taken based on the difference between each model’s AICc value and the AICc of the best model (the  $\Delta$ AICc). Only models with a  $\Delta$ AICc of less than 4 were retained, a cut-off threshold used to prevent the inclusion of overly complex models (Grueber *et al.* 2011). The retained models within  $\Delta$ AICc <4 were then model-averaged to obtain a final, weighted model. Model-averaged products for each response variable include the set of top models that explain hyporheic conditions, and the parameter estimates, confidence and relative variable importance associated with each predictor variable.

## 4. RESULTS

### 4.1. Fish Habitat, Calcite Index, and Hyporheic Conditions

#### 4.1.1. Fish Habitat Assessment and Fish Observations

Results of the modified FHAP surveys are shown on Map 2 and Map 3 and summarized in Table 9. The raw data and photographs for individual units are provided in Appendix B. A total of 11 mesohabitat units were assessed at the 12 calcite study sites (both GH\_GH1 and GRE-CA05 were located in the same mesohabitat).

The Fording River study sites were located either in pool or run channel units, with gradients of 0 to 1.0 %. The deepest habitat was located at FRD-CA01 (average water depth of 1.20 m). The wetted width ranged from 7.0 to 9.1 m (Table 9).

In the Clode Creek Settling Pond System, study sites were located in riffle (CLO-CA01) or glide (CLO-CA02) channel units, with gradients of 0.5 to 1.0 %. The wetted width varied from 2.1 m at CLO-CA01 to 5.9 m at CLO-CA02.

In Greenhills Creek, all sites were located in riffle habitat, with the exception of GRE-CA02, which was in a glide. Wetted width ranged from 1.7 to 3.2 m across all sites and average water depth varied from 0.09 to 0.25 m. In lower Greenhills Creek (GRE-CA01 to GRE-CA03) the gradient ranged from 0.5 to 1.0 %, whereas gradient in upper Greenhills Creek (GRE-GH1 to GH\_CTF) ranged from 1.5 to 3.0 % (Table 9).

Streambed composition varied between the three study streams. Cobble and gravels dominated in the Fording River, whereas gravel and sand/fines dominated the substrate composition in Clode

Creek Settling Pond System. In the lower sections of Greenhills Creek (GRE-CA01 to GRE-CA03) gravel and sand/fines dominated, whereas cobble and gravel dominated further upstream (GRE-GH1 to GH\_CTF; Table 9). Detailed particle/grain size distributions were measured at each site and the results are provided in Section 4.1.2.2.

Stream cover available for fish was also assessed during the FHAP study (Table 9). Fording River study site mesohabitat units had a variety of cover present, including large woody debris, boulder, deep pools and undercut banks. Overhanging and instream vegetation were the predominant types of cover observed in Clode Creek Settling Pond System. Overhanging vegetation was the dominant cover type for fish at four of the six sites assessed on Greenhills Creek; the upper Greenhills Creek sites all had overhanging vegetation as the primary cover type. Other forms of available cover in Greenhills Creek included large and small woody debris and undercut banks.

During the field work, Westslope Cutthroat Trout were observed in all three study streams, though not at all locations (Table 10). Fish and redds were observed at the Clode Creek Settling Pond System sites during both trips in 2016. No redds were observed at CLO-CA02 site in 2016; although redds were seen at this site in 2015 (Scott Cope, personal observation). Small fish, redds and eggs were observed at the lower Greenhills sites (GRE-CA01 to GRE-CA03; Table 10).

**Table 9. Summary of FHAP results at each calcite study site, June 18 to June 23, 2016.**

Site	Type <sup>1</sup>	Unit Length (m)	Width (m)		Area (m <sup>2</sup> )		Average Water Depth (m)	Gradient (%)	Weighted Gradient (%)	Substrate <sup>2</sup>		Dominant Cover <sup>3</sup>		Sub-dominant Cover <sup>3</sup>	
			Wetted Width	Bankfull Width	Wetted Area	Bankfull Area				Dominant	Sub-dominant	Type	%	Type	%
FRD-CA01	Pool	15.2	9.1	12.1	138	184	1.20	0.0	0.0	GR	S/FI	DP	40	LWD	30
FRD-CA02	Run	65.0	7.0	9.4	455	611	0.30	1.0	65.0	CO	GR	BO	TR	CU	TR
FRD-CA03	Run	12.0	7.0	14.0	84	168	0.46	0.5	6.0	CO	GR	LWD	10	DP	5
CLO-CA01	Riffle	55.0	2.1	2.5	113	138	0.14	1.0	55.0	GR	S/FI	IV	10	OV	5
CLO-CA02	Glide	6.5	5.9	6.2	38	40	0.24	0.5	3.3	S/FI	GR	IV	5	OV	5
GRE-CA01	Riffle	9.2	2.9	5.7	27	52	0.09	1.0	9.2	GR	CO	OV	20	CU	TR
GRE-CA02	Glide	105.8	2.6	3.5	275	370	0.25	0.5	52.9	S/FI	GR	CU	10	LWD	5
GRE-CA03	Riffle	7.2	2.2	4.7	16	34	0.12	1.0	7.2	GR	CO	LWD	2.5	SWD	2.5
GRE-GH1	Riffle <sup>4</sup>	42.4	3.2	4.3	136	182	0.17	3.0	127.2	CO	GR	OV	5	CU	5
GRE-CA05															
GRE-CA06	Riffle	8.0	2.1	3.3	17	26	0.14	1.5	12.0	GR	BO	OV	5	SWD	TR
GH_CTF	Riffle	10.0	1.7	2.9	17	29	0.11	2.0	20.0	CO	GR	OV	20	CU	TR

<sup>1</sup> Habitat unit types and measurements were classified according to definitions in Johnston and Slaney (1996).

<sup>2</sup> BO = Boulder, CO = Cobble, GR = Gravel, S/FI = Sand/Fines

<sup>3</sup> BO = Boulder, DP = Deep Pool, LWD = Large Woody Debris, LC = Large Cobble, CU = Undercut Bank, OV = Overhead Vegetation

<sup>4</sup> GRE-GH1 and GRE-CA05 are located in the same riffle.

Category - "Primary - occupy more than 50% of the wetted width of the main channel" at all sites.

**Table 10. Westslope Cutthroat Trout observations recorded during field trips for Calcite Study, 2016.**

Location	Date/Period	Details
FRD-TRQ01	June/Aug-Sep	~200 mm fish observed in large pool near LWD structure on RR just upstream of transect
CLO-CA01	June/Aug-Sep	Redds observed just upstream of piezometer location
CLO-CA02	June/Aug-Sep	No redds observed in 2016, however redds were observed in 2015 <sup>1</sup> Approximately ten to twenty fish observed (~40-70mm)
CLO-TRQ01	June/Aug-Sep	Redds along small reach where transect is located and few fish observed (~40-70 mm)
GRE-CA01	30-Aug-2016	Small fish (~120 mm) and fry (~40 mm) observed
GRE-CA02	03-Sep-2016	Small fish (~60 mm and ~100 mm) observed
	19-Jun-2016	Viable eggs (some with embryos) detected in 0-5 cm substrate depth
	June/Aug-Sep	Redds observed mainly in middle of unit
GRE-CA03	June/Aug-Sep	2 redds observed

<sup>1</sup> Cope, pers. comm. 2016

#### 4.1.2. Calcite Measures and Substrate Composition

Calcite measures and substrate composition surveys were completed from June 19 to June 26, 2016 and again from August 30 to September 6, 2016 at the study sites in the Fording River, Clode Creek Settling Pond System (Map 2), and the upper and lower reaches of Greenhills Creek (Map 3).

##### 4.1.2.1. Calcite Index

Calcite levels varied spatially throughout the study area varied, as expected from previous studies (Minnow Environmental 2016, Robinson *et al.* 2016). The lowest CI was measured in the Fording River (all sites <0.50; Figure 4). CI at the Clode Creek Settling Pond System sites ranged from 1.00 to 1.22 (Figure 5). CI at the Greenhills Creek sites ranged from 0.50 to 2.64, generally increasing with distance upstream. The maximum possible value for the CI is 3.00, which corresponds to calcite presence and a fully concreted (immovable) condition for all pebbles evaluated. The highest CI scores (>2.50 to a maximum of 2.64) were recorded at GH\_CTF and GRE-CA06 located in the upstream reaches of Greenhills Creek (Figure 6, Table 11).

Low variability in CI was observed within each site. The absolute difference between the mesohabitat and CI piezometer sites ranged from 0.00 to 0.32; however, the majority of sites had CI differences of <0.10 (Table 11). The greatest variation in CI within a mesohabitat was measured at GH\_GH1 (absolute difference of 0.32 units measured in June) and GRE-CA05 (absolute difference of 0.31 units measured in September) (Table 11).

Comparison of the CI scores between seasons showed that sites did not vary greatly by season (Table 11, Figure 4, Figure 5, Figure 6). The CI increased slightly from June to September at the Fording River sites; however, the overall index remained low, ranging from 0 to 0.38.

The presence of calcite was also measured in relation to vertical depth within the substrate; presence ranged from surface only (Fording River sites and GRE-CA01) to a depth of 30 cm. Note that these data were meant to provide an indication of calcite depth and did not replicate the procedure used in generating the surface CI score. In some cases the ability to sample at depth was restricted by the presence of bedrock. In general, the sites with higher CI values also exhibited greater depth of calcite presence (Table 11).

Table 11. Summary of CI and calcite depth at piezometer and mesohabitat sites, 2016.

Site	CI Piezometer Site		CI Mesohabitat Site		Absolute $\Delta$ CI between Piezometer and Mesohabitat		$\Delta$ CI from June to Sept. 2016 <sup>1</sup>		Vertical Calcite Depth <sup>2</sup> (cm)
	June	Aug./Sep.	June	Aug./Sep.	June	Aug./Sep.	Piezometer	Mesohabitat	
FRD-CA01	0.05	0.38	0.06	0.31	0.01	0.07	0.33	0.25	0 (surface only)
FRD-CA02	0.15	0.38	0.16	0.29	0.01	0.09	0.23	0.13	0 (surface only)
FRD-CA03	0.01	0.01	0.00	0.18	0.01	0.17	0.00	0.18	0 (surface only)
CLO-CA01	1.22	1.12	1.13	1.12	0.09	0.00	-0.10	-0.01	0 to 10-15
CLO-CA02	1.00	1.06	1.00	1.06	0.00	0.00	0.06	0.06	30
GRE-CA01	0.81	0.81	0.86	0.89	0.05	0.08	0.00	0.03	0 (surface only)
GRE-CA02	0.60	0.69	0.50	0.69	0.10	0.00	0.09	0.19	0-6
GRE-CA03	0.89	1.32	0.90	1.38	0.01	0.06	0.43	0.48	0-10
GH_GH1	2.18	1.87	1.86	1.75	0.32	0.12	-0.31	-0.11	0-30
GRE-CA05	1.91	2.06	1.91	1.75	0.00	0.31	0.15	-0.16	0-30
GRE-CA06	2.64	2.47	2.64	2.47	0.00	0.00	-0.17	-0.17	0-15
GH_CTF	2.62	2.46	2.62	2.46	0.00	0.00	-0.16	-0.16	7-15

Note: Piezometer site is within the mesohabitat unit.

<sup>1</sup>Negative (grey shading) indicates that calcite presence/concretion level decreased from June to September 2016.

<sup>2</sup>Vertical calcite depth at CLO-CA02, GRE-CA06 and GH\_CTF was limited by bedrock.

Figure 4. Summary of CI at Fording River sites, 2016.

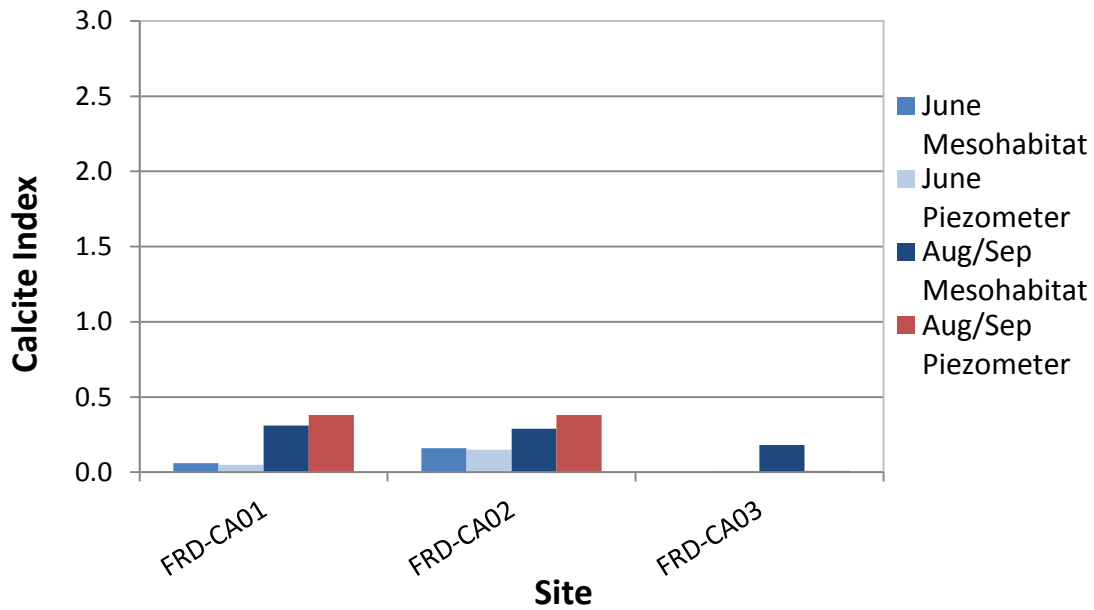


Figure 5. Summary of CI at Clode Creek Settling Pond System sites, 2016.

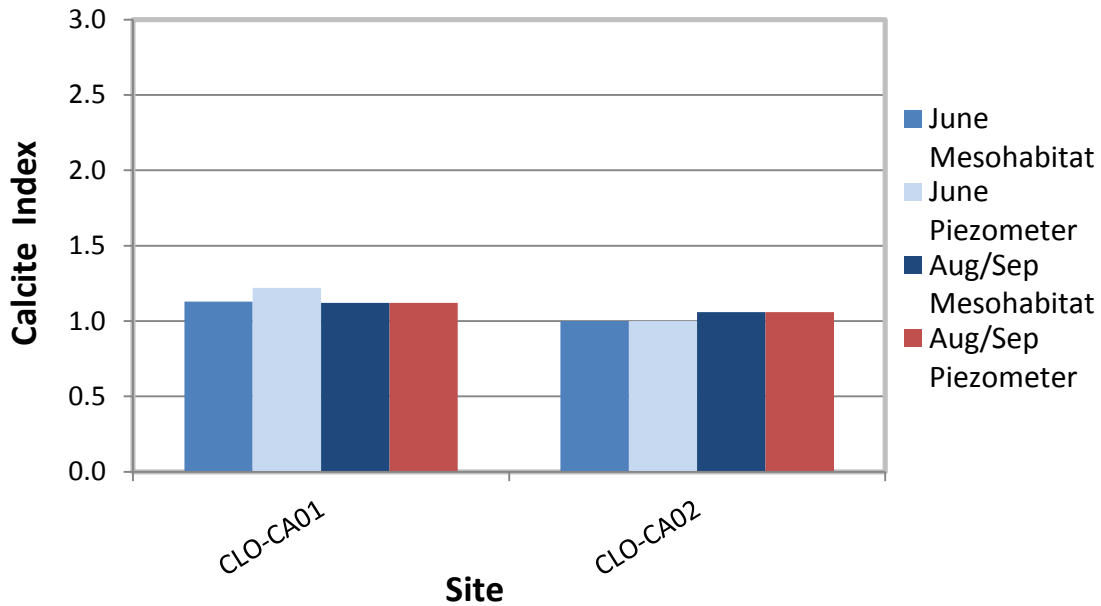
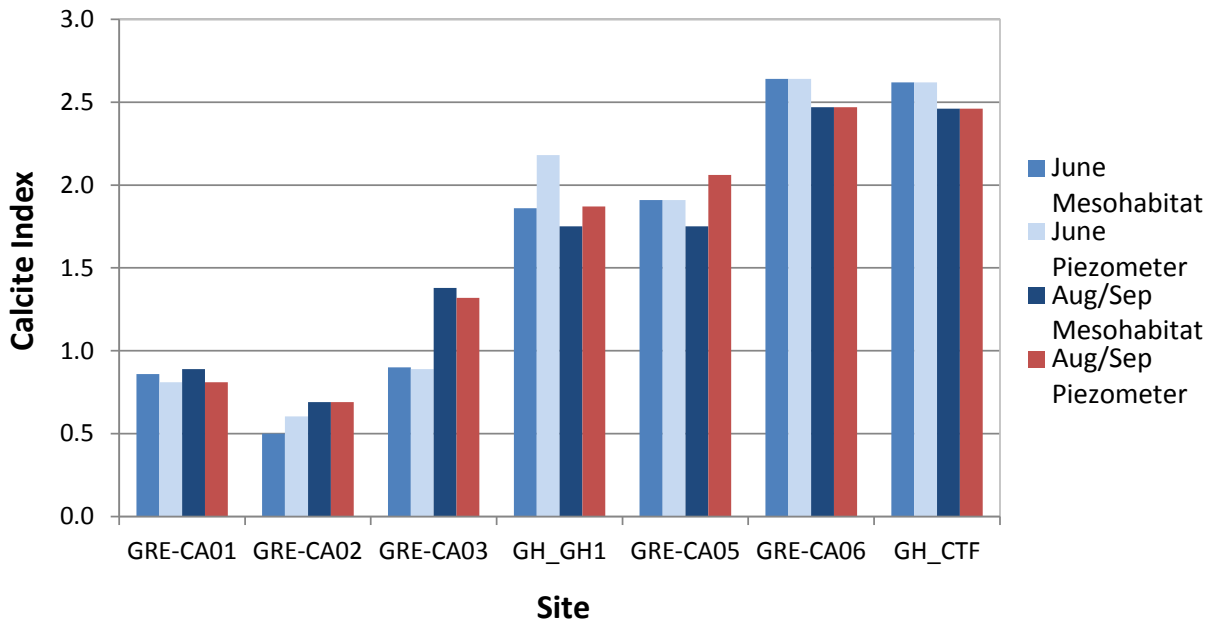


Figure 6. Summary of CI at Greenhills Creek sites, 2016.



#### 4.1.2.2. Substrate Composition

GSD was measured to provide an estimate of the thermal conductivity and porosity of each site (see Section 3.1.5.3). The cumulative particle size distribution (distribution curve) and the number of particles per size class (box plots) are provided for each site (mesohabitat and piezometer) and sampling period in Appendix C.

The Fording River and Clode Creek Settling Pond System sites exhibited similar GSD between the piezometer sites and mesohabitat sites at each of the calcite study locations. In June, the D50 (median diameter) estimates ranged from 52 to 62 mm for all sites in the Fording River (Table 12), and from 38 to 44 mm for all sites in Clode Creek Settling Pond System (Table 13). In August/September, the D50 estimates ranged from 44 to 61 mm for all sites in the Fording River (Table 12), and from 45 to 50 mm for all sites in Clode Creek Settling Pond System (Table 13).

At Greenhills Creek sites, there was greater variability in mean substrate diameter among study sites and between the piezometer and mesohabitat sites; the D50 values estimates in June ranged from 29 to 98 mm and 37 to 85 mm at the mesohabitat and piezometer sites, respectively (Table 14). In August/September, the D50 estimates ranged from 28 to 81 mm at all sites. Substrate size composition at GH-CTF was difficult to assess due to high levels of calcite concretion and the presence of bedrock; this resulted in fewer pebbles from which to assess substrate size composition and skewed the results to smaller pebble sizes.

**Table 12. Substrate size (mm) composition in the Fording River measured in the mesohabitat (meso) and piezometer (piez) sites in June and August/September 2016.**

Substrate Diameter (mm)	FRD-CA01				FRD-CA02				FRD-CA03			
	June (piez)	June (meso)	Aug/Sep (piez)	Aug/Sep (meso)	June (piez)	June (meso)	Aug/Sep (piez)	Aug/Sep (meso)	June (piez)	June (meso)	Aug/Sep (piez)	Aug/Sep (meso)
D10	32	32	19	21	27	28	27	33	31	29	20	17
D16	35	35	23	25	31	33	33	36	35	35	25	21
D40	48	46	39	40	48	45	48	52	53	55	46	41
D50	53	52	44	45	58	55	56	61	62	62	55	48
D60	58	58	51	52	69	65	65	70	74	71	63	58
D84	80	83	71	71	106	109	87	105	119	102	117	106
D90	88	91	82	82	121	128	100	122	146	124	141	128

D values represent the % grain diameter of a given size in the cumulative GSD

D50: median diameter by mass

**Table 13. Substrate size (mm) composition in Clode Creek Settling Pond System measured at the mesohabitat (meso) and piezometer (piez) sites in June and August/September 2016.**

Substrate Diameter (mm)	CLO-CA01			CLO-CA02	
	June (piez)	June (meso)	Aug/Sept (piez/meso)	June (piez/meso)	Aug/Sept (piez/meso)
D10	14	17	27	19	20
D16	19	20	30	23	24
D40	32	34	43	38	40
D50	38	41	50	44	46
D60	45	49	58	55	53
D84	64	72	80	97	78
D90	82	82	86	110	87

D values represent the % grain diameter of a given size in the cumulative GSD

D50: median diameter by mass

**Table 14. Substrate size (mm) composition in Greenhills Creek (GRE-CA01, GRE-CA02 and GRE-CA03) measured at the mesohabitat (meso) and piezometer (piez) sites in June and August/September 2016.**

Substrate Diameter (mm)	GRE-CA01				GRE-CA02			GRE-CA03				GH_GH1				GRE-CA05		GRE-CA06		GH_CTF	
	June (piez)	June (meso)	Aug/Sep (piez)	Aug/Sep (meso)	June (piez)	June (meso)	Aug/Sep (piez/meso)	June (piez)	June (meso)	Aug/Sep (piez)	Aug/Sep (meso)	June (piez)	June (meso)	Aug/Sep (piez)	Aug/Sep (meso)	June (piez/meso)	Aug/Sept (piez/meso)	June (piez/meso)	Aug/Sept (piez/meso)	June (piez/meso)	Aug/Sept (piez/meso)
D10	22	24	19	24	16	15	17	35	32	18	21	32	45	33	35	33	26	22	24	15	9
D16	26	27	22	27	19	17	20	39	35	21	25	39	55	40	42	37	33	26	28	18	10
D40	40	39	34	38	30	25	41	57	45	37	44	73	88	67	73	55	55	42	50	37	19
D50	45	44	39	42	37	29	53	65	55	43	56	85	98	78	81	62	65	53	63	40	28
D60	52	50	43	48	46	37	64	74	65	50	67	98	107	89	89	69	75	66	75	44	38
D84	75	66	63	70	88	66	89	107	89	80	90	126	136	122	122	86	108	151	156	77	64
D90	84	81	76	81	105	78	106	121	105	89	111	144	161	140	140	91	120	173	177	86	77

D values represent the % grain diameter of a given size in the cumulative GSD  
 D50: median diameter by mass

#### 4.1.3. Surface Hydrology

Water depth and velocity measurements made at each piezometer site were predictor variables hypothesized to affect hyporheic conditions (see Section 3.2). A summary of these measurements is provided in Appendix D. At many sites, water depth and velocity varied across the stream due to differences in the streambed topography and substrate. Water depths were on average 0.38 m less in August/September than in June. Water depths were highest at FRD-CA03 and lowest at CLO-CA01 and GRE-CA01 (Appendix D). Water velocities were on average 0.02 to 0.19 m/s lower at all sites in August/September than in June.

Discharge measurements collected at each stream are summarized in Section 2.4, and are provided in Appendix D. Discharge was lowest at GRE-CA02 in June (0.12 m<sup>3</sup>/s) and GRE-CA06 in August/September (0.04 m<sup>3</sup>/s); though GRE-CA02 also had low flow (0.08 m<sup>3</sup>/s) in August/September. Discharge was highest at the Fording River sites during both study periods, and highest at FRD-CA03 (0.67 m<sup>3</sup>/s in June and 0.48 m<sup>3</sup>/s in August/September).

#### 4.1.4. Hyporheic Dissolved Oxygen Concentration

Water quality summary statistics for dissolved oxygen (% saturation and mg/L), water temperature (°C), pH and specific conductivity (µS/cm) were generated for each site at each measured depth (Appendix E). Water temperature influences DO (DO saturation is usually inversely related to water temperature), and may also influence embryo development and incubation success; however, water temperature is not expected to be impacted by calcite formation and thus was not compared to BC water quality guidelines. DO concentrations at depth were found to be above the BC water quality guidelines for the protection of buried life stages (Table 8) at all the Fording River and Clode Creek Settling Pond System sites (Figure 7); however, exceedances (i.e., below) of the instantaneous minimum guideline (6 mg/L DO) were recorded at several of the Greenhills Creek sites (Figure 8). In general, DO exhibited decreasing concentration with increased depth in the substrate across the sampling sites.

At the Fording River sites, with low CI scores, DO exhibited a well-saturated condition ranging from 76.4% to 90.7% saturation and 9.00 mg/L to 10.86 mg/L concentration at all sites over both sampling periods (Figure 7). No exceedances of the BC water quality guidelines for DO were recorded and the variability in replicate data was within the guidelines provided by RISC (1998) (i.e., RSE <18%) (Appendix E). Water temperature at the Fording River sites ranged from 6.4 °C to 9.7 °C, over both sampling periods with little variation observed in relation to depth in the substrate (Figure 9, Appendix D). Specific conductivity ranged from 496 to 577 µS/cm and pH ranged from 7.92 to 8.16 and (Appendix D). Seasonally, lower DO concentrations and lower % saturation were recorded in September in comparison to June; while water temperatures were higher in September.

At the Clode Creek Settling Pond System sites, with low to moderate CI scores, DO exhibited a well-saturated condition in most cases, ranging from 75.5% to 93.4% saturation and 8.45 mg/L to 9.84 mg/L concentration over both sampling periods (Figure 7, Appendix D). No exceedance of the BC water quality guidelines for DO were recorded and the variability in triplicate data was within the

guidelines provided by RISC (1998) (i.e., RSE <18%). Water temperature at the Clode Creek Settling Pond System sites ranged from 10.9 °C to 12.5 °C, over both sampling periods with little variation observed with depth in the substrate. Some variation in pH and specific conductivity between sites was observed; pH ranged from 7.89 to 8.27 and specific conductivity ranged from 1,549 µS/cm to 1,577 µS/cm. Specific conductivity is higher than that typically observed in BC surface water, indicating a higher concentration of dissolved ions (Table 7). Seasonally, slightly lower DO concentrations and % saturation were recorded in September in Clode Creek Settling Pond System in comparison to June.

At the Greenhills Creek sites, where CI score ranged from low to high, DO and general water quality parameters exhibited greater variation among sites and in relation to depth within the substrate (Figure 8, Figure 10, Appendix D). Two of the seven Greenhills Creek sites (GRE-CA03 and GH\_GH1DO) exhibited well-saturated conditions at all depths with minimal change in DO concentration with depth; DO at these sites ranged from 81.0% to 87.2% saturation and 8.35 mg/L to 9.70 mg/L concentration, over both sampling periods (Figure 8, Appendix E). Water temperature did not change appreciably with depth (Figure 8). Slight variation in pH and specific conductivity between these sites was observed; pH ranged from 8.24 to 8.50 and specific conductivity ranged from 1,365 µS/cm to 1,379 µS/cm.

The remaining five sites exhibited more variable DO, with average values less than the instantaneous (6 mg/L) and the 30-day (8 mg/L) BC water quality guidelines for the protection of buried life stages (Table 8) at depths ranging from ~10 cm to ~43 cm (Figure 8). DO ranged from 81.0% to 87.2 % saturation and 0.99 mg/L to 10.58 mg/L concentration, over both sampling periods (lowest average concentration was measured at GRE-CA02 (~29 cm depth in June and ~43 cm depth in September; Figure 8, Figure 10).

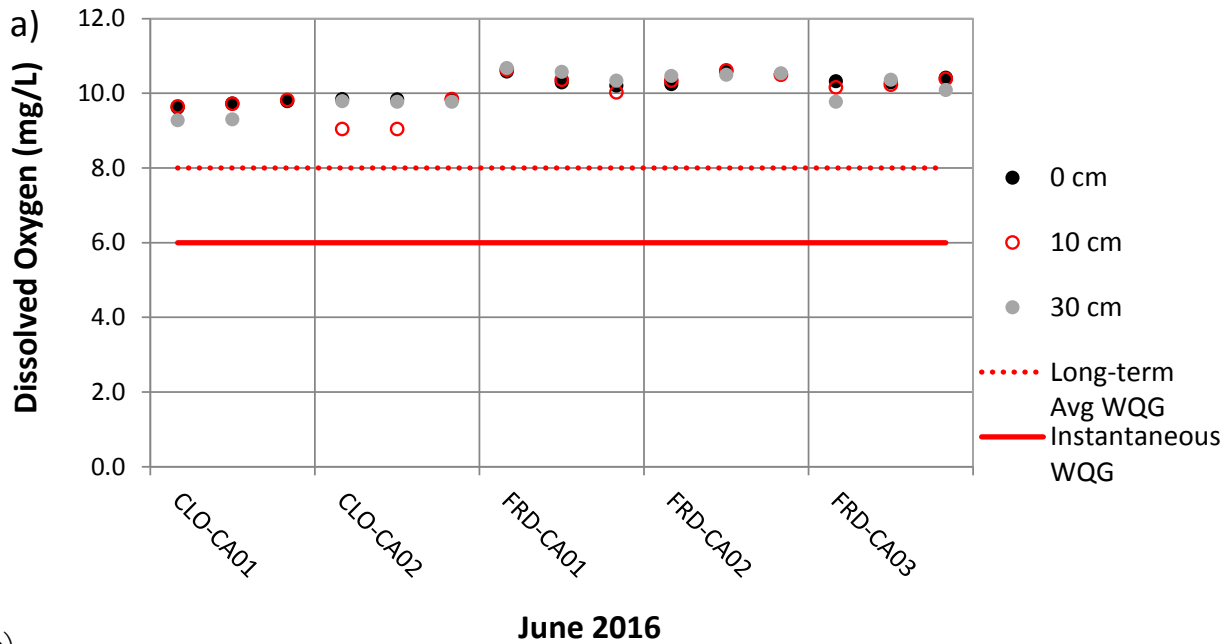
Water temperature varied between sites in Greenhills Creek as expected, based on site elevations, but not with depth (Figure 10). The Greenhills Creek sites exhibited a pH range of 7.59 to 8.54 and a specific conductivity range of 1,037 µS/cm to 2292 µS/cm. Specific conductivity was higher than typically observed in BC surface water, indicating a higher concentration of dissolved ions (Table 7).

Considering all Greenhills Creek sites seasonally, slightly lower DO concentrations and % saturation were recorded in September in comparison to June, whereas water temperatures were generally higher.

Variability in DO data between piezometer sites, but within mesohabitats, was most pronounced (>18% RSE to maximum of 70% RSE) in Greenhills Creek. High RSE values were observed at GRE-CA01, GRE-CA02, GRE-CA06 and GH\_CTF (Appendix D). At GRE-CA01, the mid-channel piezometer site consistently exhibited higher DO in comparison to the river right and river left sites for samples at 30 to 40 cm depths; suggesting heterogeneity in substrate character and interstitial or hyporheic flow within the piezometer transect. Achieving consistent depth between the piezometers was challenging, which may also have contributed to the high RSE.

Figure 7. Dissolved oxygen in relation to depth measured at the Fording River and Clode Creek Settling Pond System sites in a) June and b) August/September 2016. Water quality guidelines (WQG) include long-term average minimum DO of 8 mg/L and instantaneous DO minimum guideline 6 mg/L (MOE 2016).

a)



b)

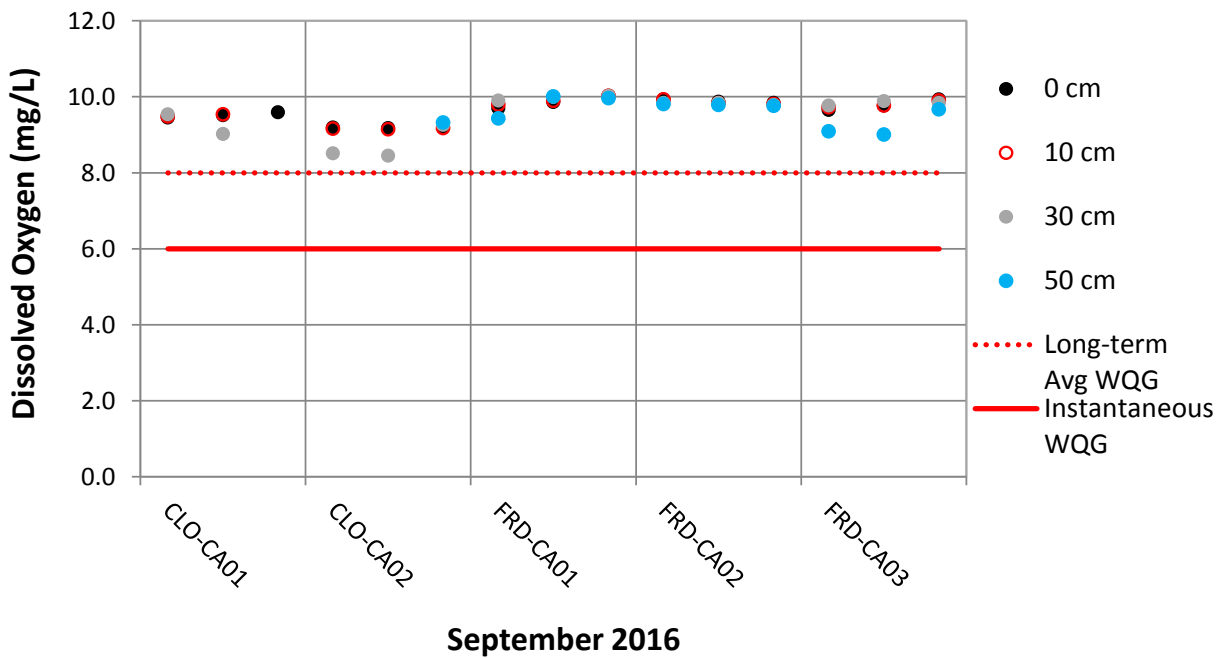


Figure 8. Dissolved oxygen in relation to depth measured at the Greenhills Creek sites in a) June and b) August/September 2016. Water quality guidelines (WQG) include long-term average minimum DO of 8 mg/L and instantaneous DO minimum guideline 6 mg/L (MOE 2016).

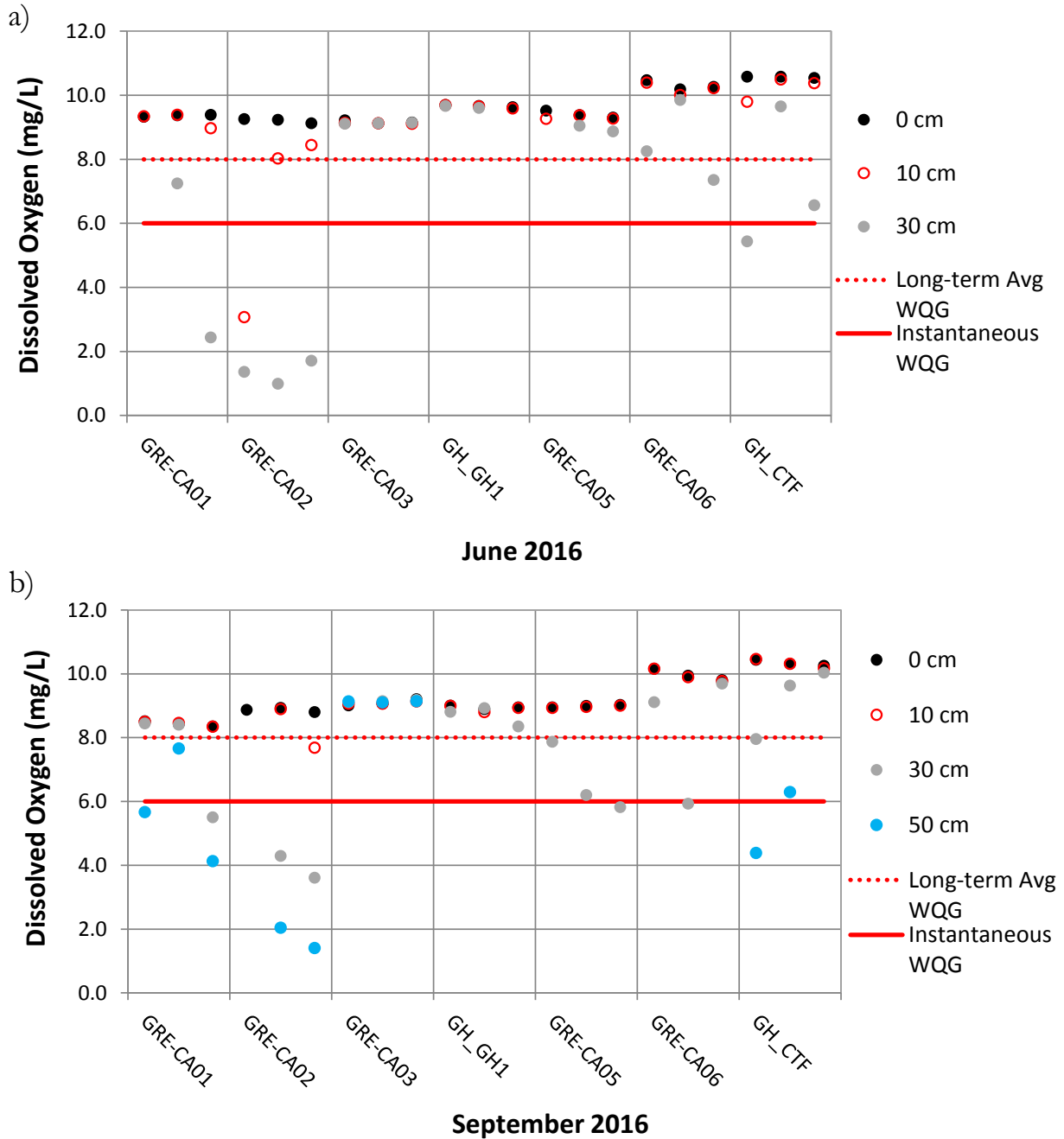


Figure 9. Water temperature in relation to depth measured at the Fording River and Clode Creek Settling Pond System sites in a) June and b) August/September 2016. Water quality guidelines (WQG) include optimum water temperature range for the incubation of Cutthroat Trout (Oliver and Fiddler 2001).

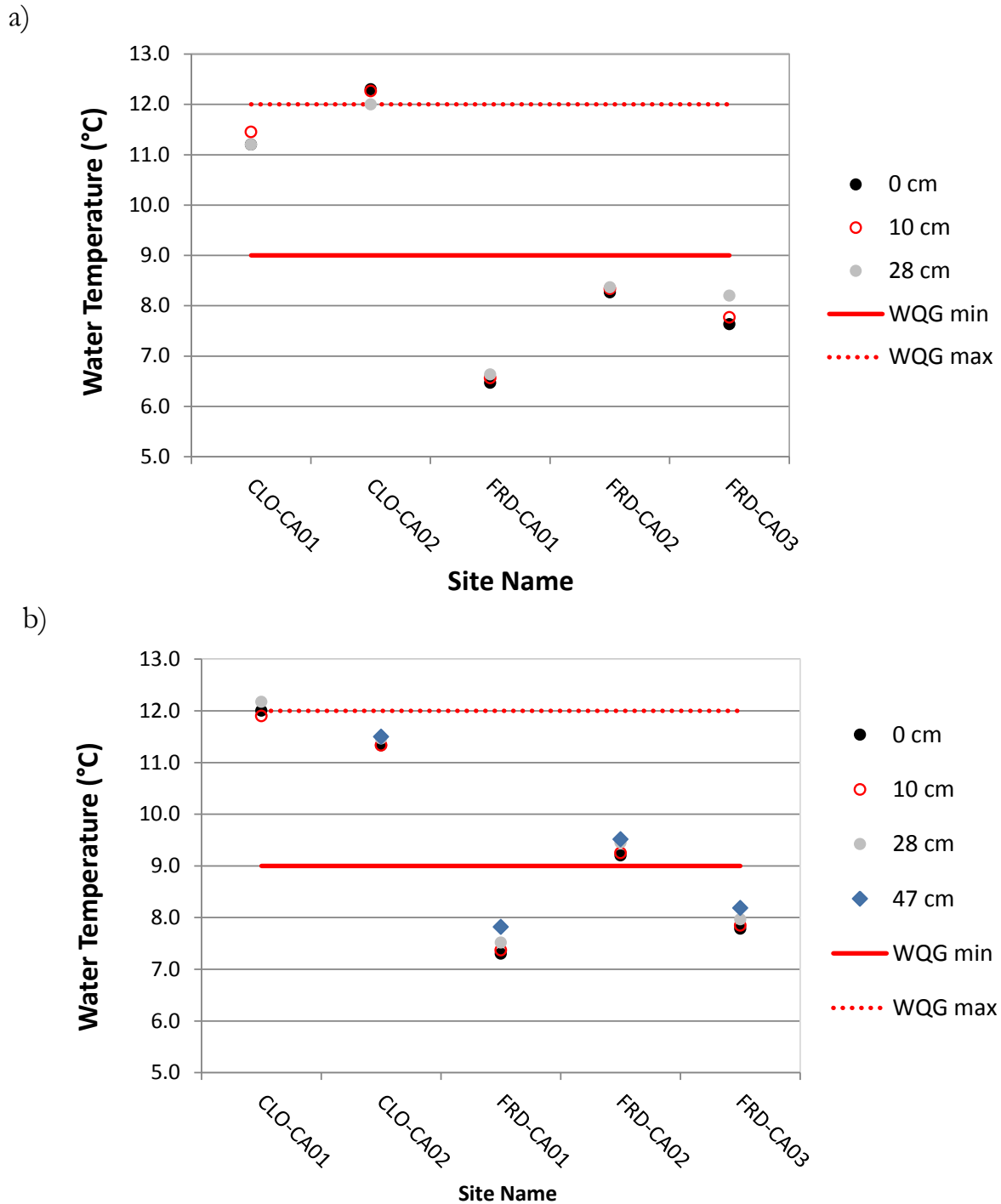
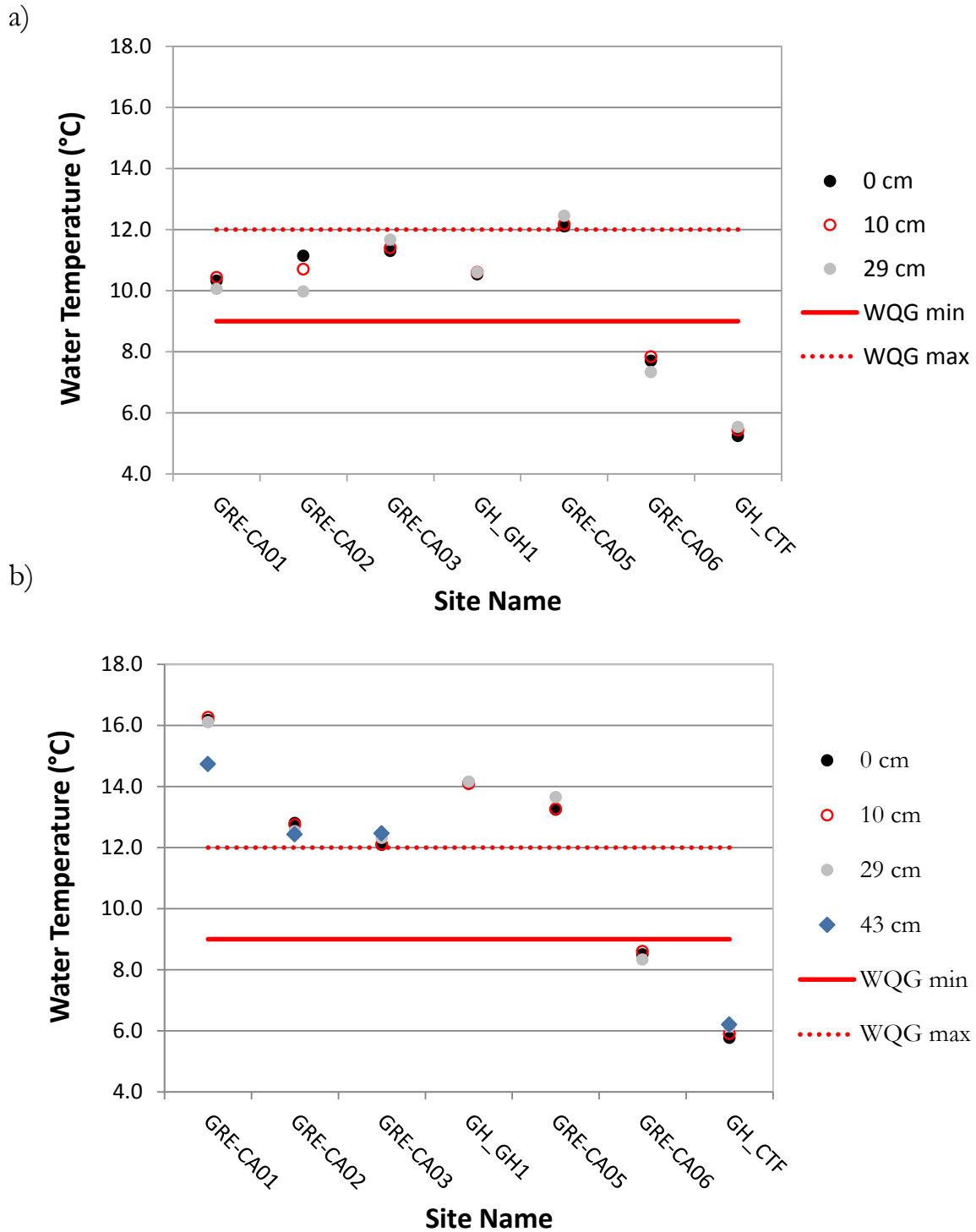


Figure 10. Water temperature in relation to depth measured at the Greenhills Creek sites in a) June and b) August/September 2016. Water quality guidelines (WQG) include the optimum water temperature range for incubation of Cutthroat Trout (Oliver and Fiddler 2001).



#### 4.1.5. Hyporheic Flow

##### 4.1.5.1. Hydraulic Head Method

Hyporheic flow estimates generated with Darcy's equation (the hydraulic head method) were found to have unrealistically high downwelling values due to uncertainty in the hydraulic head and hydraulic conductivity estimates. The hyporheic flow estimates derived from the hydraulic head method are therefore considered to be unreliable; though the estimate of direction of flow (downwelling) is considered valid. The results and implications are discussed in the *Groundwater Exchange Rate* section below.

##### *Hydraulic Head*

The hydraulic head data are summarized for each study stream in this section, and the average hydraulic head values at each site (n=3 in most cases) are summarized in Appendix D. The average hydraulic head generally increased (became more positive) with depth at all sites, indicating downwelling; although, the magnitude of the hydraulic gradient with depth varied by site.

In the Fording River, the average hydraulic head generally increased (became more positive) with depth as expected (Figure 11). FRD-CA01 and FRD-CA03 exhibited similar ranges in average hydraulic head, and FRD-CA02 exhibited greater hydraulic head at depth (Figure 11). Similar values were recorded between the two sampling periods (Appendix E).

In Clode Creek Settling Pond System, the average hydraulic head generally increased (became more positive) with depth at both sites; suggesting increased downwelling of flow with depth (Table 15). The hydraulic head at 30 cm depth was larger at CLO-CA01 (0.433 m) in comparison to CLO-CA02 (0.002 m) suggesting stronger downwelling at CLO-CA01 at this depth (Figure 11; Appendix D). Similar trends were observed in August/September. At 50 cm depth, downwelling was recorded at CLO-CA02 (this depth was not measured at CLO-CA01).

In general, increased (more positive) downwelling was recorded with increasing depth for all the sites in Greenhills Creek; however, the magnitude of the hydraulic head was relatively low (maximum of 0.159 m at approximately 50 cm depth at GRE-CA03) in comparison to the Fording River sites (maximum of 0.260 m at approximately 30 cm depth at FRD-CA03) and Clode Creek Settling Pond System (maximum of 0.433 m at approximately 30 cm CLO-CA01) (Figure 11, Table 15).

At Greenhills Creek during June, the hydraulic head at the 10 cm streambed depth ranged from -0.004 to 0.005 m, indicating both downwelling flow (GRE-CA03, GRE-CA05, GRE-CA06, and GH-CFT) and upwelling flow (GRE-CA01, GRE-CA02, and GH-GH1). The hydraulic head measurements at 30 cm streambed depth were higher than those recorded at the 10 cm depth (ranging from 0.002 to 0.034 m) indicating downwelling flow into the streambed. In June 2016, no measurements for the 50 cm depth of streambed were conducted.

At Greenhills Creek during August/September, both downwelling (GRE-CA02 and GH-CFT) and upwelling (GRE-CA01, GRE-CA03, GH-GH1, GRE-CA05, and GRE-CA06) flow patterns were

recorded at 10 cm streambed depth; hydraulic head ranged from -0.013 to 0.007 m (Appendix D). The hydraulic head measurements at 30 and 50 cm depths all indicated downwelling, except at GH-GH1 for 30 cm depth. The hydraulic head increased with increasing depth in streambed from 30 and 50 cm, ranging from 0.002 to 0.050 m for 30 cm depth and 0.034 to 0.159 m for 50 cm depth of streambed (Appendix D).

The direction of groundwater exchange sometimes changed at different depths within the same profile (e.g., CLO-CA02 during September, and GH-GH1 during June). This discrepancy may be a result of inherently high variance in the hydraulic head measurements. Water levels fluctuated up to 6 cm inside and outside of the piezometers over the measurement period, primarily due to turbulence in surface water flow. This turbulence was at times greater than the observed hydraulic head differential. Uncertainties in the measurements are further identified in Section 4.1.5.3.

Figure 11. Hydraulic head measured at depth in Fording River and Clode Creek Settling Pond System in a) June and b) August/September 2016.

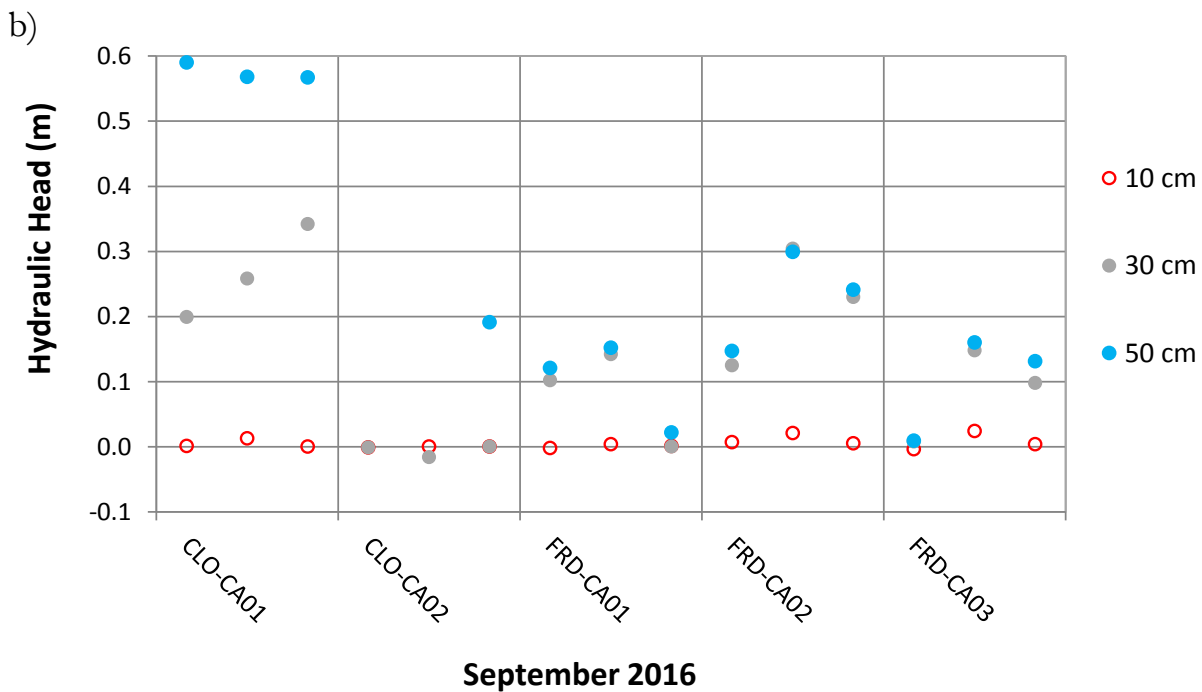
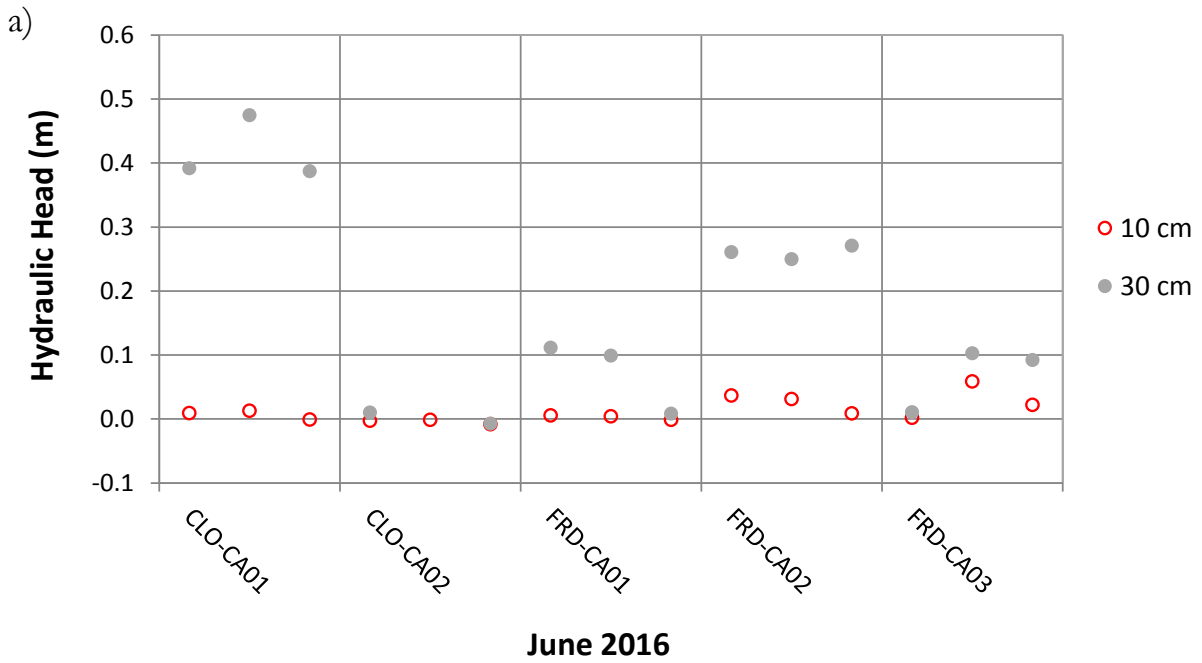
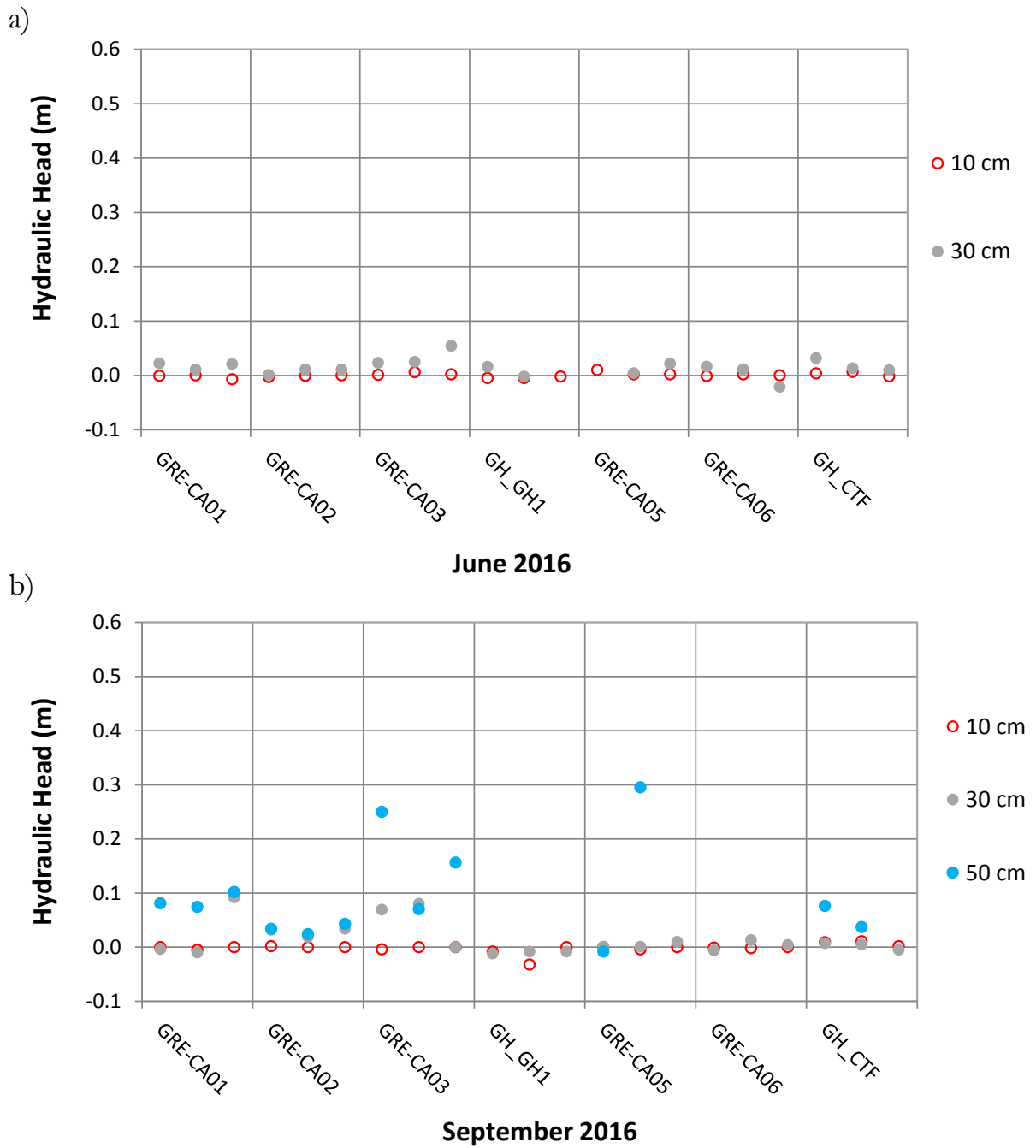


Figure 12. Hydraulic head measured at depth in Greenhills Creek in a) June and b) August/September 2016.



*Groundwater Exchange Rate*

The groundwater exchange rates estimated using the hydraulic head data were highly variable between sites and unrealistic compared to literature values. Thus, the groundwater exchange rates provided here should be used for comparison purposes only.

The vertical head gradient (VHG) at 0.35 m was calculated for each of the hydraulic head values presented in Figure 11 and Figure 12. Hydraulic conductivity (K) was estimated using GSD based relations and groundwater exchange rates were calculated from these values using Darcy's equation (Table 15). On average, the downwelling rate was weaker during the August/September study period at Fording River and Clode Creek Settling Pond System, and stronger at Greenhills Creek; although, the direction of change varied between sites at each stream. The strongest downwelling rates were observed at Fording Creek, followed by Clode Creek Settling Pond System; although, Clode Creek Settling Pond System had strong downwelling at only one of the two sites, resulting in an inflated average.

The majority of groundwater exchange rates were unrealistically high at Fording River given typical groundwater exchange rates observed in the literature (e.g., maximum of 1 m/d from Birkel *et al.* (2016), maximum of 0.47 m/d from Bianchin *et al.* (2010), and range of -0.12 to -0.35 m/d from Briggs *et al.* (2013), and infiltration rates observed in storm water management ponds (maximum of 51 m/d from Massman and Butchart (2001)). The percentage of measurements that produced groundwater exchange rates greater than 51 m/d or less than -51 m/d was 67%. The high values are likely the result of variance in VHG measurements given the difficulty in obtaining accurate piezometer readings at the Fording River sites (these sites had the greatest fluctuations in water level), and poor estimates of K. Estimation of K based on pebble counts and visual assessment of fines distribution has greater uncertainty than other methods. Obtaining better K estimates could be achieved using a sieve analysis of the GSD; however, estimation using the temperature method is expected to be an easier and more accurate method. It is therefore recommended that the groundwater exchange rates obtained from the hydraulic head method be treated as indicative of direction of flow and relative magnitude, but with unreliable estimates of absolute magnitude.

**Table 15. Groundwater exchange rate calculated with Darcy's equation using GSD based K estimates.**

Site	Fines %	Fines class <sup>1</sup>	Mean porosity <sup>2</sup>	Mean K (m/d) <sup>3</sup>	Mean hydraulic head at 0.35 (m)		q using Darcy's equation (m/d)	
					June	Aug/Sept	June	Aug/Sept
FRD-CA01	2.0	80% C, 20% M	0.47	4069.4	0.086	0.091	<b>995.3</b>	<b>1055.4</b>
FRD-CA02	5.0	95% C, 5% M	0.45	3478.3	0.316	0.222	<b>3135.6</b>	<b>2209.3</b>
FRD-CA03	3.3	95% C, 5% M	0.46	3542.5	0.088	0.090	<b>887.6</b>	<b>913.5</b>
CLO-CA01	33.7	90% C, 10% M	0.22	810.7	0.557	0.279	<b>1290.2</b>	<b>646.3</b>
CLO-CA02	42.5	90% C, 10% M	0.24	796.2	0.002	0.013	<b>4.5</b>	<b>29.6</b>
GRE-CA01	24.3	95% C, 5% F	0.29	1305.6	0.022	0.078	<b>80.4</b>	<b>289.8</b>
GRE-CA02	46.7	80% C, 20% F	0.29	633.4	0.009	0.031	<b>16.2</b>	<b>55.8</b>
GRE-CA03	4.3	95% C, 5% F	0.46	3361.1	0.040	0.095	<b>380.9</b>	<b>914.7</b>
GH-GH1	2.3	95% C, 5% F	0.47	3869.9	0.008	-0.012	<b>90.3</b>	<b>-129.0</b>
GRE-CA05	2.3	95% C, 5% F	0.47	3682.1	0.016	0.027	<b>172.4</b>	<b>286.4</b>
GRE-CA06	4.3	not measured	0.46	3435.3	0.003	0.007	<b>29.8</b>	<b>65.0</b>
GH-CTF	3.0	not measured	0.46	3043.1	0.021	0.021	<b>184.1</b>	<b>183.8</b>

<sup>1</sup> Fines class estimated visually from field samples; C = coarse sand, M = medium sand, F = fine sand.

<sup>2</sup> Based on analytical model from She *et al.* (2006).

<sup>3</sup> Mean of estimates from She *et al.* (2006) and Salarashayeri & Siosemarde (2012).

#### 4.1.5.2. Temperature Method

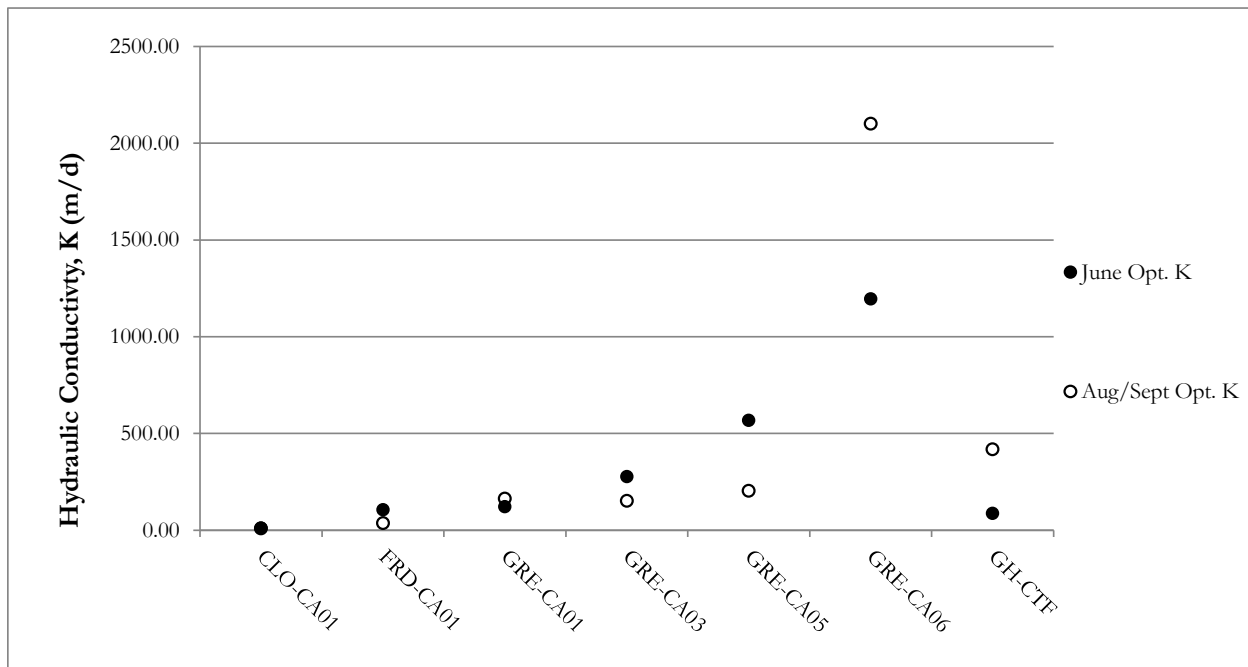
Hyporheic flow estimates generated with the temperature method were within the expected range and are considered reasonable. The 1DTempPro K optimization module produced accurate temperature gradients with a reasonable signal to noise ratio, indicating that the associated downwelling rates were reliable. Spatial variability, hydraulic head measurements, and disturbance associated with the thermistor installations are the greatest sources of uncertainty with the results.

##### *Hydraulic conductivity (K) and porosity estimation*

The estimates of K for each site using GSD relationships are provided in Table 15. These initial estimates were used as a starting point to numerically optimize K within 1DTempPro (Figure 13). The difference between GSD-based estimates and 1DTempPro optimized estimates are presented in Table 16. During June, the 1DTempPro K estimates ranged from 9.9 m/d at CLO-CA01 to 1195.7 m/d at GRE-CA06. During August/September, the 1DTempPro estimates ranged from 9.2 m/d at CLO-CA01 to 2100 m/d at GRE-CA06.

The 1DTempPro optimized K estimates are expected to be more accurate than those using GSD relations. The optimized K values ranged from 1.2% to 61.15% of GSD based estimates (100% being a perfect match), which suggests that the GSD-based methods consistently overestimated relative to 1DTempPro. The K for substrate should remain constant through time, assuming no transport of bed material. 1DTempPro optimized K estimates from the June and August/September study periods were found to vary substantially; however, the difference between sites remained somewhat similar. The differences ranged from 66% decreases to 79% increases with no dominant seasonal trend. These differences are expected to result from measurement uncertainties (e.g., uncertainty in heat transport parameters of the sediment, or various differences in characteristics of sampling locations) rather than sediment transport.

Porosity estimates based on GSD are also presented in Table 15. Porosities ranged from 0.22 at CLO-CA01 to 0.47 at each of FRD-CA01, GH-GH1, and GRE-CA05, with an average of 0.39. The relatively high porosities result from the low fines percentage at many of the sites.

**Figure 13. Modelled K values using the K optimizer module in 1DTempPro.**

#### *Heat transport properties parameterization*

Groundwater exchange estimates were found to vary minimally when varying the thermal conductivity, sediment heat capacity, and dispersivity; therefore, these parameters were held constant for each stream and site. The parameters applied to each site and date included the following:

- 2.3 Watts/m<sup>2</sup>°C for thermal conductivity, which was the average from Lapham (1989) based on an approximate bulk density range of 1850 to 1950 g/cc estimated using the methods of Wright *et al.* (2005);
- 0.055 m for dispersivity using Zheng and Bennett (2002); and
- 2384880 Joules/m<sup>3</sup> °C for sediment heat capacity, which was the average of values provided by Lapham (1989) and Bianchin *et al.* (2010).

Groundwater exchange estimates varied greatly for K and VH<sub>G</sub>, as expected, and minimally for porosity.

#### *Modelled groundwater exchange using 1DTempPro*

Modelled groundwater exchange rates using the K optimization module in 1DTempPro are shown in Table 16 and Figure 14. Time series of measured and modelled thermal profiles are provided for each site and date in Appendix F and Appendix G. Since hydraulic head values at 0.35 m depth were averaged at each site and transect, resulting in mean flow direction being downwelling for all sites

and periods. The range of values was much smaller than that of the hydraulic head method, and closer to typical values cited in the literature.

On average, the downwelling rate was weaker during the August/September study period at Fording River and Clode Creek Settling Pond System, and stronger at Greenhills Creek, similar to the results of the hydraulic head method. The strongest downwelling rates were observed at Fording Creek, followed by Clode Creek Settling Pond System, which is also consistent with the hydraulic head method.

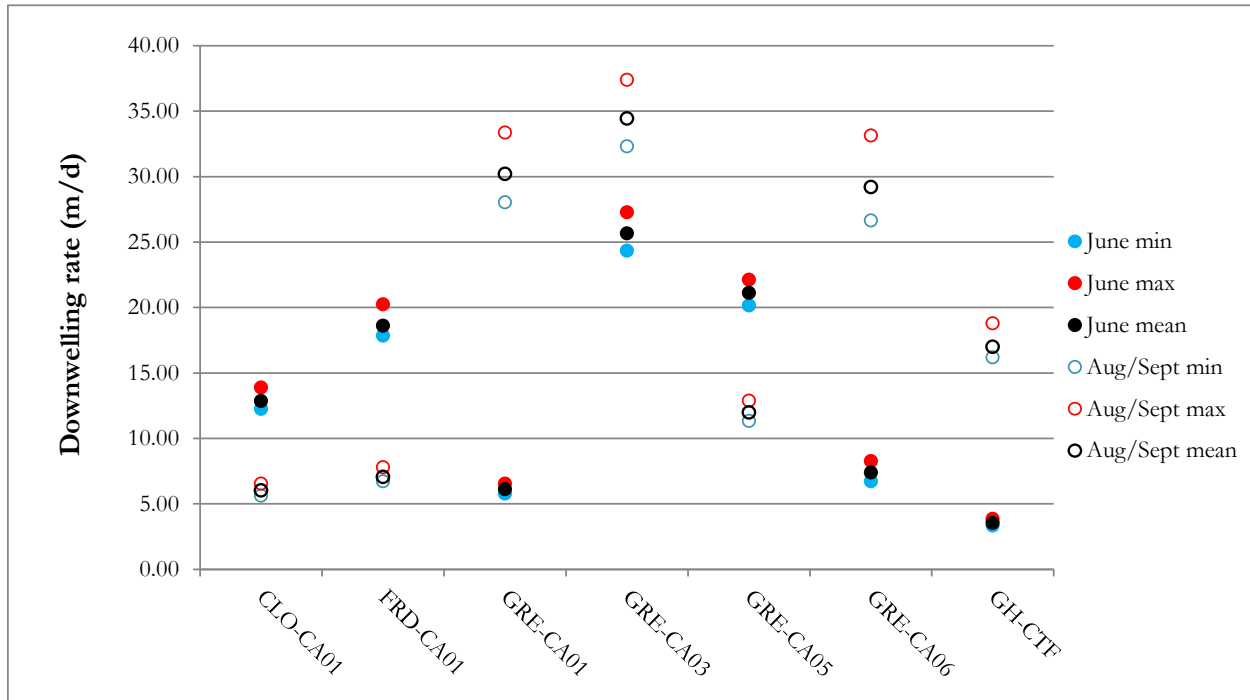
Downwelling rates in Table 16 were averaged over the approximately five days of each study period. In Figure 14, the minimum and maximum rates per period are also shown. The rates were typically strongest in the evening and weakest in the morning, as expected from daily increase in evapotranspiration demand (Gribovszki *et al.* 2010).

The root mean squared error (RMSE) of the measured vs. modelled thermal gradient using 1DTempPro was calculated for each site and date (Table 16). The RMS values were all lower than the Tidbit accuracy of 0.2 °C, indicating that the results were reliable. The RMS ranged from 0.015 °C to 0.167 °C with an average of 0.083 °C. The highest RMS values were at GH-CTF, which resulted from a change in thermal gradient midway through the June study period, which may have been from bed material transport. When only modelling the first half of the June study period, the GH-CTF RMS reduces to 0.065 °C.

**Table 16. Modelled groundwater exchange rates using the K optimizer module in 1DTempPro.**

Site	Optimized K (m/d)		Diff. between Opt. and Est. K (%)		Modelled q using Opt. K (m/d)		June to Aug/Sept Δq (%)	Modelled accuracy (RMS, °C)			
	June	Aug/Sept	June	Aug/Sept	June	Aug/Sept		June		Aug/Sept	
								Opt. K	Est. K	Opt. K	Est. K
FRD-CA01	106.0	36.3	2.6%	0.9%	<b>18.6</b>	<b>7.1</b>	38%	0.046	0.057	0.094	0.132
CLO-CA01	9.9	9.2	1.2%	1.1%	<b>12.9</b>	<b>6.0</b>	47%	0.085	0.094	0.033	0.075
GRE-CA01	121.0	162.4	9.3%	12.4%	<b>6.1</b>	<b>30.2</b>	494%	0.080	0.113	0.065	0.078
GRE-CA03	276.8	150.8	8.2%	4.5%	<b>25.6</b>	<b>34.4</b>	134%	0.039	0.043	0.015	0.021
GRE-CA05	567.4	203.6	15.4%	5.5%	<b>21.1</b>	<b>12.0</b>	57%	0.072	0.076	0.072	0.088
GRE-CA06	1195.7	2100.0	34.8%	61.1%	<b>7.4</b>	<b>29.2</b>	395%	0.115	0.132	0.043	0.044
GH_CTF	86.4	417.0	3%	14%	<b>3.5</b>	<b>17.0</b>	480%	0.167	0.167	0.130	0.135

Figure 14. Modelled groundwater exchange rates using the K optimizer module in 1DTempPro.



*Theoretical wetted channel length*

The theoretical wetted channel lengths were each lower than expected based on channel morphology, indicating that the downwelling was likely hyporheic rather than flow loss (Table 17). Longer theoretical channel lengths would be expected based on assessment of tributary confluence frequency and observations that the channels are wetted in Google Earth images from August 31, 2013. However, inflows were not calculated and would increase the theoretical wetted length. The June theoretical wetted lengths ranged from 97 m for CLO-CA01 to 2476 m for GH-CTF, with an average of 844 m. The August/September theoretical wetted lengths ranged from 37 m for GRE-CA06 to 762 m for FRD-CA01, with an average of 200 m.

**Table 17. Theoretical wetted length based on downwelling rates modelled with 1DTempPro, assuming all downwelling flows are lost.**

Site	Width (m)	Downwelling, q (m/d)		Nearest measured streamflow (cms)		Theoretical wetted length (m) <sup>1</sup>	
		June	Aug/Sept	June	Aug/Sept	June	Aug/Sept
FRD-CA01	9.8	18.61	7.06	1.31	0.61	621	762
CLO-CA01	5.03	12.86	6.02	0.07	0.13	97	371
GRE-CA01	3.12	6.12	30.21	0.24	0.04	1086	37
GRE-CA03	2.28	25.65	34.43	0.24	0.04	355	44
GRE-CA05	4.2	21.11	11.97	0.24	0.04	234	69
GRE-CA06	2.25	7.39	29.20	0.20	0.03	1039	39
GH-CTF	1.97	3.54	16.99	0.20	0.03	2476	77

<sup>1</sup> Assumes downwelling flow is lost from the system, i.e. no hyporheic exchange.

#### 4.1.5.3. Uncertainty in Hyporheic Flow Estimates

The assumption of a uniform substrate column required for 1DTempPro K optimization is not supported by the apparent variance in VHG found at different depths within the substrate, which adds uncertainty to the hyporheic flow estimates. Variation in VHG at different depths within the streambed was also observed by Birkel *et al.* (2016), which suggests that vertical variations in K may be common. Since the piezometer sites where VHGs were measured were not at the exact location of the thermal profiles, and VHG at each depth varied within transects, it was assumed that estimating a transect-averaged stratigraphy may introduce more uncertainty. It is also not possible to optimize K with varying stratigraphy in the current version of 1DTempPro; the advantages of using the K optimizer were expected to outweigh the uncertainty associated with varying stratigraphy.

Hyporheic exchange rate, including both downwelling and upwelling, is positively correlated with stream gradient and sinuosity (Moore *et al.* 2005). Inspection of the thermal profile study sites (Appendix A) suggests that GRE-CA03 and GRE-CA06 should have the strongest downwelling potential, without considering the effects of substrate GSD. The GRE-CA03 site was adjacent to a lower elevation side channel that may have resulted in lateral hyporheic flow, and as expected, GRE-CA03 had the strongest 1DTempPro modelled downwelling during the June and August/September periods. The GRE-CA06 downwelling potential appeared high based on visual observations of the relatively steep gradient, and this site had the third strongest downwelling during the August/September period; however, it was the third weakest in June.

The strength of the thermal gradient and variation in timing and strength of diurnal temperature signal with depth was moderate at most sites, but trace at CLO-CA01, FRD-CA01, and GRE-CA03 during both study periods. The reason for the lack of these signals is unclear, as the downwelling at

CLO-CA01 and FRD-CA01 were similar to other sites where thermal gradient was strong and variation in diurnal signal with depth was more pronounced.

It should be noted that the hyporheic exchange rate estimations using 1DTempPro represent a spatial point estimate; exchange rates may vary spatially within and among channel units (Birkel *et al.* 2016). Based on an understanding of substrate heat exchange rates, it is conceivable that strong downwelling at the head of a riffle with subsequent lateral flow to a thermistor site may be hard to distinguish from weak downwelling at the measurement site. Hyporheic flow paths may be complicated within a channel unit, which was evidenced by the variable head differential measurements across transects. Therefore, approximations of channel unit-scale exchange rates based on a single point are not recommended.

The variable head differential measurements at piezometer sites and across the transects is likely due to natural heterogeneity of interstitial flow at different points across the stream. Variance may be a function of several factors, including measurement error, piezometer water level not stabilizing, and fluctuations in river and interstitial flow (especially at 10 cm depth). To obtain accurate water level measurements and ensure that flow within the piezometer had reached equilibrium (i.e., water levels inside and outside of the piezometers remained consistent and stable), water levels measurements were repeated a minimum of three times (and until equilibrium was reached) at each piezometer. Even with these replicates, water levels differed among replicate measurements by up to 6 cm at some sites. In September, one of the piezometers at GRE-CA06 did not reach equilibrium before the end of the field day and measurements had to be abandoned (measurements had been made over a 3-hour period prior). Equilibrium times at this site were considerably longer than the 15 minute equilibrium seen at GRE-CA02, GRE-CA05 and GH-CTF. Fortunately, inaccurate hydraulic head estimates are largely compensated for in 1DTempPro by changes to the K value during optimization. For example, changing the hydraulic head value from 0.557 m to 0.01 m for the CLO-CA01 June model only resulted in a decrease in downwelling rate from 12.86 to approximately 12.7 m/d.

Surface flow across the piezometer transect was variable at some sites (e.g., CLO-CA01, GRE-CA01, and GRE-CA05) with the presence of preferential flow paths due to differences in streambed topography that may also have had an impact on interstitial flow paths resulting in higher amounts of downwelling at some piezometer sites than others. The different directions in flow may also be due to substrate characteristics at depth, particularly at Clode Creek Settling Pond System where the bed had been constructed by machinery.

The installation of thermistors within the bed was also expected to influence preferential flow paths by breaking up surface calcite and mixing of substrates where arrays were buried; this may have exaggerated downwelling rates. If a confining layer, such as calcite, restricted downwelling, the act of digging a hole to install thermistors may have opened a preferential flow path to a sublayer of lower hydraulic head. However, this process would not explain the strong downwelling observed at sites without a confining layer (e.g., FRD-CA01).

## 4.2. Testing the Impact Hypothesis

### 4.2.1. Statistical Modelling of Hyporheic Conditions vs. Calcite

CI was an important predictor of DO conditions in the substrate, but not of either response variable of hyporheic flow. Table 18 shows the top model (i.e., the best combination of variables) for each response variable quantified using the Akaike Information Criterion, corrected for small sample sizes (AICc). The top model weight refers to the likelihood that the specified top model is the best model among all other possible combinations of predictor variables considered.

For DO, the top model included CI score, depth in the substrate, the CI score\*depth interaction, and percent fines as predictors (Figure 15, Figure 16). This model is 88% likely to be the best model at predicting DO among the candidate models considered (Table 18). The effect of surface CI was influenced by depth in the substrate (i.e., there was a significant CI by depth interaction). At shallow depths in the substrate, surface CI was found to not have a strong effect on DO. In contrast, DO at deeper depths was influenced by surface CI (Figure 15). The model-averaged coefficients (with 95% confidence intervals) are plotted in Figure 16 for each predictor variable found in the set of top models with  $\Delta AICc < 4$ . Relative variable importance (RVI) scores indicate the likelihood that each variable shown occurs in the top set of models and is a measure of variable importance relative to other variables. DO also decreased with depth in the substrate and with increasing % fines of the substrate.

Hyporheic flow calculated via the hydraulic head method increased with increasing depth in the substrate, but was not affected by CI score (Figure 17, Table 18). The top model included only depth as a predictor, while the averaged model included percent fines. However, depth was the only coefficient in the averaged model to be significantly different from zero, suggesting it is the only variable to have a significant relationship with hyporheic flow. CI did not affect hyporheic flow as calculated via the hydraulic head method; however, it should be noted that the actual estimates of hyporheic flow were considered to be unreliable.

Hyporheic flow calculated via the temperature method was not predicted strongly by CI score or any of the habitat variables (Figure 18, Table 18). The intercept-only model was the top model. While the averaged model included substrate size, flow, percent fines, and season as predictors, all of these variables had importance values of  $\sim 0.1$  and p-values greater than 0.05, indicating weak relationships between these predictors and hyporheic flow as calculated via the temperature method.

The results of this modelling analysis suggest that CI score has no significant relationship with hyporheic flow calculated from either method. However, there is evidence that surface CI has a depth-dependent relationship with dissolved oxygen concentration.

Figure 15. Scatterplot of DO in the substrate versus CI score. Lines indicate the predicted relationships between DO and CI at different depths in the substrate based on the model that best predicts DO.

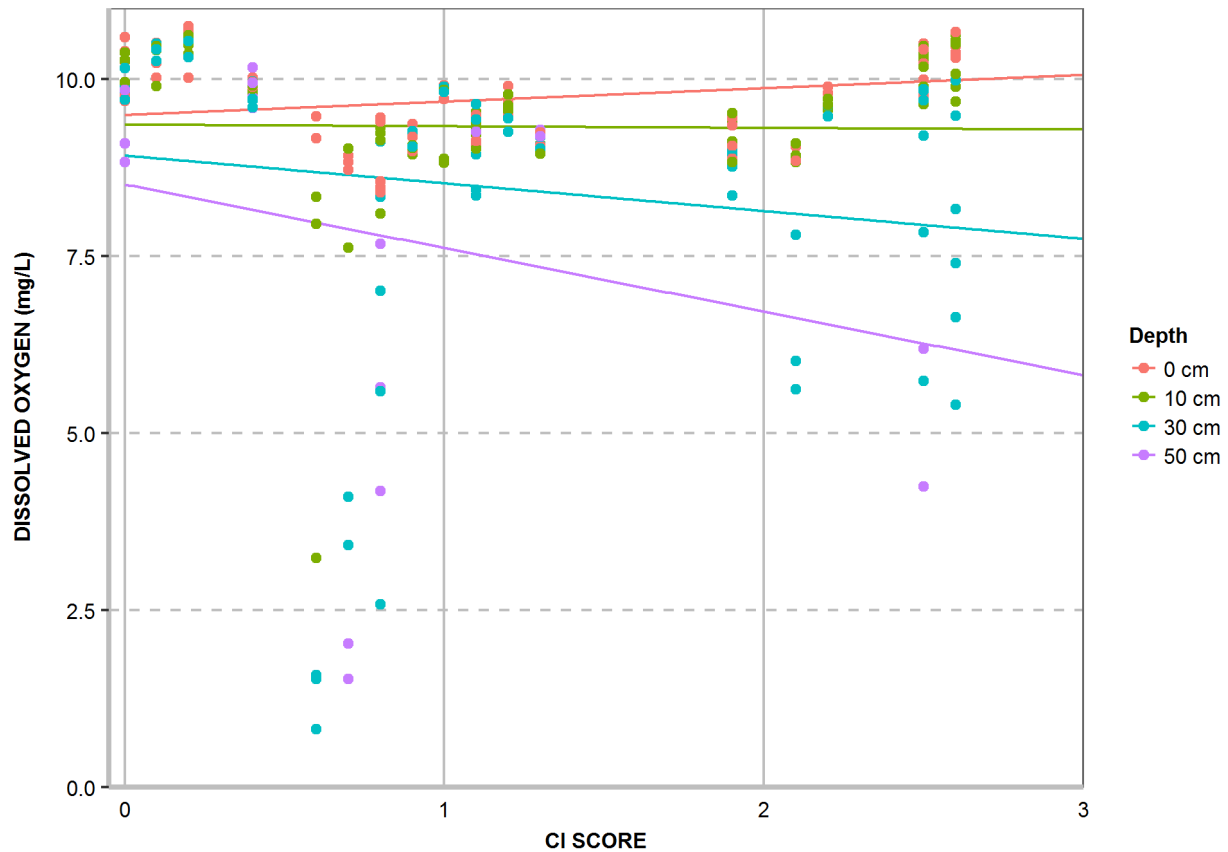


Table 18. Summary of top models for each of three response variables representing hyporheic conditions.

Response Variable <sup>2</sup>	Fixed Effects <sup>2</sup>	df	AICc	$\Delta$ AICc <sup>3</sup>	Weight <sup>4</sup>
Dissolved Oxygen	CI Score, Depth, CI Score*Depth, % Fines	7	758.70	3.92	0.877
Hyporheic Flow (Hydraulic Head Method)	Intercept, Depth	4	130.80	3.59	0.857
Hyporheic Flow (Temperature Method)	Intercept Only	3	30.80	3.42	0.601

<sup>1</sup> Random effects: Site

<sup>2</sup> All variables except for Dissolved Oxygen were scaled by subtracting the mean and dividing by twice the standard deviation

<sup>3</sup> Change in AICc from top model to next best model

<sup>4</sup> Weight in averaged model

**Figure 16.** Model averaged coefficients (with 95% confidence intervals) indicating the most important variables predicting hyporheic dissolved oxygen. RVI = Relative Variable Importance scores, where a score of 1 indicates that a predictor variable occurs in all top models with  $\Delta AICc < 4$ . p-values represent probability that the coefficient is equal to 0.

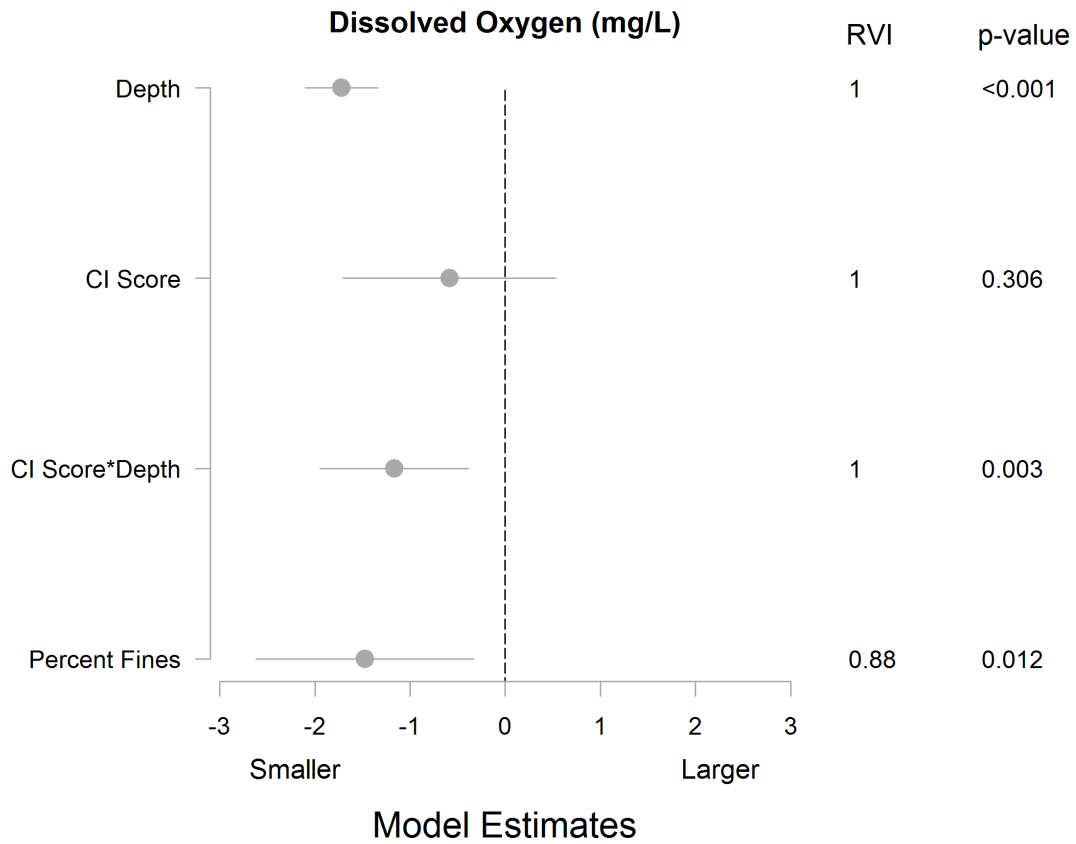


**Figure 17.** Model averaged coefficients (with 95% confidence intervals) indicating the most important variables predicting hyporheic flow using the hydraulic head method. RVI = Relative Variable Importance scores, where a score of 1 indicates that a predictor variable occurs in all top models with  $\Delta AICc < 4$ . p-values represent probability that the coefficient is equal to 0.

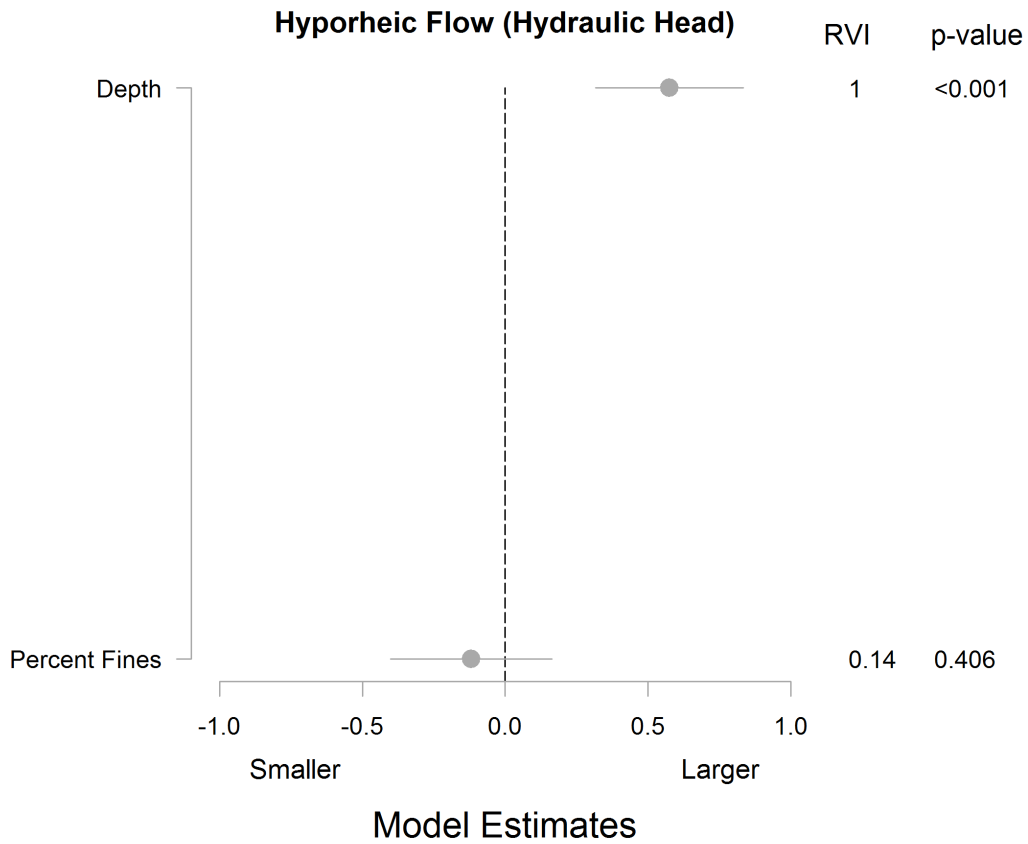
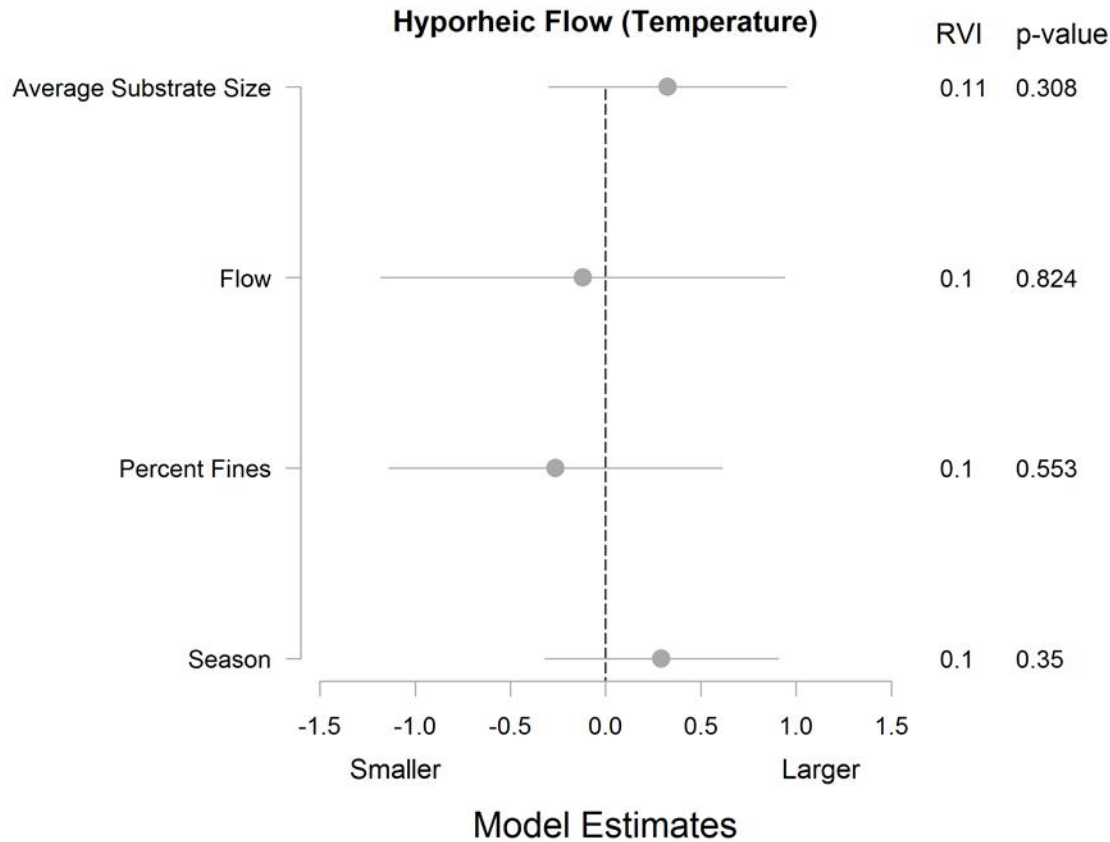


**Figure 18.** Model averaged coefficients (with 95% confidence intervals) indicating the most important variables predicting hyporheic flow using the temperature method. RVI = Relative Variable Importance scores, where a score of 1 indicates that a predictor variable occurs in all top models with  $\Delta AICc < 4$ . p-values represent probability that the coefficient is equal to 0.



## 5. DISCUSSION AND CONSIDERATIONS

### 5.1. Fish Habitat, Calcite Index, and Hyporheic Conditions

The purpose of this study was to assess the extent to which hyporheic DO and flow are influenced by calcite in the Upper Fording watershed. A number of physical and chemical habitat variables were measured along with hyporheic and calcite conditions to test for potential covariates when relating hyporheic DO and flow to calcite. Hyporheic DO and flow are of interest due to their influence on incubation success of salmonid eggs buried in stream substrates.

CI measured at the mesohabitat scale showed good agreement and low variance with CI measured within the mesohabitat, suggesting that the CI score at the mesohabitat scale is representative of calcite presence and concretion at smaller scales within the mesohabitat. A number of seasonal

factors can contribute to the precipitation or dissolution of calcite, including physical forces (e.g., scouring of the substrate during high flow turbid periods) and water chemistry (water temperature, pH, composition of dissolved ions and minerals), therefore timing and location of calcite formation can sometimes be difficult to predict (Minnow Environmental 2016). That said, there was low variation in CI score by season of collection (June vs. August/September) for the sites we studied. Data presented here show relative consistency in CI within each mesohabitat unit, but there was high spatial and temporal variance in the response and predictor variables within the sites.

In general, DO declined with increased depth in the substrate. However, DO varied among sites and depths; for example, DO ranged from 0.99 mg/L to 10.8 mg/L among measurements in Greenhills Creek. Logistical challenges in the measurement of DO included difficulties in achieving consistent sampling depths at piezometer sites.

Piezometers were also used to measure hyporheic flows. These results showed consistent direction in flow across seasons, though the magnitude likely has some error. The hyporheic flow estimates derived from the hydraulic head method (using Darcy's equation) had high uncertainty due to variation in hydraulic head readings within the same transect, and due to the difficulty in accurately estimating hydraulic conductivity based on GSD relations (Section 4.1.5.3). A more accurate estimate of hydraulic head may be possible with the installation of pressure transducers and data loggers inside and outside of the piezometers over a few days to average the noise in the data caused by rapid fluctuations in water level associated with turbulence. However, this would require a substantial increase in effort. Use of a stilling well around the piezometer may also improve the measurements.

The hyporheic downwelling rates estimated using the K optimization module in 1DTempPro are thought to be reasonably reliable; the RMS error of the measured vs. modelled thermal gradient using 1DTempPro calculated for each site and date were all lower than the Tidbit accuracy (Section 4.1.5.2). Thermistor installation could be improved by inserting sensors into a specialized piezometer before installing them into the streambed. This would reduce disturbance to the streambed and potentially result in a greater substrate-hydraulic connection with the temperature sensor. However, this would require a substantial increase in effort.

No relationship in downwelling rates among sites could be discerned using the estimates from thermistor arrays. This result may be partially due to the low number of sites (n=7) and lack of replication with this method. The downwelling rates modelled with the temperature method were higher than other similar studies but within the range of infiltration/downwelling rates for sand-gravel substrate. The higher than expected downwelling rates could be a result of a low floodplain groundwater table relative to stream water elevation, since the tributary streams investigated are influenced by settling ponds except GH\_CTF and GRE-CA06. A comparison of the wetted lengths in relation to the channel morphology at the study sites showed that the measured groundwater exchange is largely hyporheic as opposed to lateral inflow, which is not surprising given that the measurements were taken within shallow substrate (Section 4.1.5.2).

The direction of flow measured by the hydraulic head method was consistent among and within piezometer sites, streams, and seasons, even in areas with high calcite presence. Though there is high discrepancy in the magnitude of downwelling exchange we are confident that the direction of flow is correct given the number of sites showing this head differential with depth; this result was reinforced by the temperature method results. Though hyporheic flow estimates from the hydraulic head method tended to be unrealistic, the magnitude of downwelling estimated from the temperature method was more in line with literature values.

Several precautions were taken to ensure that the piezometers were not simply sampling surface water. Hydraulic head, flow, DO and other water quality measurements showed a gradient with depth from the streambed surface, which strongly suggests consistent sampling of hyporheic water rather than surface water. Time to reach equilibrium was tested at a number of sites during both study periods; these times were consistent, suggesting we sampled under steady-state conditions. Measurements were not recorded until water levels inside and outside of the piezometer were consistent for a minimum of 20 minutes. A dowel was used during installation to prevent water from entering the inside of the piezometer as it was being hammered into the substrate. In future, we recommend use of a slightly smaller screen height for the piezometer (e.g., 10 cm rather than the 14 cm height used here). We also suggest testing other ways to purge the piezometer of any surface water (e.g., pumping out the piezometer), and comparing results to methods used here.

## 5.2. Testing the Impact Hypothesis

Analyses using this relatively small pilot dataset show that the CI score was an important predictor of DO in the substrate but not of hyporheic flow. DO in the substrate decreased with increasing depth in the substrate and with higher % fines. For example, the lower Greenhills sites (GRE-CA01 and GRE-CA02) had high % fines and low DO, particularly deeper in the substrate. However, DO was not explained solely by depth and percent fines. The Clode Creek Settling Pond System sites (CLO-CA01 and CLO-CA02) also had high percent fines and these sites did not exhibit low DO in the substrate.

CI was an important predictor of DO concentrations in the substrate, but this effect increased with depth in the substrate. This result is intuitive, in that shallow depths within the substrate likely experience DO and water exchange with the surface water column even in the presence of high CI. Such exchange may be generally sufficient to replenish DO and offset biological and chemical DO consumption in shallow substrates, whereas the exchange is less at greater depths within the substrate and therefore more influenced by biological and chemical DO consumption. The model for DO predicts that average instantaneous DO would not decrease below 6 mg/L at a depth of 30 cm, even at a CI score of 3 (blue predicted line in Figure 15). At a depth of 50 cm, average instantaneous DO is predicted to decrease below 6 mg/L at a CI Score of near 3 (purple predicted line in Figure 15).

The average redd depth for Westslope Cutthroat Trout is between 10 and 30 cm (DeVries 1997, Magee and McMahon 1996). Using a maximum egg deposition depth of 30 cm, our model predicts

that average dissolved oxygen concentrations during incubation will be above 6 mg/L (the instantaneous minimum threshold for buried embryos/alevins from the BC Guidelines for Protection of Aquatic Life) at all levels of calcite in the stream. However, these model predictions represent mean conditions, and exceedances of the BC Guidelines are likely at some sites, particularly where fines occur in conjunction with high CI scores. We conclude that sites with high levels of calcite are likely to experience some reduction in incubation conditions for Westslope Cutthroat Trout, a rejection of the null impact hypothesis H1. Nevertheless, we caution that this is a small dataset and the effect of calcite on DO is most apparent at depths that are deeper than typical redd depths of Westslope Cutthroat Trout.

A further consideration is that Westslope Cutthroat Trout may not spawn frequently in substrates with CI scores greater than ~1 (Minnow Environmental 2016). DO concentrations below the minimum guidelines for the protection of buried life stages were observed in this study, but the most severe effects on incubation conditions are predicted at sites with CI scores higher than 1, relatively high % fines, and at depths deeper than typical redd depths. This suggests that at depths less than 30 cm, DO concentrations and interstitial flow may not be as important a limiting factor as access to high quality spawning gravels. Additional effort may therefore be better placed on understanding the relation between CI and fish spawning, the current availability of useable spawning habitats, and any trends in availability.

CI was not a predictor of hyporheic flow as measured with the hydraulic head or temperature methods. Estimates from the hydraulic head method were considered unreliable, at least in terms of absolute magnitude. By comparison, the temperature method-derived hyporheic flow estimates were within published ranges, but the sample size was limited and there is some uncertainty as to whether the estimates were accurate enough to adequately test H<sub>1</sub>. A preliminary conclusion would be that calcite presence and concretion does not substantively impede surface flow into the substrate, which is reinforced by the DO results.

We acknowledge that the results of this study were obtained from two tributaries and one mainstem site, which may not fully represent the conditions occurring throughout the larger area of interest. Nevertheless, the methods were employed at 12 sites in three very different streams with large variations in environmental conditions (e.g., CI, stream width, substrate type and size, flow velocity, and water depth), and repeated in early summer and late summer. Hyporheic and environmental conditions were highly heterogeneous both among and within the 12 sites, the 36 piezometer sampling points (72 including the late summer sampling period), and with depth. Despite the range in conditions, the DO and hydraulic head measurements were relatively consistent across sites, lending confidence that these methods and results are applicable to a wider range of settings in the Elk Valley. The results presented in this report should be considered by Teck and the Environmental Monitoring Committee in relation to future work on calcite and potential effects to Westslope Cutthroat Trout in the Elk Valley watershed.

**REFERENCES**

- Bates, D., Maechler, M., Bolker, B. and Walker, S. 2015. Fitting linear mixed-effects models using lme4. *Journal of Statistical Software* 67(1): 1-48.
- B.C. Research. 1981. Greenhills surface coal mining project stage II environmental assessment. Prepared for Kaiser Resources Ltd., Sparwood, B.C. Prepared by B.C. Research, Vancouver, B.C.
- Beswick, S.M. 2007. Greenhills Creek fish stream identification. Report prepared for Elk Valley Coal Corporation, Elkford, B.C. Prepared by Kootenay Natural Resource Consulting. 14 p.
- Bianchin M., L. Smith and R. Beckie. 2010. Quantifying Hyporheic Exchange in a Tidal River Using Temperature Time Series. *Water Resources Research*,. doi:10.1029/2009WR008365.
- Birkel, C., C. Soulsby, D.J. Irvine, I. Malcolm, L.K. Lautz and D. Tetzlaff. 2016. Heat-Based Hyporheic Flux Calculations in Heterogeneous Salmon Spawning Gravels. *Aquatic Sciences* 78 (2). Springer Basel: 203–13. doi:10.1007/s00027-015-0417-4.
- Briggs, M.A., E.B., Voytek, F.D. Day-Lewis, D.O. Rosenberry and J.W. Lane. 2013. Understanding Water Column and Streambed Thermal Refugia for Endangered Mussels in the Delaware River [Link exits the USGS web site]: *Environmental Sciences and Technology*: v. 47, no. 20, p. 11423-11431. doi:10.1021/es4018893.
- Clark, M.J.R.E. 2003. British Columbia Field Sampling Manual. Water, Air and Climate Change Branch, Ministry of Water, Land and Air Protection, Victoria, BC, Canada. 312 pp.
- Cope, S., C.J. Schwarz, A. Prince and J. Bisset. 2016. Upper Fording River Westslope Cutthroat Trout Population Assessment and Telemetry Project: Final Report. Report Prepared for Teck Coal Limited4, Sparwood, BC. Report Prepared by Westslope Fisheries Ltd., Cranbrook, BC. 259 p.
- DeVries, P.E. 1997. Riverine Salmonid Egg Burial Depths: Review of Published Data and Implications for Scour Studies. *Canadian Journal of Aquatic and Fisheries Science* 54: 1685-1698.
- Domenico, P.A. and F.W. Schwartz. 1990. *Physical and Chemical Hydrogeology*. Wiley Press, p. 324.
- Gribovszki, Z., J. Szilágyi and P. Kalicz. 2010. Diurnal Fluctuations in Shallow Groundwater Levels and Streamflow Rates and Their Interpretation – A Review. *Journal of Hydrology* 385 (1-4). Elsevier B.V.: 371–83. doi:10.1016/j.jhydrol.2010.02.001.
- Grueber, C.E., S. Nakagawa, R.J. Laws and I.G. Jamieson. 2011. Multimodel inference in ecology and evolution: challenges and solutions. *Journal of Evolutionary Biology* 24: 699-711.

- Johnston, N.T. and P.A. Slaney. 1996. Fish habitat assessment procedures. Watershed Restoration Technical Circular No. 8 (revised April 1996). Watershed Restoration Program. Ministry of Environment, Lands and Parks and Ministry of Forests, Victoria BC.
- Kalbus, E., F. Reinstorf and M. Schirmer. 2006. Measuring Methods for Groundwater - Surface Water Interactions: A Review. *Hydrology and Earth System Sciences* 10 (6): 873–87.
- Koch, F.W., E.B. Voytek, F.D. Day-Lewis, R. Healy, M.A. Briggs, D. Werkema, and J.W. Lane, Jr. 2015. 1DTempPro: A program for analysis of vertical one-dimensional (1D) temperature profiles v2.0: U.S. Geological Survey Software Release, 23 July 2015, <http://dx.doi.org/10.5066/F76T0JQS>.
- Lapham, WW. 1989. Use of temperature profiles beneath streams to determine rates of vertical ground-water flow and vertical hydraulic conductivity. USGS Water-Supply Paper 2337, 35 p.
- Lewis, A., T. Hatfield, B. Chilibeck and C. Roberts. 2004. Assessment methods for aquatic habitat and instream flow characteristics in support of applications to dam, divert, or extract water from streams in British Columbia. Report prepared for the Ministry of Water, Land and Air Protection and the Ministry of Sustainable Resource Management. Available online at: [http://www.env.gov.bc.ca/wld/documents/bmp/assessment\\_methods\\_instreamflow\\_in\\_b.c.pdf](http://www.env.gov.bc.ca/wld/documents/bmp/assessment_methods_instreamflow_in_b.c.pdf). Last Accessed November 17, 2016
- Lister and Kerr Wood Leidal (Lister, D.B. and Associates Ltd. and Kerr Wood Leidal Associates Ltd). 1980. Fording River Aquatic Environment Study. Prepared for Fording Coal Limited, Elkford, B.C. 77 pp. + app.
- Magee, J.P. and T.E. McMahon. 1996. Spatial Variation in Spawning Habitat of Cutthroat Trout in a Sediment-Rich Stream Basin. *American Fisheries Society* 125:768-779. 1996. Available online at: <http://www.montana.edu/mcmahon/Magee%20basin%20Sed%20TAFS%20'96.pdf>. Accessed on December 8, 2016.
- Massman, J.W. and C.D. Butchart. 2001. Infiltration Characteristics, Performance, and Design of Storm Water Facilities. Prepared for Washington State Transportation Commission, May, 2001.
- Minnow Environmental Ltd. 2014. Evaluation of Calcite Effects On Benthic Invertebrate Communities and Periphyton Productivity in the Elk River Watershed (2014) Prepared for Teck Coal Limited Sparwood, BC, September 2014.
- Minnow Environmental Ltd. 2015. Design for the Regional Aquatic Effects Monitoring Program (RAEMP), Elk River Watershed. Prepared for Teck Coal Limited Sparwood, BC, March 2015.
- Minnow Environmental Inc. 2016. Evaluation of calcite effects on aquatic biota in the Elk Valley (2014 & 2015). Prepared for Teck Coal Ltd. 44 pp + appendices.

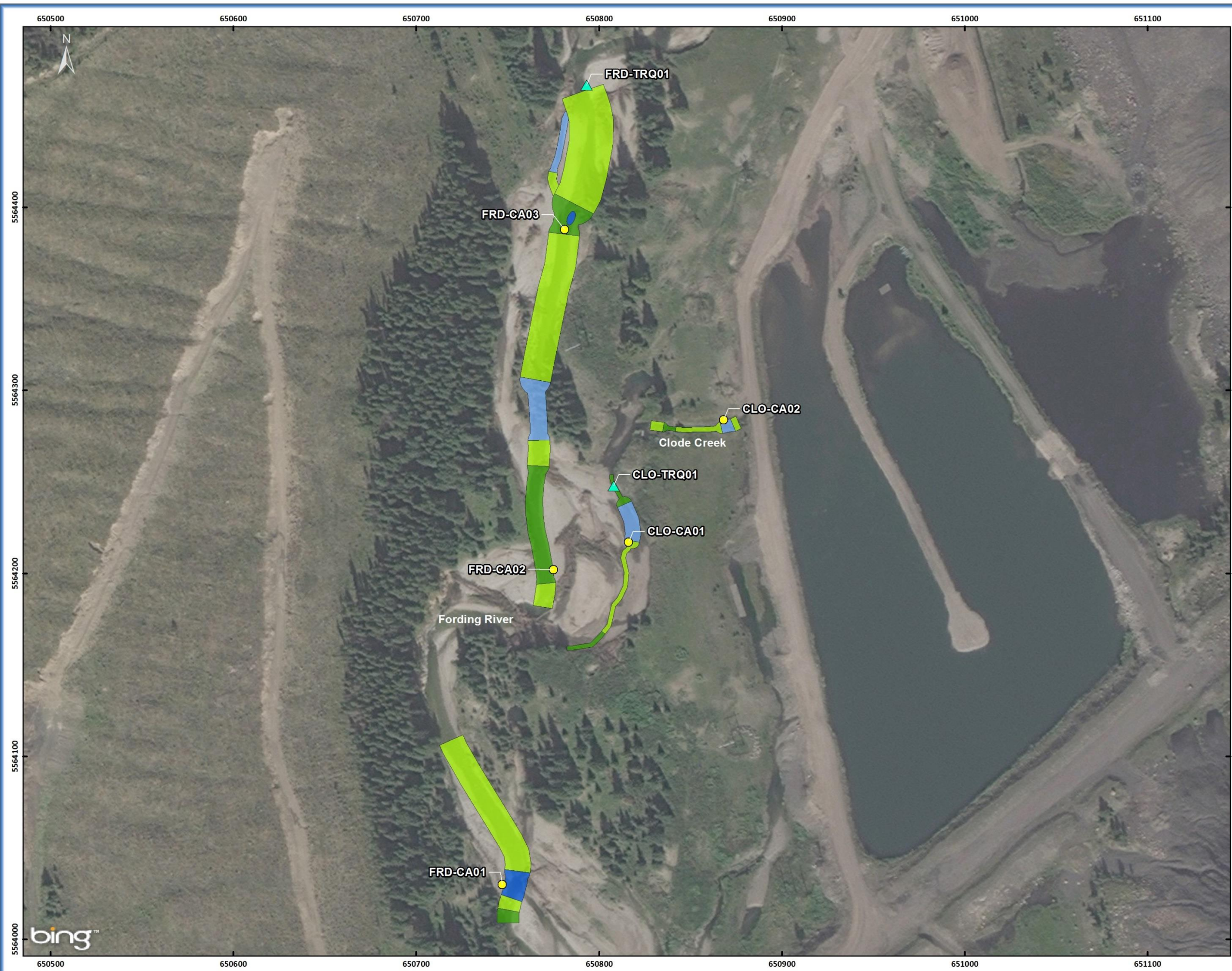
- MOE (B.C. Ministry of Environment). 1997a. Ambient water quality criteria for dissolved oxygen: overview report. Prepared pursuant to Section 2(e) of the Environment Management Act, 1981. Signed by Don Fast, Assistant Deputy Minister, Environment Lands HQ Division. Available online at: [http://www.env.gov.bc.ca/wat/wq/BCguidelines/do/do\\_over.html](http://www.env.gov.bc.ca/wat/wq/BCguidelines/do/do_over.html). Accessed on January 11, 2015.
- MOE (B.C. Ministry of Environment). 1997b. Ambient water quality criteria for dissolved oxygen: technical appendix. Prepared pursuant to Section 2(e) of the Environment Management Act, 1981. Signed by Don Fast, Assistant Deputy Minister, Environment and Lands HQ Division. Available online at: <http://www.env.gov.bc.ca/wat/wq/BCguidelines/do/index.html>. Accessed on January 11, 2015.
- MOE (B.C. Ministry of Environment). 2016. Approved Water Quality Guidelines. Available online at: <http://www2.gov.bc.ca/gov/content/environment/air-land-water/water/water-quality/water-quality-guidelines/approved-water-quality-guidelines>. Accessed on July 6, 2016.
- Moore, R.D., D. L. Spittlehouse and A. Story. 2005. Riparian Microclimate and Stream Temperature Response to Forest Harvesting: A Review. *Journal of the American Water Resources Association (JAWRA)* 41(4):813-834.
- Oliver, G.G. 1999. Fish and Fish Habitat Assessment at Designated Sites in the Upper Fording River. Prepared by Interior Reforestation Co. Ltd., Cranbrook, BC. Prepared for Fording Coal Limited (Fording River Operations), Elkford, B.C. 47 pp. + app.
- Oliver, G. G., and L. E. Fidler. 2001. Towards a water quality guideline for temperature in the Province of British Columbia. Prepared for Ministry of Environment, Lands and Parks, Water Management Branch, Water Quality Section, Victoria, B.C. Prepared by Aspen Applied Sciences Ltd., Cranbrook, BC. Available online at: <http://www2.gov.bc.ca/assets/gov/environment/air-land-water/water/waterquality/wqgs-wqos/approved-wqgs/temperature-tech.pdf>. Accessed on April 18, 2017.
- Rantz, S.E. and others. 1982. Measurement and Computation of Streamflow: Volume 1. Measurement of Stage and Discharge. Geological Survey Water Supply Paper 2175. 284 pp. Available online at: [http://pubs.usgs.gov/wsp/wsp2175/pdf/WSP2175\\_vol1a.pdf](http://pubs.usgs.gov/wsp/wsp2175/pdf/WSP2175_vol1a.pdf) Last Accessed November 28, 2016.
- RISC. 1998. Guidelines for Interpreting Water Quality Data. Prepared by the BC Ministry of Environment, Lands and Parks for the Resource Inventory Commission. Available online at: <http://archive.ilmb.gov.bc.ca/risc/pubs/aquatic/interp/index.htm>. Accessed on January 11, 2015.
- RISC. 2003. Ambient Freshwater and Effluent Sampling Manual. Prepared by the Resource Inventory Standards Committee. Available online at:

- [http://www.for.gov.bc.ca/hts/risc/pubs/aquatic/ambient/part\\_e\\_water\\_and\\_wastewater\\_sampling\\_ambient\\_freshwater\\_and\\_effluent\\_sampling\\_simulate\\_template.pdf](http://www.for.gov.bc.ca/hts/risc/pubs/aquatic/ambient/part_e_water_and_wastewater_sampling_ambient_freshwater_and_effluent_sampling_simulate_template.pdf). Accessed on January 12, 2014.
- RISC. 2009. Manual of British Columbia hydrometric standards (Version 1.0). Prepared by Ministry of Environment, Science and Information Branch, Victoria, BC. Available online at: [https://www.for.gov.bc.ca/hts/risc/pubs/aquatic/hydrometric/man\\_BC\\_hydrometric\\_standard\\_V1.0.pdf](https://www.for.gov.bc.ca/hts/risc/pubs/aquatic/hydrometric/man_BC_hydrometric_standard_V1.0.pdf) Accessed November 27, 2015.
- Robinson, M.D. and R.J. MacDonald. 2014. Teck Coal Ltd 2013 Calcite Monitoring Program - Elk Valley Operations Summary Report. Prepared by Lotic Environmental Ltd. Available online at: [http://www2.gov.bc.ca/assets/gov/environment/waste-management/industrial-waste/industrial-waste/mining-smelt-energy/area-based-man-plan/annexes/j3\\_2013\\_calcite\\_monitoring\\_program.pdf](http://www2.gov.bc.ca/assets/gov/environment/waste-management/industrial-waste/industrial-waste/mining-smelt-energy/area-based-man-plan/annexes/j3_2013_calcite_monitoring_program.pdf). Accessed on October 28, 2016.
- Robinson, M.D., M. Chernos, K. Baranowska and R.J. MacDonald. 2016. Teck Coal Ltd. – Elk Valley 2015 Calcite Monitoring Program Annual Report and Program Assessment. Prepared for Teck Coal Ltd. by Lotic Environmental Ltd. 17 pp. + appendices.
- Salarashayeri, A.F. and M. Siosemarde. 2012. Prediction of Soil Hydraulic Conductivity from Particle-Size Distribution. *International Journal of Environmental, Chemical, Ecological, Geological and Geophysical Engineering*, Vol 6 (1): 16–20.
- She, K., D.P. Horn and P. Canning. 2006. Porosity and Hydraulic Conductivity of Mixed Sand-Gravel Sediment. In *Flood and Coastal Risk Management*, At York.
- Teck Resources Limited. 2014. Elk Valley Water Quality Plan. Sparwood, BC. Available at: [http://www.teck.com/media/2015-Water-elk\\_valley\\_water\\_quality\\_plan\\_T3.2.3.2.pdf](http://www.teck.com/media/2015-Water-elk_valley_water_quality_plan_T3.2.3.2.pdf)
- Weaver, T.M. and J.J. Fraley. 1993. A Method to Measure Emergence Success of Westslope Cutthroat Trout Fry from Varying Substrate Compositions in a Natural Stream Channel. *North American Journal of Fisheries Management*, 13(4):817-822.
- Windward Environmental, Minnow Environmental Inc. and CH2M Hill Limited. 2014. Elk River watershed and Lake Koocanusa, British Columbia Aquatic environment synthesis report 2014. Report Prepared for Teck Coal Limited, Sparwood, B.C. 223 p. including 5 app.
- Wright, J., L. Amos and A. Edeburn. 2001. 2000 Fish and Fish Habitat Monitoring in the Henretta Creek Drainage. Report prepared for Fording Coal Limited, Elkford, B.C. Prepared by Interior Reforestation Co. Ltd. Cranbrook, BC. -58 pp.
- Wright, J., F. Nixon, S. Dallimore, J. Henniges and M. Côté. 2005. Thermal conductivity of sediments within the gas-hydrate-bearing interval at the JAPEX/JNOC/GSC et al. Mallik 5L- 38 gas hydrate production research well. *Bulletin-Geological Survey of Canada*, 585, 129.

Zheng, C. and G.D. Bennett. 2002. Applied Contaminant Transport Modeling, 2nd Edition, ISBN: 978-0-471-38477-9.

Zuur, A.F., E. N. Ieno, N.J. Walker, A.A. Saveliev and G.M. Smith. 2009. Mixed effects models and extensions in ecology with R. Springer, New York.

## PROJECT MAPS

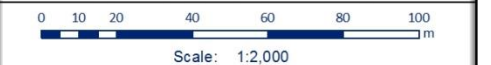


TECK COAL LTD.  
**Clode Creek and Fording River  
 Calcite Monitoring Sites, FHAP  
 Type and Discharge Locations**

- Legend**
- Calcite Monitoring Site
  - ▲ Discharge Measurement Location
- FHAP Type**
- Glide
  - Pool
  - Riffle
  - Run



**MAP SHOULD NOT BE USED FOR LEGAL  
 OR NAVIGATIONAL PURPOSES**



NO.	DATE	REVISION	BY
1	16/11/2016	1229_CalciteEffectsStudy_2016Oct27	CGA
2			
3			
4			
5			

Date Saved: 16/11/2016  
 Coordinate System: NAD 1983 UTM Zone 11N


Map 2



TECK COAL LTD.  
**Greenhills Creek, GH-CTF  
 Calcite Monitoring Site and  
 FHAP Type**

- Legend**
- Calcite Monitoring Site
  - FHAP Type**
  - Cascade
  - Riffle



**MAP SHOULD NOT BE USED FOR LEGAL  
 OR NAVIGATIONAL PURPOSES**

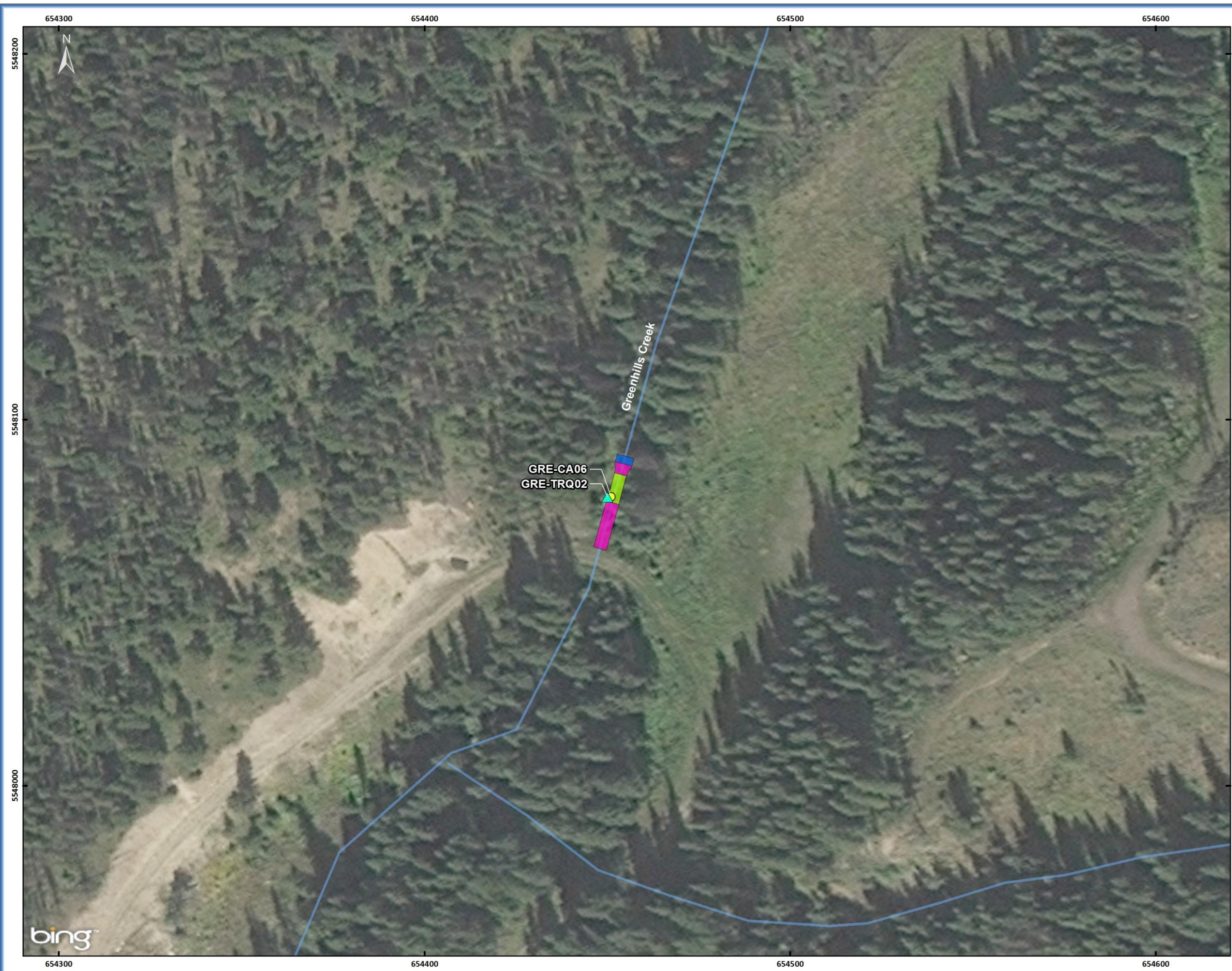


NO.	DATE	REVISION	BY
1	16/11/2016	1229_CalciteEffectsStudy_2016Oct27	CGA
2			
3			
4			
5			

Date Saved: 16/11/2016  
 Coordinate System: NAD 1983 UTM Zone 11N


Map 3





TECK COAL LTD.  
**Greenhills Creek GRE-CA06  
 Calcite Monitoring Site, FHAP  
 Type and Discharge Location**

- Legend**
- Calcite Monitoring Site
  - ▲ Discharge Measurement Location
- FHAP Type**
- Cascade
  - Pool
  - Riffle



**MAP SHOULD NOT BE USED FOR LEGAL  
 OR NAVIGATIONAL PURPOSES**



NO.	DATE	REVISION	BY
1	16/11/2016	1229_CalciteEffectsStudy_2016Oct27	CGA
2			
3			
4			
5			

Date Saved: 16/11/2016  
 Coordinate System: NAD 1983 UTM Zone 11N


Map 4



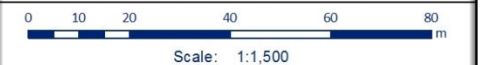


TECK COAL LTD.  
**Greenhills Creek Calcite  
 Monitoring Sites, FHAP Type  
 and Discharge Locations**

- Legend**
- Calcite Monitoring Site
  - ▲ Discharge Measurement Location
- FHAP Type**
- Glide
  - Pool
  - Riffle



**MAP SHOULD NOT BE USED FOR LEGAL  
 OR NAVIGATIONAL PURPOSES**



NO.	DATE	REVISION	BY
1	16/11/2016	1229_CalciteEffectsStudy_2016Oct27	CGA
2			
3			
4			
5			

Date Saved: 16/11/2016  
 Coordinate System: NAD 1983 UTM Zone 11N

Map 5

## APPENDICES

**Appendix A. Calcite Study Site Photographs.**

**LIST OF FIGURES**

Figure 1. Looking downstream at GRE-CA01 on June 19, 2016.....1

Figure 2. Looking RR to RL at GRE-CA01 temperature array on June 18, 2016. ....1

Figure 3. Looking downstream at GRE-CA01 on August 30, 2016. ....2

Figure 4. Looking RR to RL at GRE-CA01 temperature array on August 29, 2016.....2

Figure 5. Looking downstream at GRE-CA02 on June 19, 2016.....3

Figure 6. Looking downstream at GRE-CA02 on September 3, 2016.....3

Figure 7. Looking upstream at GRE-CA03 on June 21, 2016. ....4

Figure 8. Looking RL to RR at GRE-CA03 temperature array on June 18, 2016. ....4

Figure 9. Looking upstream at GRE-CA03 on September 3, 2016.....5

Figure 10. Looking RL to RR at GRE-CA03 temperature array on August 29, 2016.....5

Figure 11. Looking upstream at GH\_GH1 on June 20, 2016.....6

Figure 12. Looking downstream at GH\_GH1 on June 20, 2016.....6

Figure 13. Looking upstream at GH\_GH1 on September 2, 2016. ....7

Figure 14. Looking downstream at GH\_GH1 on September 2, 2016.....7

Figure 15. Looking upstream at GRE-CA05 on June 20, 2016. ....8

Figure 16. Looking RR to RL at GRE-CA05 temperature array on June 18, 2016. ....8

Figure 17. Looking upstream at GRE-CA05 on September 2, 2016.....9

Figure 18. Looking RR to RL at GRE-CA05 temperature array on August 29, 2016.....9

Figure 19. Looking RL to RR at GRE-CA06 on June 26, 2016. ....10

Figure 20. Looking RL to RR at GRE-CA06 temperature array on June 24, 2016. ....10

Figure 21. Looking upstream at GRE-CA06 on September 1, 2016.....11

Figure 22. Looking RL to RR at GRE-CA06 temperature array on August 30, 2016.....11

Figure 23. Looking RL to RR at GH\_CTF on June 26, 2016.....12

Figure 24. Looking downstream at GH\_CTF temperature array on June 24, 2016. ....12

Figure 25. Looking RL to RR at GH\_CTF on September 1, 2016. ....13

Figure 26. Looking downstream at GH\_CTF temperature array on August 30, 2016.....13

Figure 27. Looking upstream at CLO-CA01 on June 25, 2016.....14

Figure 28. Looking RL to RR at CLO-CA01 temperature array on June 21, 2016.....14

Figure 29. Looking upstream at CLO-CA01 on September 4, 2016.....15

Figure 30. Looking downstream at CLO-CA01 temperature array on August 31, 2016. ....15

Figure 31. Looking downstream at CLO-CA02 on June 23, 2016. ....16

Figure 32. Looking RL to RR at CLO-CA02 on June 23, 2016.....16

Figure 33. Looking downstream at CLO-CA02 on September 4, 2016. ....17

Figure 34. Looking RL to RR at CLO-CA02 on June 23, 2016.....17

Figure 35. Looking RL to RR at FRD-CA01 on June 25, 2016.....18

Figure 36. Looking upstream at FRD-CA01 on June 25, 2016.....18

Figure 37. Looking downstream at FRD-CA01 temperature array on June 25, 2016. ....19

Figure 38. Looking RL to RR at FRD-CA01 on September 5, 2016.....19

Figure 39. Looking upstream at FRD-CA01 on September 5, 2016.....20

Figure 40. Looking downstream at FRD-CA01 temperature array on August 31, 2016.....20

Figure 41. Looking downstream at FRD-CA02 on June 25, 2016. ....21

Figure 42. Looking RL to RR at FRD-CA02 on June 25, 2016.....21

Figure 43. Looking upstream at FRD-CA02 on September 5, 2016.....22

Figure 44. Looking RL to RR at FRD-CA02 on September 5, 2016. ....22

Figure 45. Looking upstream at FRD-CA03 on June 22, 2016.....23

Figure 46. Looking downstream at FRD-CA03 on June 22, 2016. ....23

Figure 47. Looking RL to RR at FRD-CA03 on June 22, 2016.....24

Figure 48. Looking upstream at FRD-CA03 on September 6, 2016.....24

Figure 49. Looking downstream at FRD-CA03 on September 6, 2016.....25

Figure 50. Looking RL to RR at FRD-CA03 on September 6, 2016. ....25

Figure 1. Looking downstream at GRE-CA01 on June 19, 2016.



Figure 2. Looking RR to RL at GRE-CA01 temperature array on June 18, 2016.



Figure 3. Looking downstream at GRE-CA01 on August 30, 2016.



Figure 4. Looking RR to RL at GRE-CA01 temperature array on August 29, 2016.



Figure 5. Looking downstream at GRE-CA02 on June 19, 2016.



Figure 6. Looking downstream at GRE-CA02 on September 3, 2016.



Figure 7. Looking upstream at GRE-CA03 on June 21, 2016.



Figure 8. Looking RL to RR at GRE-CA03 temperature array on June 18, 2016.



Figure 9. Looking upstream at GRE-CA03 on September 3, 2016.



Figure 10. Looking RL to RR at GRE-CA03 temperature array on August 29, 2016.



Figure 11. Looking upstream at GH\_GH1 on June 20, 2016.



Figure 12. Looking downstream at GH\_GH1 on June 20, 2016.



Figure 13. Looking upstream at GH\_GH1 on September 2, 2016.



Figure 14. Looking downstream at GH\_GH1 on September 2, 2016.



Figure 15. Looking upstream at GRE-CA05 on June 20, 2016.



Figure 16. Looking RR to RL at GRE-CA05 temperature array on June 18, 2016.



Figure 17. Looking upstream at GRE-CA05 on Septmeber 2, 2016.



Figure 18. Looking RR to RL at GRE-CA05 temperature array on August 29, 2016.



Figure 19. Looking RL to RR at GRE-CA06 on June 26, 2016.



Figure 20. Looking RL to RR at GRE-CA06 temperature array on June 24, 2016.



Figure 21. Looking upstream at GRE-CA06 on September 1, 2016.



Figure 22. Looking RL to RR at GRE-CA06 temperature array on August 30, 2016.



Figure 23. Looking RL to RR at GH\_CTF on June 26, 2016.



Figure 24. Looking downstream at GH\_CTF temperature array on June 24, 2016.



Figure 25. Looking RL to RR at GH\_CTF on September 1, 2016.



Figure 26. Looking downstream at GH\_CTF temperature array on August 30, 2016.



Figure 27. Looking upstream at CLO-CA01 on June 25, 2016.



Figure 28. Looking RL to RR at CLO-CA01 temperature array on June 21, 2016.



Figure 29. Looking upstream at CLO-CA01 on September 4, 2016.



Figure 30. Looking downstream at CLO-CA01 temperature array on August 31, 2016.



Figure 31. Looking downstream at CLO-CA02 on June 23, 2016.



Figure 32. Looking RL to RR at CLO-CA02 on June 23, 2016.



Figure 33. Looking downstream at CLO-CA02 on September 4, 2016.



Figure 34. Looking RL to RR at CLO-CA02 on June 23, 2016.



Figure 35. Looking RL to RR at FRD-CA01 on June 25, 2016.



Figure 36. Looking upstream at FRD-CA01 on June 25, 2016.



Figure 37. Looking downstream at FRD-CA01 temperature array on June 25, 2016.



Figure 38. Looking RL to RR at FRD-CA01 on September 5, 2016.



Figure 39. Looking upstream at FRD-CA01 on September 5, 2016.



Figure 40. Looking downstream at FRD-CA01 temperature array on August 31, 2016.



Figure 41. Looking downstream at FRD-CA02 on June 25, 2016.



Figure 42. Looking RL to RR at FRD-CA02 on June 25, 2016.



Figure 43. Looking upstream at FRD-CA02 on September 5, 2016.



Figure 44. Looking RL to RR at FRD-CA02 on September 5, 2016.



Figure 45. Looking upstream at FRD-CA03 on June 22, 2016.



Figure 46. Looking downstream at FRD-CA03 on June 22, 2016.



Figure 47. Looking RL to RR at FRD-CA03 on June 22, 2016.



Figure 48. Looking upstream at FRD-CA03 on September 6, 2016.



Figure 49. Looking downstream at FRD-CA03 on September 6, 2016.



Figure 50. Looking RL to RR at FRD-CA03 on September 6, 2016.



**Appendix B. Fish Habitat Assessment Procedure (FHAP) Data and Photographs**

**LIST OF TABLES**

Table 1.	FHAP Assessment information for FRD-CA01 collected on June 21, 2016. ....	1
Table 2.	FHAP Assessment information for FRD-CA02 collected on June 23, 2016. ....	1
Table 3.	FHAP Assessment information for FRD-CA03 collected on June 22, 2016. ....	1
Table 4.	FHAP Assessment information for CLO-CA01 collected on June 23, 2016. ....	2
Table 5.	FHAP Assessment information for CLO-CA02 collected on June 23, 2016. ....	2
Table 6.	FHAP Assessment information for GRE-CA01 collected on June 18, 2016. ....	2
Table 7.	FHAP Assessment information for GRE-CA02 collected on June 18, 2016. ....	3
Table 8.	FHAP Assessment information for GRE-CA03 collected on June 18, 2016. ....	3
Table 9.	FHAP Assessment information for GH_GH1/GRE-CA05 collected on June 18, 2016. ....	3
Table 10.	FHAP Assessment information for GRE-CA06 collected on June 24, 2016. ....	4
Table 11.	FHAP Assessment information for GH_CTF collected on June 24, 2016. ....	4

**LIST OF FIGURES**

Figure 1. Looking upstream at FRD-CA01 FHAP assessment Unit 1 on June 21, 2016.....5

Figure 2. Looking upstream at FRD-CA01 FHAP assessment Unit 2 on June 21, 2016.....5

Figure 3. Looking upstream at FRD-CA01 FHAP assessment Unit 3 on June 21, 2016.....6

Figure 4. Looking upstream at FRD-CA01 FHAP assessment Unit 4 on June 21, 2016.....6

Figure 5. Looking upstream at FRD-CA02 FHAP assessment Unit 1 on June 23, 2016.....7

Figure 6. Looking upstream at FRD-CA02 FHAP assessment Unit 2 on June 23, 2016.....7

Figure 7. Looking upstream at FRD-CA02 FHAP assessment Unit 3 on June 23, 2016.....8

Figure 8. Looking upstream at FRD-CA02 FHAP assessment Unit 4 on June 23, 2016.....8

Figure 9. Looking upstream at FRD-CA03 FHAP assessment Unit 1 on June 22, 2016.....9

Figure 10. Looking upstream at FRD-CA03 FHAP assessment Unit 2 on June 22, 2016.....9

Figure 11. Looking upstream at FRD-CA03 FHAP assessment Unit 2A on June 22, 2016.....10

Figure 12. Looking upstream at FRD-CA03 FHAP assessment Unit 3 on June 22, 2016.....10

Figure 13. Looking upstream at FRD-CA03 FHAP assessment Unit 3A on June 22, 2016.....11

Figure 14. Looking upstream at FRD-CA03 FHAP assessment Unit 3B on June 22, 2016.....11

Figure 15. Looking upstream at CLO-CA01 FHAP assessment Unit 1 on June 23, 2016.....12

Figure 16. Looking upstream at CLO-CA01 FHAP assessment Unit 2 on June 23, 2016.....12

Figure 17. Looking upstream at CLO-CA01 FHAP assessment Unit 3 on June 23, 2016.....13

Figure 18. Looking upstream at CLO-CA01 FHAP assessment Unit 4 on June 23, 2016.....13

Figure 19. Looking upstream at CLO-CA02 FHAP assessment Unit 1 on June 23, 2016.....14

Figure 20. Looking upstream at CLO-CA02 FHAP assessment Unit 2 on June 23, 2016.....14

Figure 21. Looking downstream at CLO-CA02 FHAP assessment Unit 3 on June 23, 2016.....15

Figure 22. Looking upstream at CLO-CA02 FHAP assessment Unit 4 on June 23, 2016.....15

Figure 23. Looking river-left to river-right at CLO-CA02 FHAP assessment Unit 5 on June 23, 2016. ....16

Figure 24. Looking upstream at GRE-CA01 FHAP assessment Unit 1 on June 18, 2016.....16

Figure 25. Looking upstream at GRE-CA01 FHAP assessment Unit 2 on June 18, 2016.....17

Figure 26. Looking upstream at GRE-CA02 FHAP assessment Unit 1 on June 18, 2016.....17

Figure 27. Looking upstream at GRE-CA02 FHAP assessment Unit 2 on June 18, 2016.....18

Figure 28. Looking upstream at GRE-CA03 FHAP assessment Unit 1 on June 18, 2016.....18

Figure 29. Looking upstream at GRE-CA03 FHAP assessment Unit 2 on June 18, 2016.....19

Figure 30. Looking upstream at GRE-CA03 FHAP assessment Unit 3 on June 18, 2016.....19

Figure 31. Looking upstream at GRE-CA03 FHAP assessment Unit 4 on June 18, 2016.....20

Figure 32. Looking upstream at GH\_GH1/GRE-CA05 FHAP assessment Unit 1 on June 18, 2016.  
.....20

Figure 33. Looking upstream at GH\_GH1/GRE-CA05 FHAP assessment Unit 2 on June 18, 2016.  
.....21

Figure 34. Looking upstream at GRE-CA06 FHAP assessment Unit 1 on June 24, 2016.....21

Figure 35. Looking upstream at GRE-CA06 FHAP assessment Unit 2 on June 24, 2016.....22

Figure 36. Looking upstream at GRE-CA06 FHAP assessment Unit 3 on June 24, 2016.....22

Figure 37. Looking upstream at GRE-CA06 FHAP assessment Unit 4 on June 24, 2016.....23

Figure 38. Looking upstream at GH\_CTF FHAP assessment Unit 1 on June 24, 2016. ....23

Figure 39. Looking upstream at GH\_CTF FHAP assessment Unit 2 on June 24, 2016. ....24

Figure 40. Looking upstream at GH\_CTF FHAP assessment Unit 3 on June 24, 2016. ....24

**Table 1. FHAP Assessment information for FRD-CA01 collected on June 21, 2016.**

Unit Number	Type	Category	Unit Length (m)	Width		Area		Average Water Depth (m)	Gradient (%)	Weighted Gradient (%)	Substrate <sup>1</sup>		Dominant Cover <sup>2</sup>		Sub-dominant Cover <sup>2</sup>	
				Wetted Width (m)	Bankfull Width (m)	Wetted Area (m <sup>2</sup> )	Bankfull Area (m <sup>2</sup> )				Dominant	Sub-dominant	Type	%	Type	%
1	Run	Primary	7.0	6.1	12.0	42.7	84.0	0.78	0.5	3.5	GR	CO	LWD	5	CU	5
2	Riffle	Primary	6.8	7.0	12.0	47.6	81.6	0.44	1.5	10.2	CO	GR	OV	TR	CU	TR
3	Pool <sup>3</sup>	Primary	15.2	9.1	12.1	138.3	183.9	1.20	0.0	0.0	GR	S/FI	DP	40	LWD	30
4	Riffle	Primary	75.0	9.0	14.0	675.0	1050.0	0.41	2.5	187.5	CO	GR	-	-	-	-

<sup>1</sup> BO = Boulder, CO = Cobble, GR = Gravel, S/FI = Sand/Fines

<sup>2</sup> BO = Boulder, DP = Deep Pool, LWD = Large Woody Debris, LC = Large Cobble, CU = Undercut Bank, OV = Overhead Vegetation

<sup>3</sup> Location of monitoring site.

**Table 2. FHAP Assessment information for FRD-CA02 collected on June 23, 2016.**

Unit Number	Type	Category	Unit Length (m)	Width		Area		Average Water Depth (m)	Gradient (%)	Weighted Gradient (%)	Substrate <sup>1</sup>		Dominant Cover <sup>2</sup>		Sub-dominant Cover <sup>2</sup>	
				Wetted Width (m)	Bankfull Width (m)	Wetted Area (m <sup>2</sup> )	Bankfull Area (m <sup>2</sup> )				Dominant	Sub-dominant	Type	%	Type	%
1	Riffle	Primary	13.0	9.1	10.7	118.3	139.1	0.28	2.5	32.5	BO	CO	BO	5	LWD	TR
2	Run <sup>3</sup>	Primary	65.0	7.0	9.4	455.0	611.0	0.30	1.0	65.0	CO	GR	BO	TR	CU	TR
3	Riffle	Primary	14.0	8.0	12.0	112.0	168.0	0.27	2.0	28.0	CO	GR	LWD	TR	OV	TR
4	Glide	Primary	28.0	7.5	9.6	210.0	268.8	0.79	0.5	14.0	GR	CO	LWD	5	CU	5

<sup>1</sup> BO = Boulder, CO = Cobble, GR = Gravel, S/FI = Sand/Fines

<sup>2</sup> BO = Boulder, DP = Deep Pool, LWD = Large Woody Debris, LC = Large Cobble, CU = Undercut Bank, OV = Overhead Vegetation

<sup>3</sup> Location of monitoring site.

**Table 3. FHAP Assessment information for FRD-CA03 collected on June 22, 2016.**

Unit Number	Type	Category	Unit Length (m)	Width		Area		Average Water Depth (m)	Gradient (%)	Weighted Gradient (%)	Substrate <sup>1</sup>		Dominant Cover <sup>2</sup>		Sub-dominant Cover <sup>2</sup>	
				Wetted Width (m)	Bankfull Width (m)	Wetted Area (m <sup>2</sup> )	Bankfull Area (m <sup>2</sup> )				Dominant	Sub-dominant	Type	%	Type	%
1	Riffle	Primary	87.0	11.0	17.0	957.0	1479.0	0.34	1.0	87.0	CO	GR	CU	TR	OV	TR
2	Run	Primary <sup>3</sup>	12.0	7.0	14.0	84.0	168.0	0.46	0.5	6.0	CO	GR	LWD	10	DP	5
2A	Pool	Tertiary	8.0	2.1	-	16.8	0.0	0.71	0.0	0.0	GR	CO	LWD	40	DP	30
3	Riffle	Primary	62.0	9.0	24.0	558.0	1488.0	0.36	1.0	62.0	CO	GR	LWD	TR	CU	TR
3A	Riffle	Secondary	24.0	2.8	4.9	67.2	117.6	0.08	1.5	36.0	GR	CO	BO	TR	SWD	TR
3B	Glide	Secondary	35.0	2.6	3.6	91.0	126.0	0.19	0.5	17.5	S/FI	GR	CU	5	SWD	TR

<sup>1</sup> BO = Boulder, CO = Cobble, GR = Gravel, S/FI = Sand/Fines

<sup>2</sup> BO = Boulder, DP = Deep Pool, LWD = Large Woody Debris, LC = Large Cobble, CU = Undercut Bank, OV = Overhead Vegetation

<sup>3</sup> Location of monitoring site.

**Table 4. FHAP Assessment information for CLO-CA01 collected on June 23, 2016.**

Unit Number	Type	Category	Unit Length (m)	Width		Area		Average Water Depth (m)	Gradient (%)	Weighted Gradient (%)	Substrate <sup>1</sup>		Dominant Cover <sup>2</sup>		Sub-dominant Cover <sup>2</sup>	
				Wetted Width (m)	Bankfull Width (m)	Wetted Area (m <sup>2</sup> )	Bankfull Area (m <sup>2</sup> )				Dominant	Sub-dominant	Type	%	Type	%
1	Run	Primary	23.0	2.15	2.35	49.5	54.1	0.13	0.50	11.5	GR	S/FI	LWD	TR	OV	TR
2	Riffle <sup>3</sup>	Primary	55.0	2.05	2.50	112.8	137.5	0.14	1.00	55.0	GR	S/FI	IV	10	OV	5
3	Glide	Primary	21.0	6.60	8.40	138.6	176.4	0.10	0.25	5.3	S/FI	GR	IV	3	OV	TR
4	Run	Primary	18.0	1.90	2.05	34.2	36.9	0.16	0.50	9.0	GR	S/FI	IV	5	OV	TR

<sup>1</sup> BO = Boulder, CO = Cobble, GR = Gravel, S/FI = Sand/Fines

<sup>2</sup> BO = Boulder, DP = Deep Pool, LWD = Large Woody Debris, LC = Large Cobble, CU = Undercut Bank, OV = Overhead Vegetation

<sup>3</sup> Location of monitoring site.

**Table 5. FHAP Assessment information for CLO-CA02 collected on June 23, 2016.**

Unit Number	Type	Category	Unit Length (m)	Width		Area		Average Water Depth (m)	Gradient (%)	Weighted Gradient (%)	Substrate <sup>1</sup>		Dominant Cover <sup>2</sup>		Sub-dominant Cover <sup>2</sup>	
				Wetted Width (m)	Bankfull Width (m)	Wetted Area (m <sup>2</sup> )	Bankfull Area (m <sup>2</sup> )				Dominant	Sub-dominant	Type	%	Type	%
1	Riffle	Primary	7.0	4.9	5.20	34	36	0.13	1.0	7.0	GR	CO	IV	30	OV	25
2	Run	Primary	7.0	2.2	2.25	15	16	0.35	0.5	3.5	GR	CO	OV	5	IV	5
3	Riffle	Primary	25.0	2.5	2.80	63	70	0.23	1.5	37.5	CO	GR	IV	90	OV	5
4	Glide <sup>3</sup>	Primary	6.5	5.9	6.20	38	40	0.24	0.5	3.3	S/FI	GR	IV	5	OV	5
5	Riffle	Primary	1.9	7.0	7.30	13	14	0.16	1.0	1.9	BO	GR	BO	50	OV	TR

<sup>1</sup> BO = Boulder, CO = Cobble, GR = Gravel, S/FI = Sand/Fines

<sup>2</sup> BO = Boulder, DP = Deep Pool, LWD = Large Woody Debris, LC = Large Cobble, CU = Undercut Bank, OV = Overhead Vegetation

<sup>3</sup> Location of monitoring site.

**Table 6. FHAP Assessment information for GRE-CA01 collected on June 18, 2016.**

Unit Number	Type	Category	Unit Length (m)	Width		Area		Average Water Depth (m)	Gradient (%)	Weighted Gradient (%)	Substrate <sup>1</sup>		Dominant Cover <sup>2</sup>		Sub-dominant Cover <sup>2</sup>	
				Wetted Width (m)	Bankfull Width (m)	Wetted Area (m <sup>2</sup> )	Bankfull Area (m <sup>2</sup> )				Dominant	Sub-dominant	Type	%	Type	%
1	Riffle	Primary <sup>3</sup>	9.2	2.9	5.7	26.7	52.4	0.09	1.0	9.2	GR	CO	OV	20	CU	TR
2	Glide	Primary	21	2.5	3.5	52.5	73.5	0.20	0.5	10.5	GR	S/FI	CU	10	OV	10

<sup>1</sup> BO = Boulder, CO = Cobble, GR = Gravel, S/FI = Sand/Fines

<sup>2</sup> BO = Boulder, DP = Deep Pool, LWD = Large Woody Debris, LC = Large Cobble, CU = Undercut Bank, OV = Overhead Vegetation

<sup>3</sup> Location of monitoring site.

**Table 7. FHAP Assessment information for GRE-CA02 collected on June 18, 2016.**

Unit Number	Type	Category	Unit Length (m)	Width		Area		Average Water Depth (m)	Gradient (%)	Weighted Gradient (%)	Substrate <sup>1</sup>		Dominant Cover <sup>2</sup>		Sub-dominant Cover <sup>2</sup>	
				Wetted Width (m)	Bankfull Width (m)	Wetted Area (m <sup>2</sup> )	Bankfull Area (m <sup>2</sup> )				Dominant	Sub-dominant	Type	%	Type	%
1	Riffle	Primary	6.1	2.5	3.8	15.3	23.2	0.11	1.0	6.1	GR	CO	OV	10	CU	10
2	Glide	Primary <sup>3</sup>	105.8	2.6	3.5	275.1	370.3	0.25	0.5	52.9	S/FI	GR	CU	10	LWD	5

<sup>1</sup> BO = Boulder, CO = Cobble, GR = Gravel, S/FI = Sand/Fines

<sup>2</sup> BO = Boulder, DP = Deep Pool, LWD = Large Woody Debris, LC = Large Cobble, CU = Undercut Bank, OV = Overhead Vegetation

<sup>3</sup> Location of monitoring site.

**Table 8. FHAP Assessment information for GRE-CA03 collected on June 18, 2016.**

Unit Number	Type	Category	Unit Length (m)	Width		Area		Average Water Depth (m)	Gradient (%)	Weighted Gradient (%)	Substrate <sup>1</sup>		Dominant Cover <sup>2</sup>		Sub-dominant Cover <sup>2</sup>	
				Wetted Width (m)	Bankfull Width (m)	Wetted Area (m <sup>2</sup> )	Bankfull Area (m <sup>2</sup> )				Dominant	Sub-dominant	Type	%	Type	%
1	Glide	Primary	3.4	3.3	3.6	11.1	12.1	0.21	0.5	1.7	GR	CO	LWD	7.5	SWD	7.5
2	Riffle	Primary <sup>3</sup>	7.2	2.2	4.7	15.8	33.8	0.12	1.0	7.2	GR	CO	LWD	2.5	SWD	2.5
3	Glide	Primary	3.9	3.0	4.9	11.7	19.1	0.16	0.5	2.0	GR	CO	LWD	7.5	SWD	7.5
4	Riffle	Primary	15.8	3.0	6.4	47.4	101.1	0.14	2.0	31.6	CO	CO	LWD	5	SWD	5

<sup>1</sup> BO = Boulder, CO = Cobble, GR = Gravel, S/FI = Sand/Fines

<sup>2</sup> BO = Boulder, DP = Deep Pool, LWD = Large Woody Debris, LC = Large Cobble, CU = Undercut Bank, OV = Overhead Vegetation

<sup>3</sup> Location of monitoring site.

**Table 9. FHAP Assessment information for GH\_GH1/GRE-CA05 collected on June 18, 2016.**

Unit Number	Type	Category	Unit Length (m)	Width		Area		Average Water Depth (m)	Gradient (%)	Weighted Gradient (%)	Substrate <sup>1</sup>		Dominant Cover <sup>2</sup>		Sub-dominant Cover <sup>2</sup>	
				Wetted Width (m)	Bankfull Width (m)	Wetted Area (m <sup>2</sup> )	Bankfull Area (m <sup>2</sup> )				Dominant	Sub-dominant	Type	%	Type	%
1	Riffle	Primary <sup>3</sup>	42.4	3.2	4.3	135.7	182.3	0.17	3.0	127.2	CO	GR	OV	5	CU	5
2	Pool	Primary	6.0	5.6	7.5	33.6	45.0	1.07	0.0	0.0	CO	GR	DP	65	CU	TR

<sup>1</sup> BO = Boulder, CO = Cobble, GR = Gravel, S/FI = Sand/Fines

<sup>2</sup> BO = Boulder, DP = Deep Pool, LWD = Large Woody Debris, LC = Large Cobble, CU = Undercut Bank, OV = Overhead Vegetation

<sup>3</sup> Location of monitoring site.

**Table 10. FHAP Assessment information for GRE-CA06 collected on June 24, 2016.**

Unit Number	Type	Category	Unit Length (m)	Width		Area		Average Water Depth (m)	Gradient (%)	Weighted Gradient (%)	Substrate <sup>1</sup>		Dominant Cover <sup>2</sup>		Sub-dominant Cover <sup>2</sup>	
				Wetted Width (m)	Bankfull Width (m)	Wetted Area (m <sup>2</sup> )	Bankfull Area (m <sup>2</sup> )				Dominant	Sub-dominant	Type	%	Type	%
1	Cascade	Primary	13.0	2.5	3.6	32.5	46.8	0.17	7.0	91.0	CO	BO	OV	10	BO	5
2	Riffle	Primary <sup>3</sup>	8.0	2.1	3.3	16.8	26.4	0.14	1.5	12.0	GR	BO	OV	5	SWD	TR
3	Cascade	Primary	3.0	2.4	3.5	7.2	10.5	0.14	12.0	36.0	BO	CO	BO	25	OV	5
4	Pool	Primary	2.2	3.4	4.8	7.37	10.45	0.34	0.0	0.0	BO	S/FI	DP	50	LWD	5

<sup>1</sup> BO = Boulder, CO = Cobble, GR = Gravel, S/FI = Sand/Fines

<sup>2</sup> BO = Boulder, DP = Deep Pool, LWD = Large Woody Debris, LC = Large Cobble, CU = Undercut Bank, OV = Overhead Vegetation

<sup>3</sup> Location of monitoring site.

**Table 11. FHAP Assessment information for GH\_CTF collected on June 24, 2016.**

Unit Number	Type	Category	Unit Length (m)	Width		Area		Average Water Depth (m)	Gradient (%)	Weighted Gradient (%)	Substrate <sup>1</sup>		Dominant Cover <sup>2</sup>		Sub-dominant Cover <sup>2</sup>	
				Wetted Width (m)	Bankfull Width (m)	Wetted Area (m <sup>2</sup> )	Bankfull Area (m <sup>2</sup> )				Dominant	Sub-dominant	Type	%	Type	%
1	Cascade	Primary	15.0	2.2	3.1	33.0	46.5	0.18	5.0	75.0	CO	GR	OV	75	CU	5
2	Riffle	Primary <sup>3</sup>	10.0	1.7	2.9	16.5	28.5	0.11	2.0	20.0	CO	GR	OV	20	CU	TR
3	Cascade	Primary	15.0	1.8	2.8	26.3	41.3	0.14	5.0	75.0	CO	GR	OV	75	CU	5

<sup>1</sup> BO = Boulder, CO = Cobble, GR = Gravel, S/FI = Sand/Fines

<sup>2</sup> BO = Boulder, DP = Deep Pool, LWD = Large Woody Debris, LC = Large Cobble, CU = Undercut Bank, OV = Overhead Vegetation

<sup>3</sup> Location of monitoring site.

Figure 1. Looking upstream at FRD-CA01 FHAP assessment Unit 1 on June 21, 2016.



Figure 2. Looking upstream at FRD-CA01 FHAP assessment Unit 2 on June 21, 2016.



Figure 3. Looking upstream at FRD-CA01 FHAP assessment Unit 3 on June 21, 2016.



Figure 4. Looking upstream at FRD-CA01 FHAP assessment Unit 4 on June 21, 2016.



Figure 5. Looking upstream at FRD-CA02 FHAP assessment Unit 1 on June 23, 2016.



Figure 6. Looking upstream at FRD-CA02 FHAP assessment Unit 2 on June 23, 2016.



Figure 7. Looking upstream at FRD-CA02 FHAP assessment Unit 3 on June 23, 2016.



Figure 8. Looking upstream at FRD-CA02 FHAP assessment Unit 4 on June 23, 2016.



Figure 9. Looking upstream at FRD-CA03 FHAP assessment Unit 1 on June 22, 2016.



Figure 10. Looking upstream at FRD-CA03 FHAP assessment Unit 2 on June 22, 2016.



Figure 11. Looking upstream at FRD-CA03 FHAP assessment Unit 2A on June 22, 2016.



Figure 12. Looking upstream at FRD-CA03 FHAP assessment Unit 3 on June 22, 2016.



Figure 13. Looking upstream at FRD-CA03 FHAP assessment Unit 3A on June 22, 2016.



Figure 14. Looking upstream at FRD-CA03 FHAP assessment Unit 3B on June 22, 2016.



Figure 15. Looking upstream at CLO-CA01 FHAP assessment Unit 1 on June 23, 2016.



Figure 16. Looking upstream at CLO-CA01 FHAP assessment Unit 2 on June 23, 2016.



Figure 17. Looking upstream at CLO-CA01 FHAP assessment Unit 3 on June 23, 2016.



Figure 18. Looking upstream at CLO-CA01 FHAP assessment Unit 4 on June 23, 2016.



Figure 19. Looking upstream at CLO-CA02 FHAP assessment Unit 1 on June 23, 2016.



Figure 20. Looking upstream at CLO-CA02 FHAP assessment Unit 2 on June 23, 2016.



Figure 21. Looking downstream at CLO-CA02 FHAP assessment Unit 3 on June 23, 2016.



Figure 22. Looking upstream at CLO-CA02 FHAP assessment Unit 4 on June 23, 2016.



Figure 23. Looking river-left to river-right at CLO-CA02 FHAP assessment Unit 5 on June 23, 2016.



Figure 24. Looking upstream at GRE-CA01 FHAP assessment Unit 1 on June 18, 2016.



Figure 25. Looking upstream at GRE-CA01 FHAP assessment Unit 2 on June 18, 2016.



Figure 26. Looking upstream at GRE-CA02 FHAP assessment Unit 1 on June 18, 2016.



Figure 27. Looking upstream at GRE-CA02 FHAP assessment Unit 2 on June 18, 2016.



Figure 28. Looking upstream at GRE-CA03 FHAP assessment Unit 1 on June 18, 2016.



Figure 29. Looking upstream at GRE-CA03 FHAP assessment Unit 2 on June 18, 2016.



Figure 30. Looking upstream at GRE-CA03 FHAP assessment Unit 3 on June 18, 2016.



Figure 31. Looking upstream at GRE-CA03 FHAP assessment Unit 4 on June 18, 2016.



Figure 32. Looking upstream at GH\_GH1/GRE-CA05 FHAP assessment Unit 1 on June 18, 2016.



Figure 33. Looking upstream at GH\_GH1/GRE-CA05 FHAP assessment Unit 2 on June 18, 2016.



Figure 34. Looking upstream at GRE-CA06 FHAP assessment Unit 1 on June 24, 2016.



Figure 35. Looking upstream at GRE-CA06 FHAP assessment Unit 2 on June 24, 2016.



Figure 36. Looking upstream at GRE-CA06 FHAP assessment Unit 3 on June 24, 2016.



Figure 37. Looking upstream at GRE-CA06 FHAP assessment Unit 4 on June 24, 2016.



Figure 38. Looking upstream at GH\_CTF FHAP assessment Unit 1 on June 24, 2016.



Figure 39. Looking upstream at GH\_CTF FHAP assessment Unit 2 on June 24, 2016.



Figure 40. Looking upstream at GH\_CTF FHAP assessment Unit 3 on June 24, 2016.



Appendix C Substrate grain distribution plots.

**LIST OF FIGURES**

Figure 1. Substrate Grain Distribution at FRD-CA01 (mesohabitat site) in Fording River on June, 2016. (a) cumulative particle size distribution and (b) number of particles per size class. .1

Figure 2. Substrate Grain Distribution at FRD-CA01 (piezometer site) in Fording River on June, 2016. (a) cumulative particle size distribution and (b) number of particles per size class. .2

Figure 3. Substrate Grain Distribution at FRD-CA02 (mesohabitat site) in Fording River on June, 2016. (a) cumulative particle size distribution and (b) number of particles per size class. .3

Figure 4. Substrate Grain Distribution at FRD-CA02 (piezometer site) in Fording River on June, 2016. (a) cumulative particle size distribution and (b) number of particles per size class. .4

Figure 5. Substrate Grain Distribution at FRD-CA03 (mesohabitat site) in Fording River on June, 2016. (a) cumulative particle size distribution and (b) number of particles per size class. .5

Figure 6. Substrate Grain Distribution at FRD-CA03 (piezometer site) in Fording River on June, 2016. (a) cumulative particle size distribution and (b) number of particles per size class. .6

Figure 7. Substrate Grain Distribution at FRD-CA01 (mesohabitat site) in the Fording River on August/September, 2016. (a) cumulative particle size distribution and (b) number of particles per size class.....7

Figure 8. Substrate Grain Distribution at FRD-CA01 (piezometer site) in the Fording River on August/September, 2016. (a) cumulative particle size distribution and (b) number of particles per size class.....8

Figure 9. Substrate Grain Distribution at FRD-CA02 (piezometer site) in the Fording River on August/September, 2016. (a) cumulative particle size distribution and (b) number of particles per size class.....9

Figure 10. Substrate Grain Distribution at FRD-CA02 (mesohabitat site) in the Fording River on August/September, 2016. (a) cumulative particle size distribution and (b) number of particles per size class.....10

Figure 11. Substrate Grain Distribution at FRD-CA03 (mesohabitat site) in Fording River on August/September, 2016. (a) cumulative particle size distribution and (b) number of particles per size class.....11

Figure 12. Substrate Grain Distribution at FRD-CA03 (piezometer site) in the Fording River on August/September, 2016. (a) cumulative particle size distribution and (b) number of particles per size class.....12

Figure 13. Substrate Grain Distribution at CLO-CA01 (mesohabitat site) in Clode Creek on June, 2016. (a) cumulative particle size distribution and (b) number of particles per size class. ....13

Figure 14. Substrate Grain Distribution at CLO-CA01 (piezometer site) in Clode Creek on June, 2016. (a) cumulative particle size distribution and (b) number of particles per size class. ....14

Figure 15. Substrate Grain Distribution at CLO-CA02 (mesohabitat and piezometer sites) in Clode Creek on June, 2016. (a) cumulative particle size distribution and (b) number of particles per size class. ....15

Figure 16. Substrate Grain Distribution at CLO-CA01 (mesohabitat/piezometer site) in Clode Creek on August/September, 2016. (a) cumulative particle size distribution and (b) number of particles per size class.....16

Figure 17. Substrate Grain Distribution at CLO-CA02 (mesohabitat/piezometer site) in Clode Creek on August/September, 2016. (a) cumulative particle size distribution and (b) number of particles per size class.....17

Figure 18. Substrate Grain Distribution at GRE-CA01 (piezometer site) in Greenhills Creek on June, 2016. (a) cumulative particle size distribution and (b) number of particles per size class.....18

Figure 19. Substrate Grain Distribution at GRE-CA02 (mesohabitat site) in Greenhills Creek on June, 2016. (a) cumulative particle size distribution and (b) number of particles per size class.....19

Figure 20. Substrate Grain Distribution at GRE-CA02 (piezometer site) in Greenhills Creek on June, 2016. (a) cumulative particle size distribution and (b) number of particles per size class.....20

Figure 21. Substrate Grain Distribution at GRE-CA03 (mesohabitat site) in Greenhills Creek on June, 2016. (a) cumulative particle size distribution and (b) number of particles per size class.....21

Figure 22. Substrate Grain Distribution at GRE-CA03 (piezometer site) in Greenhills Creek on June, 2016. (a) cumulative particle size distribution and (b) number of particles per size class.....22

Figure 23. Substrate Grain Distribution at GH-GH1 (mesohabitat site) in Greenhills Creek on June, 2016. (a) cumulative particle size distribution and (b) number of particles per size class. ....23

Figure 24. Substrate Grain Distribution at GH-GH1 (piezometer site) in Greenhills Creek on June, 2016. (a) cumulative particle size distribution and (b) number of particles per size class. ....24

Figure 25. Substrate Grain Distribution at GRE-CA05 (mesohabitat site) in Greenhills Creek on June, 2016. (a) cumulative particle size distribution and (b) number of particles per size class.....25

Figure 26. Substrate Grain Distribution at GRE-CA05 (piezometer site) in Greenhills Creek on June, 2016. (a) cumulative particle size distribution and (b) number of particles per size class.....26

Figure 27. Substrate Grain Distribution at GRE-CA06 (mesohabitat and piezometer sites) in Greenhills Creek on June, 2016. (a) cumulative particle size distribution and (b) number of particles per size class.....27

Figure 28. Substrate Grain Distribution at GH-CFT (mesohabitat and piezometer sites) in Greenhills Creek on June, 2016. (a) cumulative particle size distribution and (b) number of particles per size class.....28

Figure 29. Substrate Grain Distribution at GRE-CA01 (mesohabitat site) in Greenhills Creek on August/September, 2016. (a) cumulative particle size distribution and (b) number of particles per size class.....29

Figure 30. Substrate Grain Distribution at GRE-CA01 (piezometer site) in Greenhills Creek on August/September, 2016. (a) cumulative particle size distribution and (b) number of particles per size class.....30

Figure 31. Substrate Grain Distribution at GRE-CA02 (mesohabitat/piezometer site) in Greenhills Creek on August/September, 2016. (a) cumulative particle size distribution and (b) number of particles per size class.....31

Figure 32. Substrate Grain Distribution at GRE-CA03 (mesohabitat site) in Greenhills Creek on August/September, 2016. (a) cumulative particle size distribution and (b) number of particles per size class.....32

Figure 33. Substrate Grain Distribution at GRE-CA03 (piezometer site) in Greenhills Creek on August/September, 2016. (a) cumulative particle size distribution and (b) number of particles per size class.....33

Figure 34. Substrate Grain Distribution at GH\_GH1 (mesohabitat site) in Greenhills Creek on August/September, 2016. (a) cumulative particle size distribution and (b) number of particles per size class.....34

Figure 35. Substrate Grain Distribution at GH\_GH1 (piezometer site) in Greenhills Creek on August/September, 2016. (a) cumulative particle size distribution and (b) number of particles per size class.....35

Figure 36. Substrate Grain Distribution at GRE-CA05 (piezometer site) in Greenhills Creek on August/September, 2016. (a) cumulative particle size distribution and (b) number of particles per size class.....36

Figure 37. Substrate Grain Distribution at GRE-CA06 (mesohabitat/piezometer site) in Greenhills Creek on August/September, 2016. (a) cumulative particle size distribution and (b) number of particles per size class.....37

Figure 38. Substrate Grain Distribution at GRE-GH\_CTF (mesohabitat/piezometer site) in Greenhills Creek on August/September, 2016. (a) cumulative particle size distribution and (b) number of particles per size class.....38

Figure 1. Substrate Grain Distribution at FRD-CA01 (mesohabitat site) in Fording River on June, 2016. (a) cumulative particle size distribution and (b) number of particles per size class.

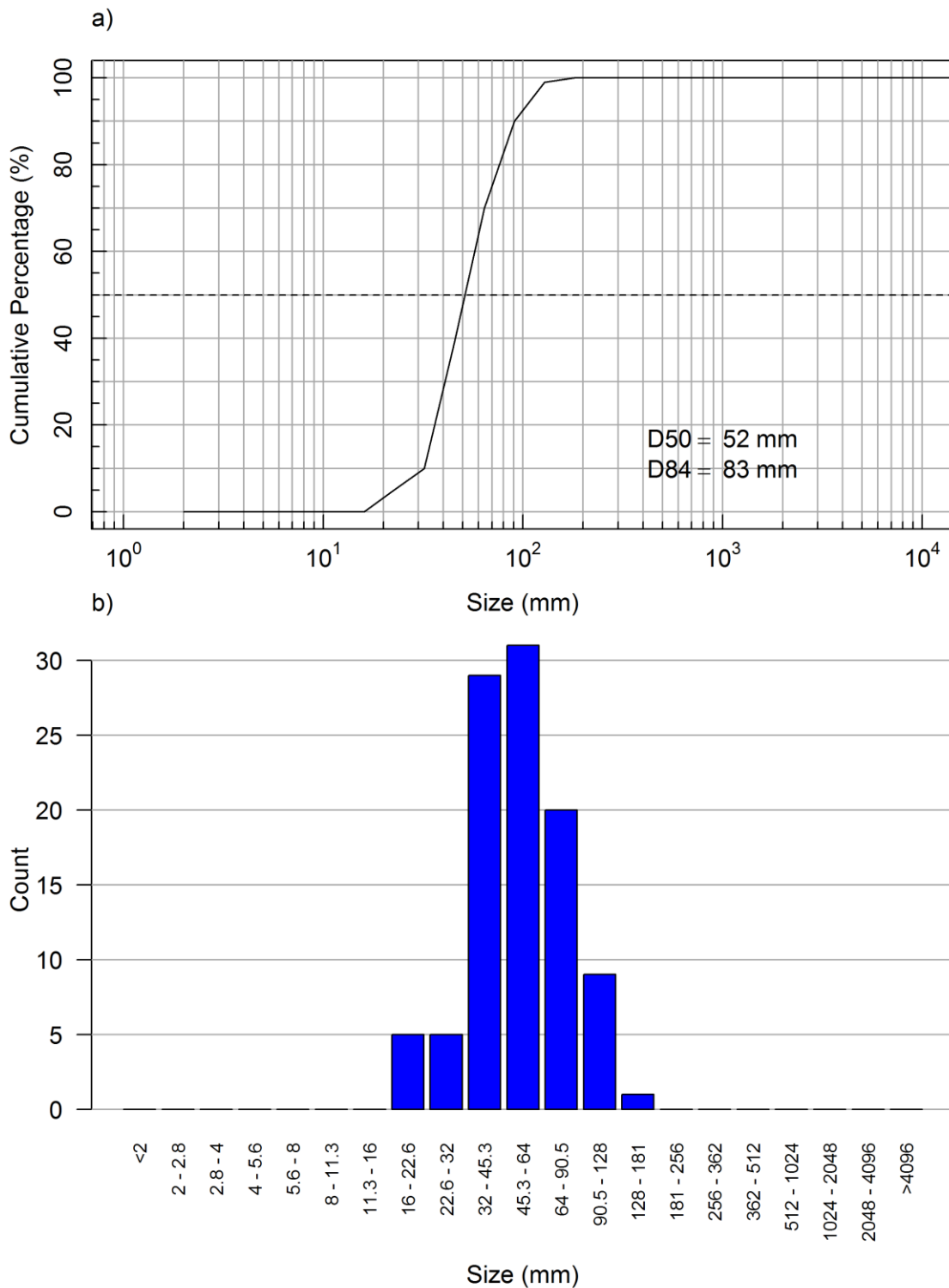


Figure 2. Substrate Grain Distribution at FRD-CA01 (piezometer site) in Fording River on June, 2016. (a) cumulative particle size distribution and (b) number of particles per size class.

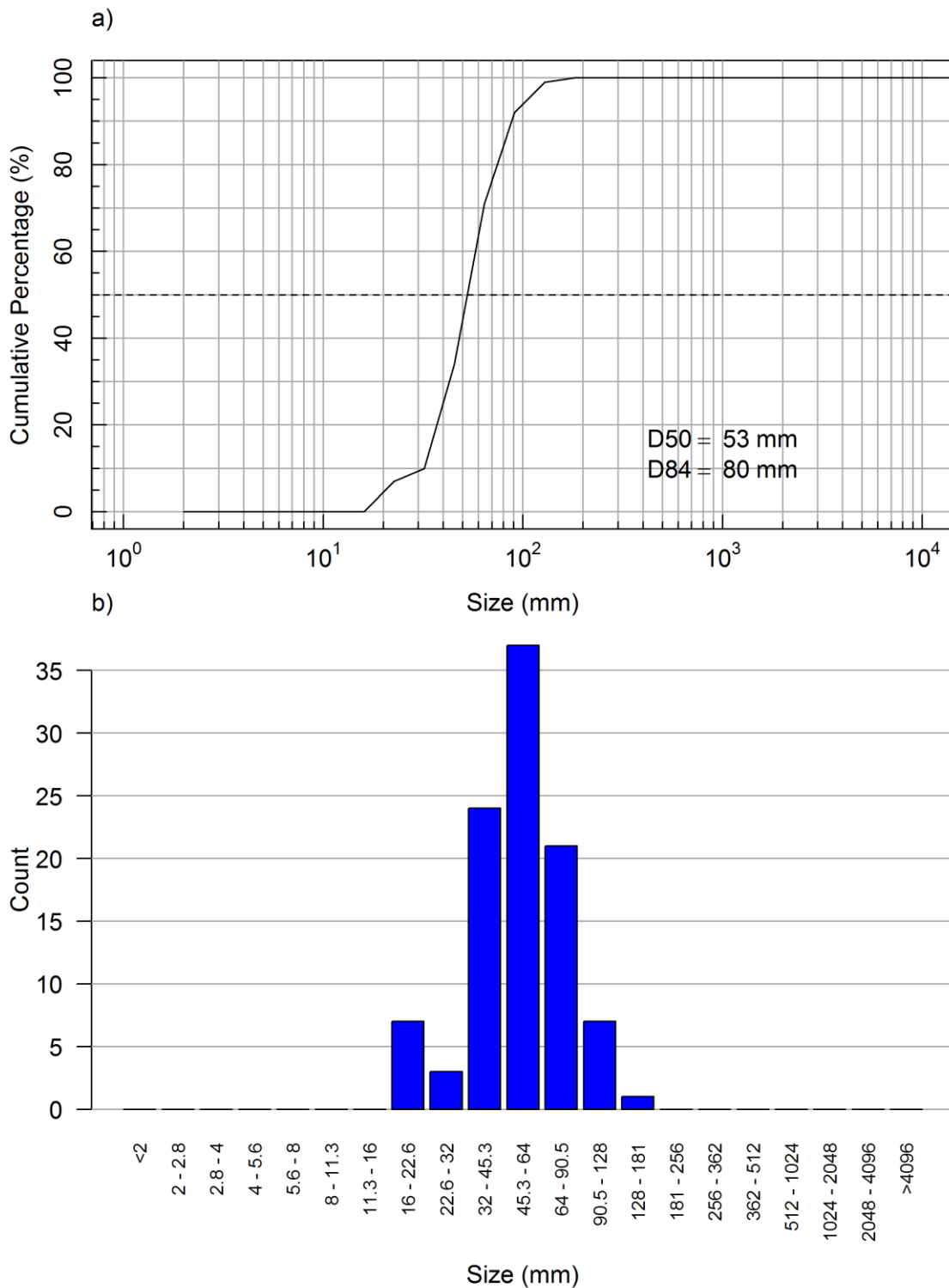


Figure 3. Substrate Grain Distribution at FRD-CA02 (mesohabitat site) in Fording River on June, 2016. (a) cumulative particle size distribution and (b) number of particles per size class.

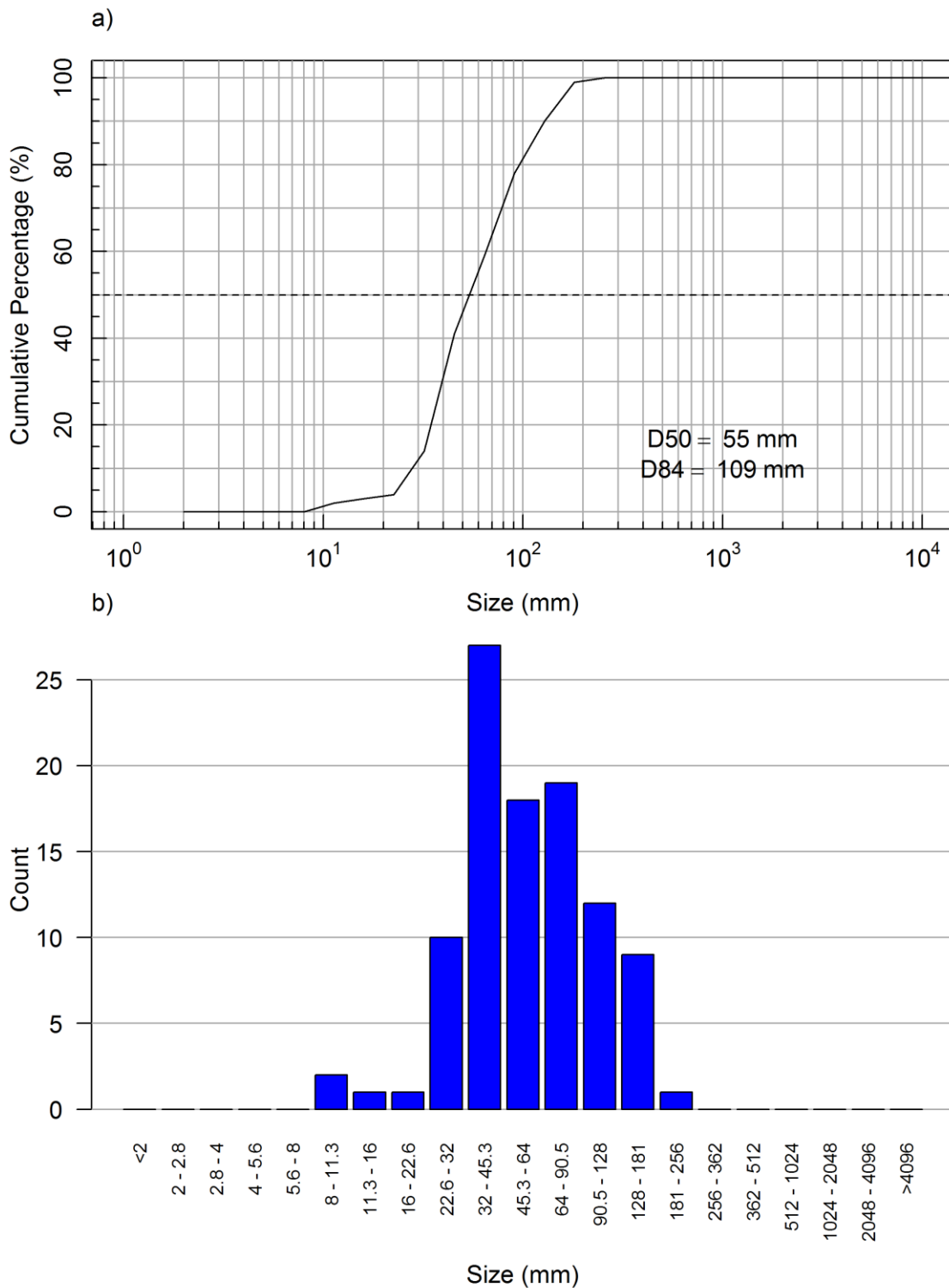


Figure 4. Substrate Grain Distribution at FRD-CA02 (piezometer site) in Fording River on June, 2016. (a) cumulative particle size distribution and (b) number of particles per size class.

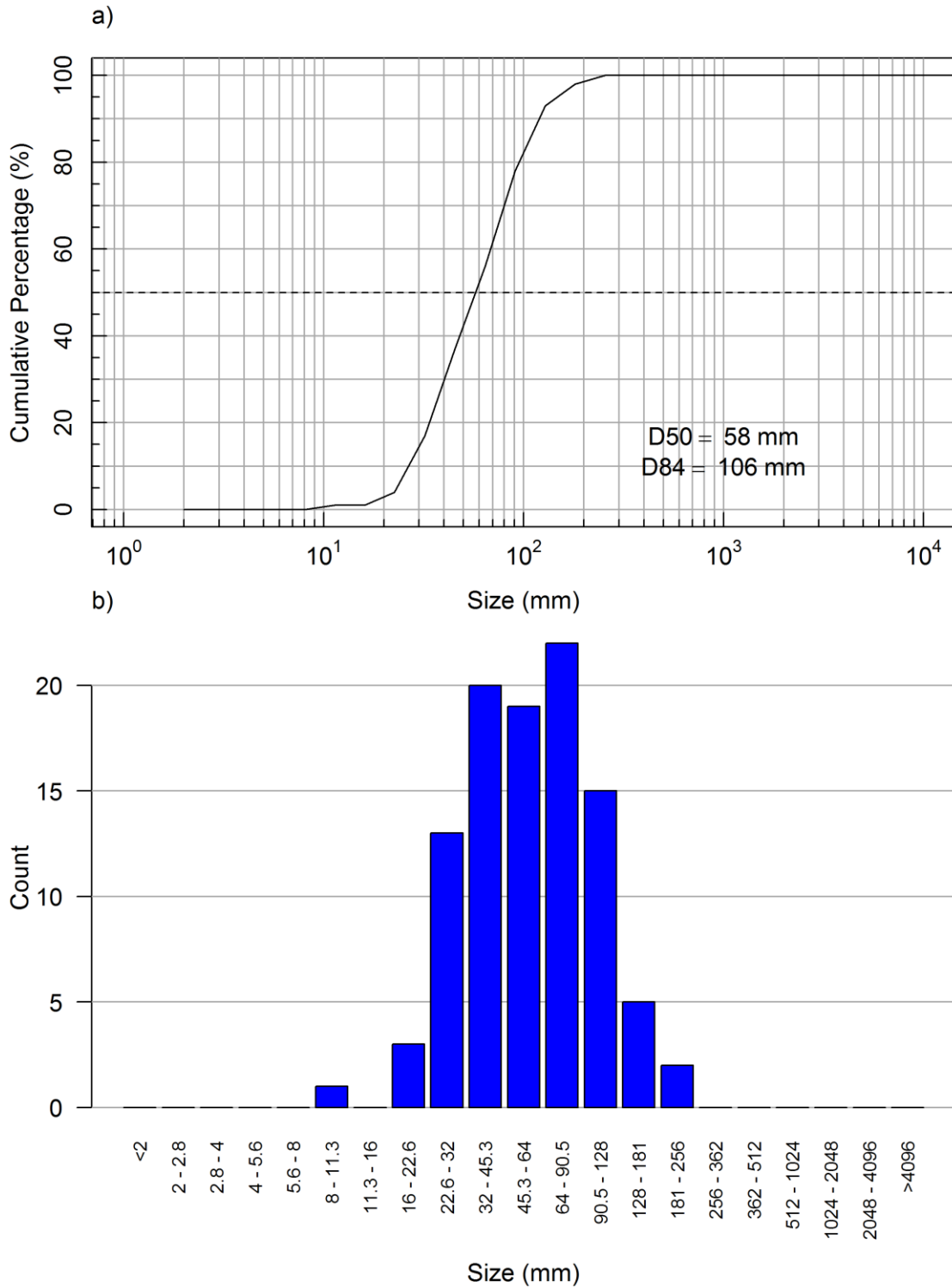


Figure 5. Substrate Grain Distribution at FRD-CA03 (mesohabitat site) in Fording River on June, 2016. (a) cumulative particle size distribution and (b) number of particles per size class.

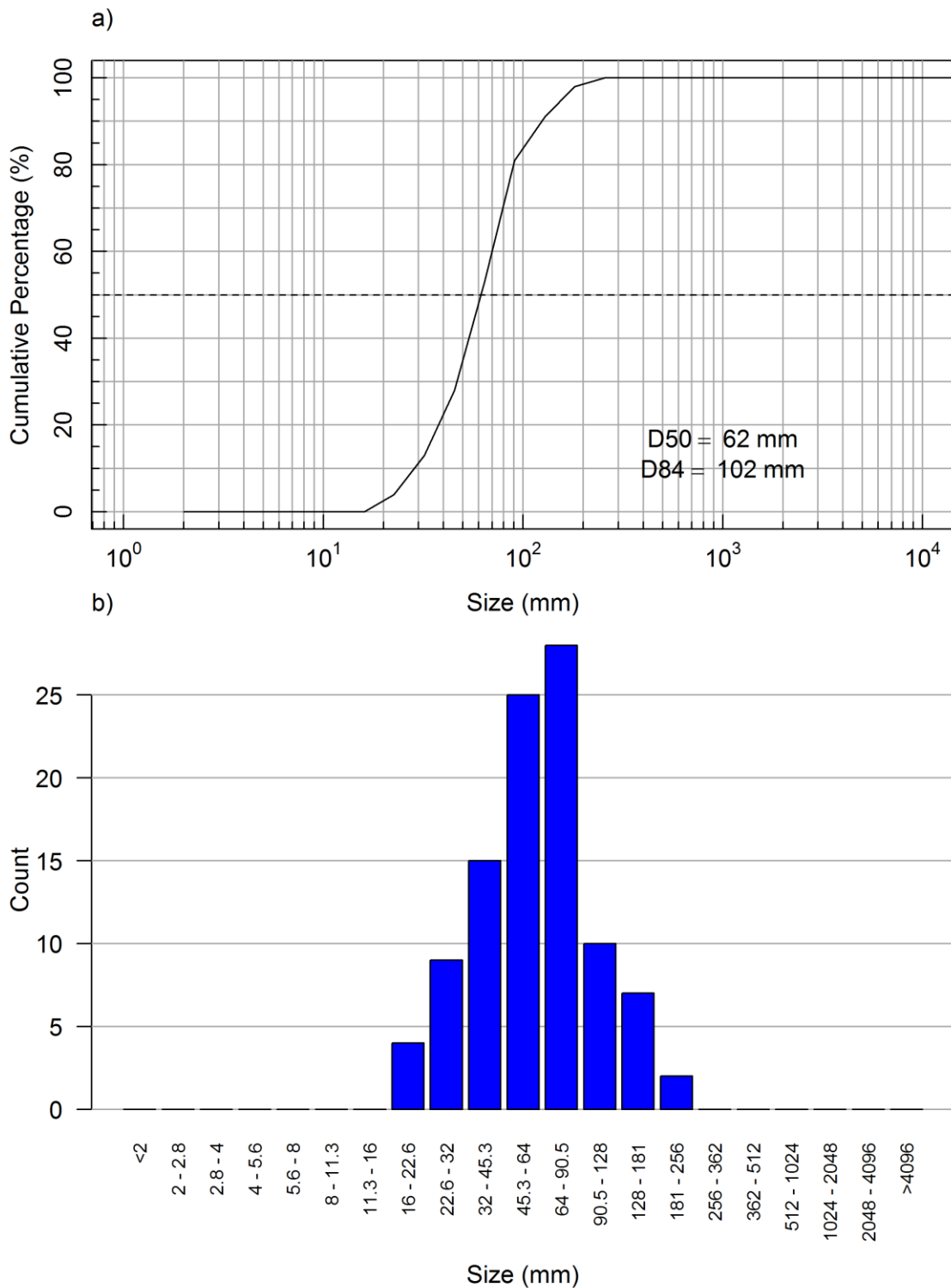


Figure 6. Substrate Grain Distribution at FRD-CA03 (piezometer site) in Fording River on June, 2016. (a) cumulative particle size distribution and (b) number of particles per size class.

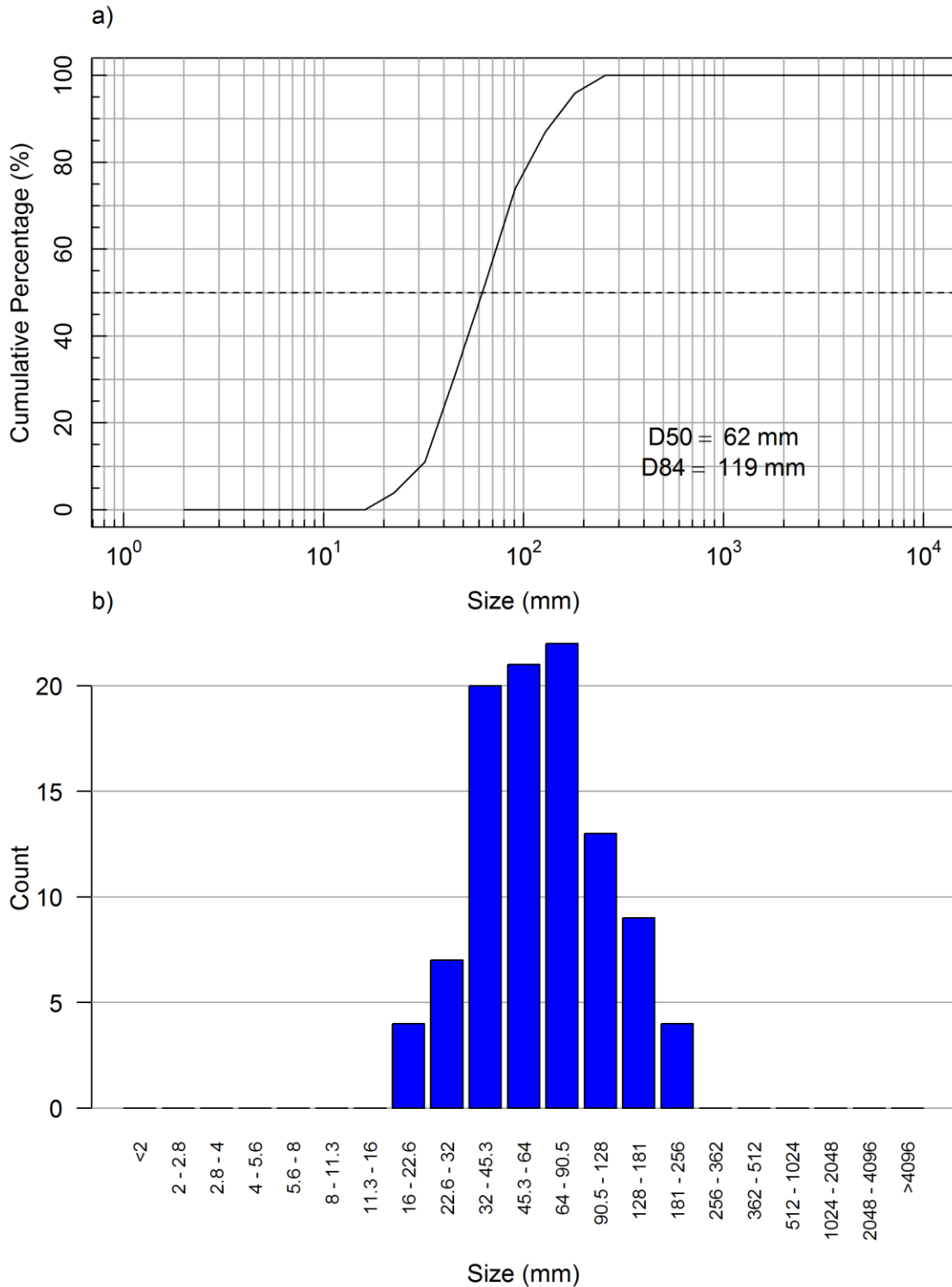


Figure 7. Substrate Grain Distribution at FRD-CA01 (mesohabitat site) in the Fording River on August/September, 2016. (a) cumulative particle size distribution and (b) number of particles per size class.

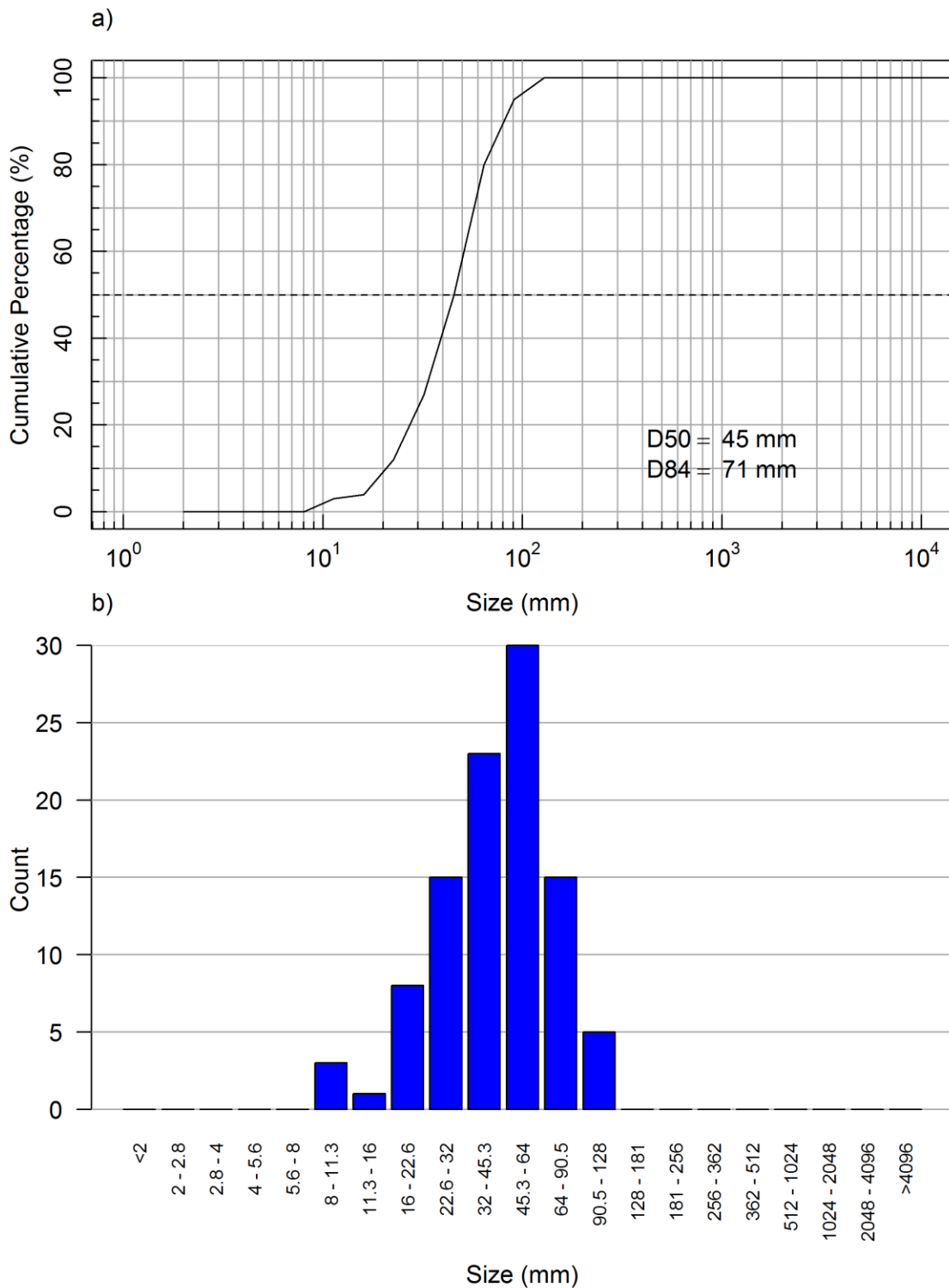


Figure 8. Substrate Grain Distribution at FRD-CA01 (piezometer site) in the Fording River on August/September, 2016. (a) cumulative particle size distribution and (b) number of particles per size class.

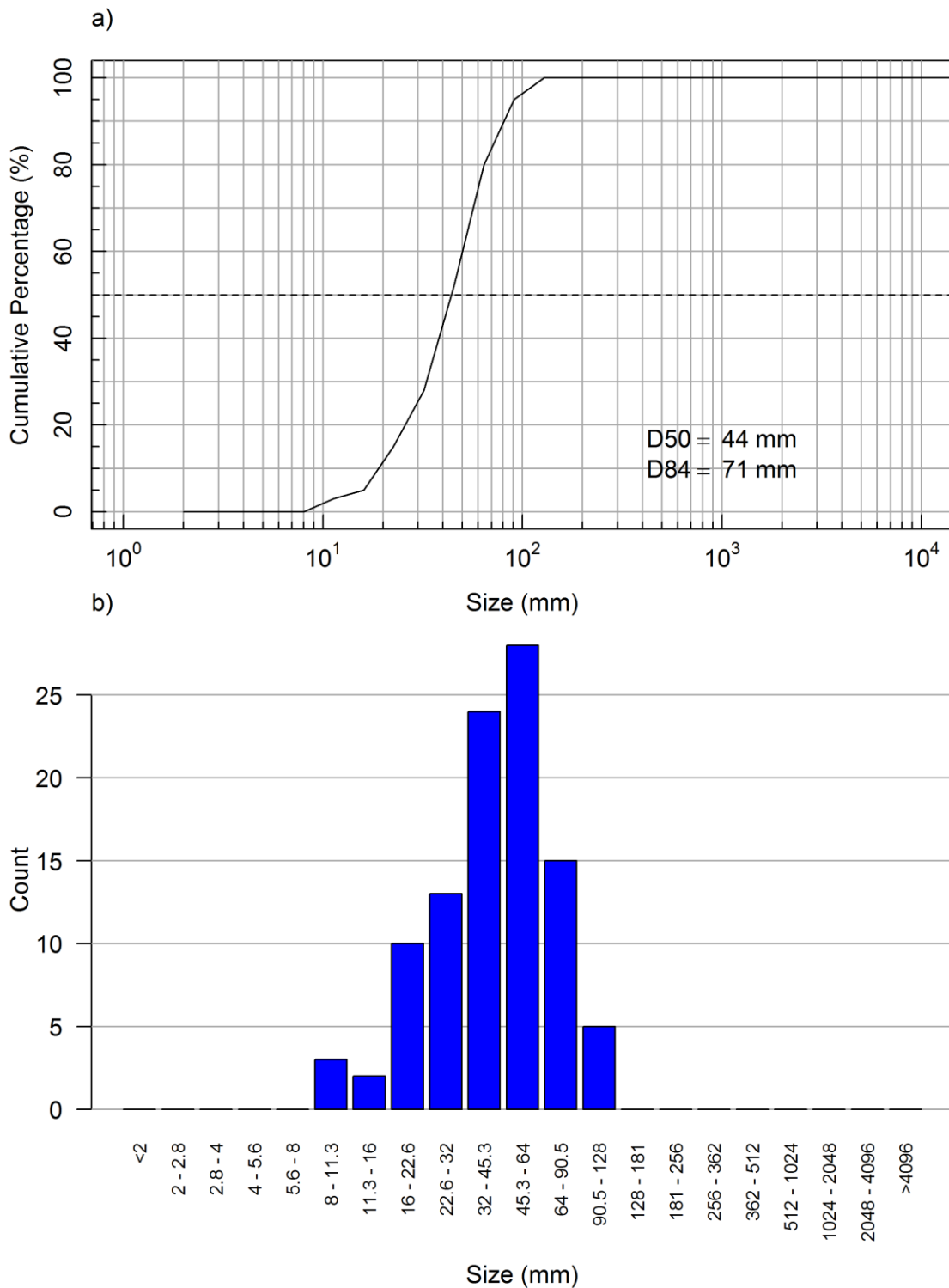


Figure 9. Substrate Grain Distribution at FRD-CA02 (piezometer site) in the Fording River on August/September, 2016. (a) cumulative particle size distribution and (b) number of particles per size class.

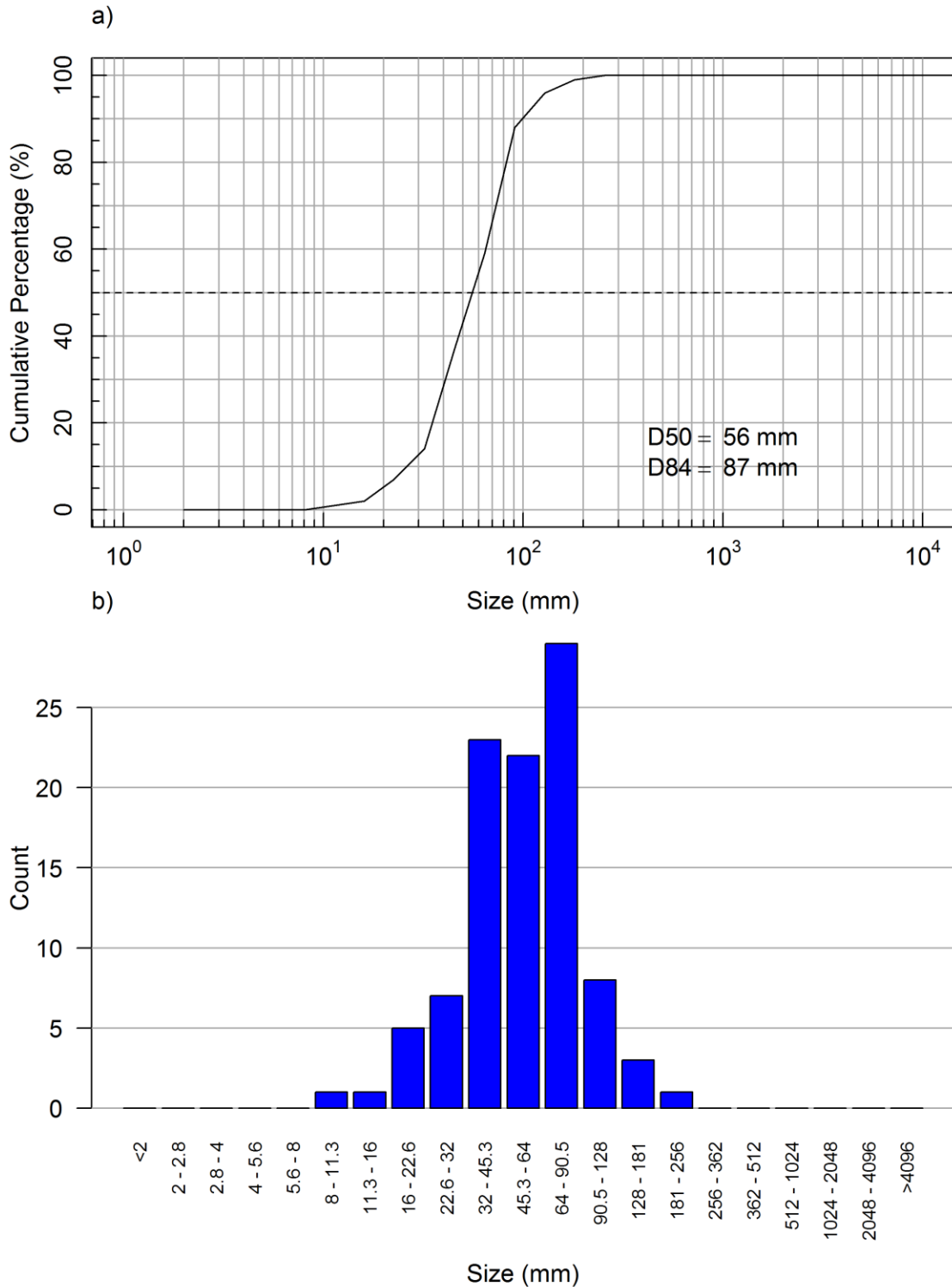


Figure 10. Substrate Grain Distribution at FRD-CA02 (mesohabitat site) in the Fording River on August/September, 2016. (a) cumulative particle size distribution and (b) number of particles per size class.

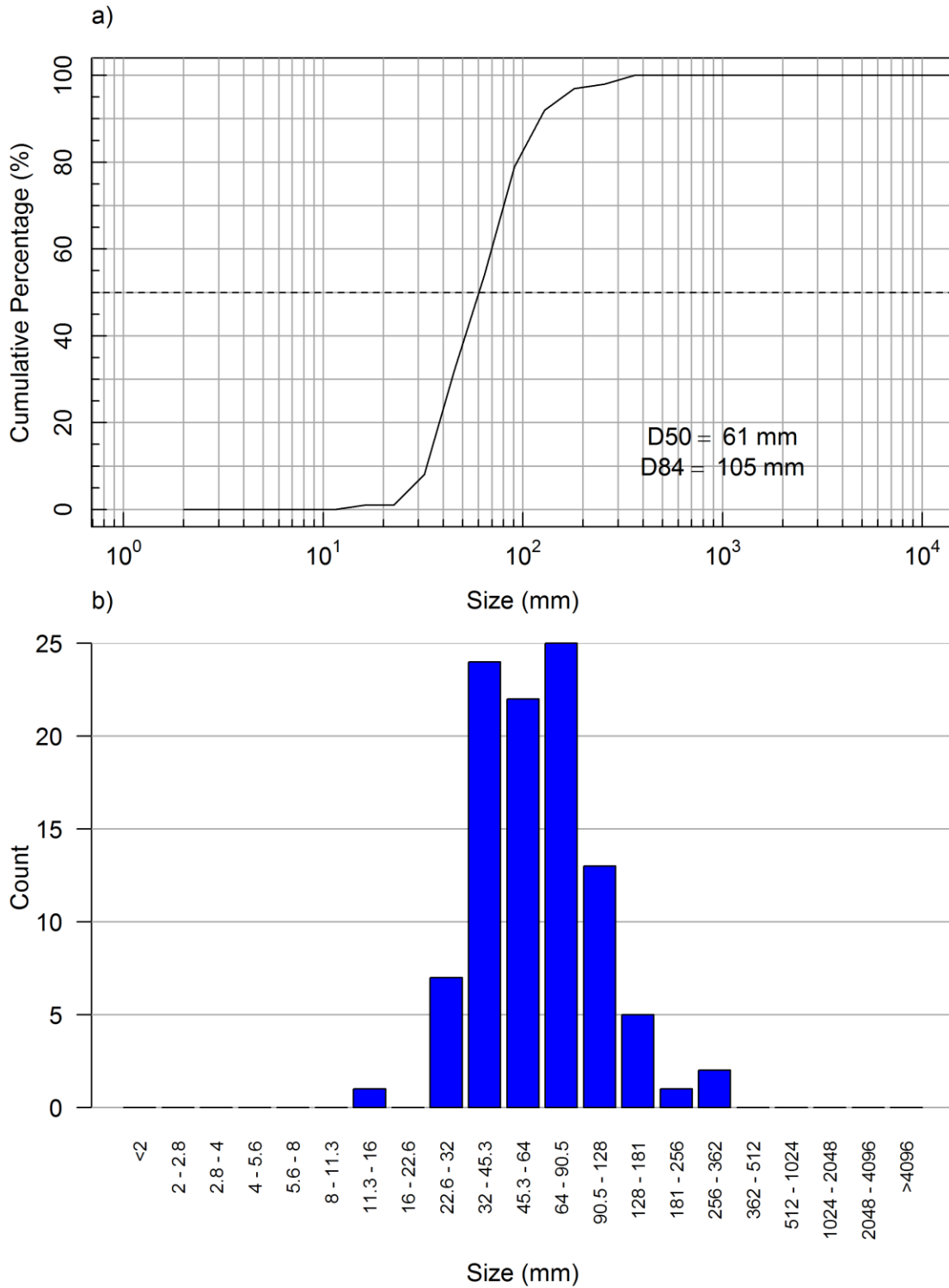


Figure 11. Substrate Grain Distribution at FRD-CA03 (mesohabitat site) in Fording River on August/September, 2016. (a) cumulative particle size distribution and (b) number of particles per size class.

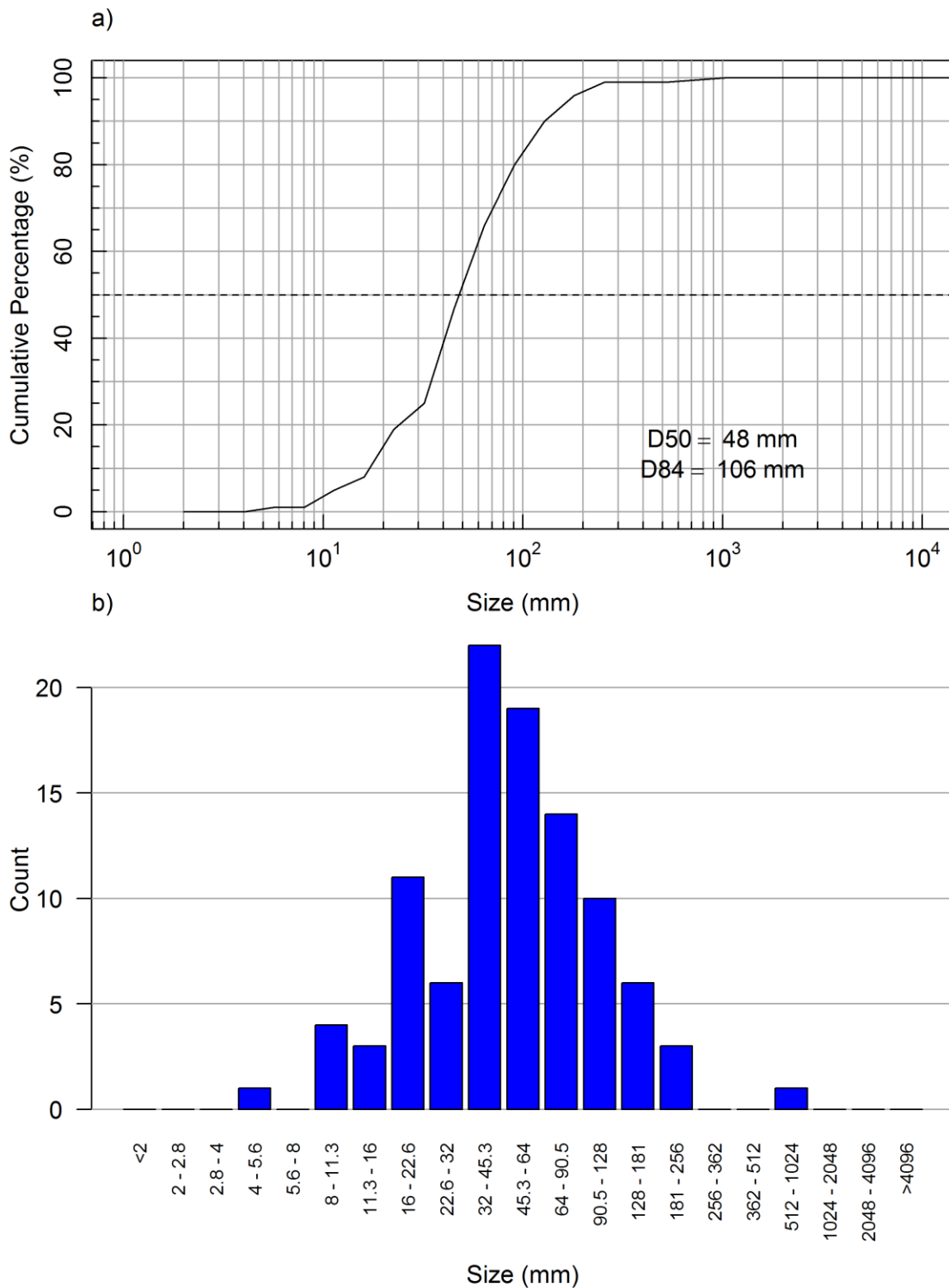


Figure 12. Substrate Grain Distribution at FRD-CA03 (piezometer site) in the Fording River on August/September, 2016. (a) cumulative particle size distribution and (b) number of particles per size class.

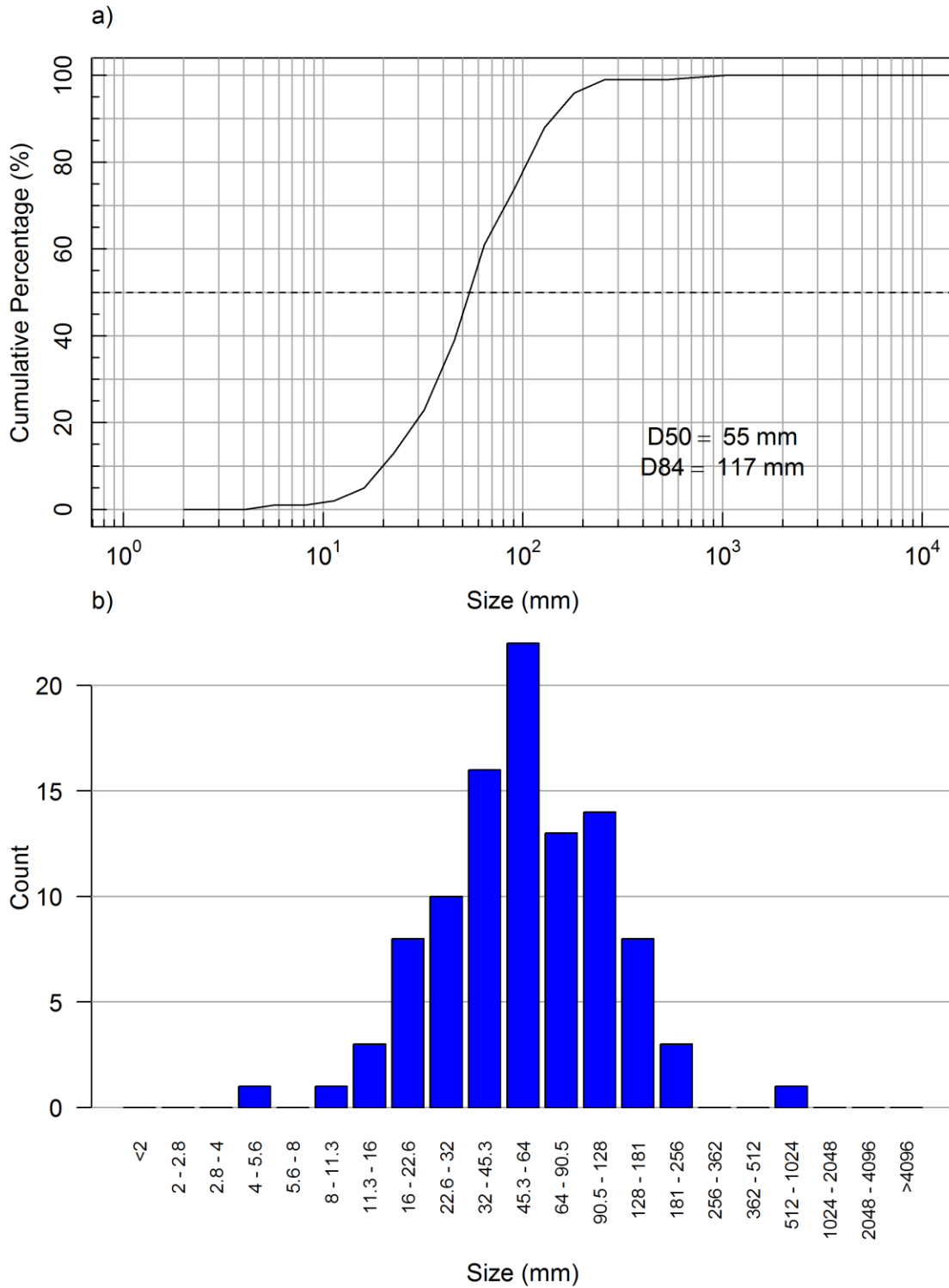


Figure 13. Substrate Grain Distribution at CLO-CA01 (mesohabitat site) in Clode Creek on June, 2016. (a) cumulative particle size distribution and (b) number of particles per size class.

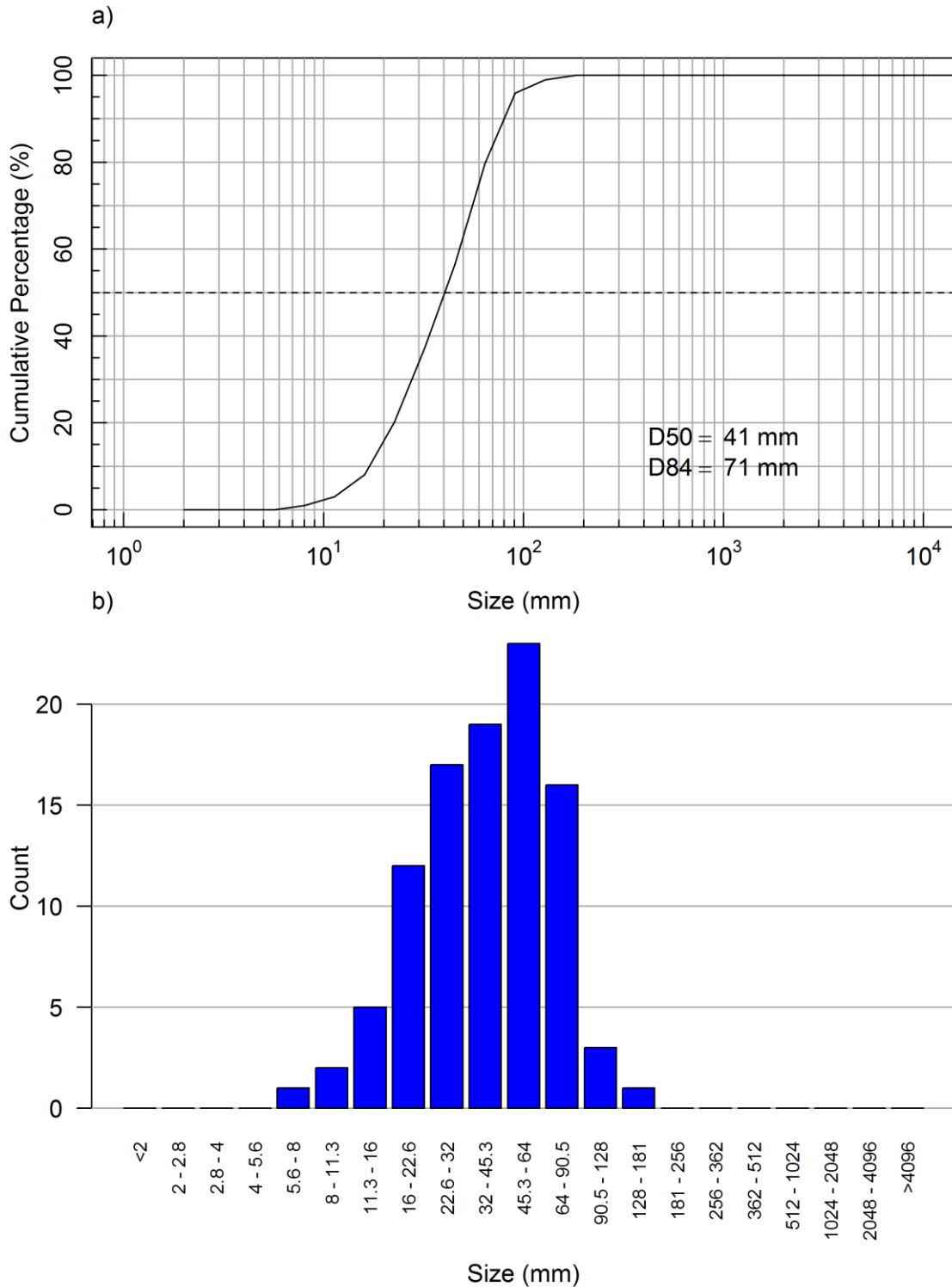


Figure 14. Substrate Grain Distribution at CLO-CA01 (piezometer site) in Clode Creek on June, 2016. (a) cumulative particle size distribution and (b) number of particles per size class.

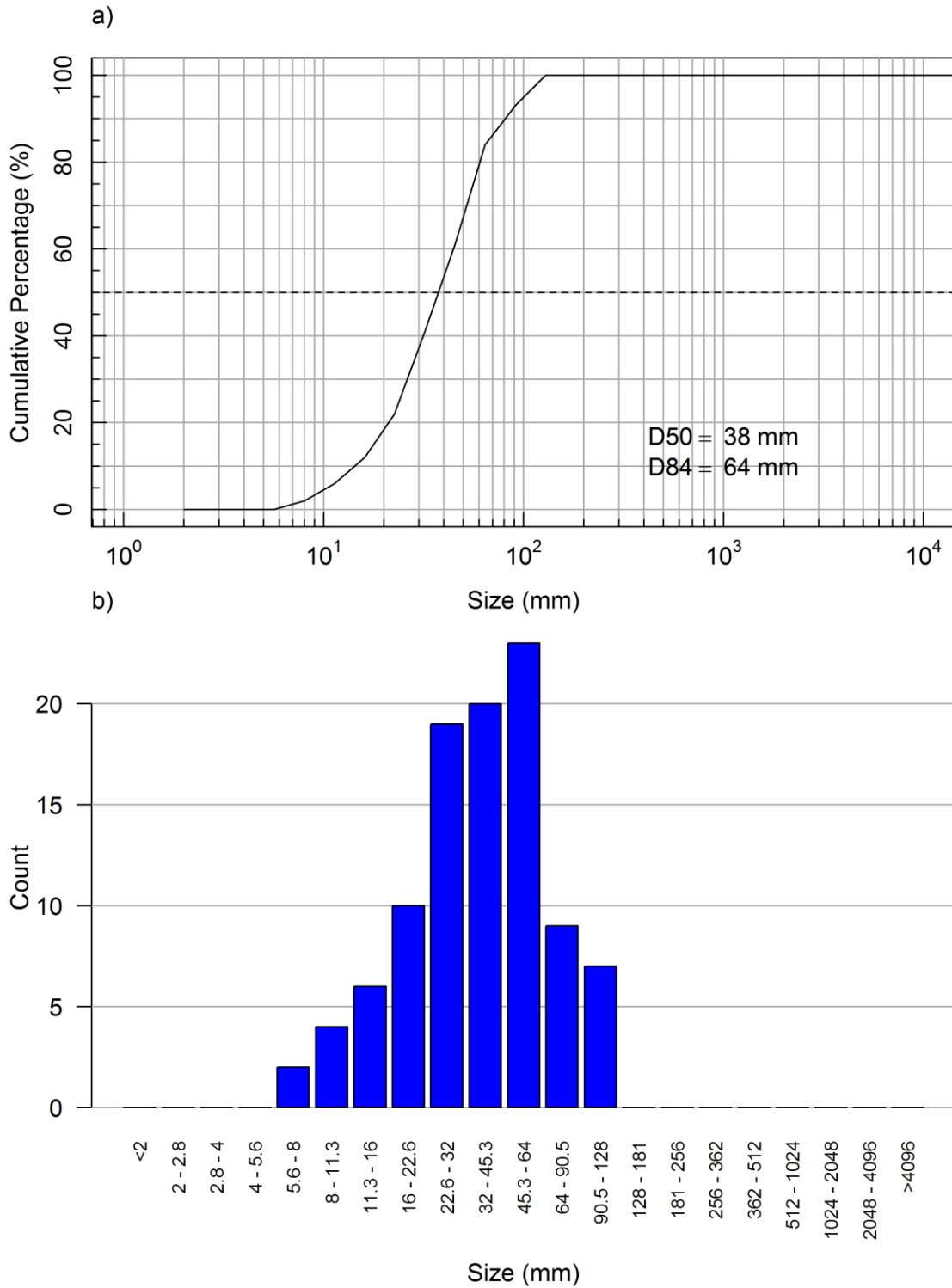


Figure 15. Substrate Grain Distribution at CLO-CA02 (mesohabitat and piezometer sites) in Clode Creek on June, 2016. (a) cumulative particle size distribution and (b) number of particles per size class.

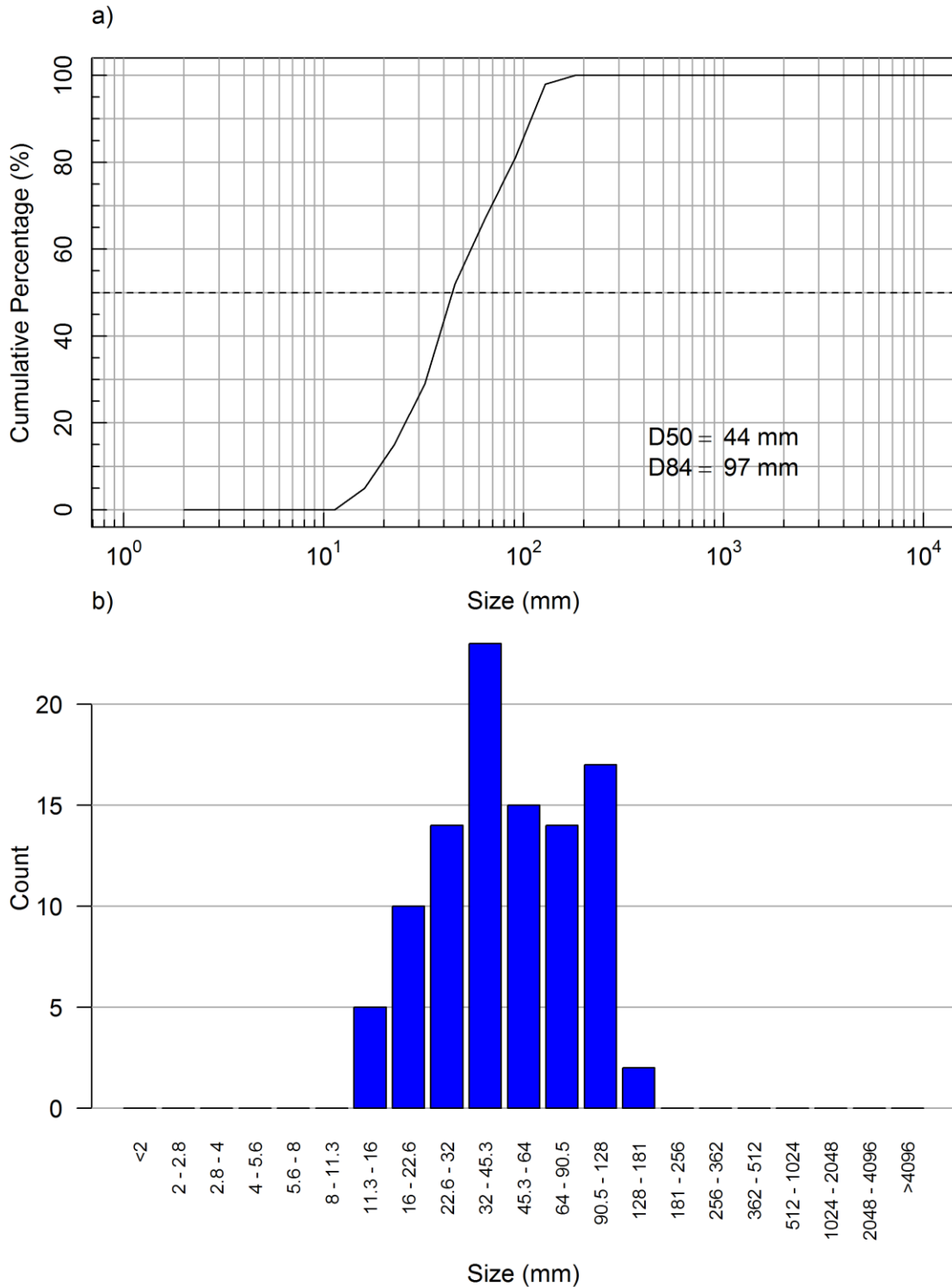


Figure 16. Substrate Grain Distribution at CLO-CA01 (mesohabitat/piezometer site) in Clode Creek on August/September, 2016. (a) cumulative particle size distribution and (b) number of particles per size class.

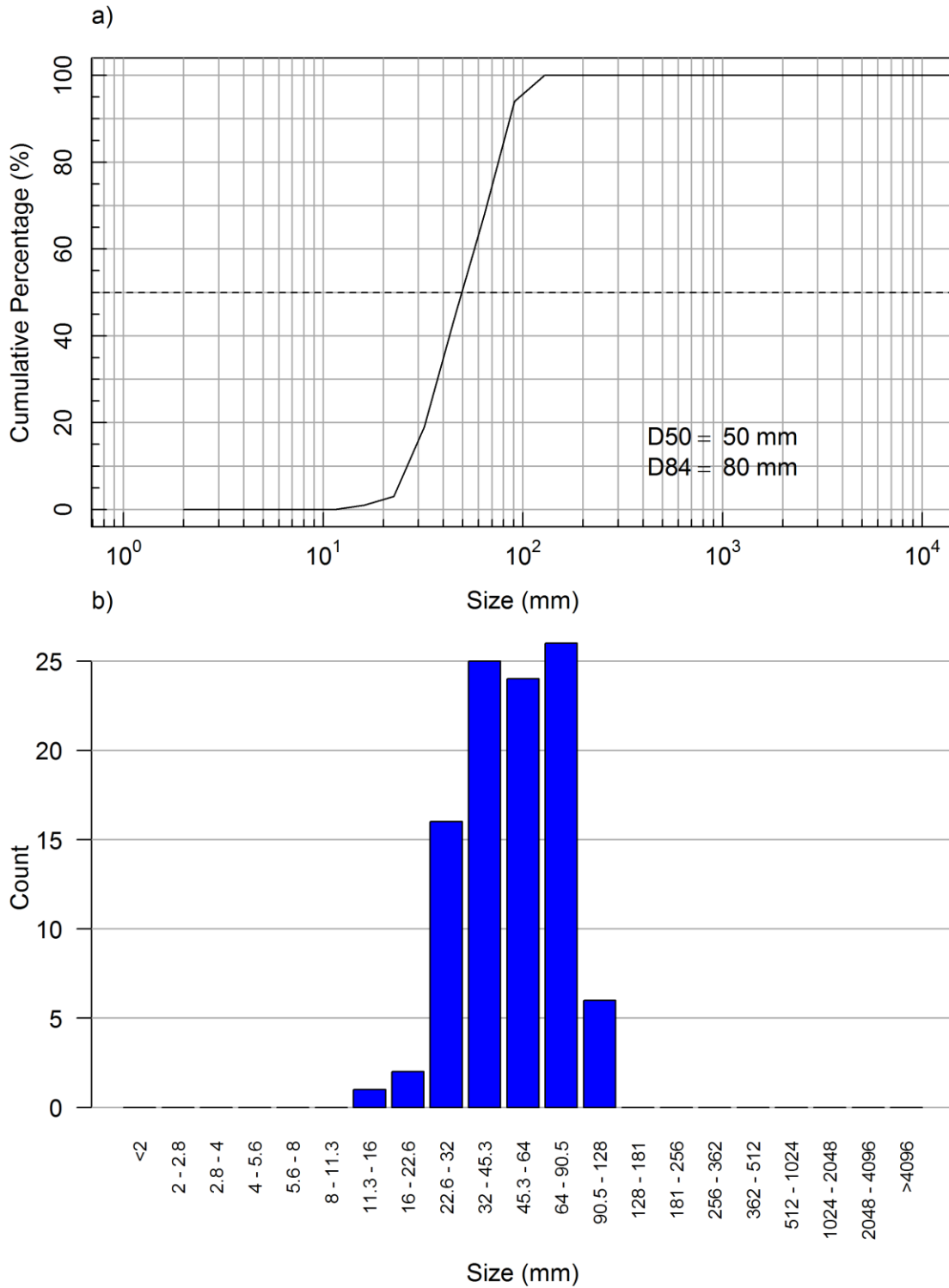


Figure 17. Substrate Grain Distribution at CLO-CA02 (mesohabitat/piezometer site) in Clode Creek on August/September, 2016. (a) cumulative particle size distribution and (b) number of particles per size class.

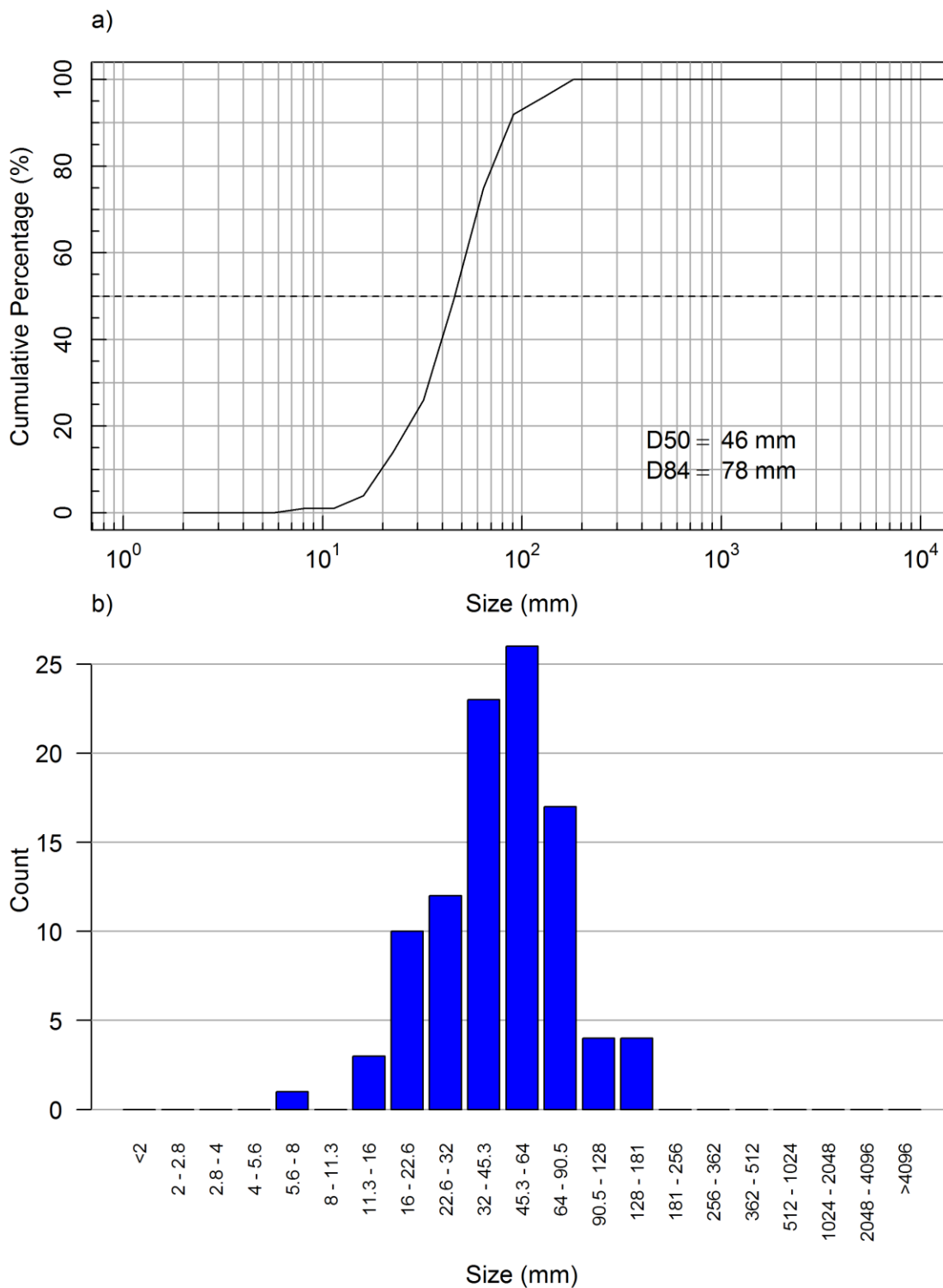


Figure 18. Substrate Grain Distribution at GRE-CA01 (piezometer site) in Greenhills Creek on June, 2016. (a) cumulative particle size distribution and (b) number of particles per size class.

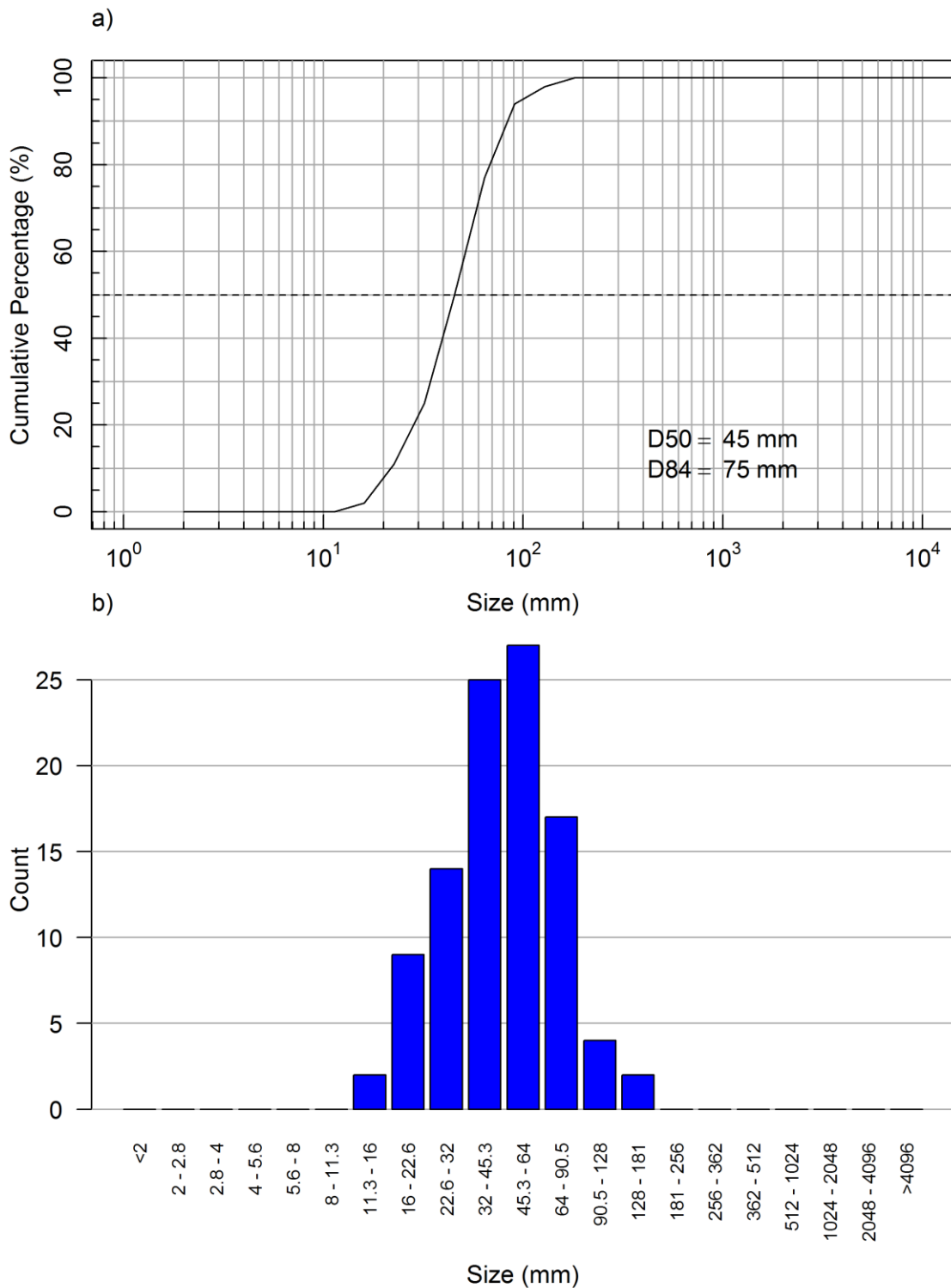


Figure 19. Substrate Grain Distribution at GRE-CA02 (mesohabitat site) in Greenhills Creek on June, 2016. (a) cumulative particle size distribution and (b) number of particles per size class.

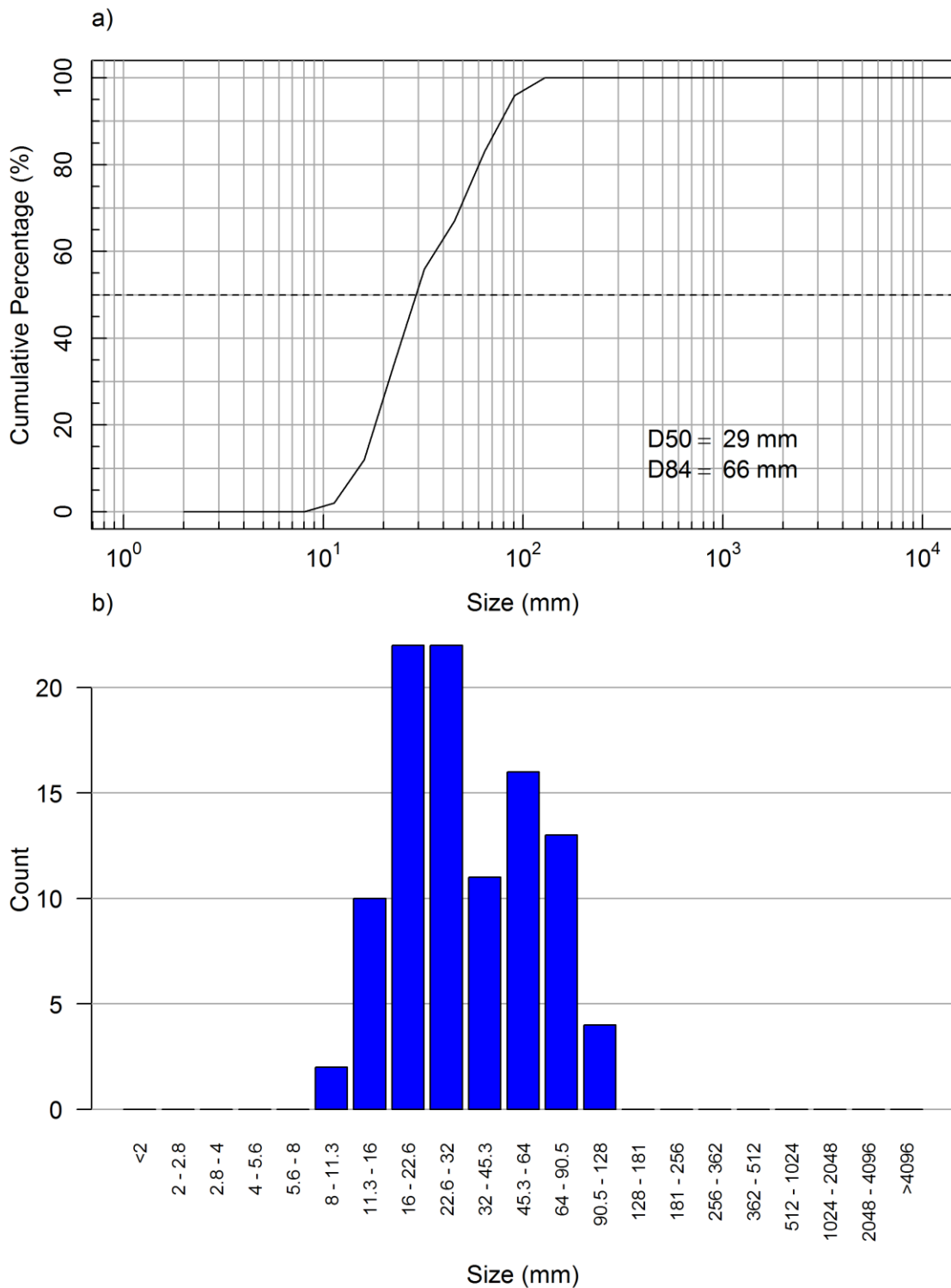


Figure 20. Substrate Grain Distribution at GRE-CA02 (piezometer site) in Greenhills Creek on June, 2016. (a) cumulative particle size distribution and (b) number of particles per size class.

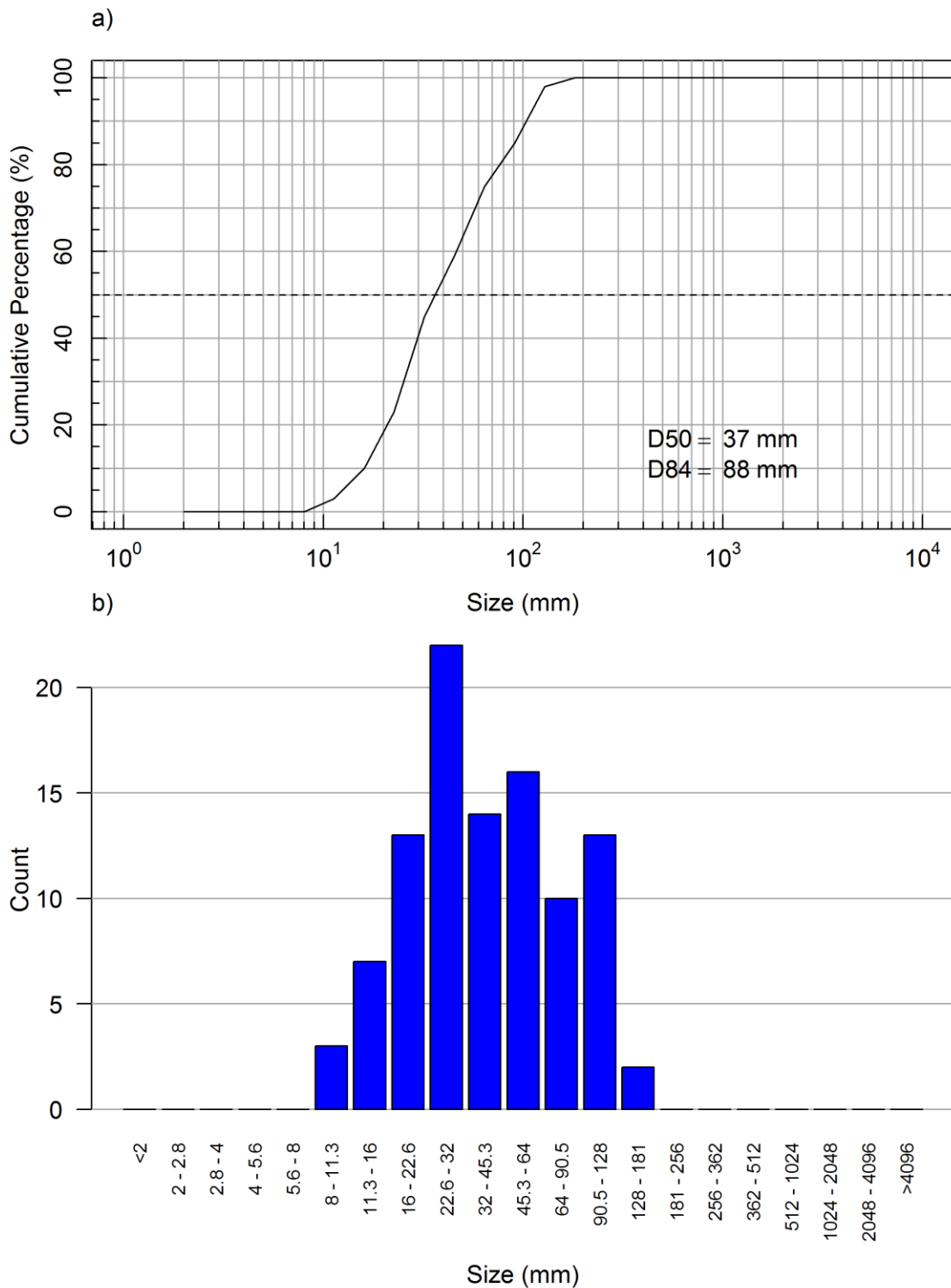


Figure 21. Substrate Grain Distribution at GRE-CA03 (mesohabitat site) in Greenhills Creek on June, 2016. (a) cumulative particle size distribution and (b) number of particles per size class.

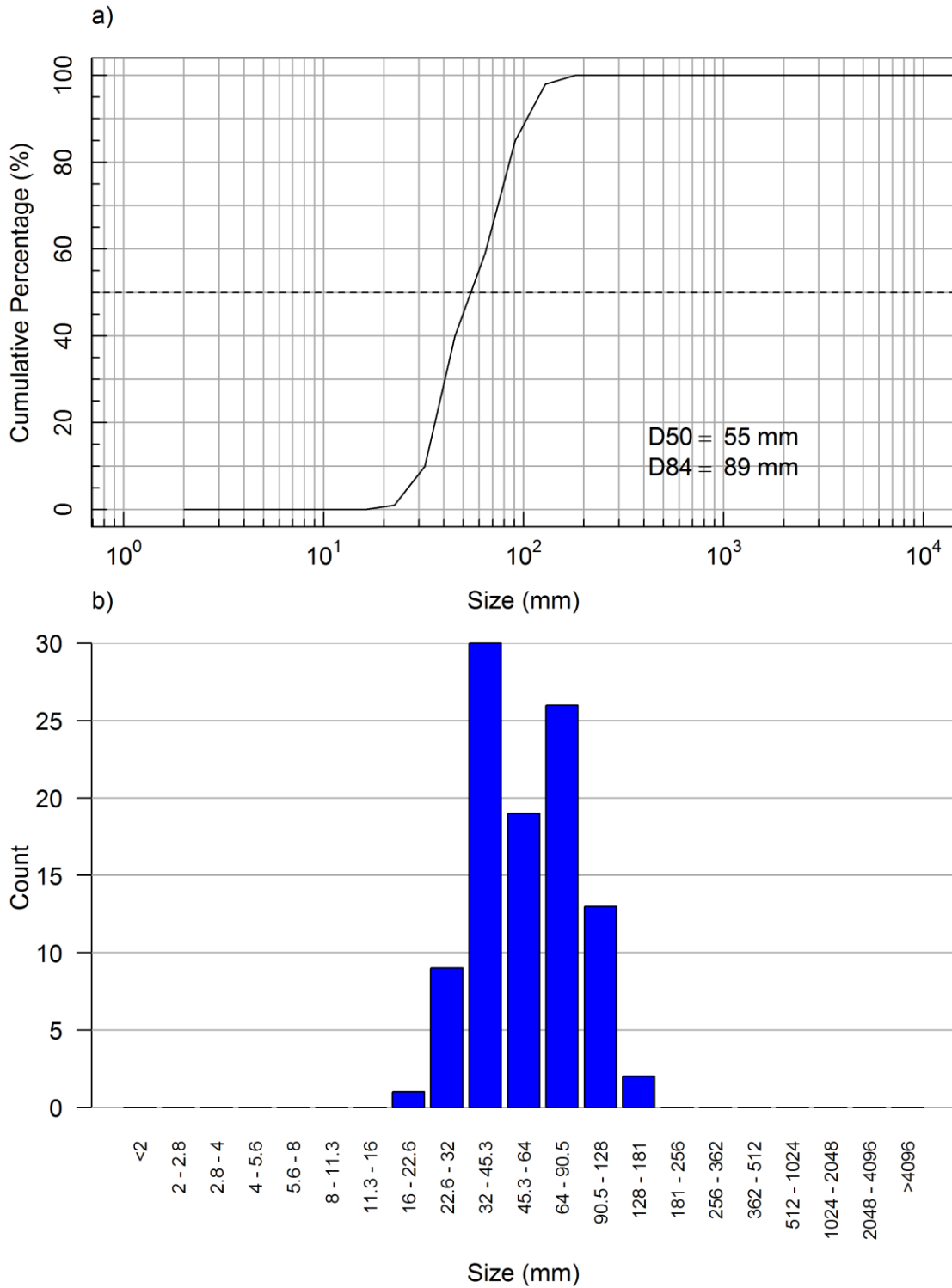


Figure 22. Substrate Grain Distribution at GRE-CA03 (piezometer site) in Greenhills Creek on June, 2016. (a) cumulative particle size distribution and (b) number of particles per size class.

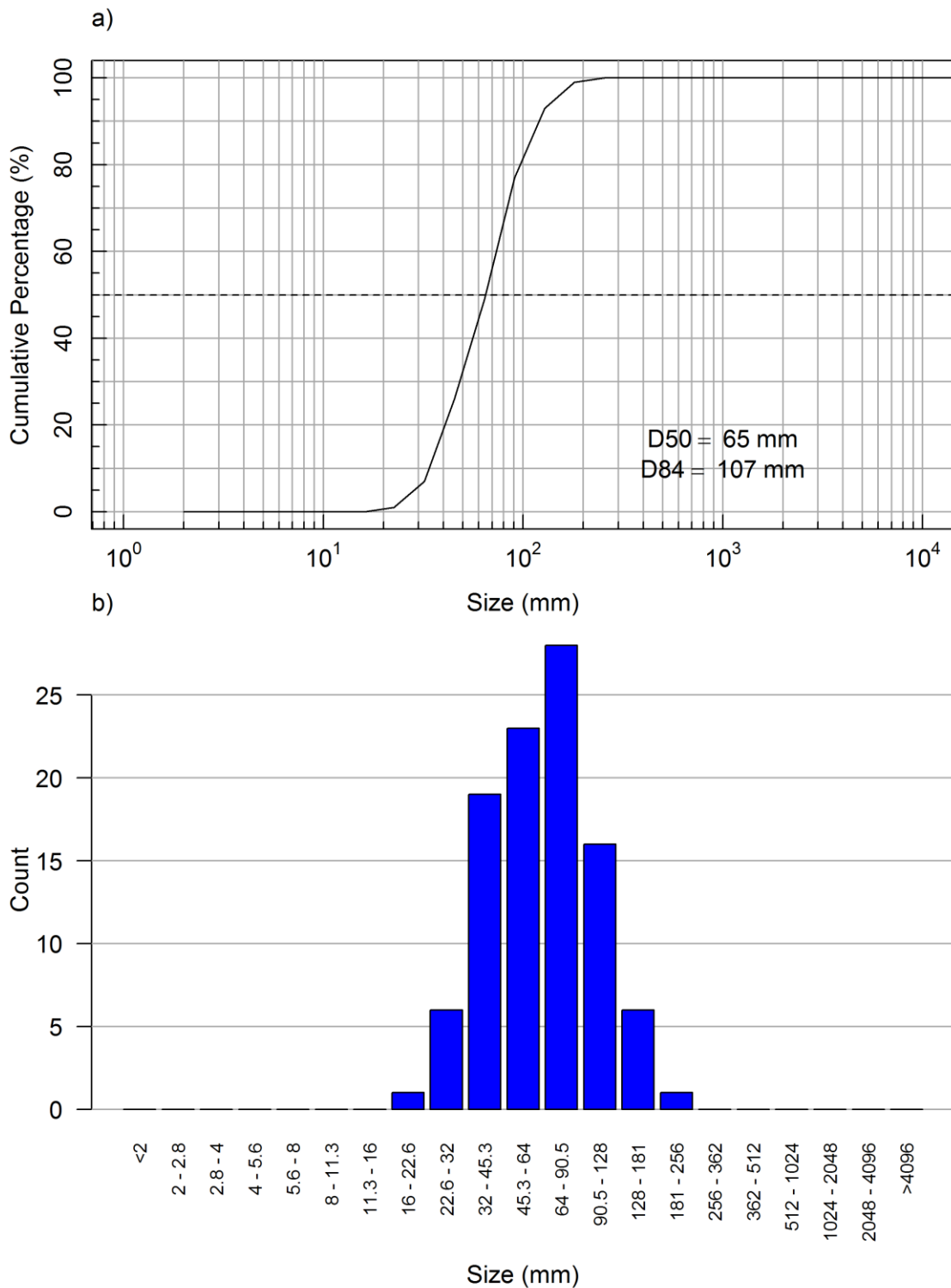


Figure 23. Substrate Grain Distribution at GH-GH1 (mesohabitat site) in Greenhills Creek on June, 2016. (a) cumulative particle size distribution and (b) number of particles per size class.

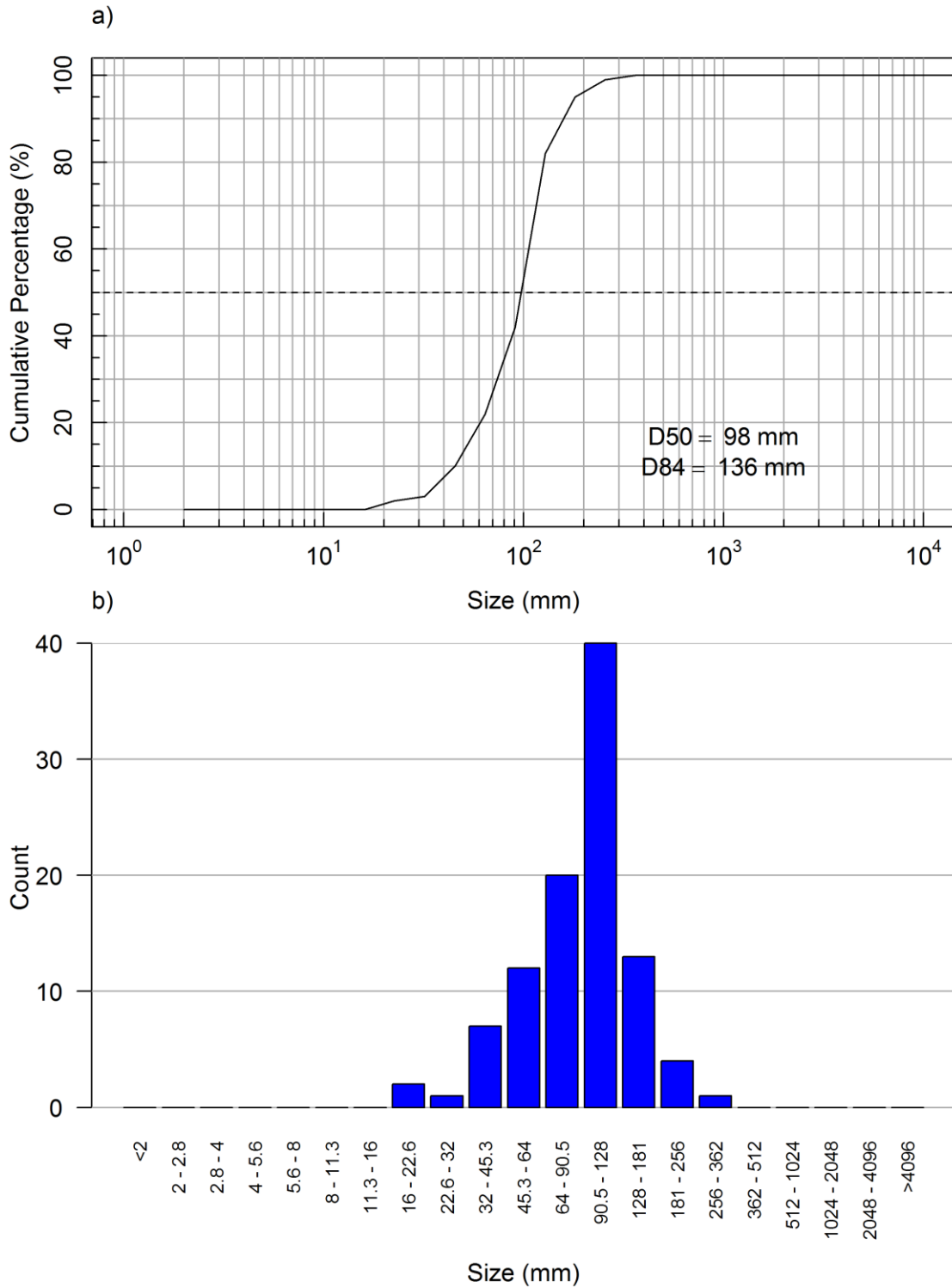


Figure 24. Substrate Grain Distribution at GH-GH1 (piezometer site) in Greenhills Creek on June, 2016. (a) cumulative particle size distribution and (b) number of particles per size class.

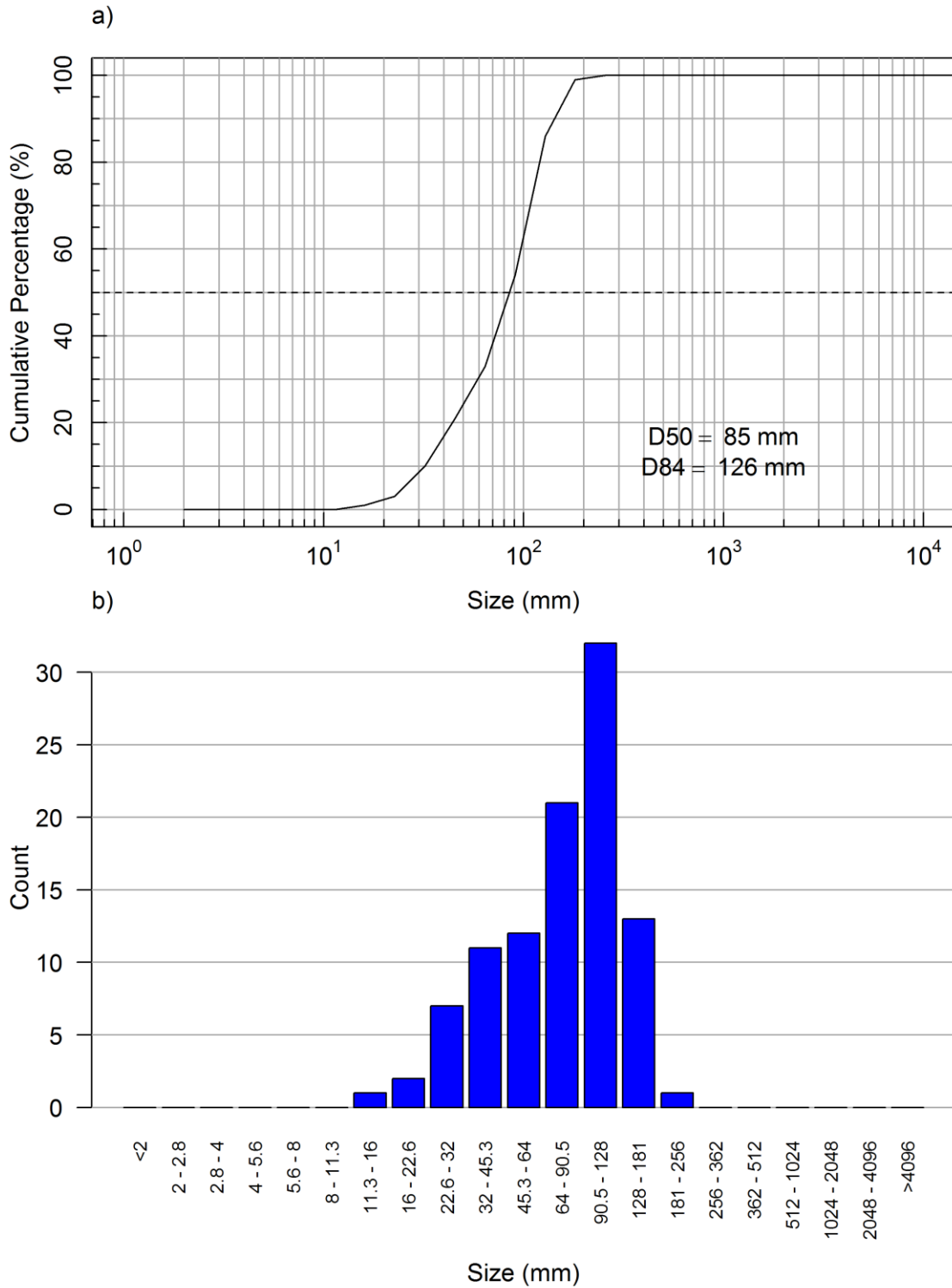


Figure 25. Substrate Grain Distribution at GRE-CA05 (mesohabitat site) in Greenhills Creek on June, 2016. (a) cumulative particle size distribution and (b) number of particles per size class.

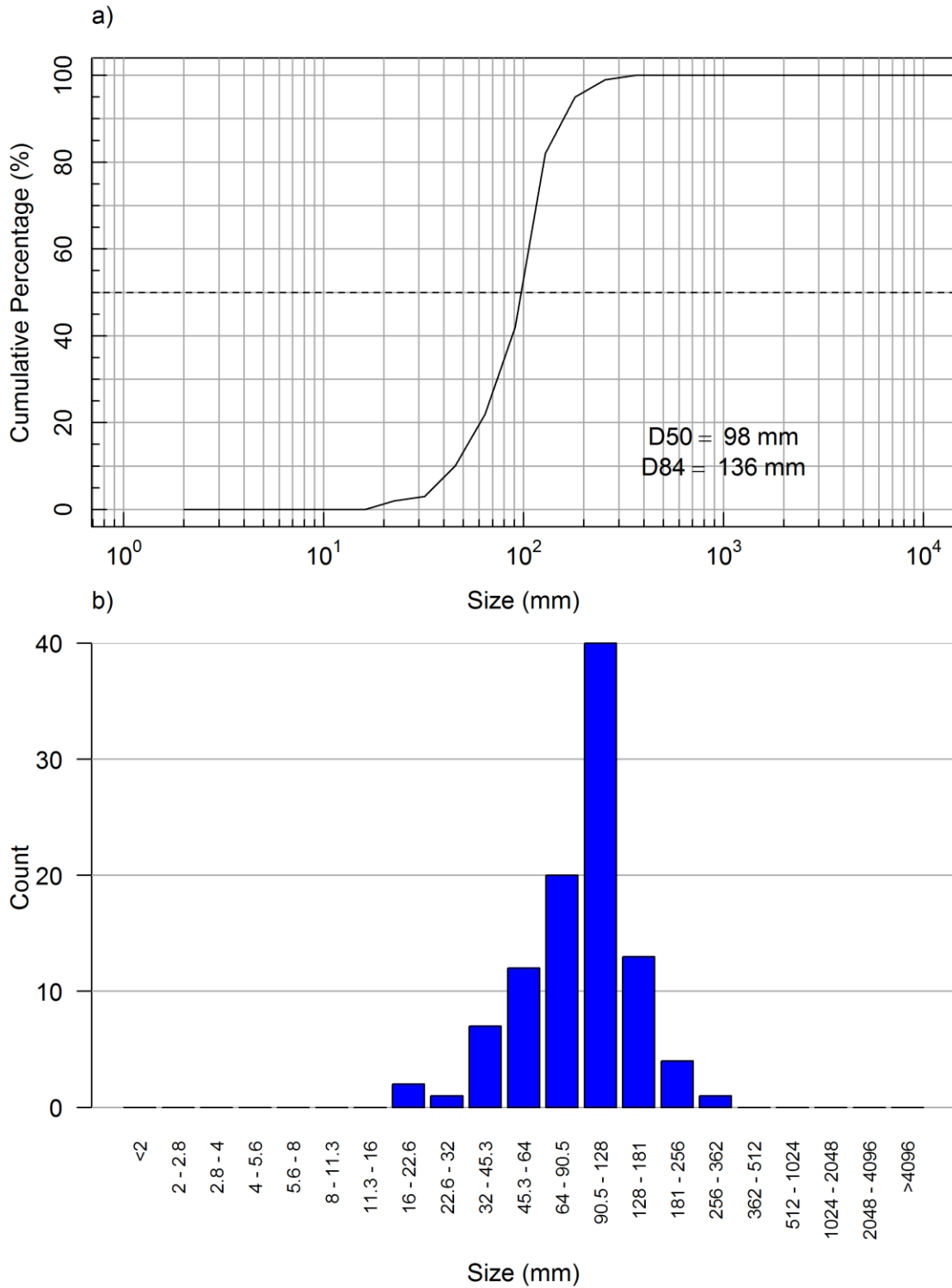


Figure 26. Substrate Grain Distribution at GRE-CA05 (piezometer site) in Greenhills Creek on June, 2016. (a) cumulative particle size distribution and (b) number of particles per size class.

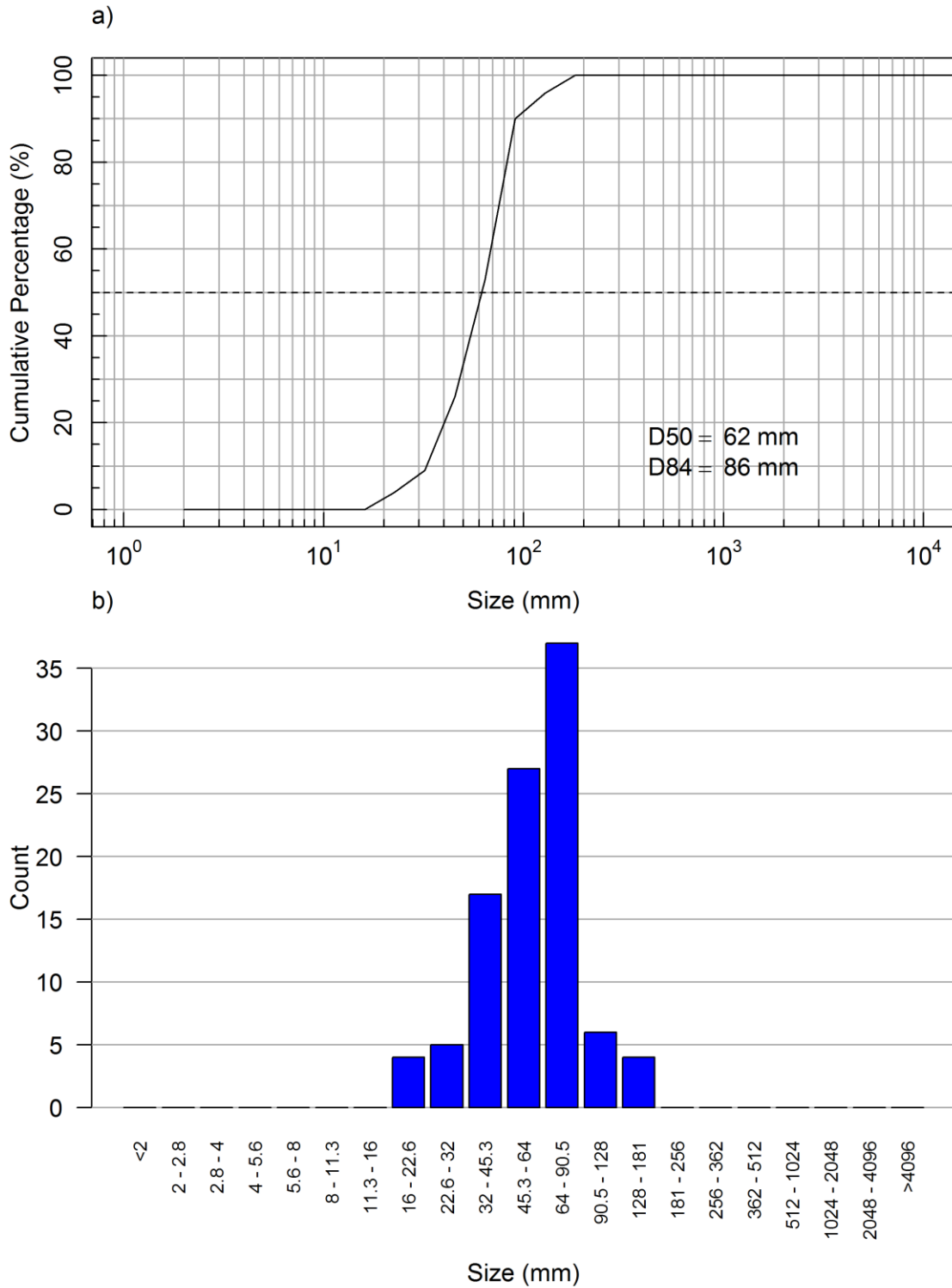


Figure 27. Substrate Grain Distribution at GRE-CA06 (mesohabitat and piezometer sites) in Greenhills Creek on June, 2016. (a) cumulative particle size distribution and (b) number of particles per size class.

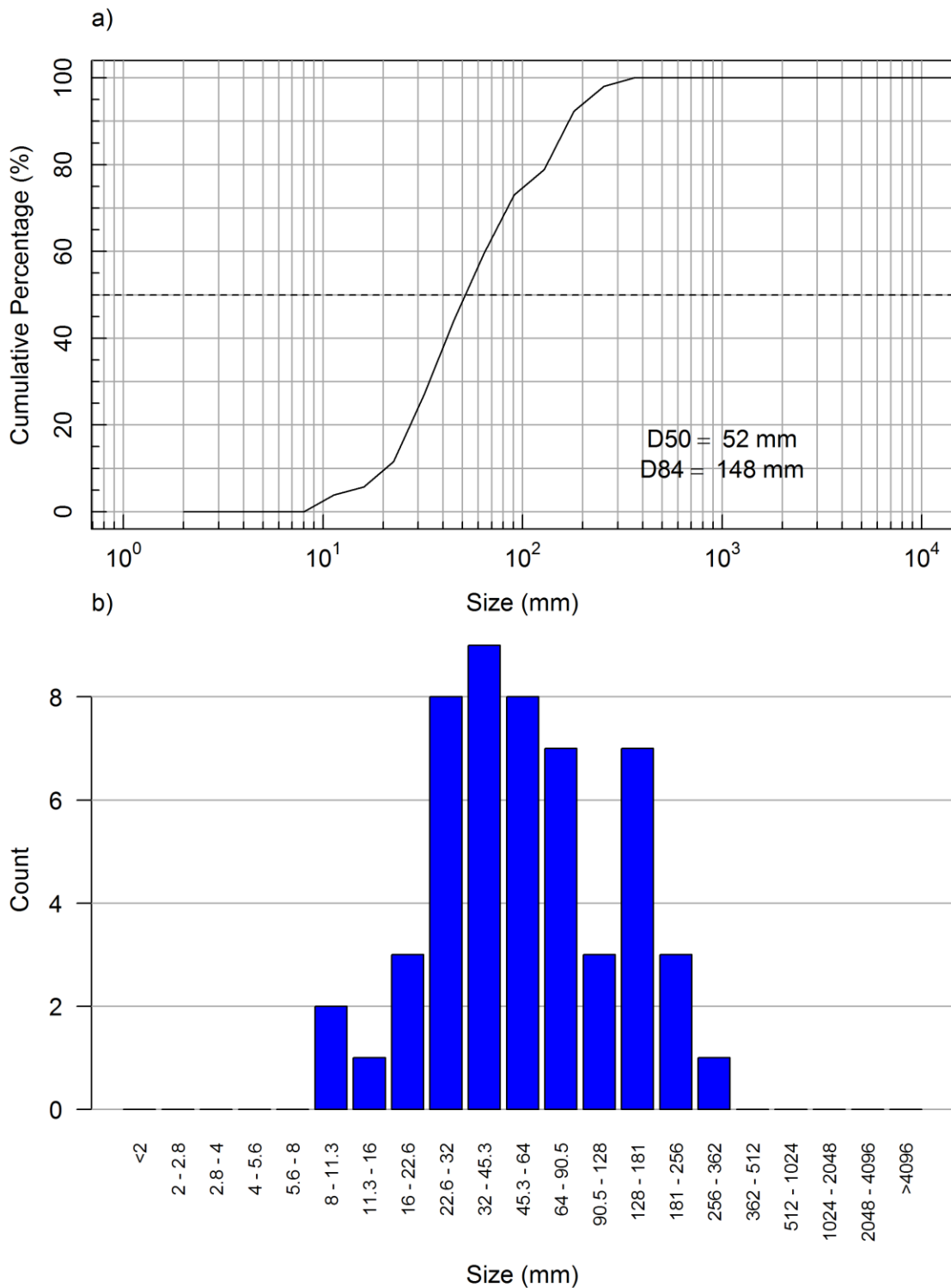


Figure 28. Substrate Grain Distribution at GH-CFT (mesohabitat and piezometer sites) in Greenhills Creek on June, 2016. (a) cumulative particle size distribution and (b) number of particles per size class.

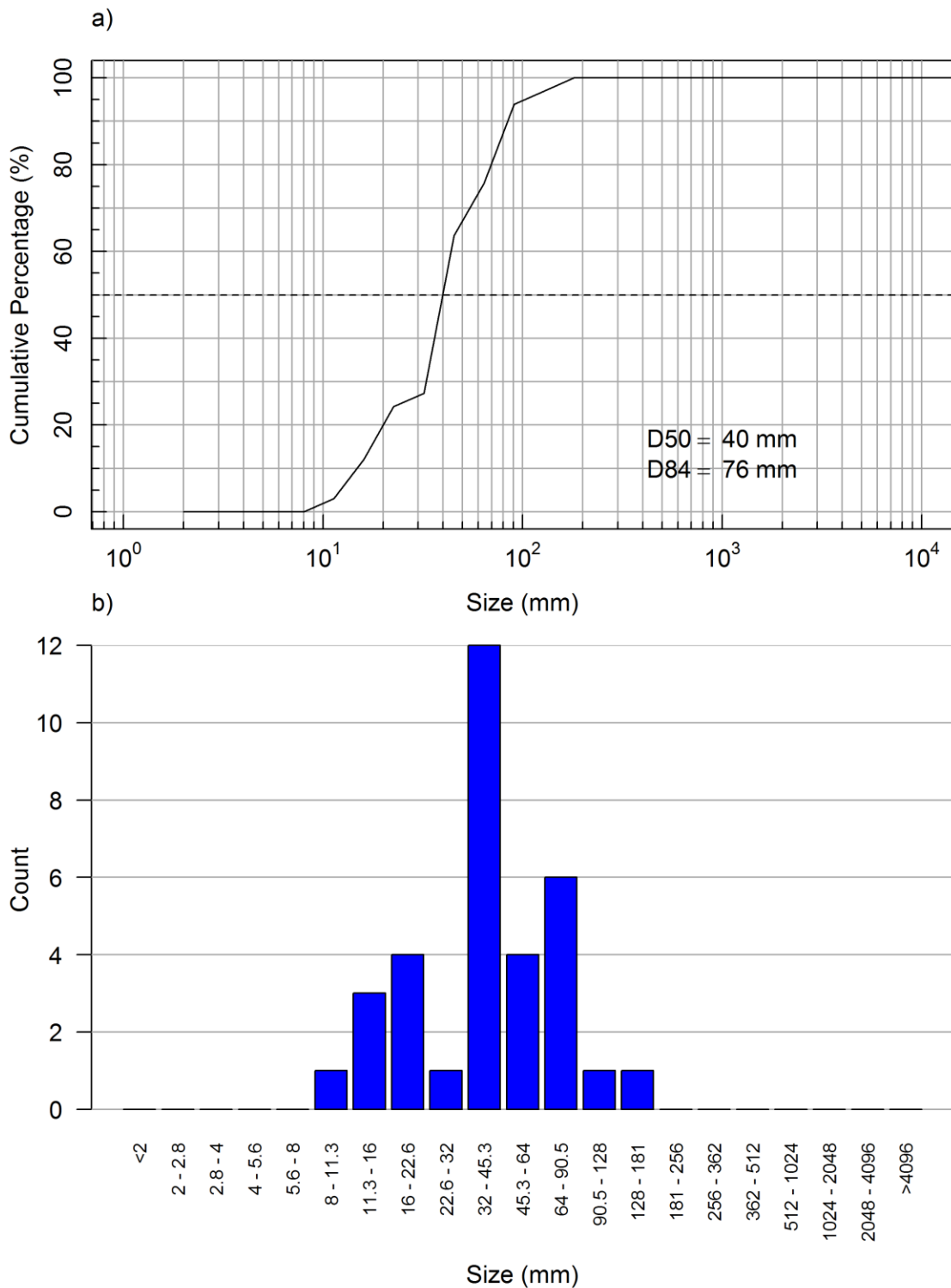


Figure 29, Substrate Grain Distribution at GRE-CA01 (mesohabitat site) in Greenhills Creek on August/September, 2016. (a) cumulative particle size distribution and (b) number of particles per size class.

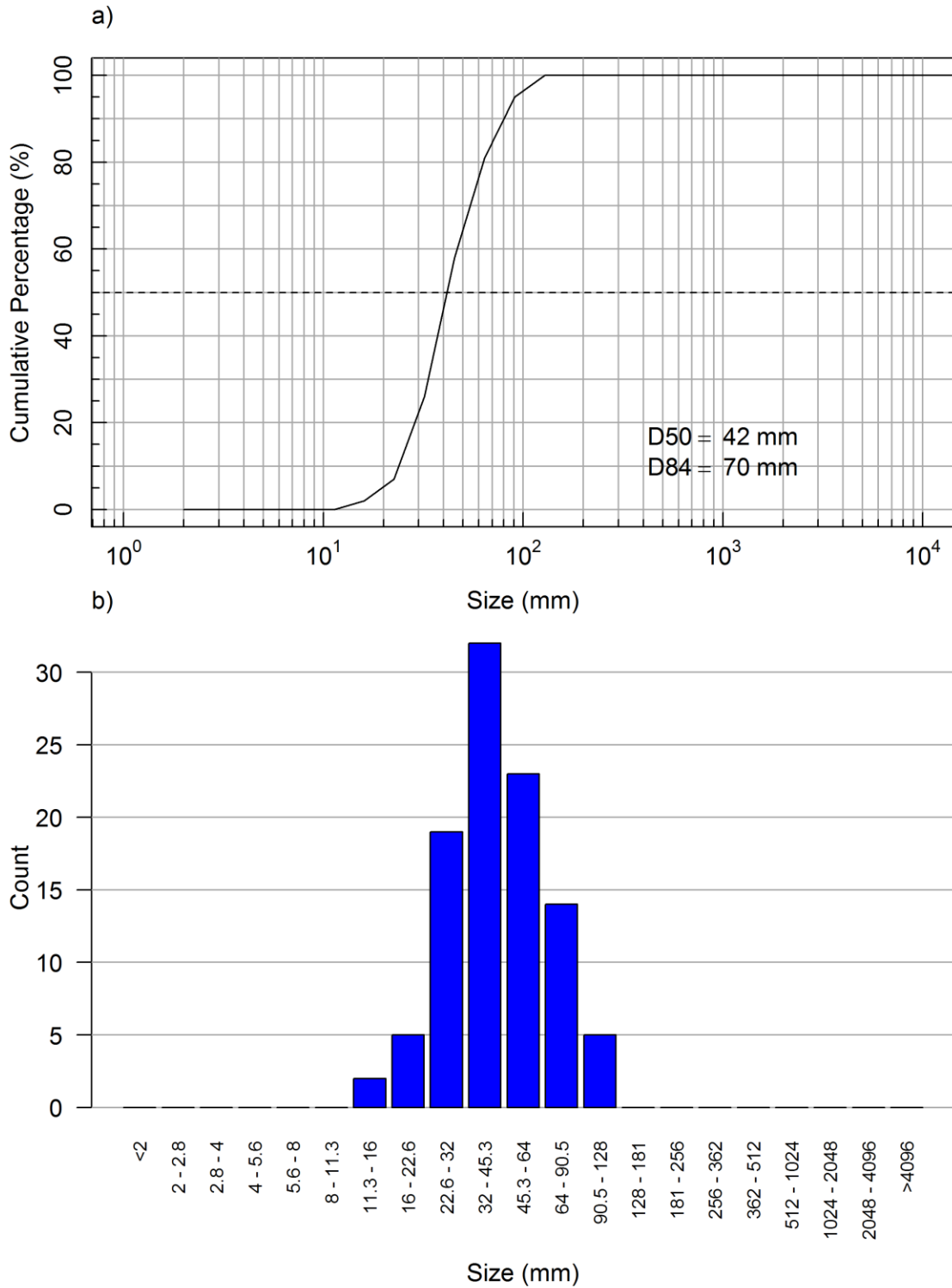


Figure 30. Substrate Grain Distribution at GRE-CA01 (piezometer site) in Greenhills Creek on August/September, 2016. (a) cumulative particle size distribution and (b) number of particles per size class.

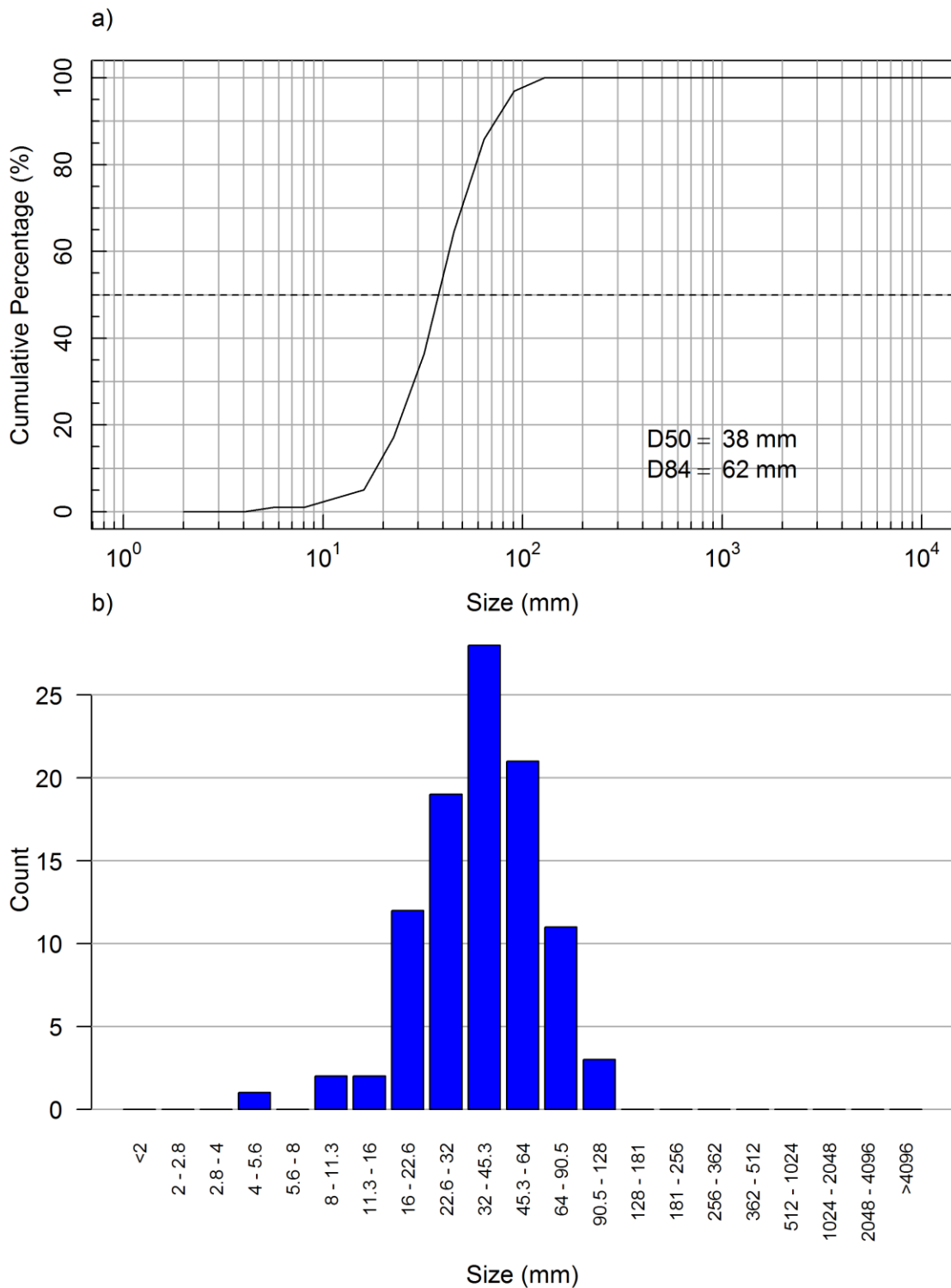


Figure 31. Substrate Grain Distribution at GRE-CA02 (mesohabitat/piezometer site) in Greenhills Creek on August/September, 2016. (a) cumulative particle size distribution and (b) number of particles per size class.

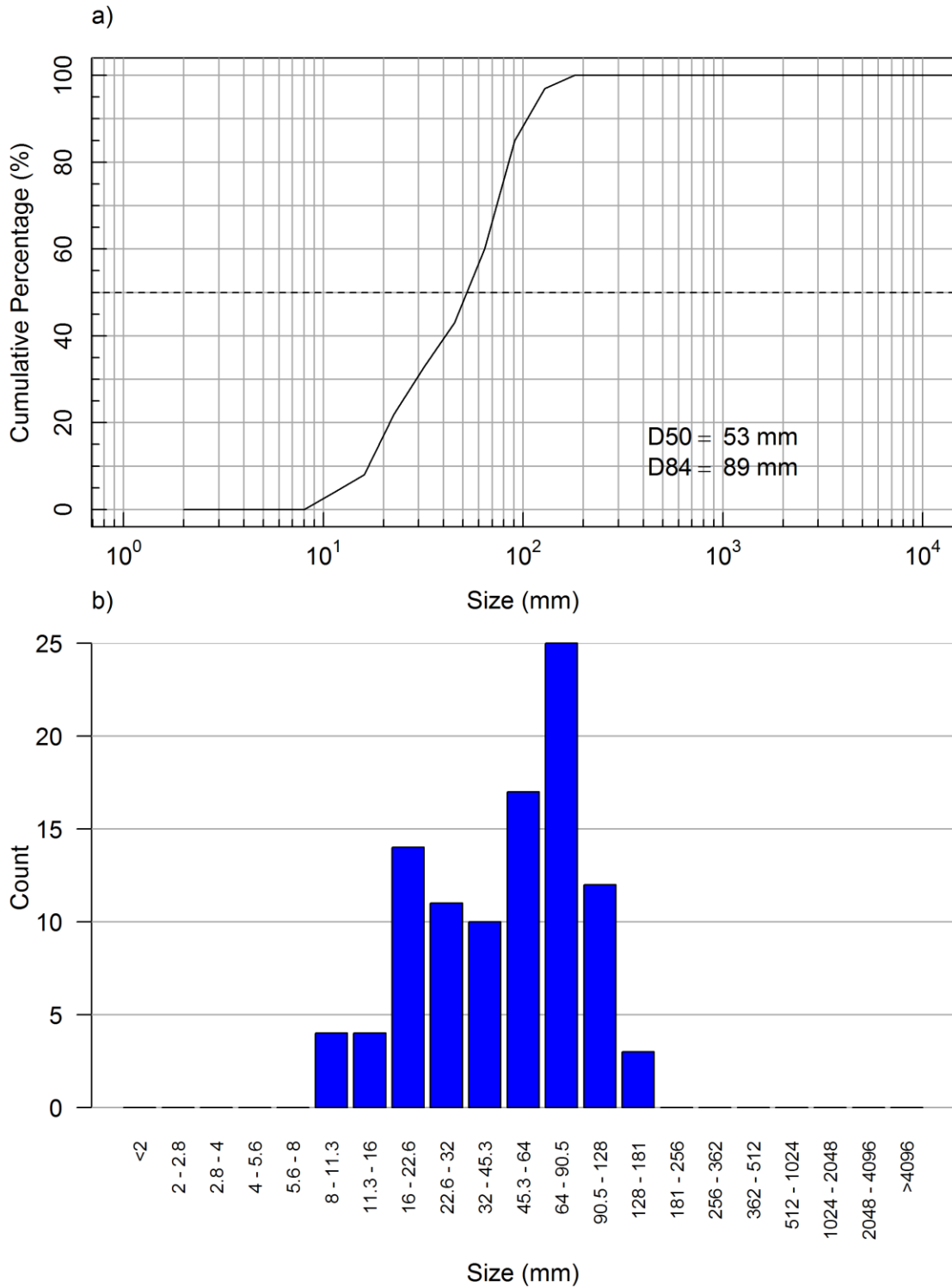


Figure 32. Substrate Grain Distribution at GRE-CA03 (mesohabitat site) in Greenhills Creek on August/September, 2016. (a) cumulative particle size distribution and (b) number of particles per size class.

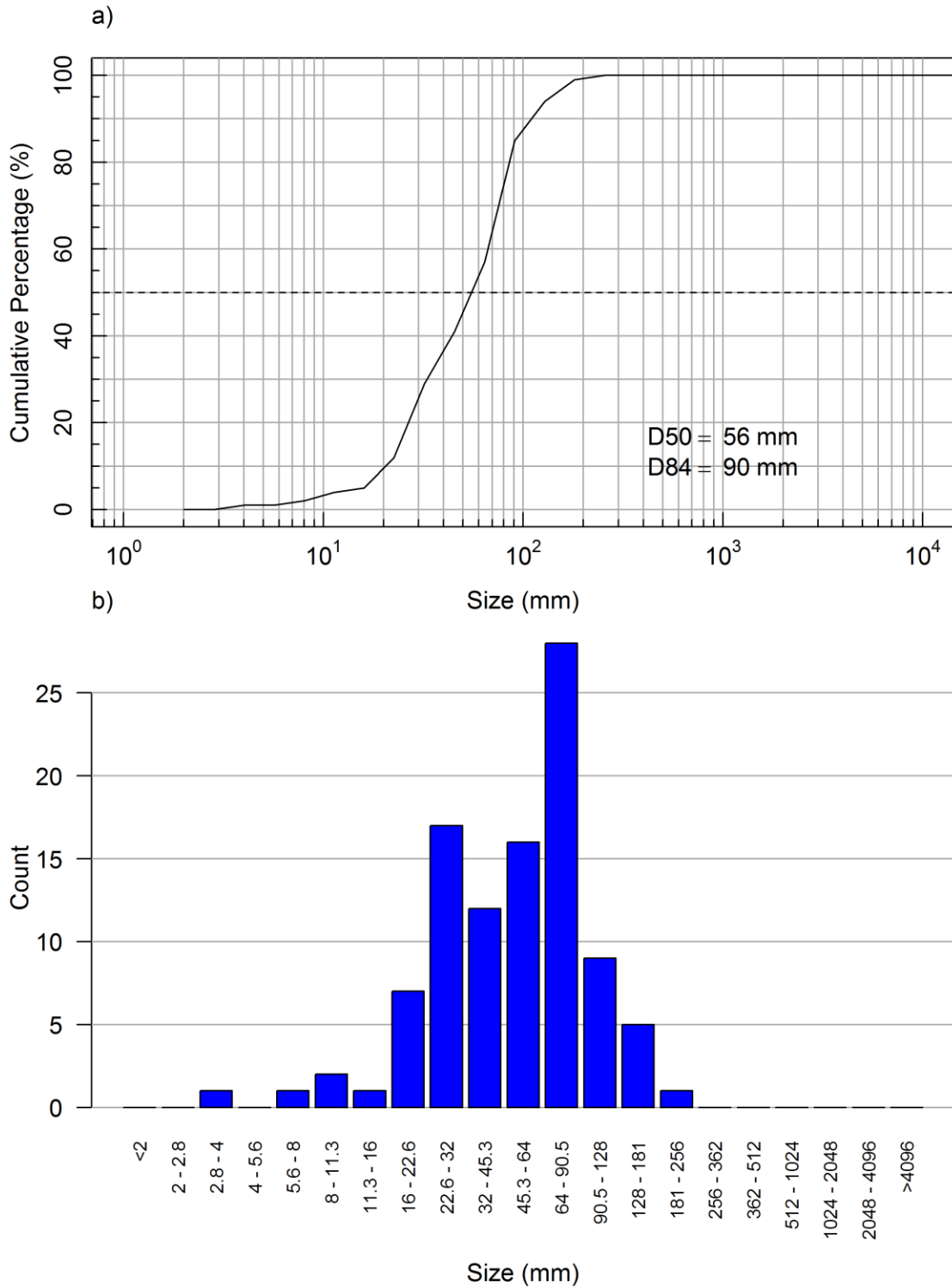


Figure 33. Substrate Grain Distribution at GRE-CA03 (piezometer site) in Greenhills Creek on August/September, 2016. (a) cumulative particle size distribution and (b) number of particles per size class.

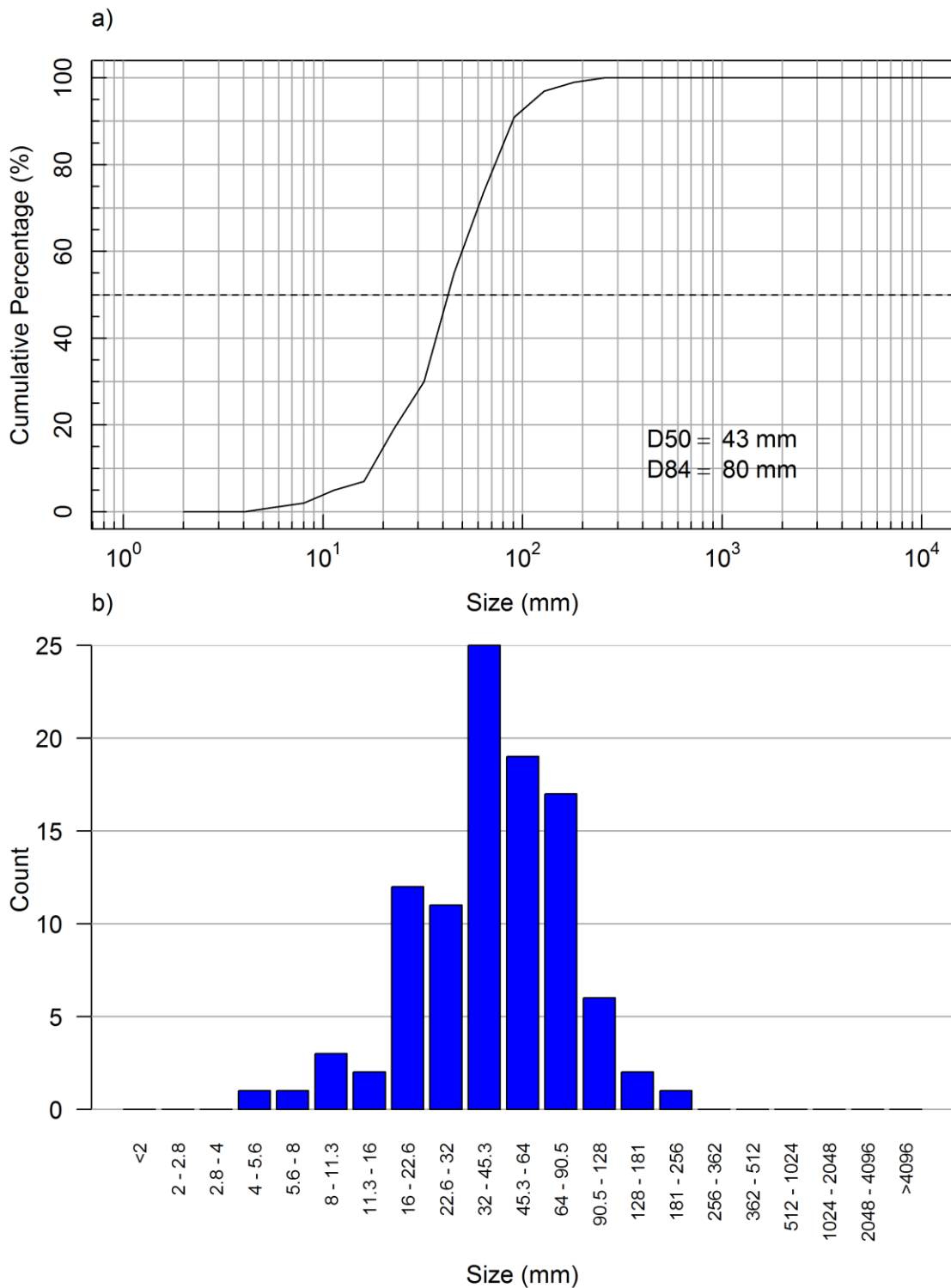


Figure 34. Substrate Grain Distribution at GH\_GH1 (mesohabitat site) in Greenhills Creek on August/September, 2016. (a) cumulative particle size distribution and (b) number of particles per size class.

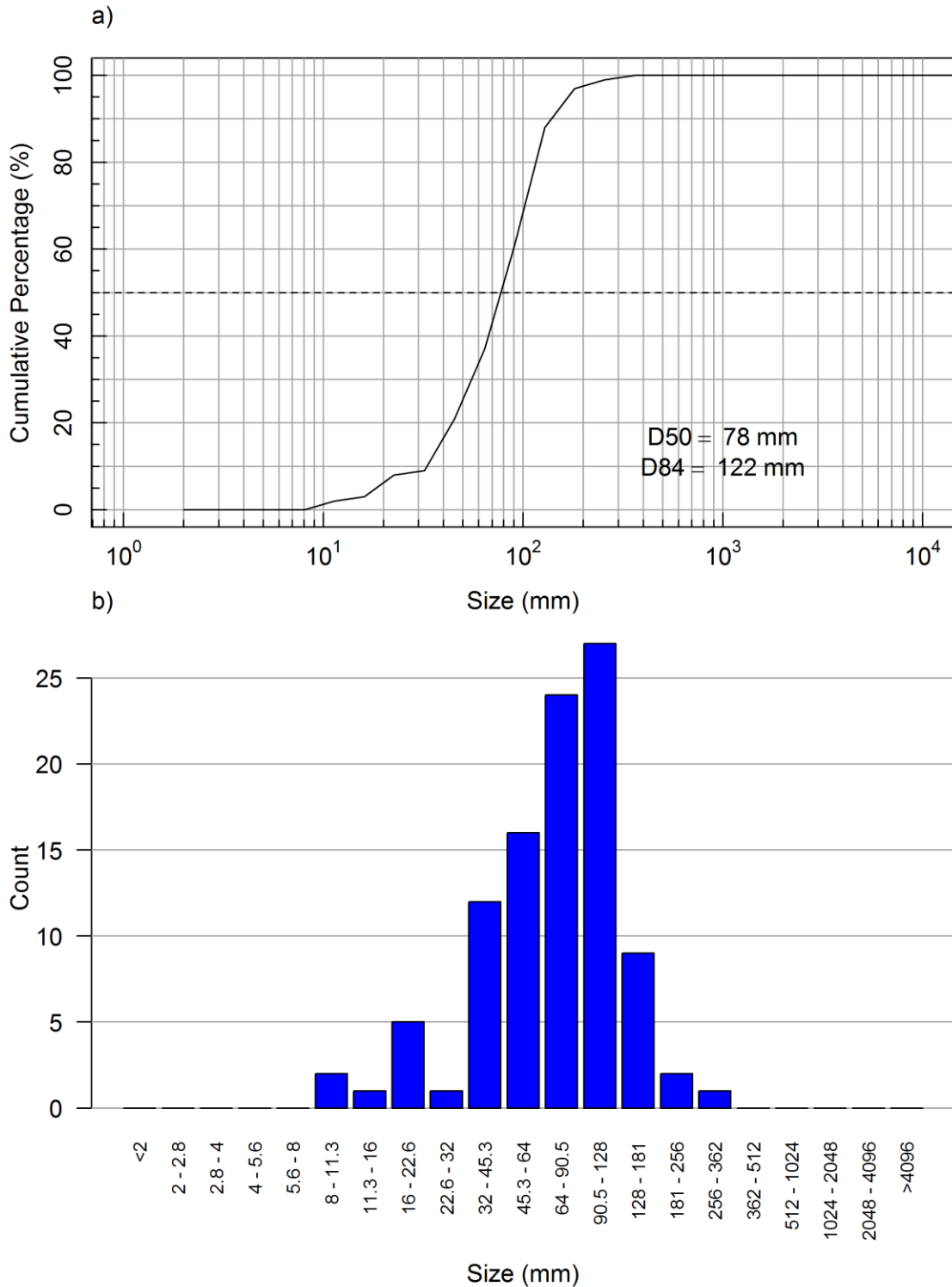


Figure 35. Substrate Grain Distribution at GH\_GH1 (piezometer site) in Greenhills Creek on August/September, 2016. (a) cumulative particle size distribution and (b) number of particles per size class.

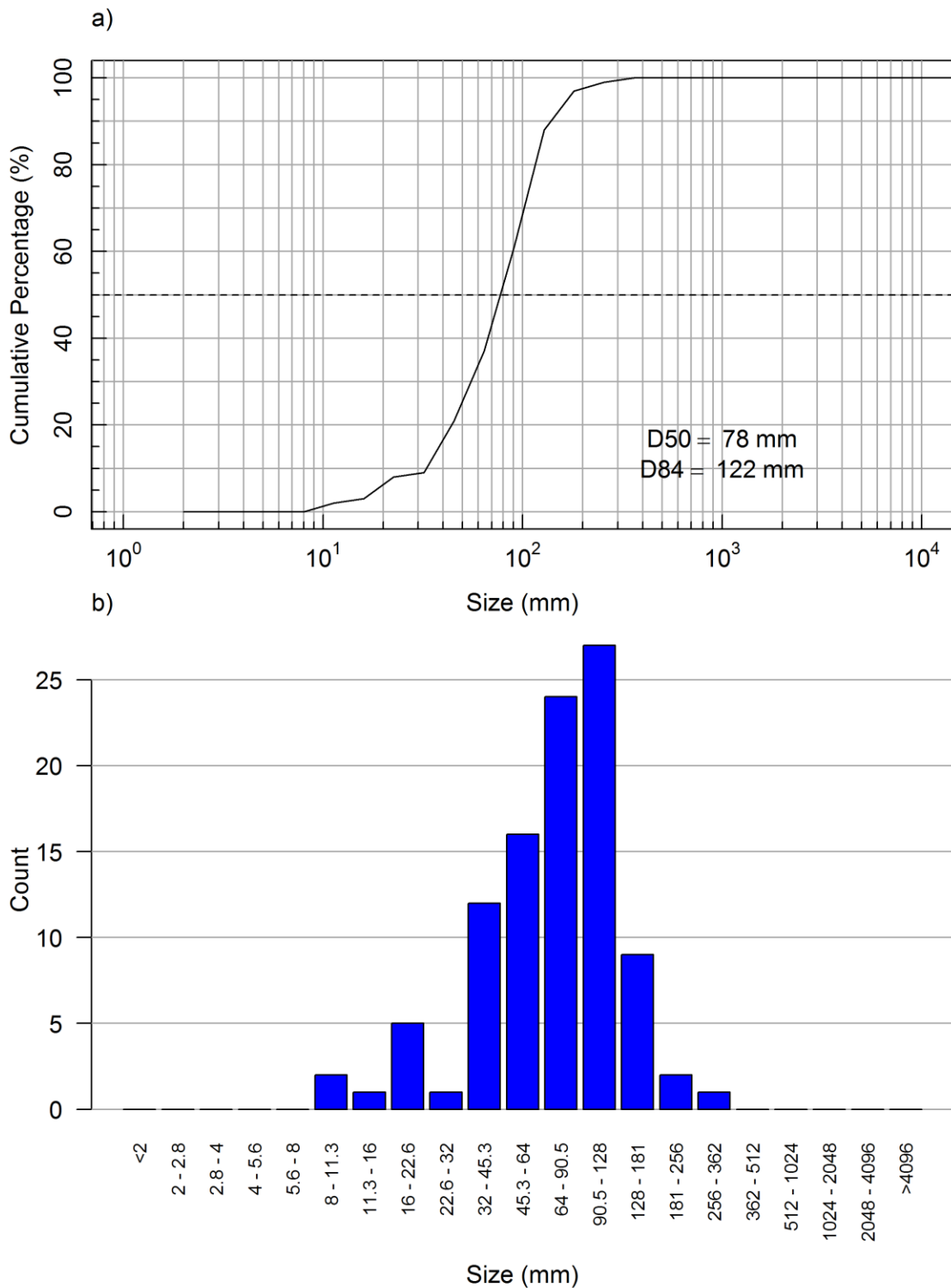


Figure 36. Substrate Grain Distribution at GRE-CA05 (piezometer site) in Greenhills Creek on August/September, 2016. (a) cumulative particle size distribution and (b) number of particles per size class.

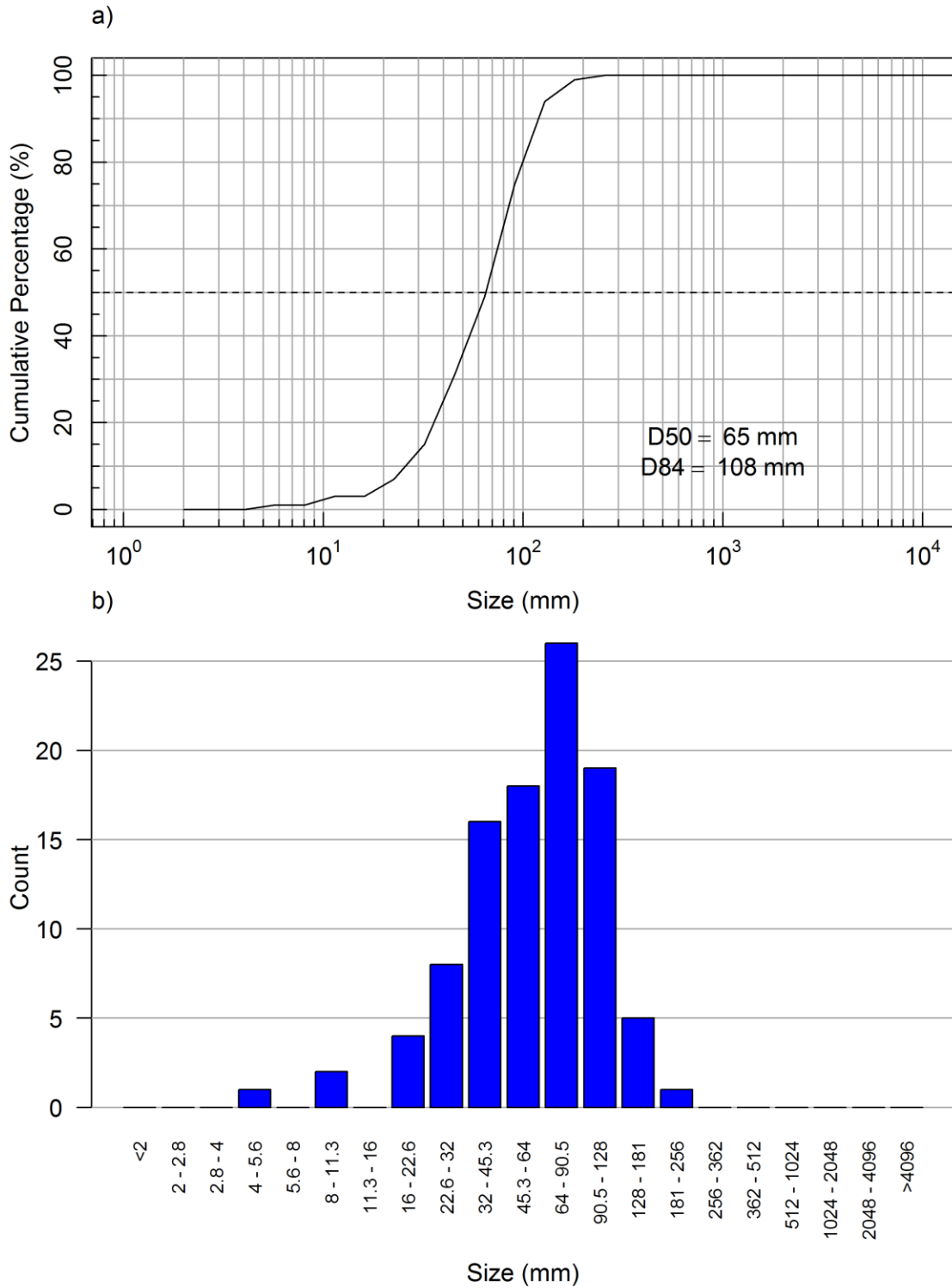


Figure 37. Substrate Grain Distribution at GRE-CA06 (mesohabitat/piezometer site) in Greenhills Creek on August/September, 2016. (a) cumulative particle size distribution and (b) number of particles per size class.

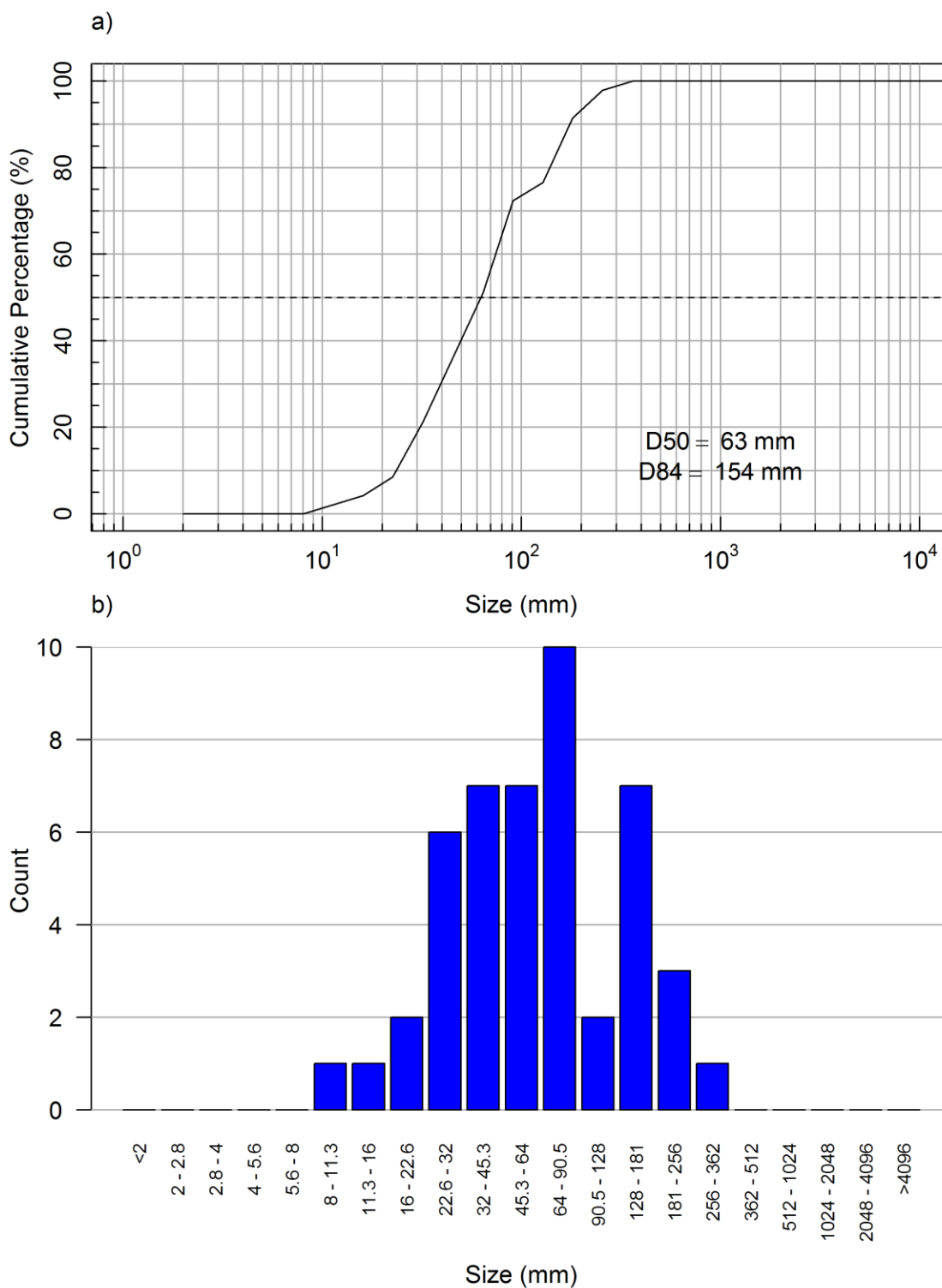
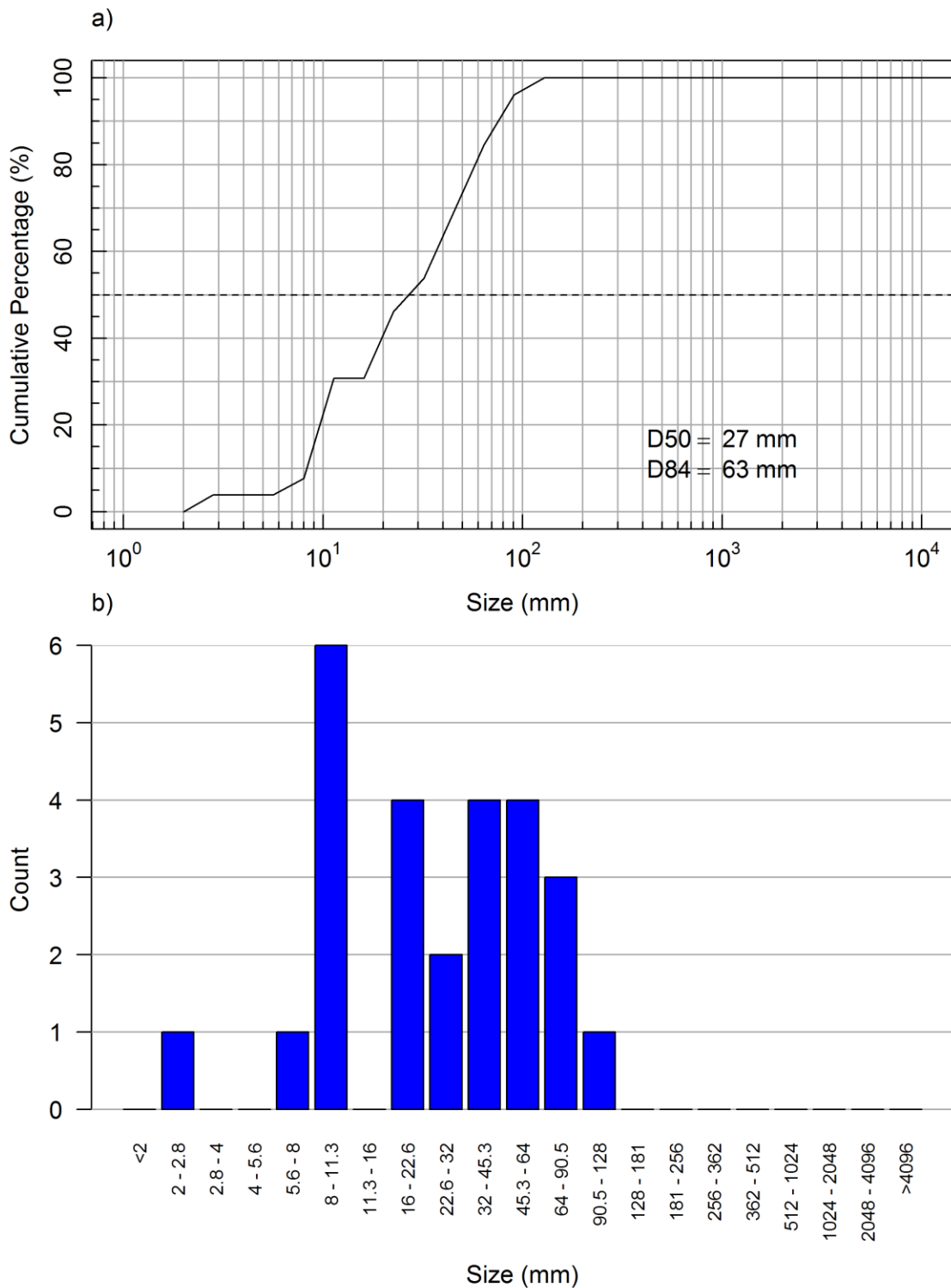


Figure 38. Substrate Grain Distribution at GRE-GH\_CTF (mesohabitat/piezometer site) in Greenhills Creek on August/September, 2016. (a) cumulative particle size distribution and (b) number of particles per size class.



Appendix D. Summary of surface hydrology results.

**LIST OF TABLES**

Table 1. Summary of surface hydrology measurements collected in June 2016. ....2  
Table 2. Summary of surface hydrology measurements collected in August, September 2016.....3

**Table 1. Summary of surface hydrology measurements collected in June 2016.**

Site Name	Measured Flow <sup>1</sup> (m <sup>3</sup> /s)	Location	Water Depth (Ruler) (m)	Water Depth (Swoffer) (m)	Flow Velocity <sup>2</sup> (m/s)
FRD-CA01	1.310	River Right	0.373	0.360	0.66
		Mid-Channel	0.463	0.440	0.50
		River Left	0.380	0.390	0.25
FRD-CA02		River Right	0.340	0.300	0.37
		Mid-Channel	0.400	0.390	0.48
		River Left	0.220	0.210	0.43
FRD-CA03		River Right	0.430	0.390	0.44
		Mid-Channel	0.440	0.460	0.79
		River Left	0.395	0.360	0.77
CLO-CA01	0.073	River Right	0.045	0.040	0.30
		Mid-Channel	0.140	0.120	0.69
		River Left	0.057	0.050	0.39
CLO-CA02		River Right	0.172	0.160	0.19
		Mid-Channel	0.159	0.140	0.22
		River Left	0.239	0.170	0.10
GRE-CA01	0.221	River Right	-	0.190	0.33
		Mid-Channel	0.085	0.070	0.30
		River Left	0.087	0.075	0.30
GRE-CA02		River Right	0.248	0.190	0.04
		Mid-Channel	0.304	0.280	0.19
		River Left	0.300	0.310	0.13
GRE-CA03		River Right	0.129	0.100	0.40
		Mid-Channel	0.170	0.140	0.52
		River Left	-	0.120	0.36
GH-GH1		River Right	0.138	0.110	0.27
		Mid-Channel	0.174	0.095	0.27
		River Left	0.196	0.150	0.27
GRE-CA05		River Right	0.103	0.050	0.27
		Mid-Channel	0.040	0.070	0.47
		River Left	0.170	0.170	0.59
GRE-CA06		River Right	0.195	0.170	0.07
		Mid-Channel	0.150	0.120	0.42
		River Left	0.107	0.077	0.27
GH-CFT		River Right	0.135	0.110	0.23
		Mid-Channel	0.150	0.130	0.41
		River Left	0.090	0.095	0.29

<sup>1</sup> Average flow using Price AA or Pygmy meter, assumed to be representative of the reach flow.

<sup>2</sup> Water velocity measured as average water column velocity using a Swoffer meter.

**Table 2. Summary of surface hydrology measurements collected in August, September 2016.**

Site Name	Measured Flow <sup>1</sup> (m <sup>3</sup> /s)	Location	Water Depth (Ruler) (m)	Water Depth (Swoffer) (m)	Flow Velocity <sup>2</sup> (m/s)
FRD-CA01	0.610	River Right	0.204	0.160	0.40
		Mid-Channel	0.365	0.200	0.38
		River Left	0.280	0.260	0.23
FRD-CA02		River Right	0.198	0.180	0.29
		Mid-Channel	0.325	0.280	0.54
		River Left	0.246	0.220	0.40
FRD-CA03		River Right	0.237	0.220	0.29
		Mid-Channel	0.395	0.340	0.56
		River Left	0.280	0.300	0.59
CLO-CA01	0.130	River Right	0.121	0.090	0.33
		Mid-Channel	0.077	0.070	0.22
		River Left	0.057	0.040	0.39
CLO-CA02		River Right	0.163	0.150	0.15
		Mid-Channel	0.192	0.188	0.11
		River Left	0.155	0.150	0.03
GRE-CA01	0.035	River Right	0.113	0.100	0.22
		Mid-Channel	0.095	0.050	0.40
		River Left	0.070	0.070	0.20
GRE-CA02		River Right	0.166	0.170	0.04
		Mid-Channel	0.285	0.260	0.11
		River Left	0.300	0.270	0.10
GRE-CA03		River Right	0.120	0.080	0.31
		Mid-Channel	0.160	0.110	0.38
		River Left	0.180	0.110	0.26
GH-GH1		River Right	0.135	0.100	0.24
		Mid-Channel	0.131	0.150	0.24
		River Left	0.130	0.130	0.28
GRE-CA05		River Right	0.060	0.040	0.02
		Mid-Channel	0.062	0.050	0.07
		River Left	0.180	0.150	0.73
GRE-CA06		River Right	0.227	0.160	0.04
		Mid-Channel	0.246	0.220	0.06
		River Left	0.050	0.050	0.02
GH-CFT		River Right	0.080	0.090	0.33
		Mid-Channel	0.130	0.130	0.40
		River Left	0.117	0.080	0.15

<sup>1</sup> Average flow using Price AA or Pygmy meter, assumed to be representative of the reach flow.

<sup>2</sup> Water velocity measured as average water column velocity using a Swoffer meter.

**Appendix E. Water quality and hydraulic head data tables and QA/QC.**

**LIST OF TABLES**

Table 1. Typical range of specific conductivity, pH and dissolved oxygen in BC surface watercourses..... 1

Table 2. BC MOE Guidelines for the Protection of Aquatic Life for dissolved oxygen (mg/L) in the water column and interstitial waters.....2

Table 3. Summary of dissolved oxygen and general water quality at Fording River and Clode Creek calcite study sites in 2016.....3

Table 4. Summary of dissolved oxygen and general water quality at Greenhills Creek study sites in 2016 (part 1 of 2).....4

Table 5. Summary of dissolved oxygen and general water quality at Greenhills Creek study sites in 2016 (part 2 of 2).....5

Table 6. Relative standard error (RSE) exceedance summary for dissolved oxygen, water temperature and specific conductivity at the calcite study sites.....6

Table 7. Summary of hydraulic head measurements at the Fording River and Clode Creek in 2016. ....7

Table 8. Summary of hydraulic head measurements at Greenhills Creek in 2016.....8

**Table 1. Typical range of specific conductivity, pH and dissolved oxygen in BC surface watercourses.**

Parameter	Unit	Typical Range in BC	Reference
Specific Conductivity	µS/cm	The typical value in coastal British Columbia streams is 100 µS/cm, while interior streams range up to 500 µS/cm	RISC (1998)
pH	pH units	Natural fresh waters have a pH range from 4 to 10, and lakes tend to have a pH ≥ 7.0.	RISC (1998)
Dissolved Oxygen	mg/L	In BC surface waters are generally well aerated and have DO concentrations greater than 10 mg/L	MOE (1997a)
Dissolved Oxygen	% saturation	In BC surface waters are generally well aerated and have DO concentrations close to equilibrium with the atmosphere (i.e., close to 100% saturation)	MOE (1997a)

**Table 2. BC MOE Guidelines for the Protection of Aquatic Life for dissolved oxygen (mg/L) in the water column and interstitial waters.**

<b>BC Guidelines for the Protection of Aquatic Life<sup>1</sup></b>			
	<b>Life Stages Other Than Buried Embryo/Alevin</b>	<b>Buried Embryo/Alevin<sup>2</sup></b>	<b>Buried Embryo/Alevin<sup>2</sup></b>
	Water column	Water column	Interstitial Water
Dissolved Oxygen Concentration	mg/L O <sub>2</sub>	mg/L O <sub>2</sub>	mg/L O <sub>2</sub>
Instantaneous minimum <sup>3</sup>	5	9	6
30-day mean <sup>4</sup>	8	11	8

<sup>1</sup> MOE (1997a) and MOE (1997b)

<sup>2</sup> For the buried embryo / alevin life stages these are in-stream concentrations from spawning to the point of yolk sac absorption or 30 days post-hatch for fish; the water column concentrations recommended to achieve interstitial dissolved oxygen values when the latter are unavailable. Interstitial oxygen measurements would supersede water column measurements in comparing to criteria.

<sup>3</sup> The instantaneous minimum level is to be maintained at all times.

<sup>4</sup> The mean is based on at least five approximately evenly spaced samples. If a diurnal cycle exists in the water body, measurements should be taken when oxygen levels are lowest (usually early morning).

**Table 3. Summary of dissolved oxygen and general water quality at Fording River and Clode Creek calcite study sites in 2016.**

Site	Date	n	Depth (cm)		Dissolved Oxygen (% sat.)				Dissolved Oxygen (mg/L)				Water Temperature (°C)				pH				Specific Conductivity (µS/cm)					
			Avg.	SD	Avg.	Min.	Max.	SD	Avg.	Min.	Max.	SD	Avg.	Min.	Max.	SD	Avg.	Min.	Max.	SD	Avg.	Min.	Max.	SD		
FRD-CA01	Jun-25	3	0	0	84.2	82.8	86.3	1.9	10.36	10.20	10.58	0.20	6.5	6.4	6.6	0.1	-	-	-	-	-	-	-	-	-	
		3	10	0	84.2	81.3	86.9	2.8	10.34	10.02	10.63	0.31	6.6	6.4	6.7	0.2	-	-	-	-	-	-	-	-	-	
		3	28	3	85.9	84.1	87.5	1.7	10.53	10.34	10.68	0.17	6.6	6.5	6.8	0.2	-	-	-	-	-	-	-	-	-	
	Sep-05	3	0	0	81.9	80.3	83.8	1.8	9.86	9.70	10.02	0.16	7.3	7.2	7.6	0.3	8.03	7.92	8.12	0.10	569	564	575	6		
		3	10	0	82.3	81.0	84.0	1.5	9.90	9.79	10.02	0.12	7.4	7.2	7.8	0.3	8.10	8.08	8.14	0.03	572	568	577	5		
		3	29	1	83.2	82.0	84.3	1.2	9.97	9.90	10.02	0.06	7.5	7.2	7.9	0.4	8.14	8.14	8.14	0.00	571	568	573	2		
		3	43	6	82.4	78.3	84.9	3.6	9.80	9.43	10.01	0.32	7.8	7.3	8.4	0.5	8.12	8.05	8.16	0.06	570	561	575	7		
	FRD-CA02	Jun-25	3	0	0	88.7	87.1	90.0	1.5	10.44	10.24	10.58	0.18	8.3	8.2	8.3	0.1	-	-	-	-	-	-	-	-	-
			3	10	0	89.2	87.9	90.7	1.4	10.48	10.34	10.61	0.14	8.3	8.2	8.5	0.2	-	-	-	-	-	-	-	-	-
3			29	2	89.4	89.2	89.6	0.2	10.50	10.46	10.54	0.04	8.4	8.3	8.4	0.1	-	-	-	-	-	-	-	-	-	
Sep-05		3	0	0	85.9	85.6	86.3	0.4	9.88	9.84	9.92	0.04	9.2	8.9	9.6	0.4	8.07	8.02	8.11	0.05	500	499	500	1		
		3	10	0	85.7	85.2	86.1	0.5	9.86	9.81	9.93	0.06	9.3	9.1	9.6	0.3	8.07	8.03	8.10	0.04	502	502	503	0		
		3	30	0	85.9	85.7	86.0	0.2	9.82	9.78	9.84	0.03	9.5	9.3	9.7	0.2	8.09	8.08	8.09	0.01	504	503	505	1		
		3	48	3	85.7	85.2	85.9	0.4	9.78	9.76	9.81	0.03	9.5	9.3	9.7	0.2	8.10	8.09	8.12	0.02	504	502	506	2		
FRD-CA03		Jun-22	3	0	0	86.5	85.8	87.8	1.1	10.34	10.29	10.41	0.07	7.6	7.1	8.3	0.6	-	-	-	-	-	-	-	-	-
			3	10	0	86.1	85.5	86.6	0.6	10.26	10.16	10.39	0.12	7.8	7.3	8.4	0.6	-	-	-	-	-	-	-	-	-
	3		28	3	85.4	83.7	87.9	2.2	10.07	9.77	10.36	0.30	8.2	7.3	9.1	0.9	-	-	-	-	-	-	-	-	-	
	Sep-06	3	0	0	82.2	80.7	84.2	1.8	9.78	9.65	9.93	0.14	7.8	7.6	8.2	0.4	8.00	7.98	8.02	0.02	498	497	499	1		
		3	10	0	82.5	81.5	84.2	1.5	9.80	9.72	9.90	0.09	7.9	7.7	8.3	0.3	8.08	8.07	8.10	0.02	499	496	501	2		
		3	27	3	83.0	82.2	83.7	0.8	9.83	9.77	9.88	0.06	8.0	7.8	8.3	0.2	8.07	8.06	8.09	0.02	500	498	501	2		
		3	47	5	78.5	76.4	82.2	3.2	9.25	9.00	9.67	0.36	8.2	8.1	8.3	0.1	8.02	7.95	8.06	0.06	502	497	506	5		
	CLO-CA01	Jun-25	3	0	0	88.5	87.0	90.2	1.6	9.71	9.62	9.79	0.09	11.2	10.9	11.7	0.4	-	-	-	-	-	-	-	-	-
			3	10	0	88.9	87.5	90.9	1.8	9.73	9.65	9.82	0.09	11.5	11.0	11.9	0.6	-	-	-	-	-	-	-	-	-
2			27	4	84.6	84.1	85.1	0.7	9.29	9.27	9.30	0.02	11.2	11.0	11.4	0.3	-	-	-	-	-	-	-	-	-	
Sep-04		3	0	0	88.3	86.9	90.0	1.6	9.52	9.45	9.59	0.07	12.0	11.6	12.5	0.5	8.22	8.20	8.23	0.02	1565	1564	1567	2		
		2	10	0	88.2	87.8	88.5	0.5	9.51	9.48	9.54	0.04	11.9	11.9	12.0	0.1	8.24	8.24	8.24	0.00	1574	1574	1574	0		
		2	30	0	86.6	84.6	88.5	2.8	9.28	9.02	9.54	0.37	12.2	12.0	12.4	0.2	8.25	8.24	8.25	0.01	1577	-	-	-		
CLO-CA02		Jun-23	3	0	0	92.4	91.9	93.4	0.9	9.84	9.84	9.84	0.00	12.3	12.3	12.3	0.0	-	-	-	-	-	-	-	-	-
			3	10	0	86.4	83.3	91.7	4.6	9.31	9.04	9.84	0.46	12.3	12.2	12.4	0.1	-	-	-	-	-	-	-	-	-
			3	27	5	86.0	75.5	91.3	9.1	9.78	9.77	9.79	0.01	12.1	11.7	12.3	0.3	-	-	-	-	-	-	-	-	-
	Sep-04	3	0	0	83.9	83.9	84.0	0.1	9.19	9.17	9.20	0.02	11.3	11.3	11.4	0.1	8.25	8.22	8.27	0.03	1567	1563	1569	3		
		3	10	0	83.7	83.6	83.9	0.2	9.16	9.14	9.17	0.02	11.3	11.3	11.4	0.0	8.05	7.89	8.23	0.17	1572	1563	1577	8		
		3	28	2	80.2	77.7	84.9	4.0	8.74	8.45	9.26	0.45	11.5	11.5	11.5	0.0	8.06	7.95	8.21	0.14	1564	1549	1577	14		
		1	48	-	85.5	-	-	-	9.32	-	-	-	-	11.5	-	-	-	8.22	-	-	-	1574	-	-	-	

Note that the Avg. is an average of three single measurements taken at three piezometer locations within each monitoring site (i.e., at river right, mid channel and at river left) unless otherwise indicated (n). Therefore variability (high standard deviation) is likely due to heterogeneous substrate composition within the monitoring site.

**Table 4. Summary of dissolved oxygen and general water quality at Greenhills Creek study sites in 2016 (part 1 of 2).**

Site	Date	n	Depth (cm)		Dissolved Oxygen (% sat.)				Dissolved Oxygen (mg/L)				Water Temperature (°C)				pH				Specific Conductivity (µS/cm)				
			Avg.	SD	Avg.	Min.	Max.	SD	Avg.	Min.	Max.	SD	Avg.	Min.	Max.	SD	Avg.	Min.	Max.	SD	Avg.	Min.	Max.	SD	
GRE-CA01	Jun-19	4	0	0	83.5	82.2	84.5	1.0	9.35	9.30	9.38	0.04	10.3	9.9	10.7	0.3	-	-	-	-	-	-	-	-	-
			3	10	0	82.6	80.4	84.1	1.9	9.23	8.97	9.38	0.23	10.4	10.3	10.5	0.1	-	-	-	-	-	-	-	-
			2	30	0	43.1	21.5	64.6	30.5	4.84	2.44	7.24	3.40	10.1	9.8	10.3	0.4	-	-	-	-	-	-	-	-
	Aug-30	3	0	0	85.6	85.5	85.8	0.2	8.43	8.35	8.51	0.08	16.2	15.6	16.6	0.5	8.27	8.09	8.42	0.17	1242	1037	1346	177	
			3	6	1	85.8	85.5	86.3	0.4	8.43	8.34	8.50	0.08	16.3	15.8	16.6	0.4	8.23	8.13	8.33	0.14	1330	1311	1349	27
			3	19	2	75.8	55.1	86.7	17.9	7.45	5.50	8.44	1.69	16.1	15.4	16.9	0.8	8.10	8.00	8.16	0.09	1365	1360	1372	6
	3	37	1	57.3	40.7	75.8	17.6	5.82	4.13	7.66	1.77	14.7	14.5	15.0	0.3	7.93	7.82	8.02	0.10	1383	1352	1415	32		
GRE-CA02	Jun-19	3	0	0	83.7	83.5	83.9	0.2	9.20	9.12	9.25	0.07	11.1	10.8	11.5	0.4	-	-	-	-	-	-	-	-	
			3	10	0	58.8	27.3	76.7	27.4	6.51	3.07	8.44	2.99	10.7	10.2	11.1	0.5	-	-	-	-	-	-	-	
			3	30	0	12.0	8.7	15.3	3.3	1.35	0.99	1.71	0.36	10.0	9.7	10.4	0.4	-	-	-	-	-	-	-	
	Sep-03	3	0	0	83.9	83.5	84.2	0.4	8.87	8.80	8.93	0.07	12.8	12.5	13.2	0.4	8.47	8.43	8.54	0.06	1361	1359	1365	3	
			2	9	1	78.5	73.0	84.0	7.8	8.29	7.68	8.89	0.86	12.8	12.4	13.1	0.4	8.14	7.86	8.36	0.25	1348	1300	1373	41
			2	27	4	37.2	34.0	40.3	4.5	3.95	3.61	4.29	0.48	12.5	12.4	12.7	0.1	7.83	7.72	7.96	0.12	1291	1212	1384	87
	2	46	6	16.2	13.2	19.1	4.2	1.72	1.40	2.04	0.45	12.4	12.4	12.5	0.0	7.66	7.59	7.75	0.08	1231	1123	1375	130		
GRE-CA03	Jun-21	3	0	0	83.7	83.3	84.3	0.6	9.16	9.12	9.22	0.05	11.3	10.9	11.7	0.4	-	-	-	-	-	-	-	-	
			3	10	0	83.5	82.8	83.9	0.6	9.12	9.10	9.13	0.01	11.4	11.0	11.7	0.4	-	-	-	-	-	-	-	
			3	30	0	84.0	83.0	85.2	1.1	9.13	9.11	9.14	0.02	11.7	11.2	12.2	0.5	-	-	-	-	-	-	-	
	Sep-03	3	0	0	84.5	83.4	86.1	1.4	9.09	9.01	9.20	0.10	12.1	11.9	12.4	0.3	8.44	8.40	8.47	0.04	1369	1368	1371	2	
			3	10	0	84.5	83.9	85.5	0.9	9.08	9.06	9.13	0.04	12.1	11.9	12.4	0.3	8.48	8.46	8.50	0.02	1377	1376	1378	1
			3	28	2	85.5	84.7	86.3	0.8	9.14	9.11	9.18	0.04	12.3	12.1	12.6	0.2	8.49	8.49	8.50	0.01	1375	1372	1378	3
	3	47	3	85.6	85.3	86.1	0.4	9.12	9.10	9.14	0.02	12.5	12.3	12.7	0.2	8.47	8.46	8.47	0.01	1373	1370	1376	3		
GH_GH1	Jun-20	3	0	0	86.7	86.3	87.1	0.4	9.66	9.63	9.70	0.03	10.5	10.2	10.9	0.4	-	-	-	-	-	-	-	-	
			3	10	0	86.6	86.2	86.9	0.4	9.64	9.58	9.69	0.05	10.6	10.2	11.0	0.4	-	-	-	-	-	-	-	
			2	30	0	86.6	86.4	86.7	0.2	9.63	9.61	9.66	0.04	10.6	10.4	10.8	0.3	-	-	-	-	-	-	-	
	Sep-02	3	0	0	87.0	86.8	87.2	0.2	8.95	8.89	9.00	0.06	14.1	13.9	14.6	0.4	8.48	8.47	8.49	0.01	1367	1365	1369	2	
			3	10	0	86.6	86.0	87.2	0.6	8.91	8.80	8.99	0.10	14.1	14.0	14.3	0.2	8.49	8.49	8.50	0.01	1376	1375	1379	2
			3	30	0	84.7	81.0	86.6	3.2	8.69	8.35	8.92	0.30	14.2	14.0	14.5	0.3	8.40	8.24	8.49	0.14	1371	1367	1378	6

Grey shading indicates that the dissolved oxygen concentration (mg/L) does not meet the BC WQ guidelines for the instantaneous minimum concentration (6 mg/L) for interstitial water (BC MOE 2016).

Blue shading indicates that the dissolved oxygen concentration (mg/L) does not meet the BC WQ guidelines for the 30-day mean concentration (8 mg/L) for interstitial water (BC MOE 2016).

Note that the Avg. is an average of three single measurements taken at three piezometer locations within each monitoring site (i.e., at river right, mid channel and at river left) unless otherwise indicated (n).

Therefore variability (high standard deviation) is likely due to heterogeneous substrate composition within the monitoring site.

The following water quality data was removed due to the presence of fines in the standpipe: 1) September 03, 2016 at GRE-CA02 piezometer site "a" (depth 3 cm, 29 cm and 50 cm; DO 1.12 mg/L, 0.25 mg/L and 1.32 mg/L respectively), 2) September 02, 2016 at GRE-CA05 piezometer site "a" (depth 44.5 cm, DO 7.61 mg/L) and piezometer site "b" (depth 50 cm; DO 4.40 mg/L).

**Table 5. Summary of dissolved oxygen and general water quality at Greenhills Creek study sites in 2016 (part 2 of 2).**

Site	Date	n	Depth (cm)		Dissolved Oxygen (% sat.)				Dissolved Oxygen (mg/L)				Water Temperature (°C)				pH				Specific Conductivity (µS/cm)					
			Avg.	SD	Avg.	Min.	Max.	SD	Avg.	Min.	Max.	SD	Avg.	Min.	Max.	SD	Avg.	Min.	Max.	SD	Avg.	Min.	Max.	SD		
GRE-CA05	Jun-20	3	0	0	87.4	87.1	87.6	0.3	9.40	9.30	9.52	0.11	12.1	11.4	12.6	0.6	-	-	-	-	-	-	-	-	-	
			3	10	0	86.6	84.8	87.7	1.6	9.30	9.27	9.37	0.06	12.2	11.4	12.7	0.7	-	-	-	-	-	-	-	-	-
			2	27	1	84.0	83.0	84.9	1.3	8.96	8.87	9.05	0.13	12.5	12.4	12.5	0.1	-	-	-	-	-	-	-	-	-
	Sep-02	3	0	0	85.8	85.4	86.2	0.4	8.99	8.95	9.02	0.04	13.2	13.2	13.3	0.1	8.47	8.46	8.49	0.02	1365	1363	1368	3		
			3	10	0	85.6	85.1	86.1	0.5	8.96	8.93	9.00	0.04	13.3	13.2	13.4	0.1	8.42	8.33	8.47	0.08	1373	1369	1376	4	
			3	28	2	63.9	56.0	75.8	10.5	6.63	5.82	7.87	1.09	13.7	13.7	13.7	0.0	8.07	8.02	8.10	0.04	1332	1280	1360	45	
GRE-CA06	Jun-26	3	0	0	86.3	86.0	86.6	0.3	10.30	10.18	10.47	0.15	7.7	6.9	8.3	0.7	-	-	-	-	-	-	-	-	-	
			3	10	0	85.8	85.6	86.1	0.3	10.21	10.00	10.39	0.19	7.8	7.0	8.6	0.8	-	-	-	-	-	-	-	-	
			3	29	2	70.8	58.6	85.6	13.7	8.48	7.35	9.85	1.27	7.3	5.7	9.2	1.8	-	-	-	-	-	-	-	-	
	Sep-01	3	0	0	85.2	84.9	85.4	0.3	9.97	9.80	10.16	0.18	8.5	7.6	9.3	0.9	8.34	8.33	8.36	0.02	2023	2000	2037	20		
			3	10	0	85.0	84.9	85.3	0.2	9.94	9.77	10.16	0.20	8.6	7.7	9.4	0.9	8.32	8.29	8.36	0.04	1765	1197	2054	492	
			3	27	5	70.3	50.1	84.4	17.9	8.24	5.93	9.69	2.02	8.3	7.7	9.3	0.9	8.05	7.78	8.34	0.28	2013	1963	2047	44	
GH_CTF	Jun-26	3	0	0	83.2	82.8	83.8	0.5	10.56	10.54	10.58	0.02	5.2	5.0	5.6	0.3	-	-	-	-	-	-	-	-		
			3	10	0	80.9	76.7	83.1	3.7	10.22	9.80	10.49	0.37	5.4	5.0	5.9	0.5	-	-	-	-	-	-	-	-	
			3	30	0	57.4	42.8	77.1	17.7	7.22	5.44	9.65	2.18	5.5	5.2	5.8	0.3	-	-	-	-	-	-	-	-	
	Sep-01	3	0	0	82.5	81.9	82.9	0.5	10.33	10.25	10.44	0.10	5.8	5.1	6.3	0.6	8.30	8.30	8.31	0.01	2265	2257	2270	7		
			3	10	0	82.5	82.3	82.8	0.3	10.31	10.17	10.46	0.15	5.9	5.2	6.5	0.7	8.26	8.18	8.30	0.07	2286	2279	2292	7	
			3	27	3	74.3	63.4	81.8	9.6	9.20	7.95	10.03	1.10	6.1	5.7	6.6	0.5	8.02	7.83	8.26	0.22	2239	2196	2266	37	
2	43	2	43.1	35.3	50.8	11.0	5.34	4.38	6.29	1.35	6.2	6.2	6.2	0.0	7.67	7.59	7.75	0.11	1996	1851	2140	204				

Grey shading indicates that the dissolved oxygen concentration (mg/L) does not meet the BC WQ guidelines for the instantaneous minimum concentration (6 mg/L) for interstitial water (BC MOE 2016).

Blue shading indicates that the dissolved oxygen concentration (mg/L) does not meet the BC WQ guidelines for the 30-day mean concentration (8 mg/L) for interstitial water (BC MOE 2016).

Note that the Avg. is an average of three single measurements taken at three piezometer locations within each monitoring site (i.e., at river right, mid channel and at river left) unless otherwise indicated (n). Therefore variability (high standard deviation) is likely due to heterogeneous substrate composition within the monitoring site.

The following water quality data was removed due to the presence of fines in the standpipe: 1) September 03, 2016 at GRE-CA02 piezometer site "a" (depth 3 cm, 29 cm and 50 cm; DO 1.12 mg/L, 0.25 mg/L and 1.32 mg/L respectively), 2) September 02, 2016 at GRE-CA05 piezometer site "a" (depth 44.5 cm, DO 7.61 mg/L) and piezometer site "b" (depth 50 cm; DO 4.40 mg/L).

**Table 6. Relative standard error (RSE) exceedance summary for dissolved oxygen, water temperature and specific conductivity at the calcite study sites.**

Site	Date	n	Depth (cm)		Dissolved Oxygen (mg/L)					Water Temperature (°C)					Specific Conductivity (µS/cm)					
			Avg.	SD	Avg.	Min.	Max.	SD	RSE	Avg.	Min.	Max.	SD	RSE	Avg.	Min.	Max.	SD	RSE	
GRE-CA01	Jun-19	4	0	0	9.35	9.30	9.38	0.04	0%	10.3	9.9	10.7	0.3	3%	-	-	-	-	-	
		3	10	0	9.23	8.97	9.38	0.23	2%	10.4	10.3	10.5	0.1	1%	-	-	-	-	-	
		2	30	0	4.84	2.44	7.24	3.40	70%	10.1	9.8	10.3	0.4	4%	-	-	-	-	-	
	Aug-30	3	0	0	8.43	8.35	8.51	0.08	1%	16.2	15.6	16.6	0.5	3%	1242	1037	1346	177	14%	
		3	6	1	8.43	8.34	8.50	0.08	1%	16.3	15.8	16.6	0.4	3%	1330	1311	1349	27	2%	
		3	19	2	7.45	5.50	8.44	1.69	23%	16.1	15.4	16.9	0.8	5%	1365	1360	1372	6	0%	
		3	37	1	5.82	4.13	7.66	1.77	30%	14.7	14.5	15.0	0.3	2%	1383	1352	1415	32	2%	
GRE-CA02	Jun-19	3	0	0	9.20	9.12	9.25	0.07	1%	11.1	10.8	11.5	0.4	3%	-	-	-	-	-	
		3	10	0	6.51	3.07	8.44	2.99	46%	10.7	10.2	11.1	0.5	4%	-	-	-	-	-	
			3	30	0	1.35	0.99	1.71	0.36	27%	10.0	9.7	10.4	0.4	4%	-	-	-	-	-
	Sep-03	3	0	0	8.87	8.80	8.93	0.07	1%	12.8	12.5	13.2	0.4	3%	1361	1359	1365	3	0%	
		2	9	1	8.29	7.68	8.89	0.86	10%	12.8	12.4	13.1	0.4	3%	1348	1300	1373	41	3%	
		2	27	4	3.95	3.61	4.29	0.48	12%	12.5	12.4	12.7	0.1	1%	1291	1212	1384	87	7%	
2		46	6	1.72	1.40	2.04	0.45	26%	12.4	12.4	12.5	0.0	0%	1231	1123	1375	130	11%		
GRE-CA06	Jun-26	3	0	0	10.30	10.18	10.47	0.15	1%	7.7	6.9	8.3	0.7	9%	-	-	-	-	-	
		3	10	0	10.21	10.00	10.39	0.19	2%	7.8	7.0	8.6	0.8	10%	-	-	-	-	-	
		3	29	2	8.48	7.35	9.85	1.27	15%	7.3	5.7	9.2	1.8	24%	-	-	-	-	-	
	Sep-01	3	0	0	9.97	9.80	10.16	0.18	2%	8.5	7.6	9.3	0.9	10%	2023	2000	2037	20	1%	
		3	10	0	9.94	9.77	10.16	0.20	2%	8.6	7.7	9.4	0.9	10%	1765	1197	2054	492	28%	
		3	27	5	8.24	5.93	9.69	2.02	25%	8.3	7.7	9.3	0.9	10%	2013	1963	2047	44	2%	
GH_CTF	Jun-26	3	0	0	10.56	10.54	10.58	0.02	0%	5.2	5.0	5.6	0.3	6%	-	-	-	-	-	
		3	10	0	10.22	9.80	10.49	0.37	4%	5.4	5.0	5.9	0.5	8%	-	-	-	-	-	
		3	30	0	7.22	5.44	9.65	2.18	30%	5.5	5.2	5.8	0.3	6%	-	-	-	-	-	
	Sep-01	3	0	0	10.33	10.25	10.44	0.10	1%	5.8	5.1	6.3	0.6	11%	2265	2257	2270	7	0%	
		3	10	0	10.31	10.17	10.46	0.15	1%	5.9	5.2	6.5	0.7	11%	2286	2279	2292	7	0%	
		3	27	3	9.20	7.95	10.03	1.10	12%	6.1	5.7	6.6	0.5	7%	2239	2196	2266	37	2%	
		2	43	2	5.34	4.38	6.29	1.35	25%	6.2	6.2	6.2	0.0	0%	1996	1851	2140	204	10%	

RSE: relative standard error (SD/Avg.%)

Grey shading indicates exceedance of the 18% RSE guideline for triplicate sampling (RISC 1998).

Note that the Avg. is an average of three single measurements taken at three piezometer locations within each monitoring site (i.e., at river right, mid channel and at river left) unless otherwise indicated (n). Therefore variability (high standard deviation) is likely due to heterogeneous substrate composition within the monitoring site.

**Table 7. Summary of hydraulic head measurements at the Fording River and Clode Creek in 2016.**

Site	Date	Depth Category (cm)	Avg. Depth (cm)	Hydraulic Head (m)				
				n	Avg.	Min.	Max.	SD
FRD-CA01	Jun-25	10	10	3	0.0028	-0.0012	0.0054	0.0035
		30	28	3	0.0728	0.0083	0.1113	0.0562
	Sep-05	10	10	3	0.0010	-0.0020	0.0040	0.0030
		30	29	3	0.0813	0.0000	0.1420	0.0732
		50	43	3	0.0983	0.0220	0.1520	0.0679
FRD-CA02	Jun-25	10	10	3	0.0254	0.0087	0.0365	0.0147
		30	29	3	0.2604	0.2498	0.2709	0.0106
	Sep-05	10	10	3	0.0110	0.0050	0.0210	0.0087
		30	30	3	0.2197	0.1250	0.3040	0.0899
		50	48	3	0.2290	0.1470	0.2990	0.0767
FRD-CA03	Jun-22	10	10	3	0.0273	0.0017	0.0585	0.0288
		30	28	3	0.0683	0.0104	0.1024	0.0504
	Sep-06	10	10	3	0.0080	-0.0040	0.0240	0.0144
		30	27	3	0.0847	0.0080	0.1480	0.0709
		50	47	3	0.1000	0.0090	0.1600	0.0801
CLO-CA01	Jun-25	10	10	3	0.0070	-0.0010	0.0129	0.0072
		30	27	2	0.4333	0.3918	0.4747	0.0586
	Sep-04	10	10	2	0.0070	0.0010	0.0130	0.0085
		30	30	2	0.2285	0.1990	0.2580	0.0417
CLO-CA02	Jun-23	10	10	3	-0.0041	-0.0082	-0.0015	0.0036
		30	27	3	0.0016	-0.0075	0.0102	0.0089
	Sep-04	10	10	3	-0.0003	-0.0010	0.0000	0.0006
		30	28	3	-0.0057	-0.0160	0.0000	0.0090
		50	48	1	0.1910	-	-	-

**Table 8. Summary of hydraulic head measurements at Greenhills Creek in 2016.**

Site	Date	Depth Category (cm)	Avg. Depth (cm)	Hydraulic Head (m)				
				n	Avg.	Min.	Max.	SD
GRE-CA01	Jun-19	10	10	3	0.0050	-0.0070	0.0220	0.0151
		30	30	2	0.0160	0.0110	0.0210	0.0071
	Aug-30	10	6	3	-0.0017	-0.0050	0.0000	0.0029
		30	19	3	0.0262	-0.0100	0.0920	0.0571
		50	37	3	0.0857	0.0740	0.1020	0.0146
GRE-CA02	Jun-19	10	10	3	-0.0013	-0.0030	0.0000	0.0015
		30	30	3	0.0077	0.0010	0.0110	0.0058
	Sep-03	10	9	2	0.0000	0.0000	0.0000	0.0000
		30	27	2	0.0265	0.0190	0.0340	0.0106
		50	46	2	0.0335	0.0240	0.0430	0.0134
GRE-CA03	Jun-21	10	10	3	0.0030	0.0010	0.0060	0.0026
		30	30	3	0.0340	0.0230	0.0540	0.0173
	Sep-03	10	10	3	-0.0013	-0.0040	0.0000	0.0023
		30	28	3	0.0497	0.0000	0.0800	0.0434
		50	47	3	0.1587	0.0700	0.2500	0.0900
GH_GH1	Jun-20	10	10	3	-0.0040	-0.0050	-0.0020	0.0017
		30	30	2	0.0070	-0.0020	0.0160	0.0127
	Sep-02	10	10	3	-0.0133	-0.0320	0.0000	0.0167
		30	30	3	-0.0093	-0.0120	-0.0080	0.0023
GRE-CA05	Jun-20	10	10	3	0.0046	0.0018	0.0100	0.0047
		30	27	2	0.0128	0.0040	0.0216	0.0124
	Sep-02	10	10	3	-0.0013	-0.0040	0.0000	0.0023
		30	28	3	0.0040	0.0010	0.0100	0.0052
GRE-CA06	Jun-26	10	10	3	0.0002	-0.0013	0.0020	0.0016
		30	29	3	0.0022	-0.0209	0.0162	0.0202
	Sep-01	10	10	3	-0.0010	-0.0020	0.0000	0.0010
		30	27	3	0.0037	-0.0060	0.0130	0.0095
GH_CTF	Jun-26	10	10	3	0.0027	-0.0017	0.0062	0.0040
		30	30	3	0.0181	0.0094	0.0318	0.0120
	Sep-01	10	10	3	0.0073	0.0020	0.0110	0.0047
		30	27	3	0.0023	-0.0050	0.0070	0.0064
		50	43	2	0.0565	0.0370	0.0760	0.0276

Appendix F. Figures from fixed hydraulic conductivity 1DTempPro runs 2016.

**LIST OF FIGURES**

Figure 1. Downwelling and thermal gradient modelled with 1DTempPro using estimated hydraulic conductivity at FRD-CA01 during June 2016. Temperatures shown as solid lines for modelled and dots for measured..... 1

Figure 2. Downwelling and thermal gradient modelled with 1DTempPro using estimated hydraulic conductivity at FRD-CA01 during October 2016. Temperatures shown as solid lines for modelled and dots for measured..... 2

Figure 3. Downwelling and thermal gradient modelled with 1DTempPro using estimated hydraulic conductivity at CLO-CA01 during June 2016. Temperatures shown as solid lines for modelled and dots for measured..... 3

Figure 4. Downwelling and thermal gradient modelled with 1DTempPro using estimated hydraulic conductivity at CLO-CA01 during October 2016. Temperatures shown as solid lines for modelled and dots for measured..... 4

Figure 5. Downwelling and thermal gradient modelled with 1DTempPro using estimated hydraulic conductivity at GRE-CA01 during June 2016. Temperatures shown as solid lines for modelled and dots for measured..... 5

Figure 6. Downwelling and thermal gradient modelled with 1DTempPro using estimated hydraulic conductivity at GRE-CA01 during October 2016. Temperatures shown as solid lines for modelled and dots for measured..... 6

Figure 7. Downwelling and thermal gradient modelled with 1DTempPro using estimated hydraulic conductivity at GRE-CA03 during June 2016. Temperatures shown as solid lines for modelled and dots for measured..... 7

Figure 8. Downwelling and thermal gradient modelled with 1DTempPro using estimated hydraulic conductivity at GRE-CA03 during October 2016. Temperatures shown as solid lines for modelled and dots for measured..... 8

Figure 9. Downwelling and thermal gradient modelled with 1DTempPro using estimated hydraulic conductivity at GRE-CA05 during June 2016. Temperatures shown as solid lines for modelled and dots for measured..... 9

Figure 10. Downwelling and thermal gradient modelled with 1DTempPro using estimated hydraulic conductivity at GRE-CA05 during October 2016. Temperatures shown as solid lines for modelled and dots for measured..... 10

Figure 11. Downwelling and thermal gradient modelled with 1DTempPro using estimated hydraulic conductivity at GRE-CA06 during June 2016. Temperatures shown as solid lines for modelled and dots for measured..... 11

Figure 12. Downwelling and thermal gradient modelled with 1DTempPro using estimated hydraulic conductivity at GRE-CA06 during October 2016. Temperatures shown as solid lines for modelled and dots for measured.....12

Figure 13. Downwelling and thermal gradient modelled with 1DTempPro using estimated hydraulic conductivity at GH-CTF during June 2016. Temperatures shown as solid lines for modelled and dots for measured. ....13

Figure 14. Downwelling and thermal gradient modelled with 1DTempPro using estimated hydraulic conductivity at GH-CTF during October 2016. Temperatures shown as solid lines for modelled and dots for measured. ....14

Figure 1. Downwelling and thermal gradient modelled with 1DTempPro using estimated hydraulic conductivity at FRD-CA01 during June 2016. Temperatures shown as solid lines for modelled and dots for measured.

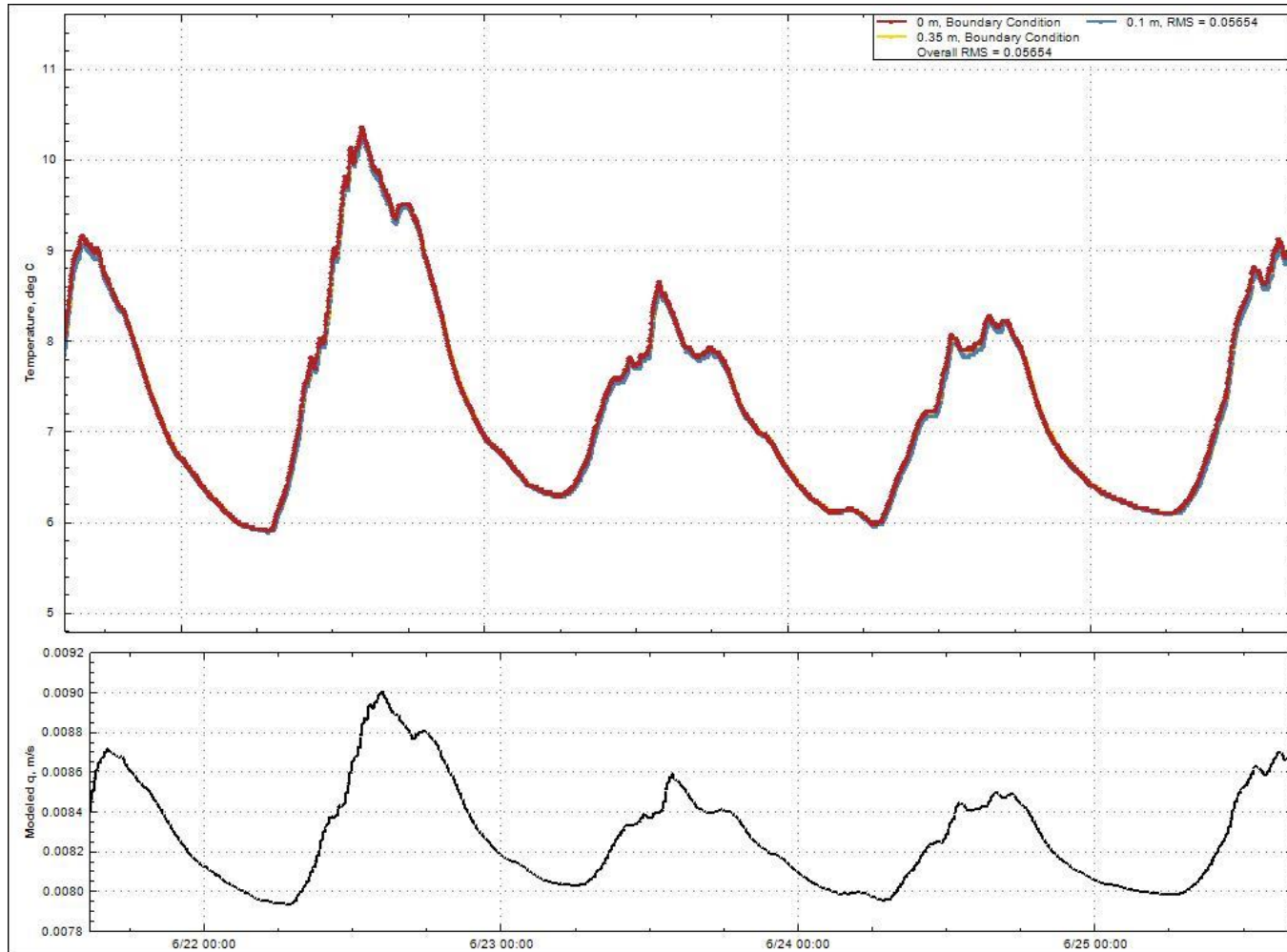


Figure 2. Downwelling and thermal gradient modelled with 1DTempPro using estimated hydraulic conductivity at FRD-CA01 during October 2016. Temperatures shown as solid lines for modelled and dots for measured.

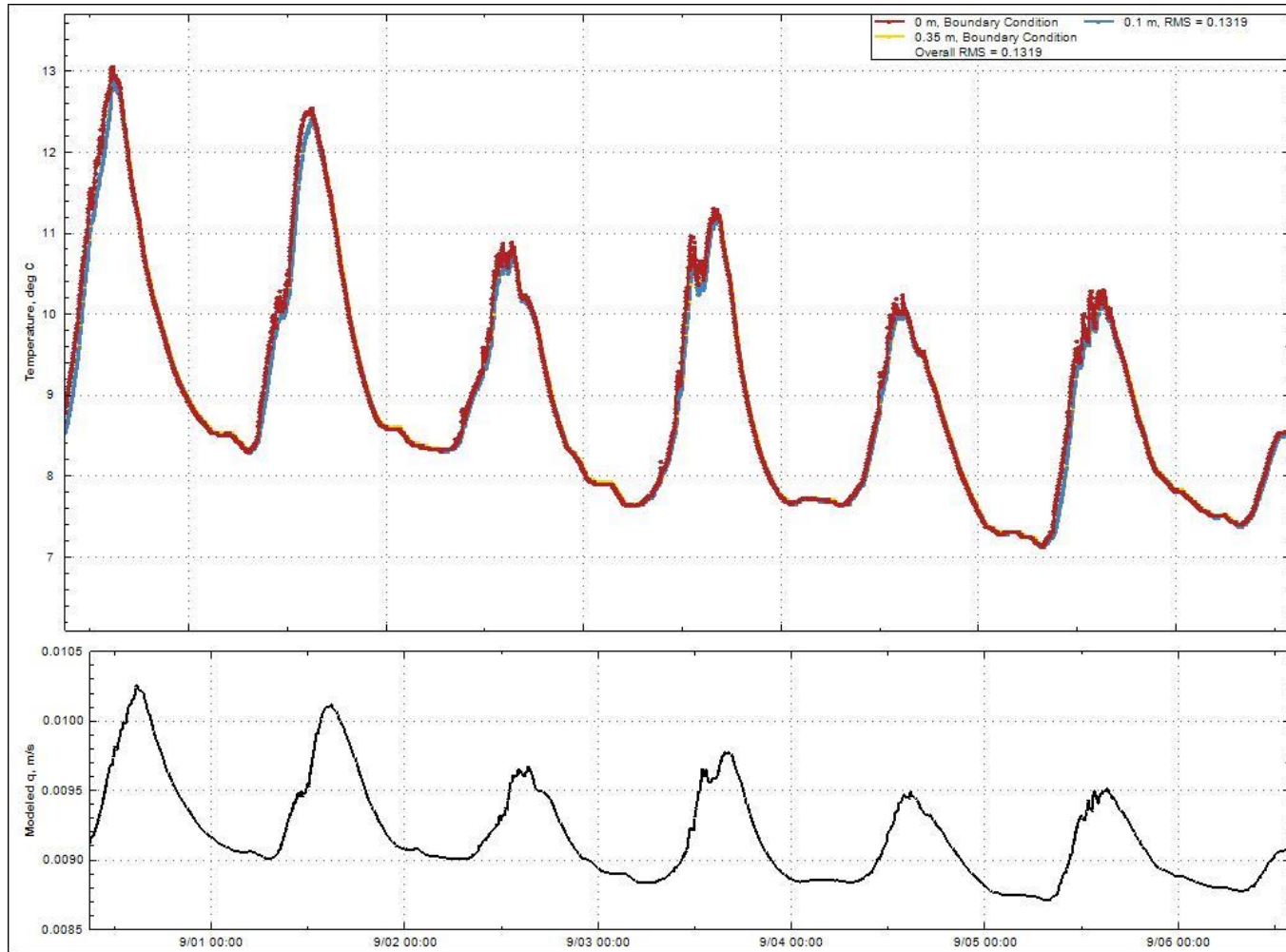


Figure 3. Downwelling and thermal gradient modelled with 1DTempPro using estimated hydraulic conductivity at CLO-CA01 during June 2016. Temperatures shown as solid lines for modelled and dots for measured.

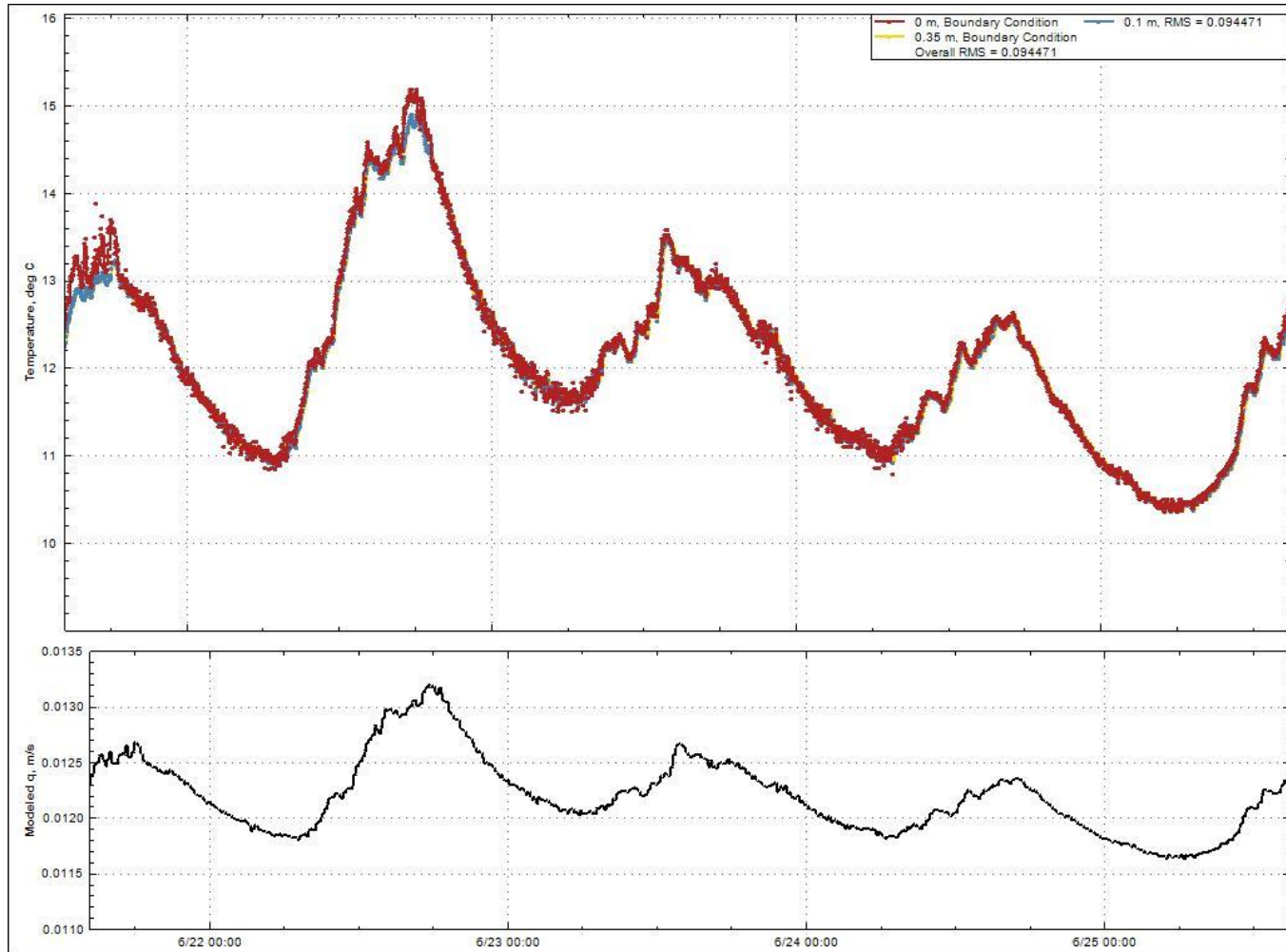


Figure 4. Downwelling and thermal gradient modelled with 1DTempPro using estimated hydraulic conductivity at CLO-CA01 during October 2016. Temperatures shown as solid lines for modelled and dots for measured.

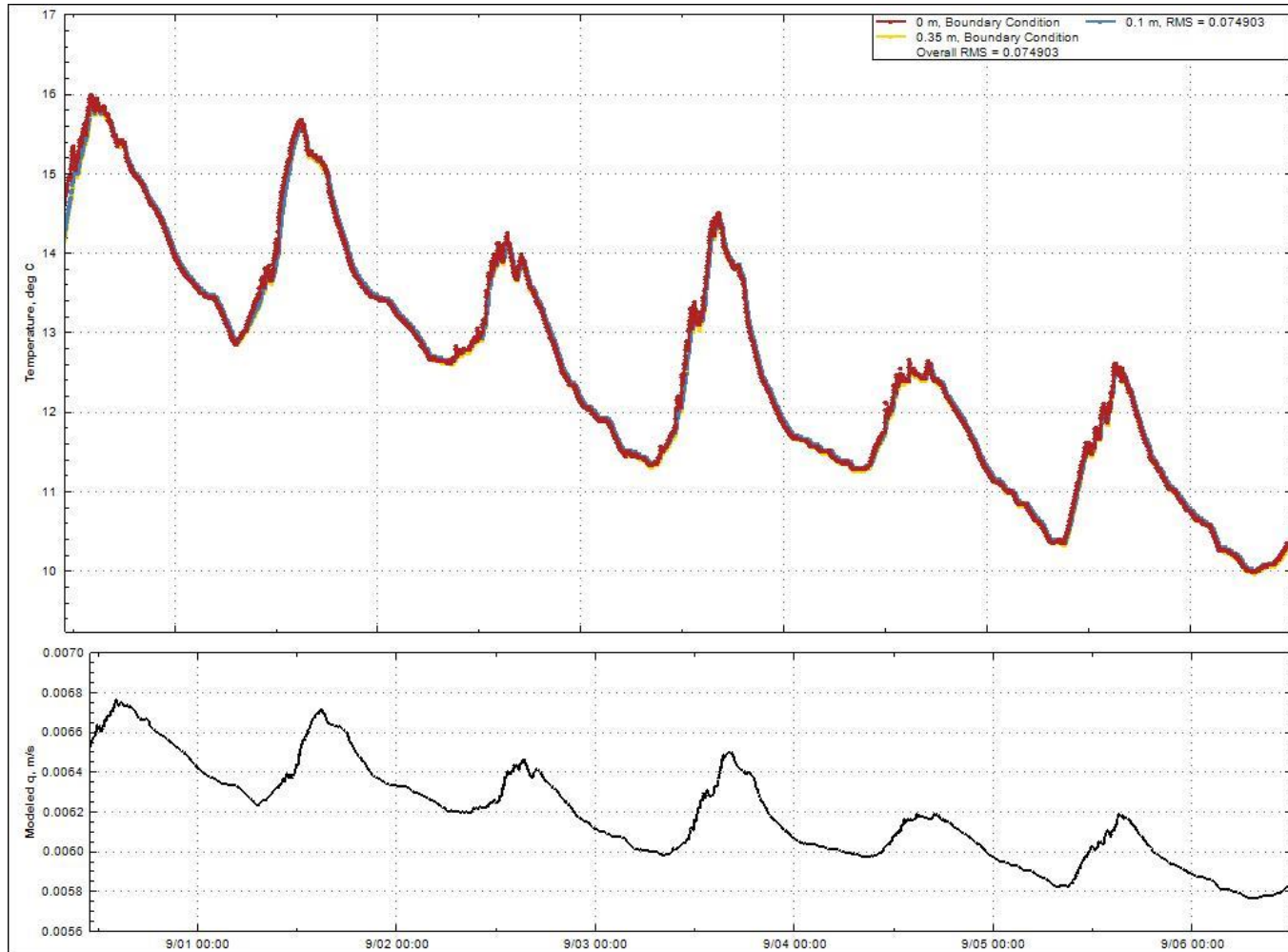


Figure 5. Downwelling and thermal gradient modelled with 1DTempPro using estimated hydraulic conductivity at GRE-CA01 during June 2016. Temperatures shown as solid lines for modelled and dots for measured.

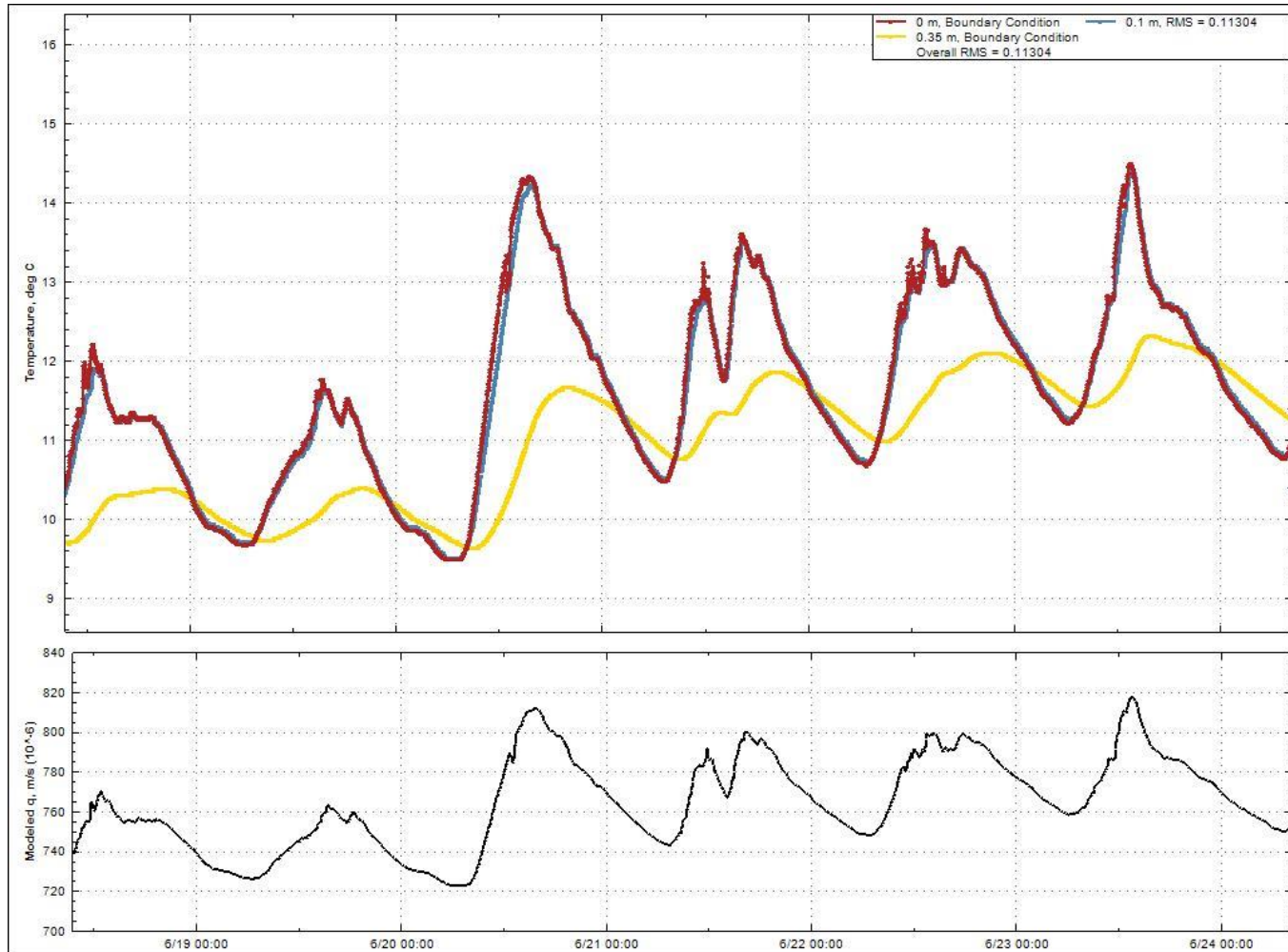


Figure 6. Downwelling and thermal gradient modelled with 1DTempPro using estimated hydraulic conductivity at GRE-CA01 during October 2016. Temperatures shown as solid lines for modelled and dots for measured.

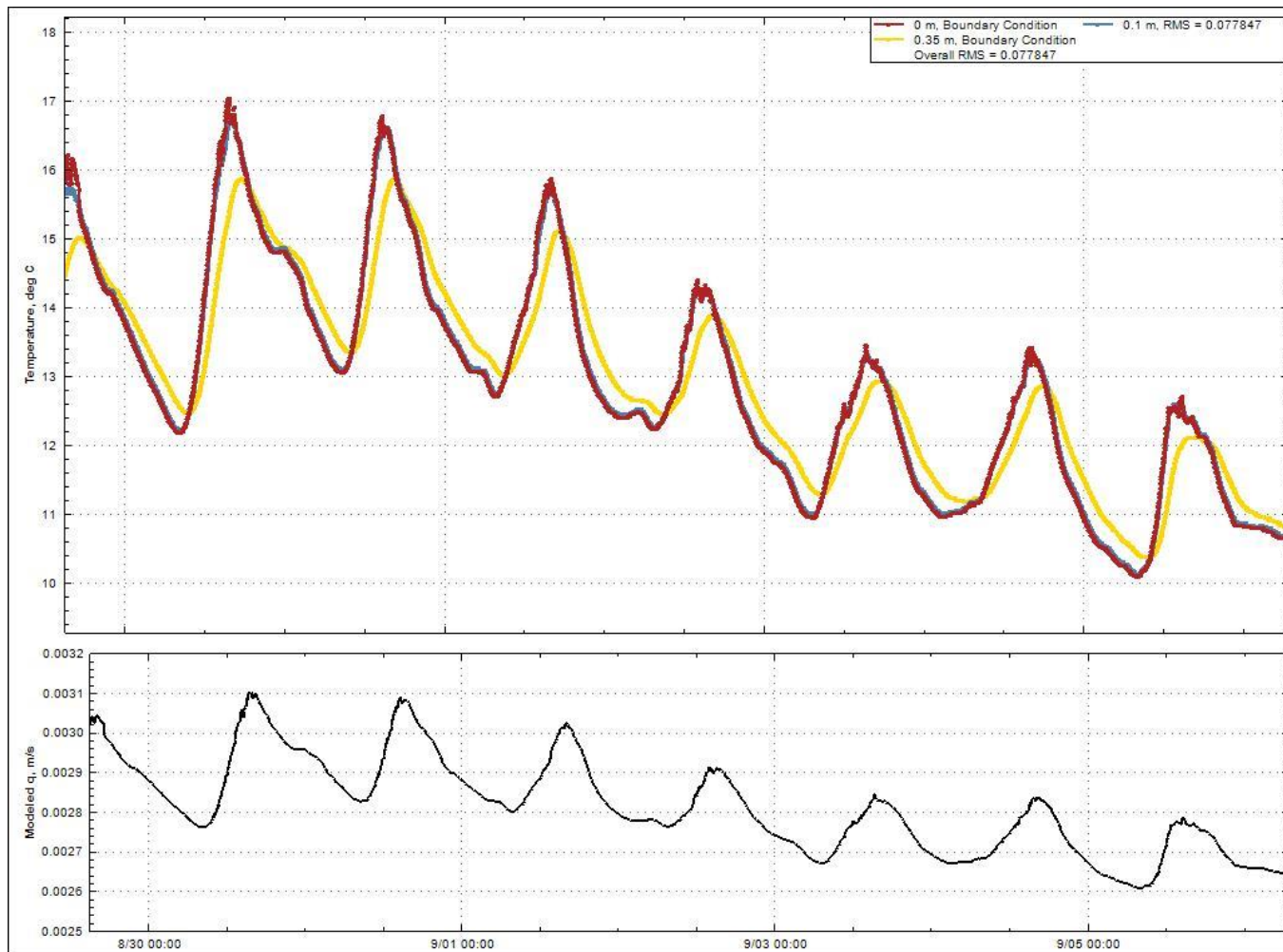


Figure 7. Downwelling and thermal gradient modelled with 1DTempPro using estimated hydraulic conductivity at GRE-CA03 during June 2016. Temperatures shown as solid lines for modelled and dots for measured.

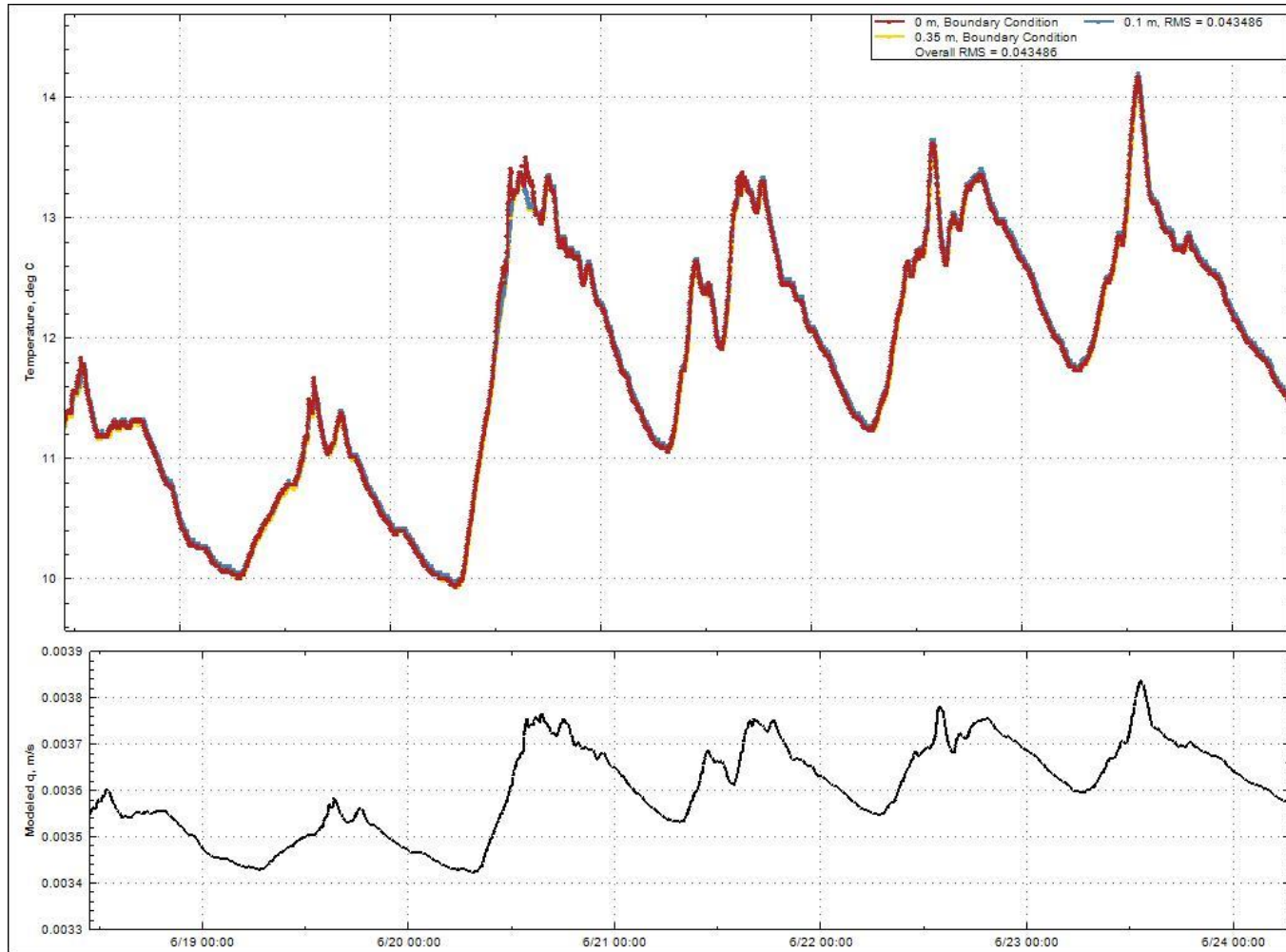


Figure 8. Downwelling and thermal gradient modelled with 1DTempPro using estimated hydraulic conductivity at GRE-CA03 during October 2016. Temperatures shown as solid lines for modelled and dots for measured.

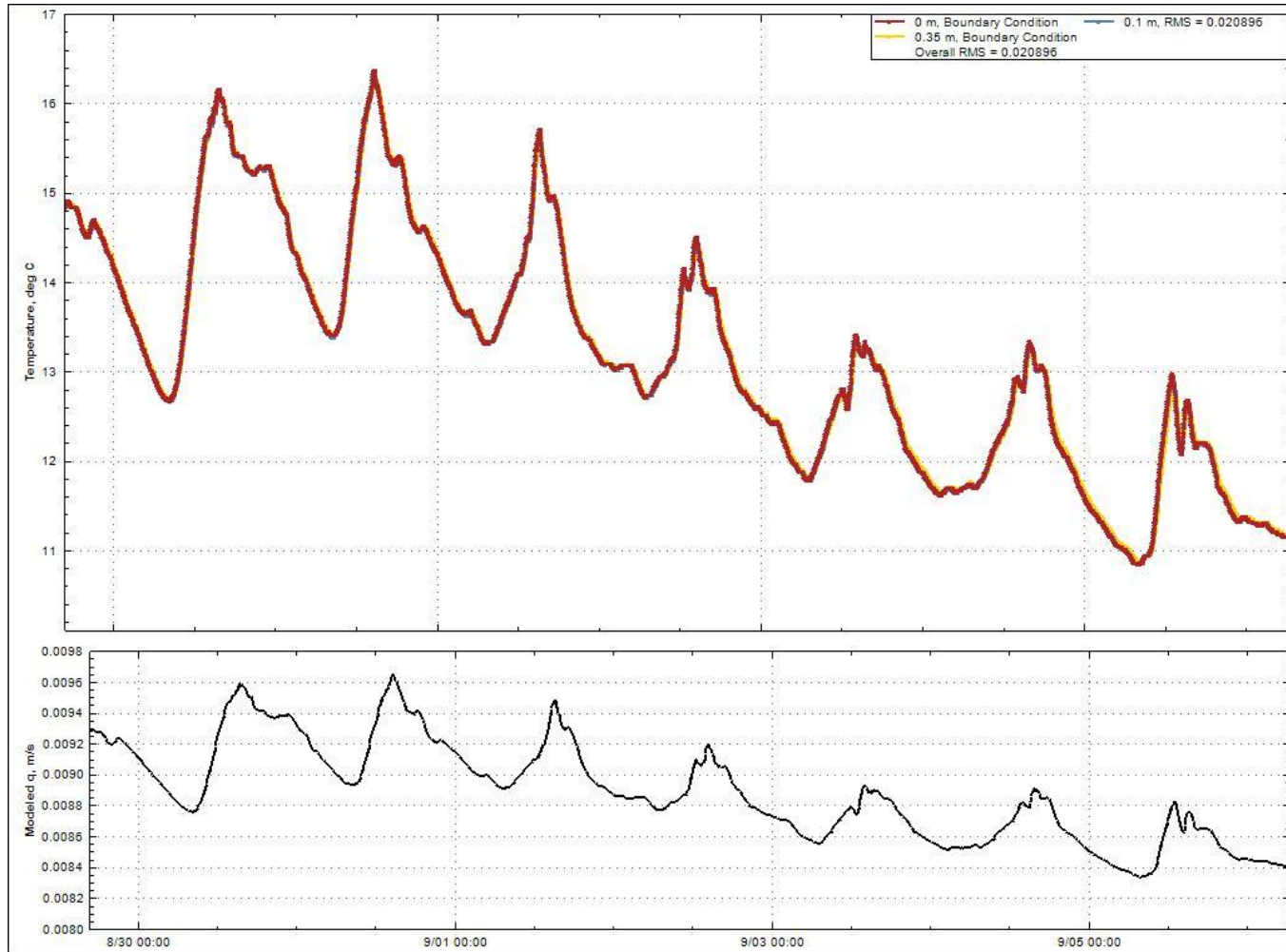


Figure 9. Downwelling and thermal gradient modelled with 1DTempPro using estimated hydraulic conductivity at GRE-CA05 during June 2016. Temperatures shown as solid lines for modelled and dots for measured.

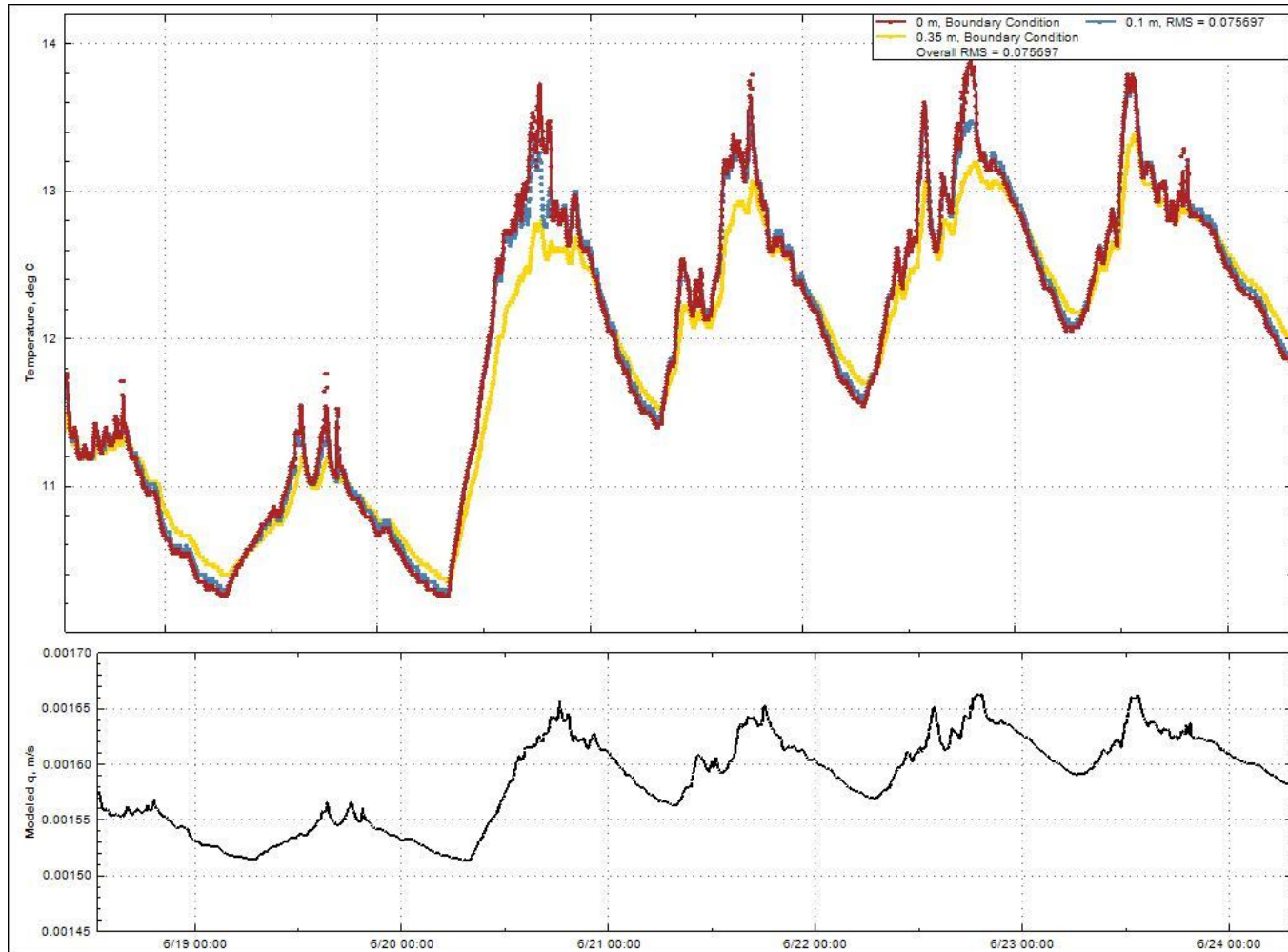


Figure 10. Downwelling and thermal gradient modelled with 1DTempPro using estimated hydraulic conductivity at GRE-CA05 during October 2016. Temperatures shown as solid lines for modelled and dots for measured.

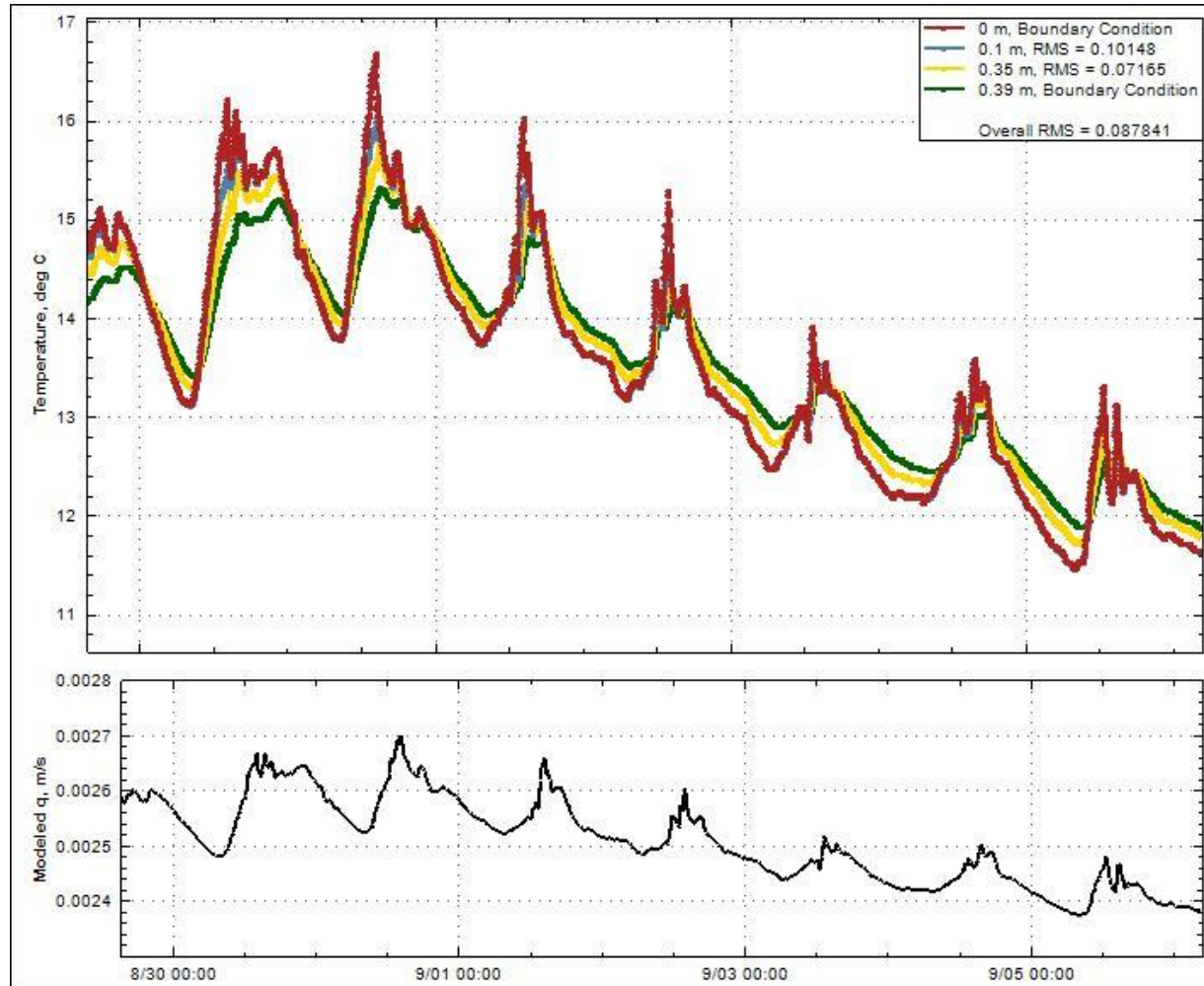


Figure 11. Downwelling and thermal gradient modelled with 1DTempPro using estimated hydraulic conductivity at GRE-CA06 during June 2016. Temperatures shown as solid lines for modelled and dots for measured.

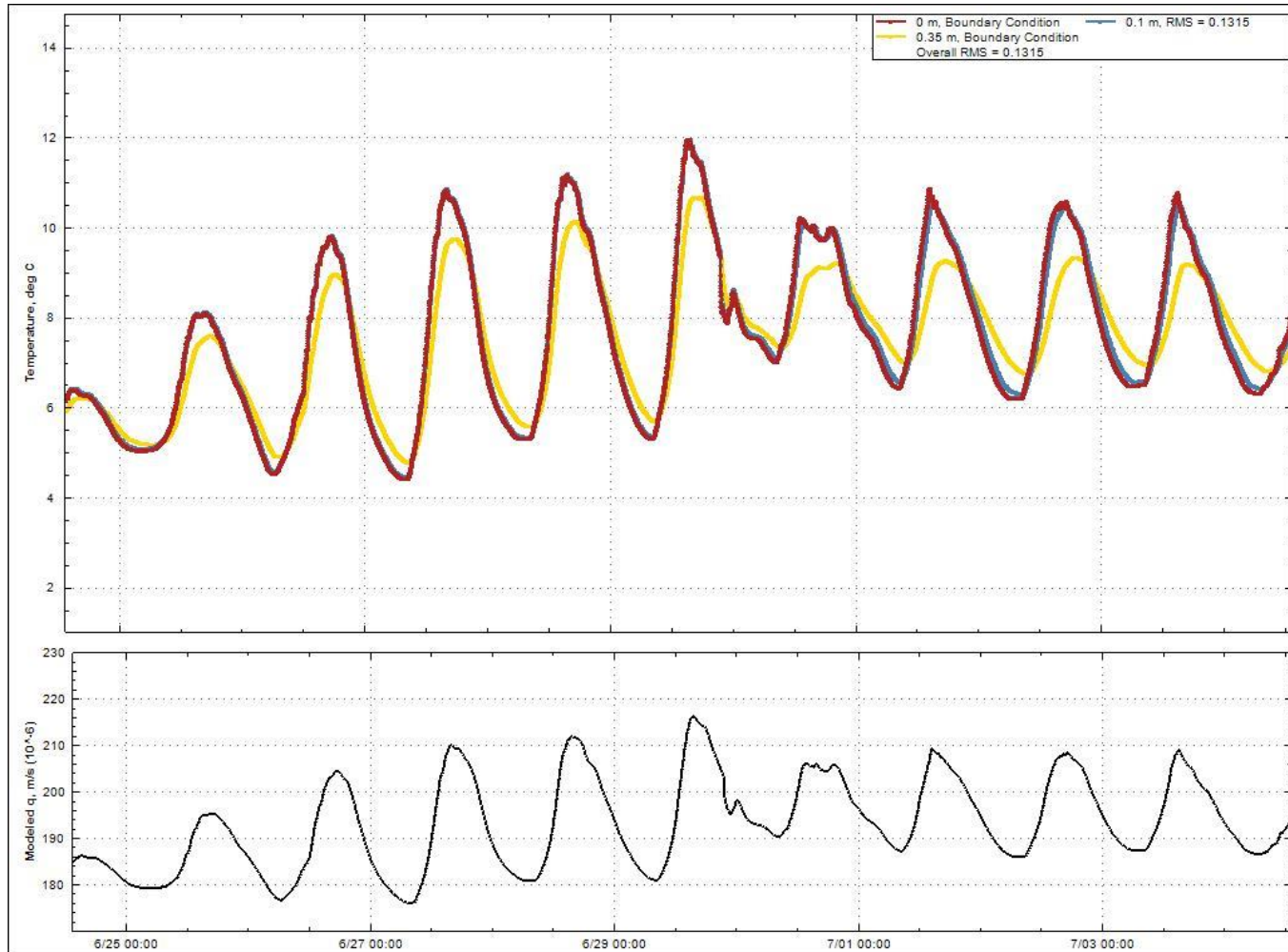


Figure 12. Downwelling and thermal gradient modelled with 1DTempPro using estimated hydraulic conductivity at GRE-CA06 during October 2016. Temperatures shown as solid lines for modelled and dots for measured.

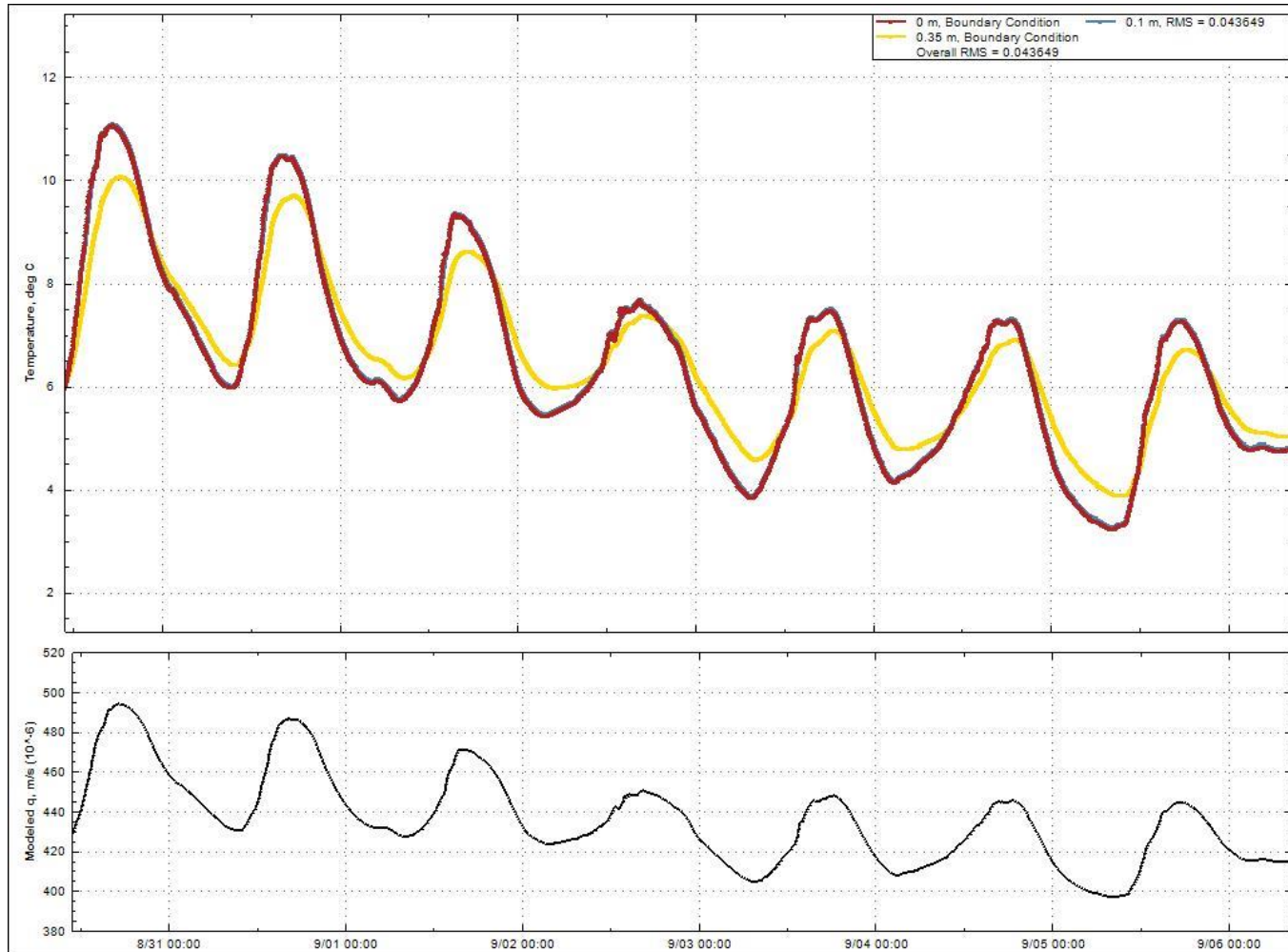


Figure 13. Downwelling and thermal gradient modelled with 1DTempPro using estimated hydraulic conductivity at GH-CTF during June 2016. Temperatures shown as solid lines for modelled and dots for measured.

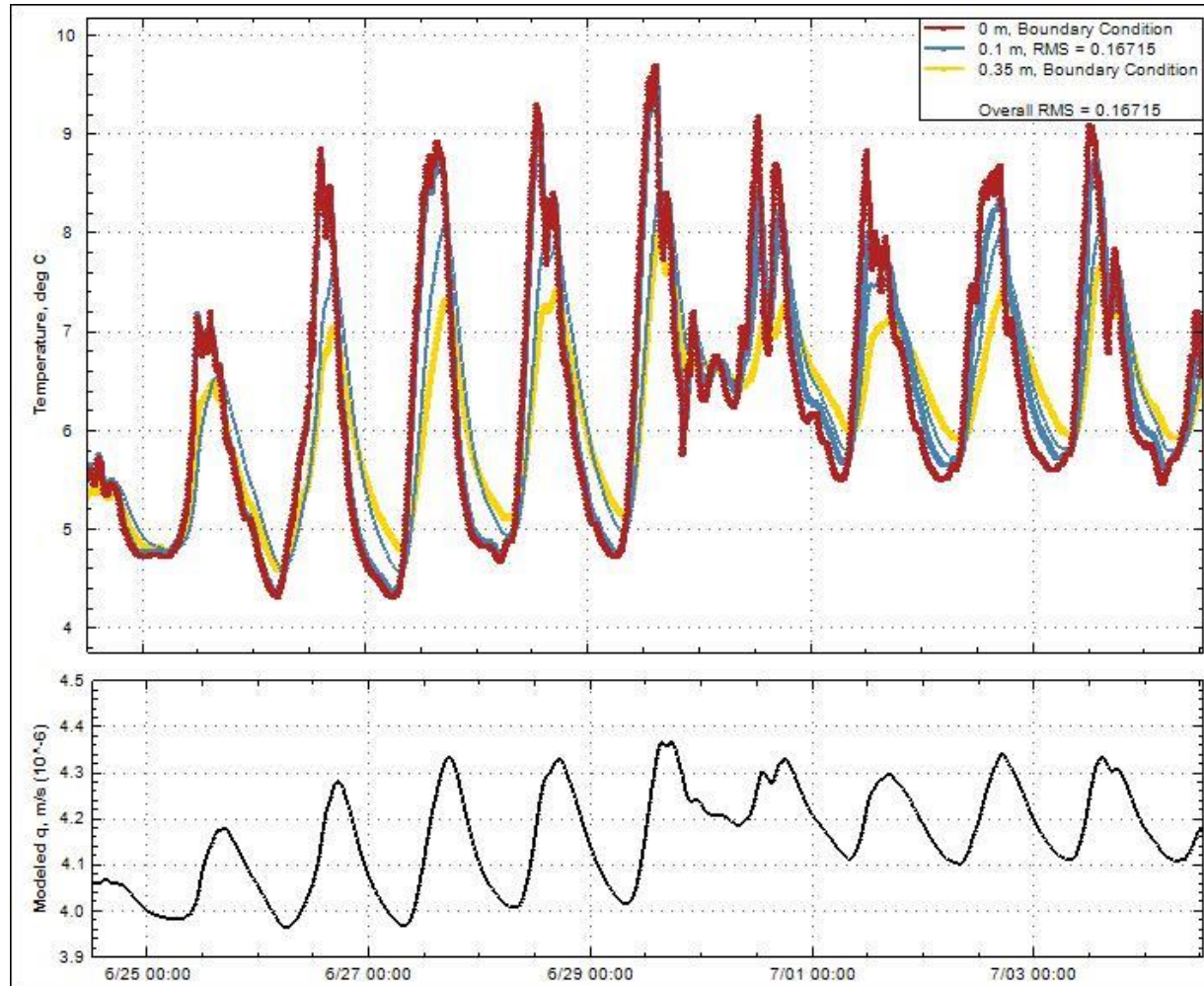
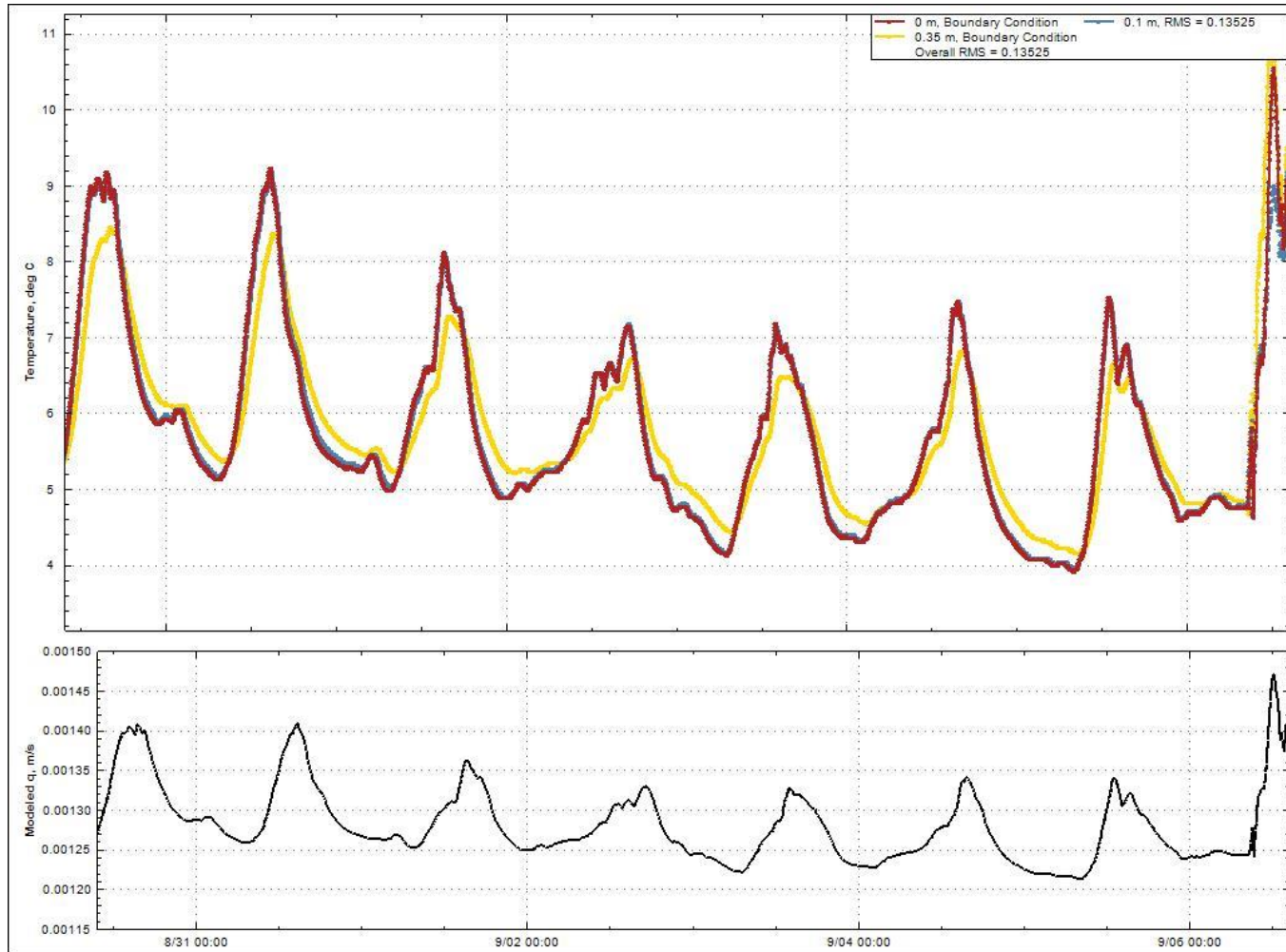


Figure 14. Downwelling and thermal gradient modelled with 1DTempPro using estimated hydraulic conductivity at GH-CTF during October 2016. Temperatures shown as solid lines for modelled and dots for measured.



Appendix G. Figures from optimized hydraulic conductivity 1DTempPro runs 2016.

**LIST OF FIGURES**

Figure 1. Downwelling and thermal gradient modelled with 1DTempPro by optimizing hydraulic conductivity at FRD-CA01 during June 2016. Temperatures shown as solid lines for modelled and dots for measured..... 1

Figure 2. Downwelling and thermal gradient modelled with 1DTempPro by optimizing hydraulic conductivity at FRD-CA01 during October 2016. Temperatures shown as solid lines for modelled and dots for measured..... 2

Figure 3. Downwelling and thermal gradient modelled with 1DTempPro by optimizing hydraulic conductivity at CLO-CA01 during June 2016. Temperatures shown as solid lines for modelled and dots for measured..... 3

Figure 4. Downwelling and thermal gradient modelled with 1DTempPro by optimizing hydraulic conductivity at CLO-CA01 during October 2016. Temperatures shown as solid lines for modelled and dots for measured..... 4

Figure 5. Downwelling and thermal gradient modelled with 1DTempPro by optimizing hydraulic conductivity at GRE-CA01 during June 2016. Temperatures shown as solid lines for modelled and dots for measured..... 5

Figure 6. Downwelling and thermal gradient modelled with 1DTempPro by optimizing hydraulic conductivity at GRE-CA01 during October 2016. Temperatures shown as solid lines for modelled and dots for measured..... 6

Figure 7. Downwelling and thermal gradient modelled with 1DTempPro by optimizing hydraulic conductivity at GRE-CA03 during June 2016. Temperatures shown as solid lines for modelled and dots for measured..... 7

Figure 8. Downwelling and thermal gradient modelled with 1DTempPro by optimizing hydraulic conductivity at GRE-CA03 during October 2016. Temperatures shown as solid lines for modelled and dots for measured..... 8

Figure 9. Downwelling and thermal gradient modelled with 1DTempPro by optimizing hydraulic conductivity at GRE-CA05 during June 2016. Temperatures shown as solid lines for modelled and dots for measured..... 9

Figure 10. Downwelling and thermal gradient modelled with 1DTempPro by optimizing hydraulic conductivity at GRE-CA05 during October 2016. Temperatures shown as solid lines for modelled and dots for measured..... 10

Figure 11. Downwelling and thermal gradient modelled with 1DTempPro by optimizing hydraulic conductivity at GRE-CA06 during June 2016. Temperatures shown as solid lines for modelled and dots for measured..... 11

Figure 12. Downwelling and thermal gradient modelled with 1DTempPro by optimizing hydraulic conductivity at GRE-CA06 during October 2016. Temperatures shown as solid lines for modelled and dots for measured.....12

Figure 13. Downwelling and thermal gradient modelled with 1DTempPro by optimizing hydraulic conductivity at GH-CTF during June 2016. Temperatures shown as solid lines for modelled and dots for measured.....13

Figure 14. Downwelling and thermal gradient modelled with 1DTempPro by optimizing hydraulic conductivity at GH-CTF during October 2016. Temperatures shown as solid lines for modelled and dots for measured.....14

Figure 1. Downwelling and thermal gradient modelled with 1DTempPro by optimizing hydraulic conductivity at FRD-CA01 during June 2016. Temperatures shown as solid lines for modelled and dots for measured.

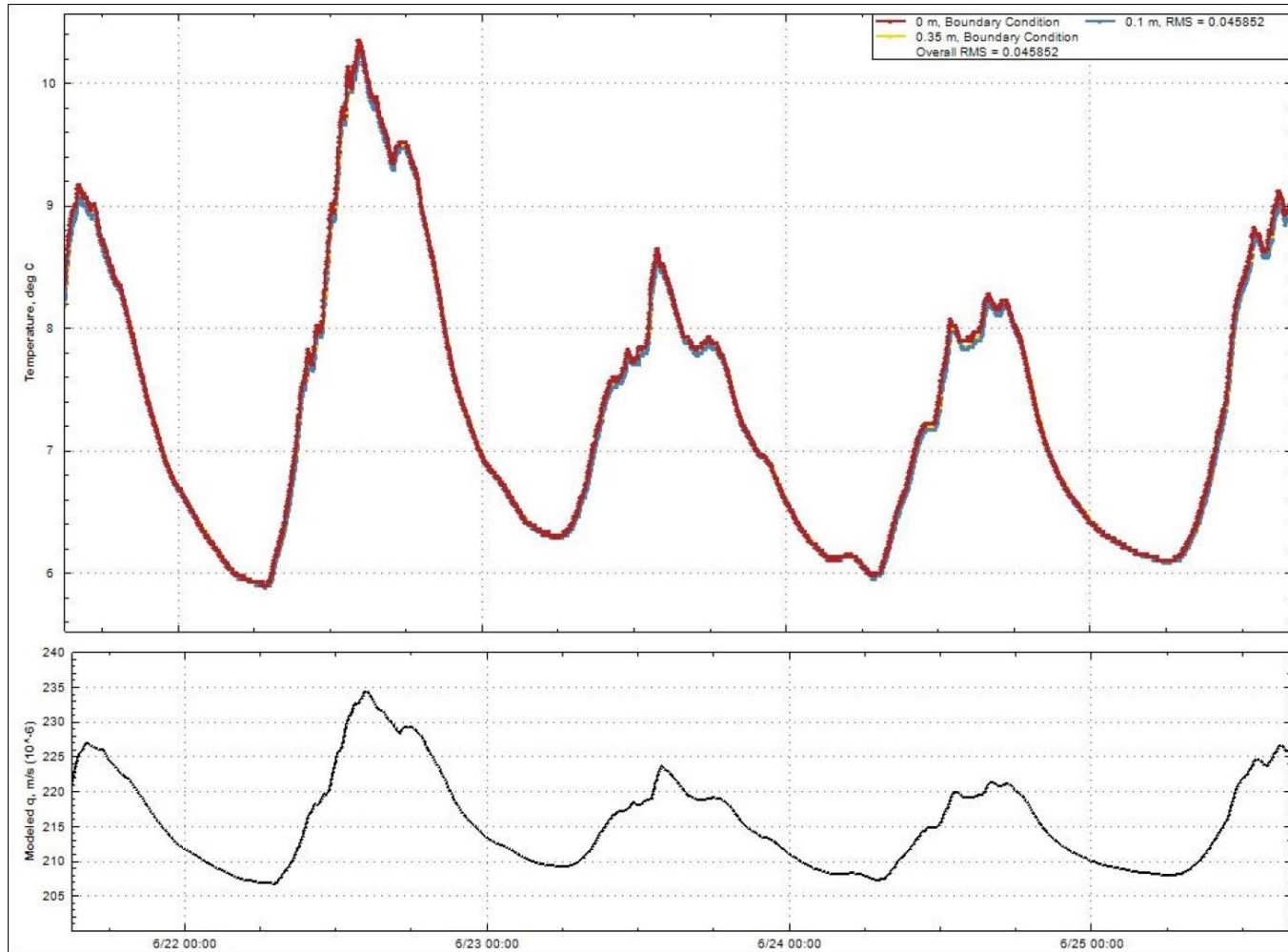


Figure 2. Downwelling and thermal gradient modelled with 1DTempPro by optimizing hydraulic conductivity at FRD-CA01 during October 2016. Temperatures shown as solid lines for modelled and dots for measured.

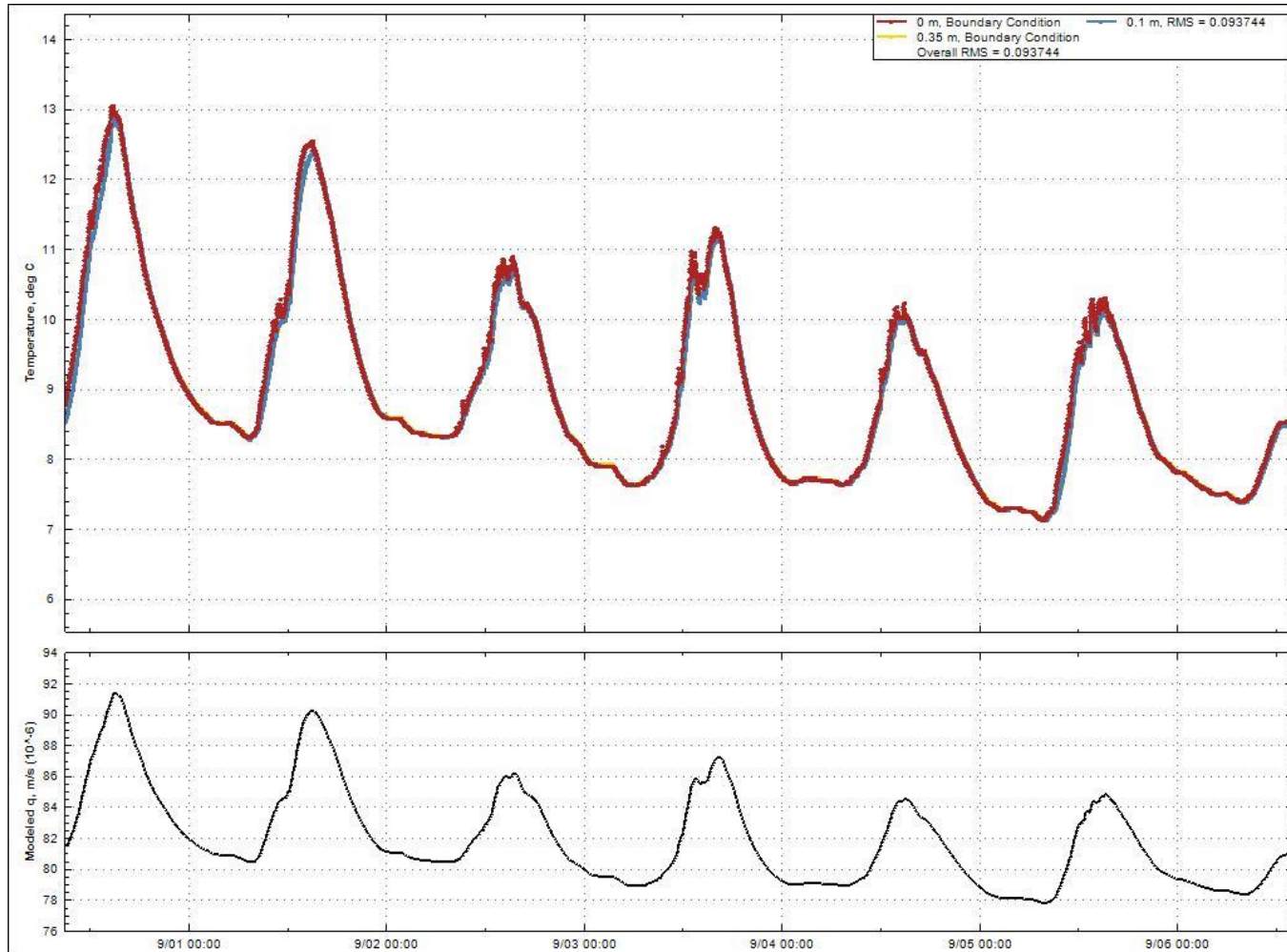


Figure 3. Downwelling and thermal gradient modelled with 1DTempPro by optimizing hydraulic conductivity at CLO-CA01 during June 2016. Temperatures shown as solid lines for modelled and dots for measured.

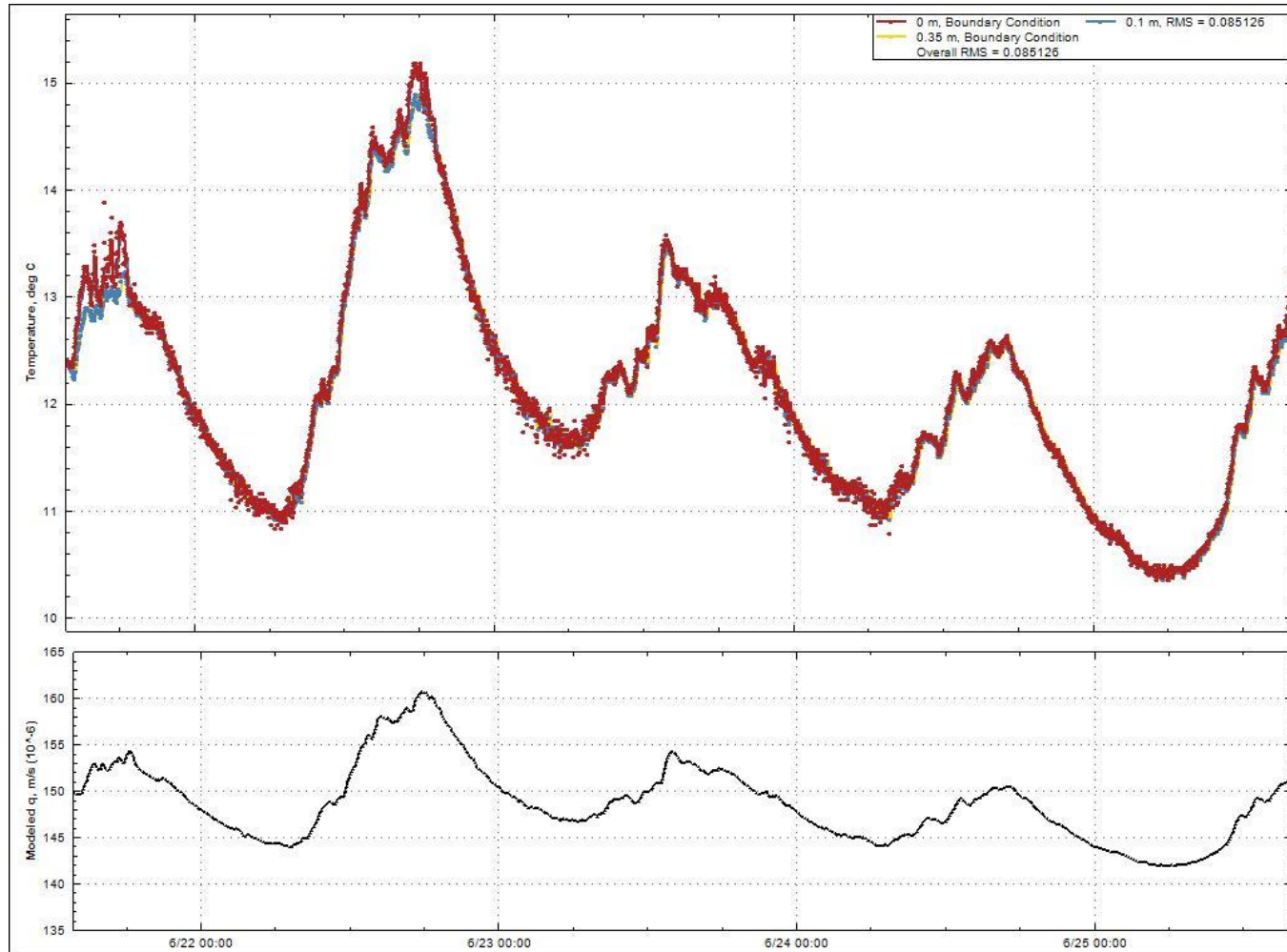


Figure 4. Downwelling and thermal gradient modelled with 1DTempPro by optimizing hydraulic conductivity at CLO-CA01 during October 2016. Temperatures shown as solid lines for modelled and dots for measured.

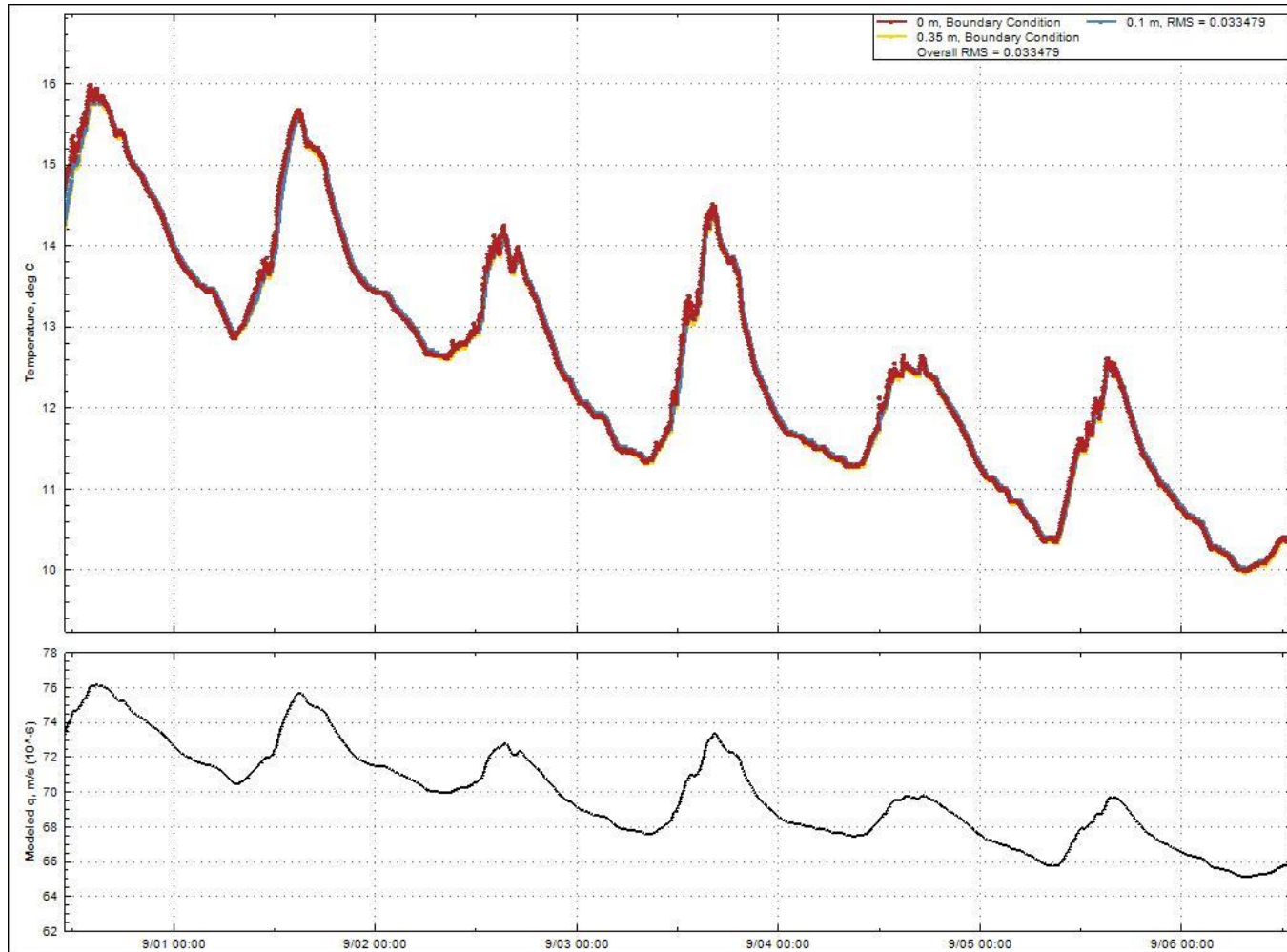


Figure 5. Downwelling and thermal gradient modelled with 1DTempPro by optimizing hydraulic conductivity at GRE-CA01 during June 2016. Temperatures shown as solid lines for modelled and dots for measured.

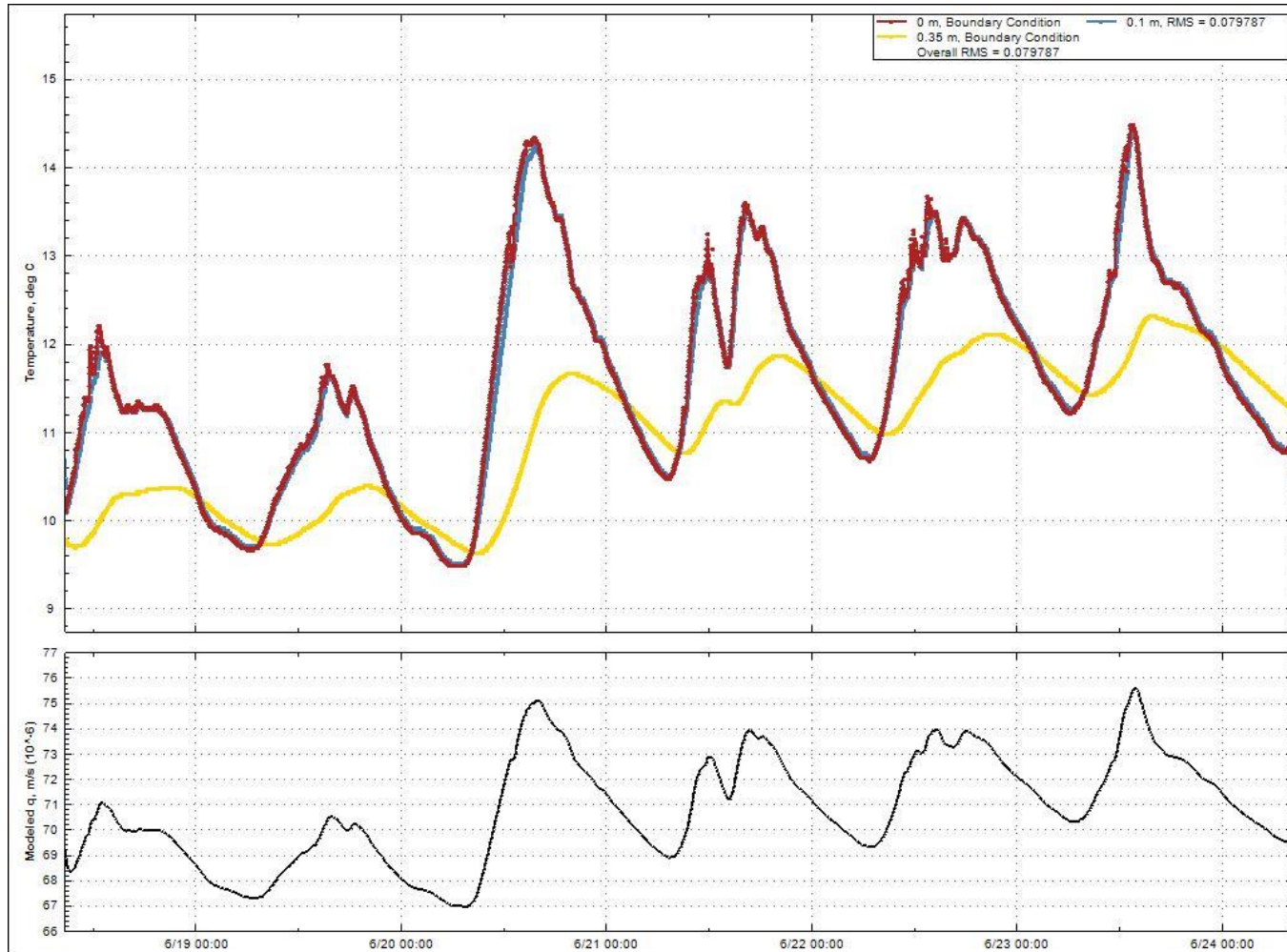


Figure 6. Downwelling and thermal gradient modelled with 1DTempPro by optimizing hydraulic conductivity at GRE-CA01 during October 2016. Temperatures shown as solid lines for modelled and dots for measured.

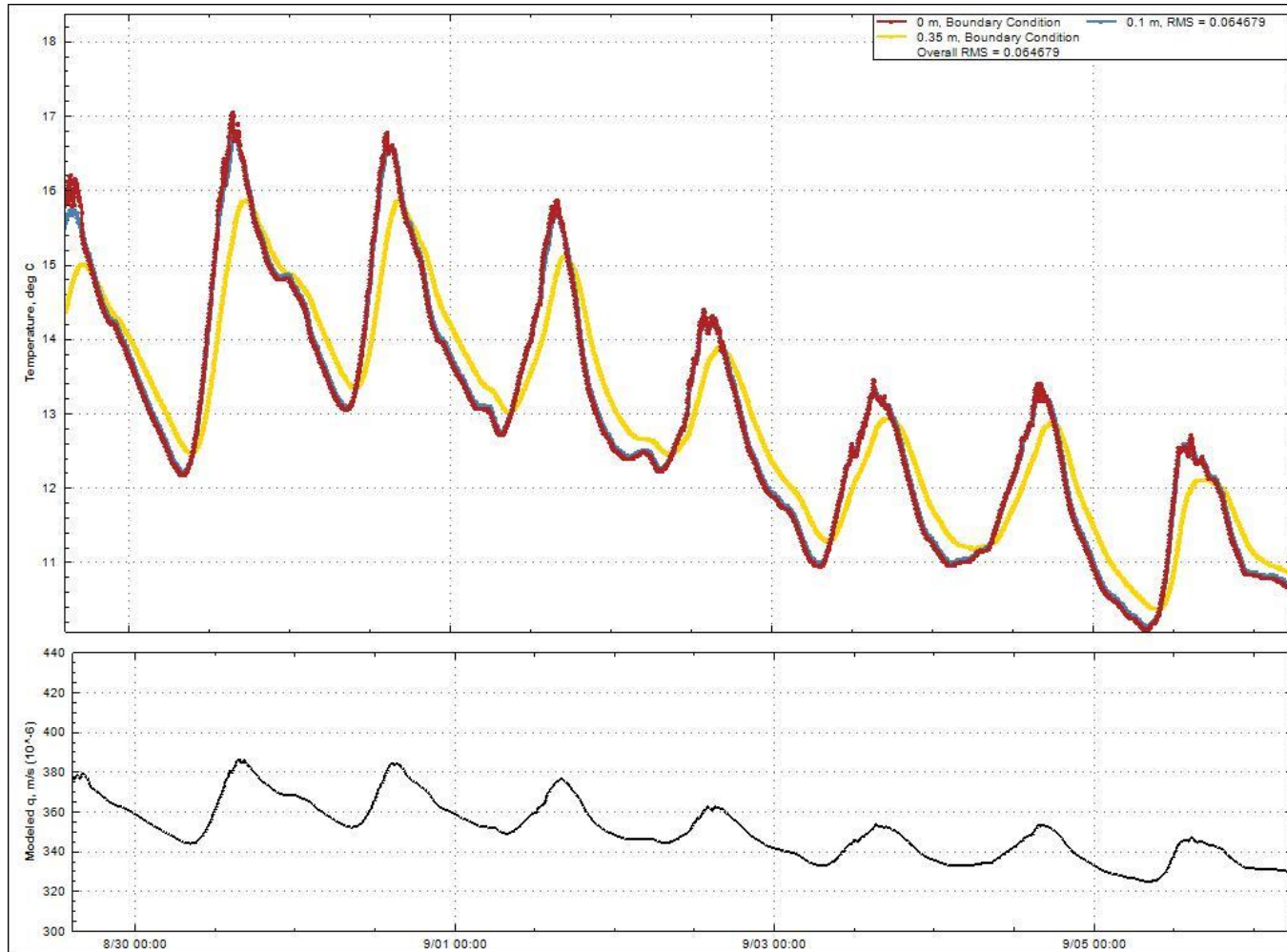


Figure 7. Downwelling and thermal gradient modelled with 1DTempPro by optimizing hydraulic conductivity at GRE-CA03 during June 2016. Temperatures shown as solid lines for modelled and dots for measured.

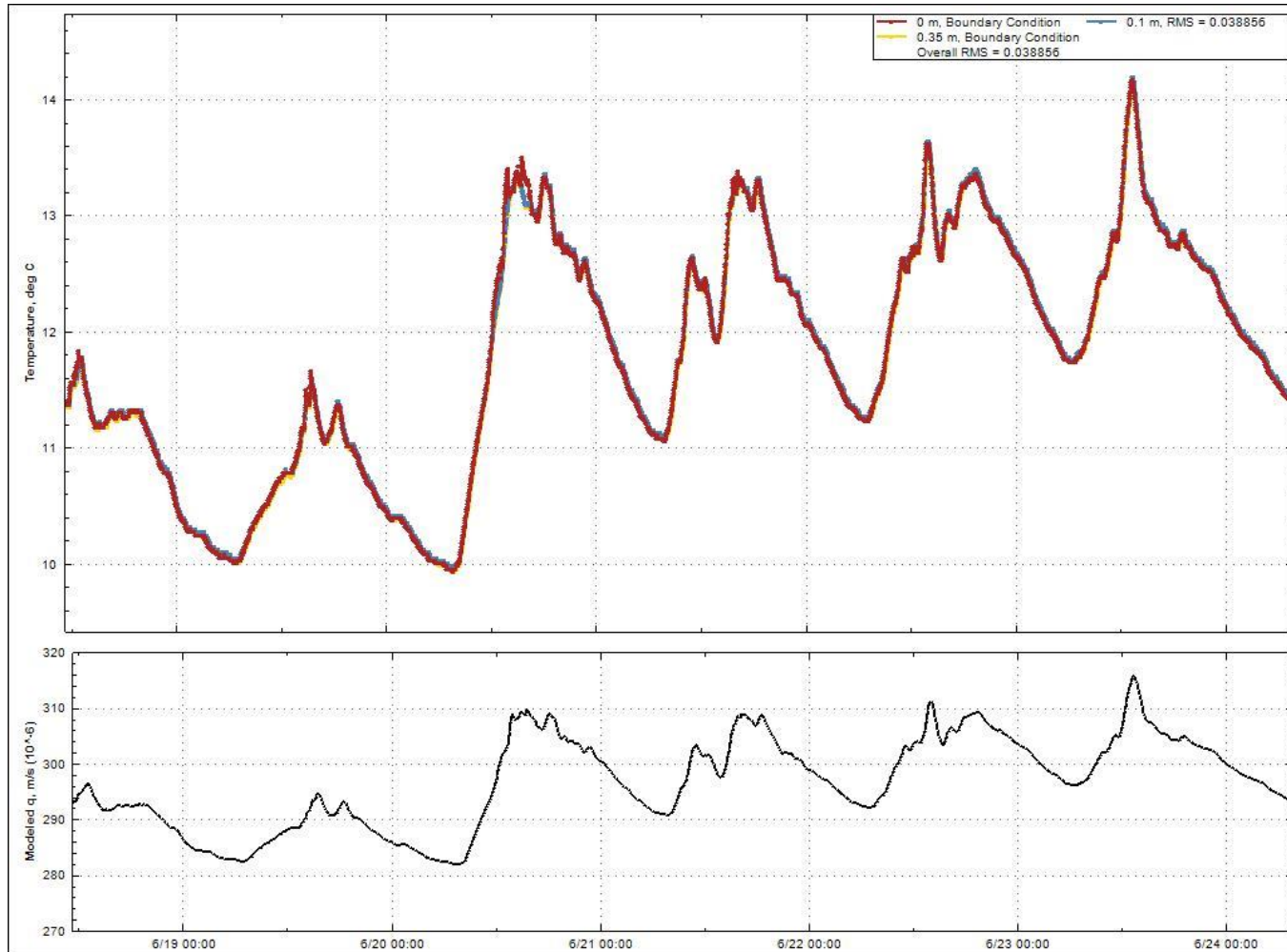


Figure 8. Downwelling and thermal gradient modelled with 1DTempPro by optimizing hydraulic conductivity at GRE-CA03 during October 2016. Temperatures shown as solid lines for modelled and dots for measured.

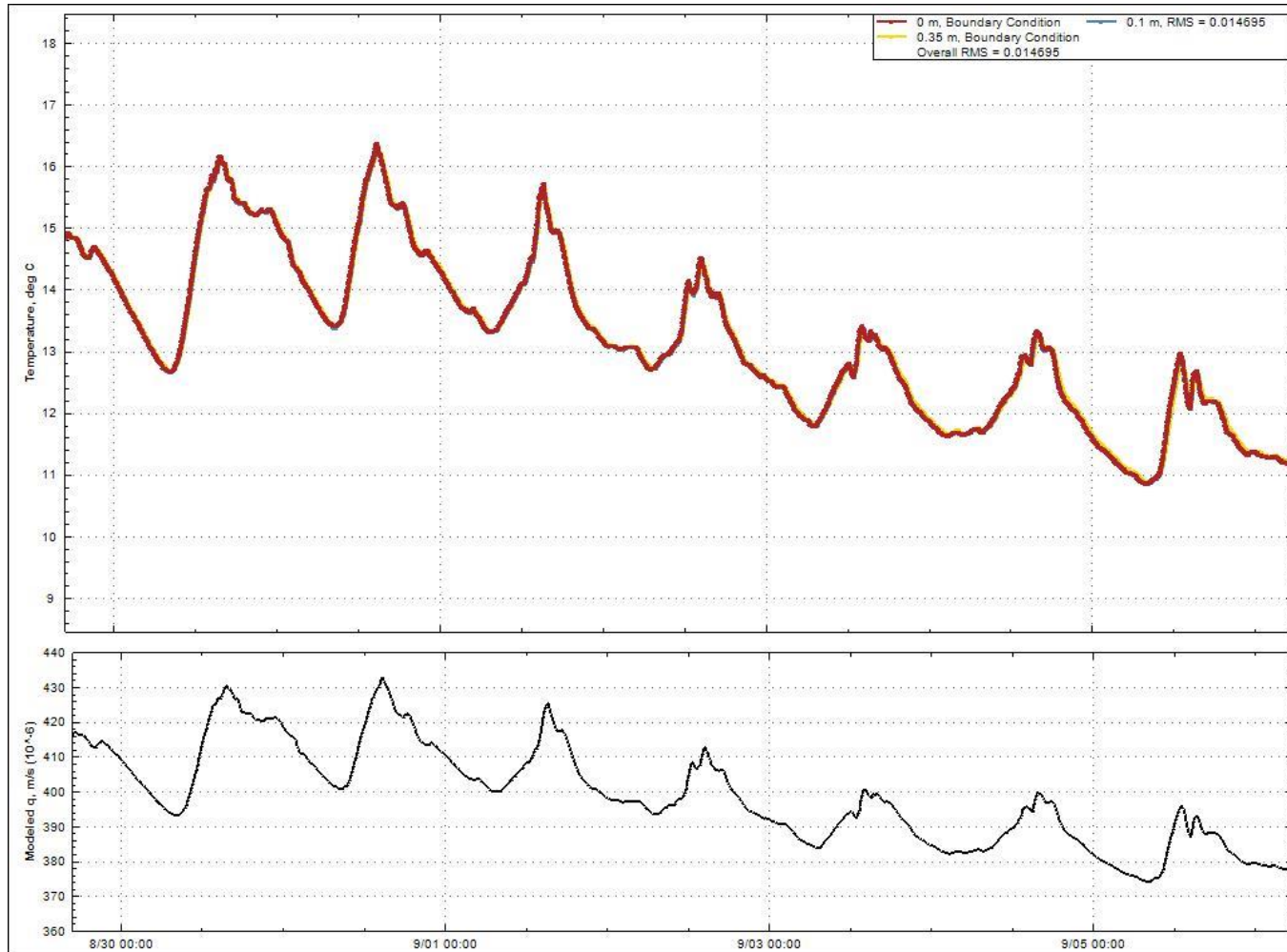


Figure 9. Downwelling and thermal gradient modelled with 1DTempPro by optimizing hydraulic conductivity at GRE-CA05 during June 2016. Temperatures shown as solid lines for modelled and dots for measured.

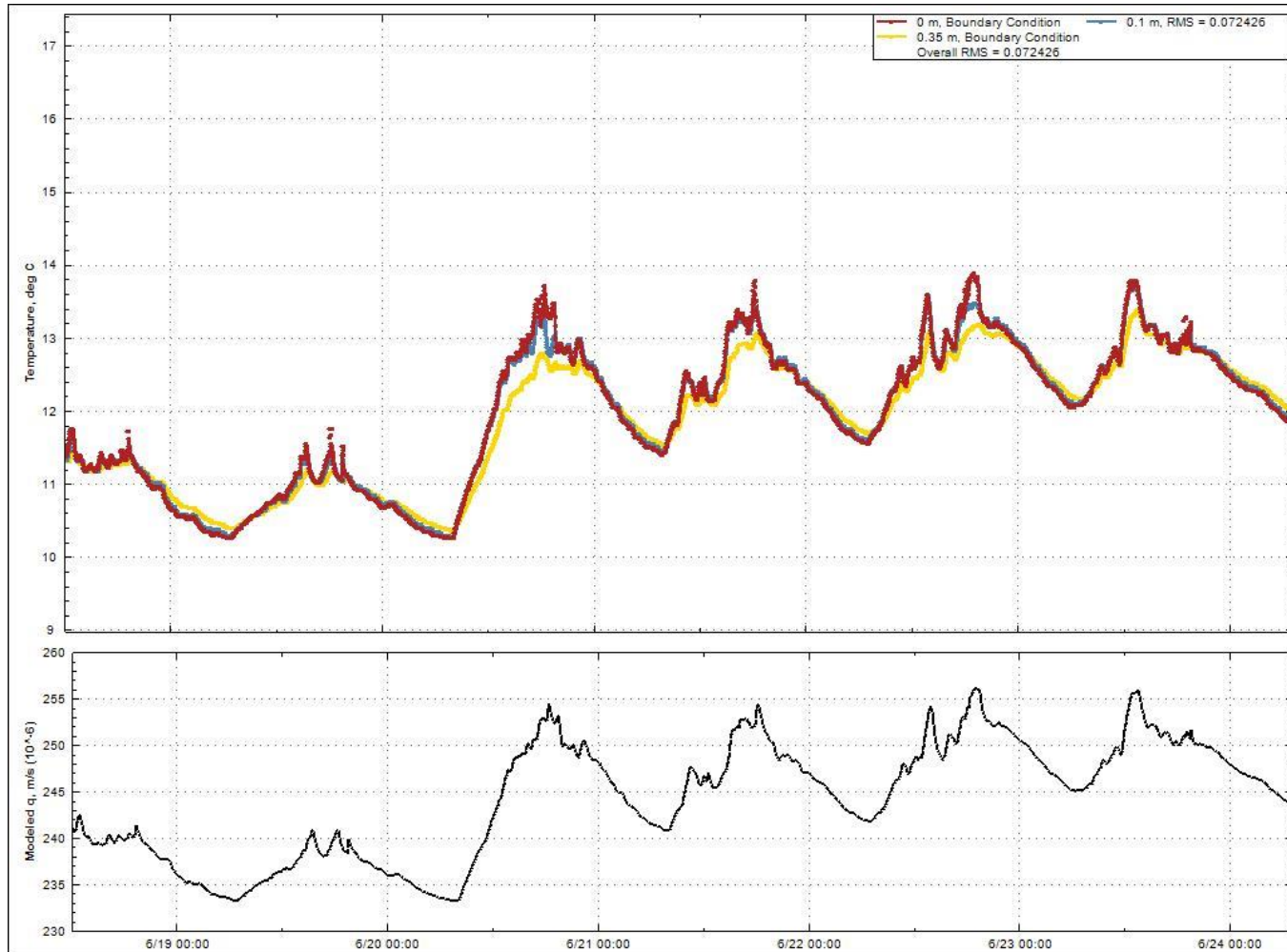


Figure 10. Downwelling and thermal gradient modelled with 1DTempPro by optimizing hydraulic conductivity at GRE-CA05 during October 2016. Temperatures shown as solid lines for modelled and dots for measured.

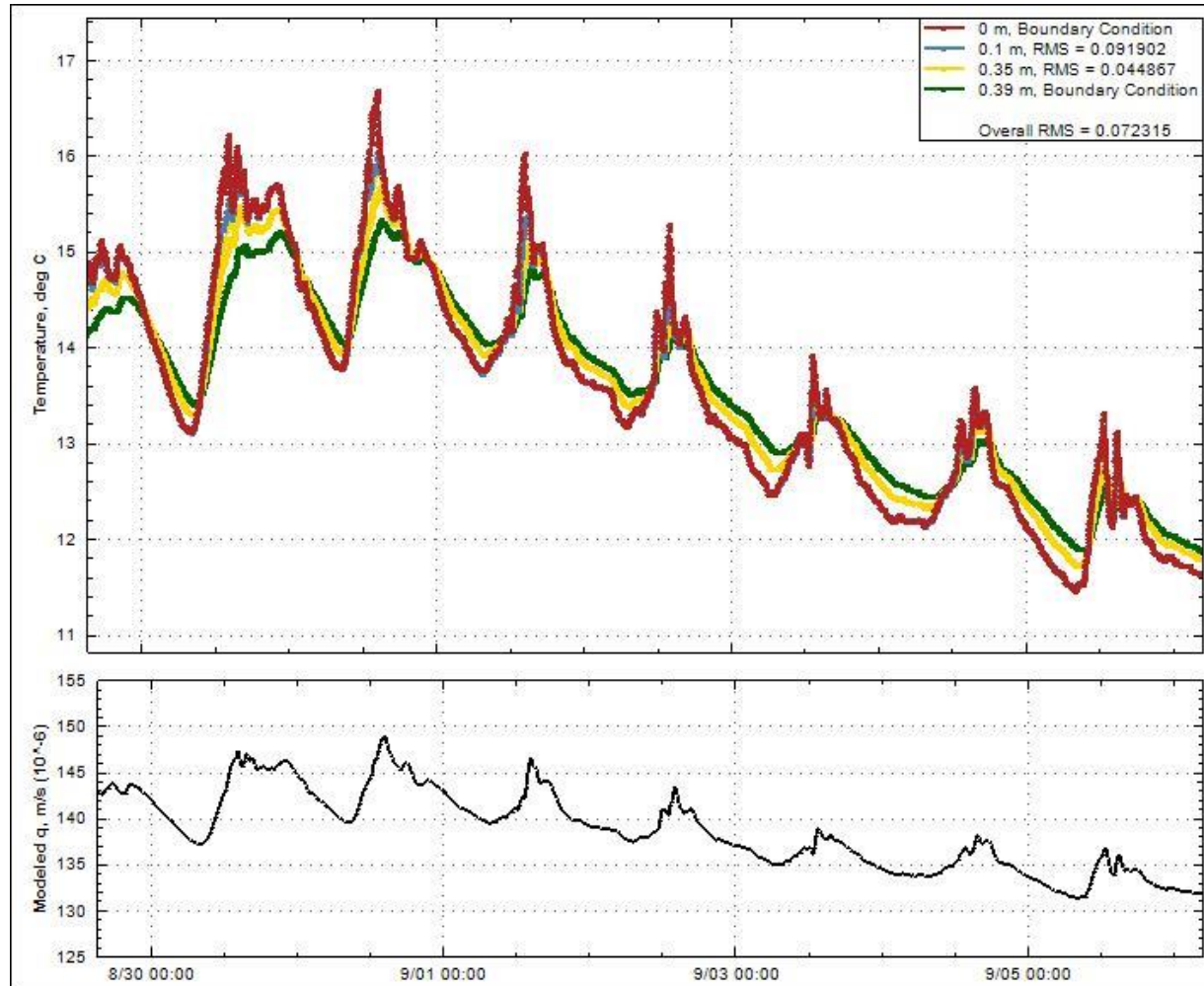


Figure 11. Downwelling and thermal gradient modelled with 1DTempPro by optimizing hydraulic conductivity at GRE-CA06 during June 2016. Temperatures shown as solid lines for modelled and dots for measured.

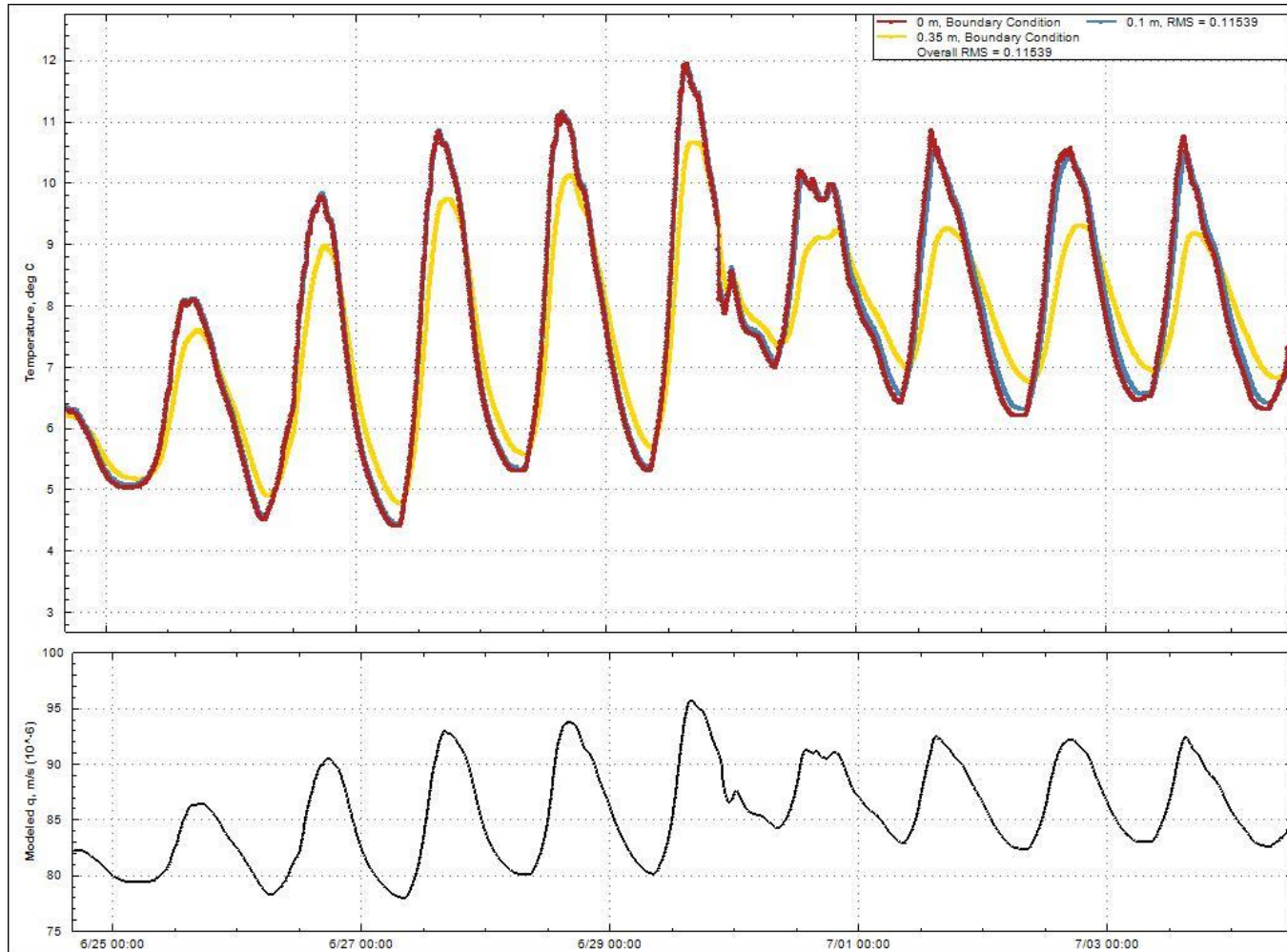


Figure 12. Downwelling and thermal gradient modelled with 1DTempPro by optimizing hydraulic conductivity at GRE-CA06 during October 2016. Temperatures shown as solid lines for modelled and dots for measured.

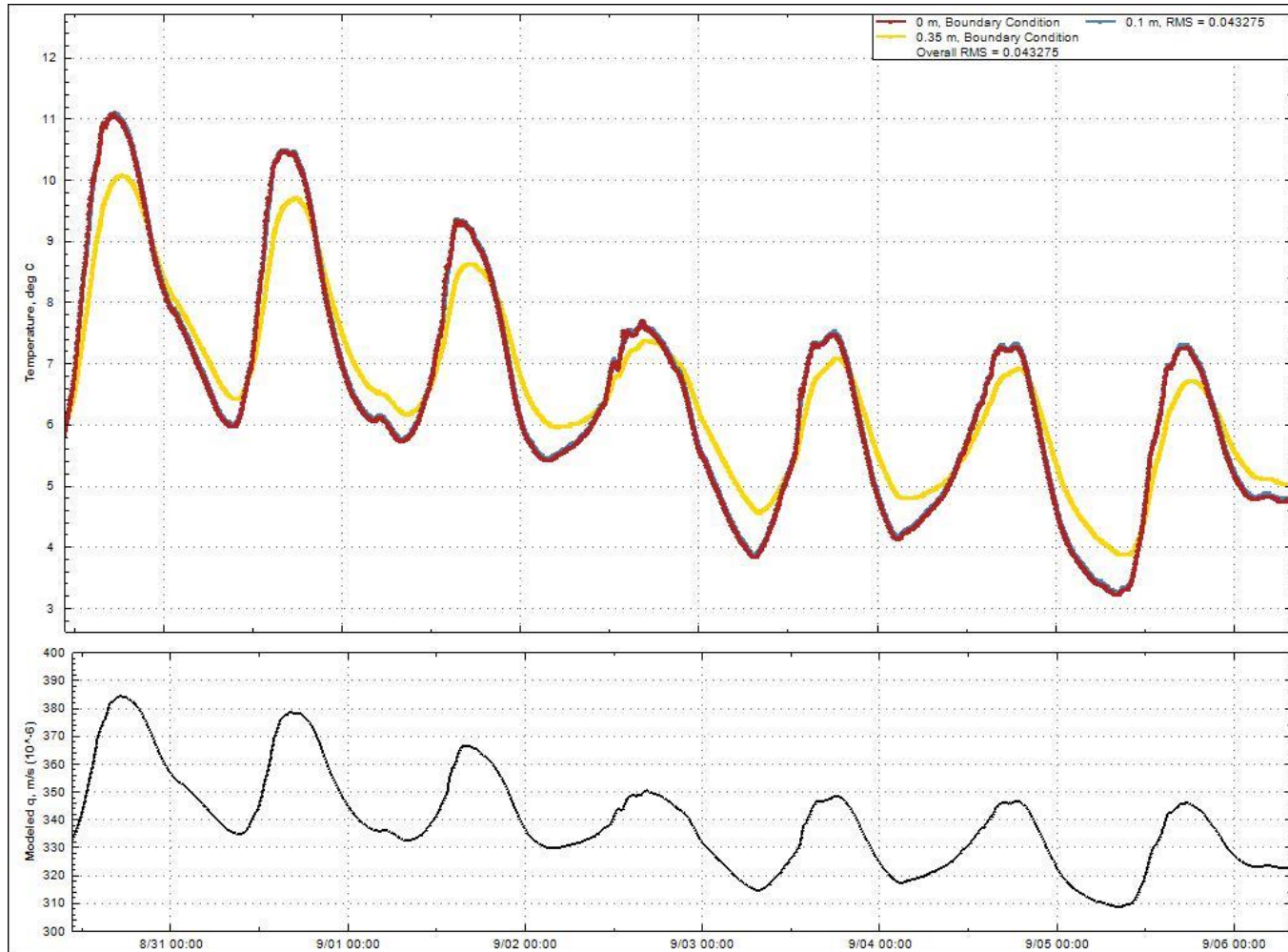


Figure 13. Downwelling and thermal gradient modelled with 1DTempPro by optimizing hydraulic conductivity at GH-CTF during June 2016. Temperatures shown as solid lines for modelled and dots for measured.

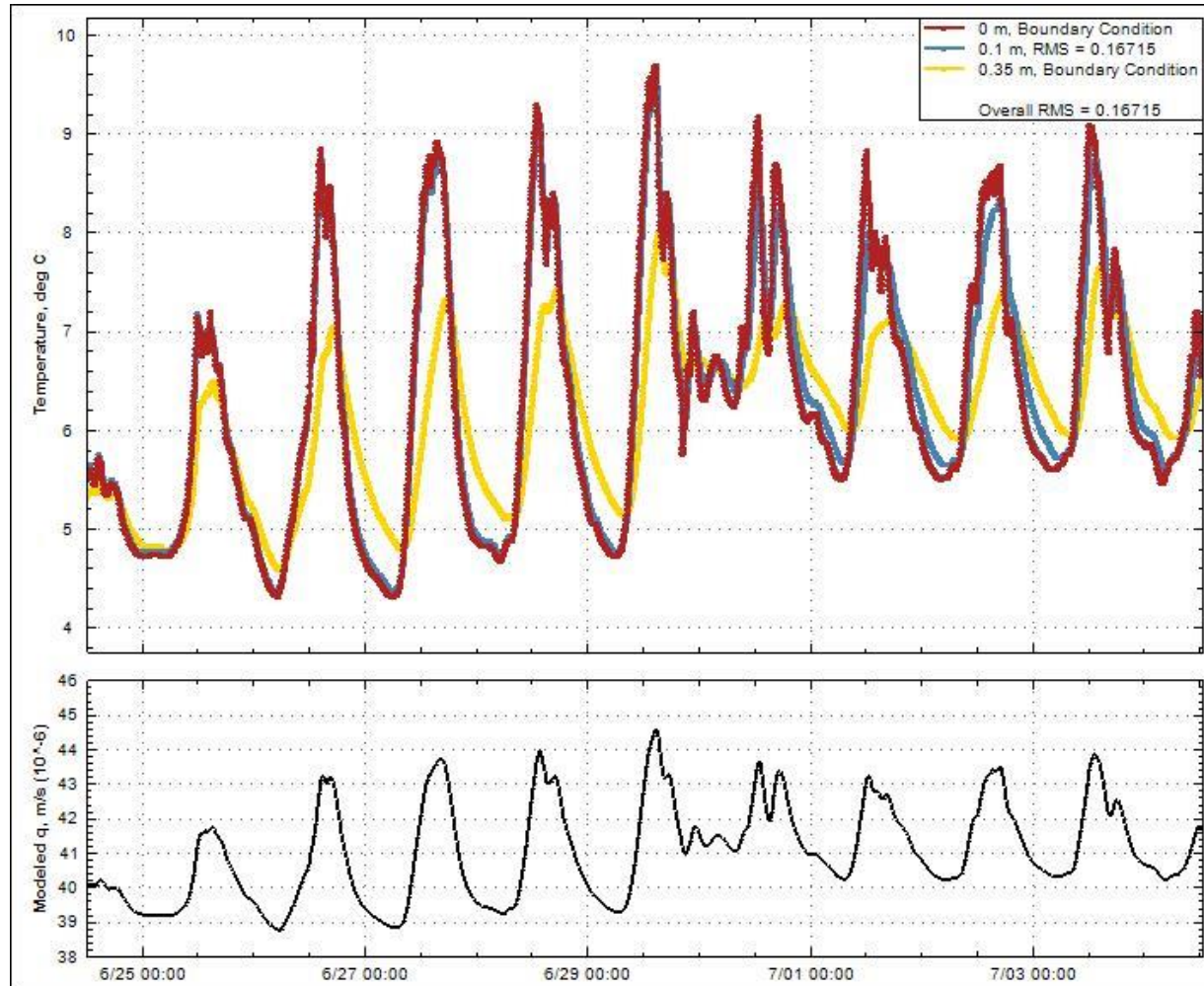


Figure 14. Downwelling and thermal gradient modelled with 1DTempPro by optimizing hydraulic conductivity at GH-CTF during October 2016. Temperatures shown as solid lines for modelled and dots for measured.

